

AD-A141 796

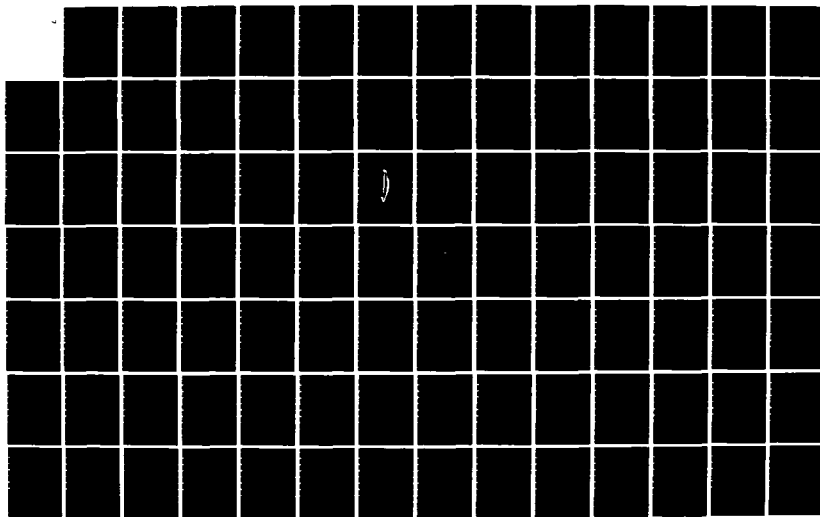
AERODYNAMIC DESIGN AND PERFORMANCE OF A TWO-STAGE
AXIAL-FLOW COMPRESSOR C. (U) IOWA STATE UNIV AMES
ENGINEERING RESEARCH INST M D HATHAWAY ET AL DEC 83
ISU-ERI-AMES-84178 AFOSR-TR-84-0417

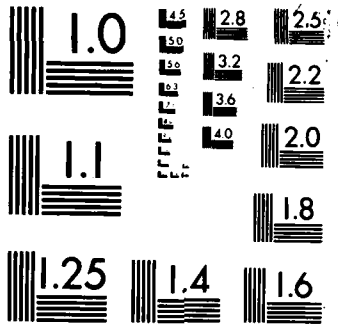
1/3

UNCLASSIFIED

F/G 21/5

NL





MICROCOPY RESOLUTION TEST CHART
NATIONAL BUREAU OF STANDARDS 1963 A

AFOSR-TR- 84-0417

M. D. HATHAWAY
T. H. OKIISHI
DECEMBER 1983

(3)

AD-A141 796

DTIC FILE COPY

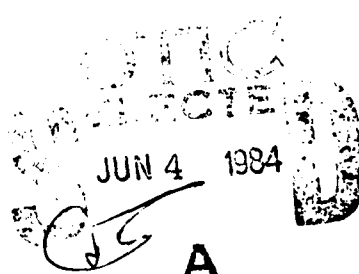
ISU-ERI-AMES-84178
TCPML-24
ERI PROJECTS 1384, 1480, 1645

AMERICAN AVIATION & SPACE RESEARCH CORPORATION
A Division of the Boeing Company
1984

AMERICAN
AVIATION &
SPACE
RESEARCH
CORPORATION
AMES

Approved for public release;
distribution unlimited.

84 05 30 055



**Qualified requestors may obtain additional copies from the
Defense Documentation Center; all others should apply
to the National Technical Information Service.**

CONDITIONS OF REPRODUCTION

**Reproduction, translation, publication, use and disposal in whole
or in part by or for the United States Government is permitted.**

TECHNICAL REPORT

AERODYNAMIC DESIGN AND PERFORMANCE OF A TWO-STAGE, AXIAL-FLOW COMPRESSOR (BASELINE)

AIR FORCE OFFICE OF SCIENTIFIC RESEARCH (AFSC)
NOTICE OF APPROVAL TO DISTRIBUTE
This technical document was reviewed and approved by Michael D. Hathaway
and Theodore H. Okilishi
December 1983
Distribution is unlimited.
MATTHEW J. KERPER
Chief, Technical Information Division

ISU-ERI-Ames-84178
TCRL-24
ERI Projects 1394, 1490, 1645

**DEPARTMENT OF MECHANICAL ENGINEERING
ENGINEERING RESEARCH INSTITUTE
IOWA STATE UNIVERSITY, AMES**

Unclassified

iii

SECURITY CLASSIFICATION OF THIS PAGE (When Data Entered)

REPORT DOCUMENTATION PAGE		READ INSTRUCTIONS BEFORE COMPLETING FORM
1. REFERENCE AFOSR-TR-84-0417 ISSUE DATE 10-17-83	2. GOVT ACCESSION NO. AD-A141	3. RECIPIENT'S CATALOG NUMBER 796
4. TITLE (and Subtitle) Aerodynamic Design and Performance of a Two-Stage, Axial-Flow Compressor (Baseline)		5. TYPE OF REPORT & PERIOD COVERED Technical Report - 1 October 1978-30 November 1982
7. AUTHOR(s) Michael D. Hathaway Theodore H. Okiishi		6. PERFORMING ORG. REPORT NUMBER TCRL-24
9. PERFORMING ORGANIZATION NAME AND ADDRESS Turbomachinery Components Research Laboratory Engineering Research Institute/Department of Mechanical Engineering Iowa State University, Ames, Iowa 50011		10. PROGRAM ELEMENT, PROJECT, TASK AREA & WORK UNIT NUMBERS 61102 F 2307/A4
11. CONTROLLING OFFICE NAME AND ADDRESS Air Force Office of Scientific Research Directorate of Aerospace Sciences (AFOSR/NA) Bolling Air Force Base, Washington, D.C.		12. REPORT DATE December 1983
		13. NUMBER OF PAGES 190 pages
14. MONITORING AGENCY NAME & ADDRESS (if different from Controlling Office)		15. SECURITY CLASS. (of this report) Unclassified
		15a. DECLASSIFICATION/DOWNGRADING SCHEDULE
16. DISTRIBUTION STATEMENT (of this Report) Approved for Public Release; Distribution Unlimited		
17. DISTRIBUTION STATEMENT (of the abstract entered in Block 20, if different from Report)		
18. SUPPLEMENTARY NOTES		
19. KEY WORDS (Continue on reverse side if necessary and identify by block number) axial-flow turbomachinery axial-flow compressor multistage axial-flow compressor		
20. ABSTRACT (Continue on reverse side if necessary and identify by block number) A two-stage, baseline configuration, low-speed, axial-flow research compressor was designed, built and tested at design flow. The design, fabrication and data acquisition and reduction details are described. Time-averaged, spatially detailed and overall flow and aerodynamic performance data for design flow operation of the compressor are presented and discussed.		

Unclassified

iv

SECURITY CLASSIFICATION OF THIS PAGE(When Data Entered)

Unclassified

SECURITY CLASSIFICATION OF THIS PAGE(When Data Entered)

TABLE OF CONTENTS

	<u>Page</u>
SYMBOLS AND NOTATION	ix
LIST OF FIGURES	xiii
LIST OF TABLES	xvii
1. INTRODUCTION	1
2. RESEARCH COMPRESSOR FACILITY	3
2.1. Axial-Flow Research Compressor	3
2.1.1. Aerodynamic Design	3
2.1.2. Mechanical Design	9
2.1.3. Blade Fabrication and Installation	13
2.2. Probe and Stationary Blade Row Actuators	20
2.3. Pressure and Temperature Sensing Instrumentation	21
2.4. Computer Control System	22
2.5. Calibration Equipment	23
3. EXPERIMENTAL PROCEDURE AND DATA REDUCTION	27
3.1. Calibration	29
3.1.1. Cobra Probe Yaw-Angle Calibration in Free-Stream Portion of Flow	31
3.1.2. Cobra Probe Calibration in Wake Portion of Flow	31
3.1.3. Spanwise Calibration of the Cobra Probe	33
3.1.4. Scanivalve Pressure Transducer Calibration	33
3.2. Data Aquisition	37
3.2.1. Overall Performance Map	37
3.2.2. Time-Averaged Measurements	39

3.3. Data Reduction	42
3.3.1. Flow-Field Parameters	43
3.3.2. Performance Parameters	45
4. PRESENTATION AND DISCUSSION OF DATA	47
4.1. Error Analysis	47
4.2. Overall Performance Map	51
4.3. Spatially Detailed Time-Averaged Measurement Results	57
4.4. Comparisons of Circumferential-Mean Data with Design Code Predictions	86
5. SUMMARY AND CONCLUSIONS	111
6. RECOMMENDATIONS FOR FURTHER RESEARCH	113
7. REFERENCES	115
8. ACKNOWLEDGEMENTS	117
9. APPENDIX A: CORRELATIONS USED IN NASA DESIGN CODE	119
9.1. Blade Loss	119
9.2. Incidence and Deviation Angle	121
10. APPENDIX B: NASA DESIGN CODE RESULTS	123
11. APPENDIX C: COMPUTER PROGRAMS AND DATA STORAGE	155
12. APPENDIX D: PARAMETER EQUATIONS	157
12.1. General Parameters	157
12.1.1. Basic Fluid Properties	157
12.1.2. Blade-Element Location	159
12.2. Flow-Field Parameters	159
12.2.1. Point and Circumferential-Average Blade Element Quantities	159
12.2.2. Global Parameters	163

12.2.3. Performance Parameters (based on cobra probe measurements)	164
12.2.4. Performance Parameters Used in Generating Performance Map	166
13. APPENDIX E: TABULATION OF EXPERIMENTALLY DETERMINED DATA	169

Approved _____
NTIS GEN#: _____
FSC TNS
University of _____
Institution _____

Date _____
Distribution _____

Available _____
Available after _____
List _____ Standard _____

A-1



SYMBOLS AND NOTATION

A	compressor flow passage annulus area, m^2
c	blade chord length, m
FCC	comparison of integrated and venturi flow coefficients (Eq. 12.34), percent
g	local acceleration of gravity, m/s^2
g_c	gravitational constant, 1.0 kgm/Ns^2
H	total head with respect to barometric pressure (Eq. 12.5 or 12.48), Nm/kg
h	static head with respect to barometric pressure, Nm/kg
h_{hg}	barometric pressure, m of Hg
h_w	annulus outer-surface end-wall static head with respect to barometric pressure (Eq. 12.9 or 12.10), Nm/kg
i	incidence angle (Fig. 12.1; Eqs. 12.25 or 12.27), deg
P_{atm}	barometric pressure (Eq. 12.1), N/m^2
P_t	total pressure with respect to barometric pressure, m of water
P_w	annulus outer-surface static wall pressure with respect to barometric pressure, m of water
PHH	percent passage height from hub (Eq. 12.4), percent
Q_a	integrated volume flow rate at probe-traversing measurement stations (Eq. 12.32), m^3/s
Q_v	venturi volume flow rate (Eq. 12.30), m^3/s
R	gas constant, $\text{Nm/kg}^\circ\text{K}$
r	radius from compressor axis, m
RPM	rotor rotational speed, rpm
S	circumferential space between blades, blade pitch, m or deg
T	compressor drive motor torque, Nm

t	temperature, °K
t_{baro}	barometer ambient temperature, °K
t_{max}	blade section maximum thickness, m
U	rotor blade velocity (Eq. 12.14), m/s
V	absolute velocity (Fig. 12.1; Eq. 12.12 or 12.13), m/s
V'	relative velocity (Eqs. 12.21 or 12.22), m/s
v_y	tangential component of absolute fluid velocity (Fig. 12.1; Eqs. 12.17 or 12.18), m/s
v'_y	tangential component of relative fluid velocity (Eqs. 12.19 or 12.20), m/s
v_z	axial component of fluid velocity (Fig. 12.1; Eqs. 12.15 or 12.16 and 12.47), m/s
γ	circumferential traversing position, deg
β_y	absolute flow angle with respect to axial direction (Fig. 12.1; Eqs. 12.7 or 12.8), deg
β'_y	relative flow angle with respect to axial direction (Eqs. 12.23 or 12.24), deg
γ_{H_2O}	specific weight of water manometer fluid (Eq. 12.3), N/m ³
γ_{Hg}	specific weight of mercury, N/m ³
P_{vent}	differential pressure across venturi, m of water
δ	deviation angle (Fig. 12.1; Eqs. 12.26 or 12.28), deg
η	hydraulic efficiency (Eqs. 12.42, 12.43, and 12.44)
κ	blade angle, angle between tangent to blade camber line and axial direction (Fig. 12.1), deg
ρ	density of air (Eq. 12.2), kg/m ³
σ	blade row solidity
ϕ	flow coefficient (Eq. 12.29)
ϕ_a	integrated flow coefficient at probe-traversing measurement stations (Eq. 12.33)
ϕ_v	venturi flow coefficient (eq. 12.31)

Ψ head-rise coefficient (Eqs. 12.36 through 12.41 and 12.49, 12.50)

w total-head loss coefficient (Eqs. 12.45 and 12.46)

Additional General Subscripts

h annulus inner surface, hub

i ideal

me mechanical

$overall$ overall compressor

pm torque meter based performance parameters

R rotor

S stator

$stage$ stage

t annulus outer surface, tip

1 blade-row inlet

2 blade-row outlet

$1R$ first rotor

$2R$ second rotor

$1S$ first stator

$2S$ second stator

Superscripts

' relative to rotor

- average; blade-to-blade circumferential average value

. mass-averaged in the radial direction

= cross-section average

LIST OF FIGURES

	<u>Page</u>
Figure 2.1 Schematic of baseline compressor showing original and redesigned components.	4
Figure 2.2 Representative rotor blade sections at three spanwise locations.	6
Figure 2.3 Representative stator blade sections at three spanwise locations.	7
Figure 2.4 Meridional-plane view of redesigned section of baseline compressor with each ring assembly identified.	10
Figure 2.5 Schematic diagram showing axial location of probe measurement stations relative to adjacent blade rows (dimensions in mm).	12
Figure 2.6 Radial and circumferential interlock design of outer ring assembly.	14
Figure 2.7 Probe access hole configuration.	15
Figure 2.8 Schematic of blade fabrication showing laminates sandwiching trunnion spline.	17
Figure 2.9 Representative eyelash drawing.	18
Figure 2.10 Schematic diagram of data acquisition system.	24
Figure 3.1 Baseline compressor overall performance curve and operating point.	28
Figure 3.2 Logic diagram of data acquisition system.	30
Figure 3.3 Cobra probe yaw-angle total-head calibration curve in free stream portion of flow for flow coefficient = 0.587 at 2400 rpm.	32
Figure 3.4 Cobra probe total-head calibration curve in wake portion of flow for flow coefficient = 0.587 at 2400 rpm.	34
Figure 3.5 Cobra and Kiel probe comparison behind first rotor and first stator for flow coefficient = 0.587 at 2400 rpm ($Y/S_S = 0.0$).	35

Figure 3.6	Blade cascade showing circumferential measurement window.	41
Figure 4.1	Predicted and measured overall performance data.	52
Figure 4.2	Blade-to-blade distribution of time-averaged total head for flow behind the first and second stage rotors ($\phi = 0.587$ at 2400 rpm).	58
Figure 4.3	Blade-to-blade distribution of time-averaged total head for flow behind the first and second stage stators ($\phi = 0.587$ at 2400 rpm).	61
Figure 4.4	Spanwise distribution of circumferential-mean data for flow behind the first and second stage rotors ($\phi = 0.587$ at 2400 rpm).	67
Figure 4.5	Spanwise distribution of circumferential-mean data for flow behind the first and second stage stators ($\phi = 0.587$ at 2400 rpm).	70
Figure 4.6	Contour map of the distribution of total head behind each blade row ($\phi = 0.587$ at 2400 rpm). Data enhancement employed.	74
Figure 4.7	Locations of actual data points used in constructing the contour map behind the first stator.	78
Figure 4.8	Contour map of the distribution of total head behind the first stator ($\phi = 0.587$ at 2400 rpm). No data enhancement.	79
Figure 4.9	Comparisons of measured circumferential-mean incidence and deviation angles for both stages ($\phi = 0.587$ at 2400 rpm).	83
Figure 4.10	Comparisons of measured and predicted velocity triangles behind the first rotor ($\phi = 0.587$ at 2400 rpm).	87
Figure 4.11	Comparisons of measured and predicted velocity triangles ahead of the second rotor ($\phi = 0.587$ at 2400 rpm).	88
Figure 4.12	Comparisons of measured and predicted velocity triangles behind the second rotor ($\phi = 0.587$ at 2400 rpm).	89
Figure 4.13	Comparisons of the measured and predicted spanwise distributions of circumferential-mean axial velocity ($\phi = 0.587$ at 2400 rpm).	91

Figure 4.14	Comparisons of the measured and predicted spanwise distributions of circumferential-mean data for the first and second stage rotors ($\phi = 0.587$ at 2400 rpm).	94
Figure 4.15	Comparisons of the measured and predicted spanwise distributions of circumferential-mean data for the first and second stage stators ($\phi = 0.587$ at 2400 rpm).	97
Figure 4.16	Spanwise distributions of design code rotor blade angles.	101
Figure 4.17	Spanwise distributions of design code stator blade angles.	104
Figure 4.18	Comparisons of measured and predicted spanwise distributions of blade loss for each blade row ($\phi = 0.587$ at 2400 rpm).	105
Figure 9.1	Blade loss correlation curves used in NASA design code.	120
Figure 10.1	Typical rotor and stator blade sections using manufacturing coordinates.	154
Figure 12.1	Sketch showing nomenclature and sign conventions (all positive except as noted) for slow-response instrument parameters.	158

LIST OF TABLES

	<u>Page</u>
Table 4.1 Uncertainty estimates of measurement parameters.	48
Table 4.2 Flow coefficient comparison between venturi and integrated measurement station flow coefficients.	51
Table 4.3 Rotor, stator, stage, and overall performance parameters.	85
Table 10.1 Design code input parameters.	124
Table 10.2 Design code predictions of aerodynamic parameters.	132
Table 10.3 Design code stage and overall performance predictions.	143
Table 10.4 Rotor blade manufacturing coordinates generated by NASA design code.	144
Table 10.5 Stator blade manufacturing coordinates generated by NASA design code.	149
Table 13.1 Point-by-point distributions of circumferential survey data.	171
Table 13.2 Circumferentially-averaged flow-field parameters.	190

1. INTRODUCTION

A significant portion of the inefficiency of axial-flow turbomachines is associated with viscous and turbulent flow phenomena in the boundary layers which develop on blade surfaces and on annulus hub and casing walls. For example, large secondary flow losses can accompany the complex, three-dimensional flow patterns of annulus-wall boundary layers passing through blade rows. This behavior affects both local work transfer and the management of the flow in subsequent blade rows. It can be appreciated, therefore, why there has been considerable interest in the possibility of reducing axial-flow turbomachine stationary-blade-row secondary and end-wall flow losses by incorporation of unusual blade configurations (e.g., Mitchell and Soileau [1]; Wisler [2]; Senoo, Taylor, Batra, and Hink [3]).

In order to initiate a local program of research to provide a clearer understanding of the potential for better controlling the secondary and end-wall flows in axial-flow turbomachines, a suitable baseline research compressor was required. The existing three-stage, axial-flow compressor [4] of the Iowa State University Turbomachinery Components Research Laboratory was evaluated for possible service in this capacity. It was decided that the best course of action would involve the design and fabrication of new blades which would be more representative of conventional compressors. However, much of the rest of the existing compressor rig such as drive system, inlet flow path, and flow-rate control and measurement duct could be used with the new blades to form the baseline compressor. The design of the new

baseline blades was accomplished with the aid of a NASA computer code [5] and included the following considerations:

1. Higher blade-chord Reynolds numbers than were previously attainable with the three-stage compressor blading.
2. A better blade material which would be more durable than that already available.
3. Conventional blade-section shapes.
4. A favorable ratio of number of rotor blades to number of stator blades.
5. Elimination of inlet guide vanes.

In order to use as much of the existing compressor rig as possible while also achieving a significantly higher blade-chord Reynolds number, a two-stage configuration without inlet guide vanes was selected.

Fiberglass blades were fabricated and fitted into specially made flow-path rings to form the baseline compressor.

This report is intended to document in detail important aspects of the design, fabrication, and aerodynamic testing of the baseline compressor configuration. Subsequent reports will deal with specific stator blade modifications for possibly improved control of end-wall and secondary flows as well as related tests and comparisons of data.

2. RESEARCH COMPRESSOR FACILITY

The axial-flow research compressor and data acquisition system of the Iowa State University Engineering Research Institute/Mechanical Engineering Department Turbomachinery Components Research Laboratory were used to accomplish the research described in this report. The compressor, instrumentation, data acquisition system, and calibration equipment are described in this section.

2.1. Axial-Flow Research Compressor

Aerodynamic considerations mentioned earlier led to the design of a new two-stage, baseline, axial-flow research compressor configuration. An existing three-stage axial-flow compressor [4] was modified to form the baseline compressor. Much of the existing compressor such as the drive system, inlet flow-path, and flow-rate control and measurement duct were incorporated into the current system. A schematic of the baseline compressor rig which indicates the extent of the redesigned section is shown in Figure 2.1.

2.1.1. Aerodynamic Design

Aerodynamic design of the two-stage baseline compressor was accomplished with the aid of an axial-flow compressor design code [5] developed at NASA Lewis Research Center. The aerodynamic portion of the code assumes steady, axisymmetric flow and uses a streamline curvature method for the iterative solution--between blade rows--of the property, continuity, and momentum equations with empirical subsonic flow viscous loss correlations provided by the user (see

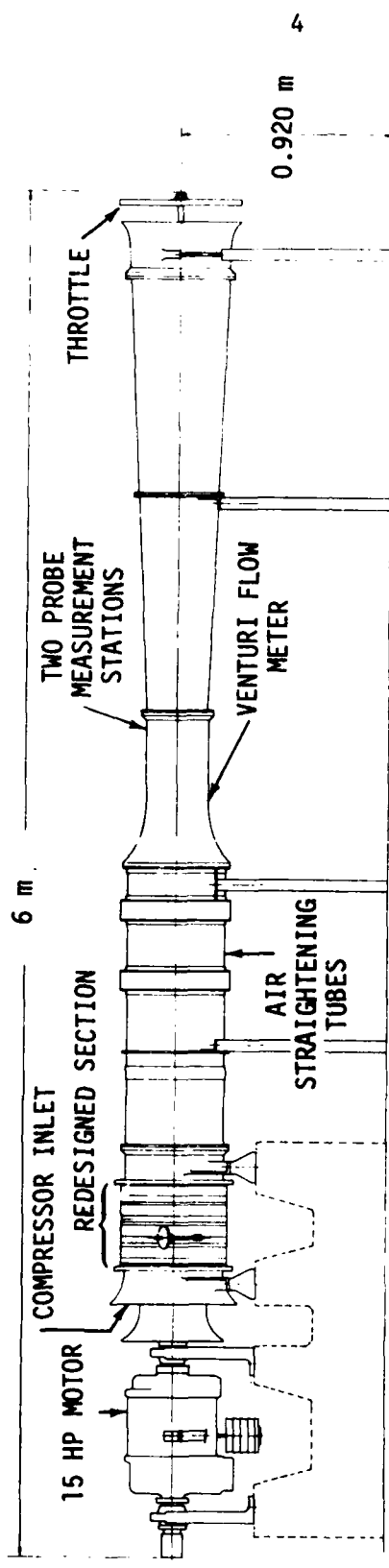


Figure 2.1 Schematic of baseline compressor showing original and redesigned components.

Appendix A). Coupled with the aerodynamic solution iterations, is a blade design procedure which constructs blade elements on specified conical surfaces and then stacks them on a user defined axis (see Reference [5]). These blade elements are positioned in the flow with incidence and deviation angle correlations selected by the user (see Appendix A). After aerodynamic and blade design solution convergence has been achieved, blade fabrication information consisting of coordinates for several blade sections--formed by the intersection of planes perpendicular to the radial direction and the blade at different radii--are provided by the code. Blade sections between elements are obtained by interpolation. Examples of such blade sections at three spanwise locations are shown in Figure 2.2, for the baseline rotor blade, and Figure 2.3, for the baseline stator blade.

The baseline compressor was designed to have high reaction stages typical of transonic compressor configurations. Further, a uniform spanwise distribution of total pressure was prescribed for each rotor exit. The stators were designed to discharge fluid axially and inlet guide vanes were not used.

The coordinates of the annular flow path for the existing compressor were retained in the baseline compressor to allow use of the existing inlet and exit flow sections. A rotor speed of 2400 rpm was selected as it was considered to be the maximum safe level obtainable with the existing equipment. A mass flow-rate of 5.25 lb/s (2.29 Kg/s) was established from preliminary design trials with a simple radial equilibrium based computer code [6] developed by Detroit Diesel Allison for NASA. An overall compressor pressure ratio of 1.0125 was obtained

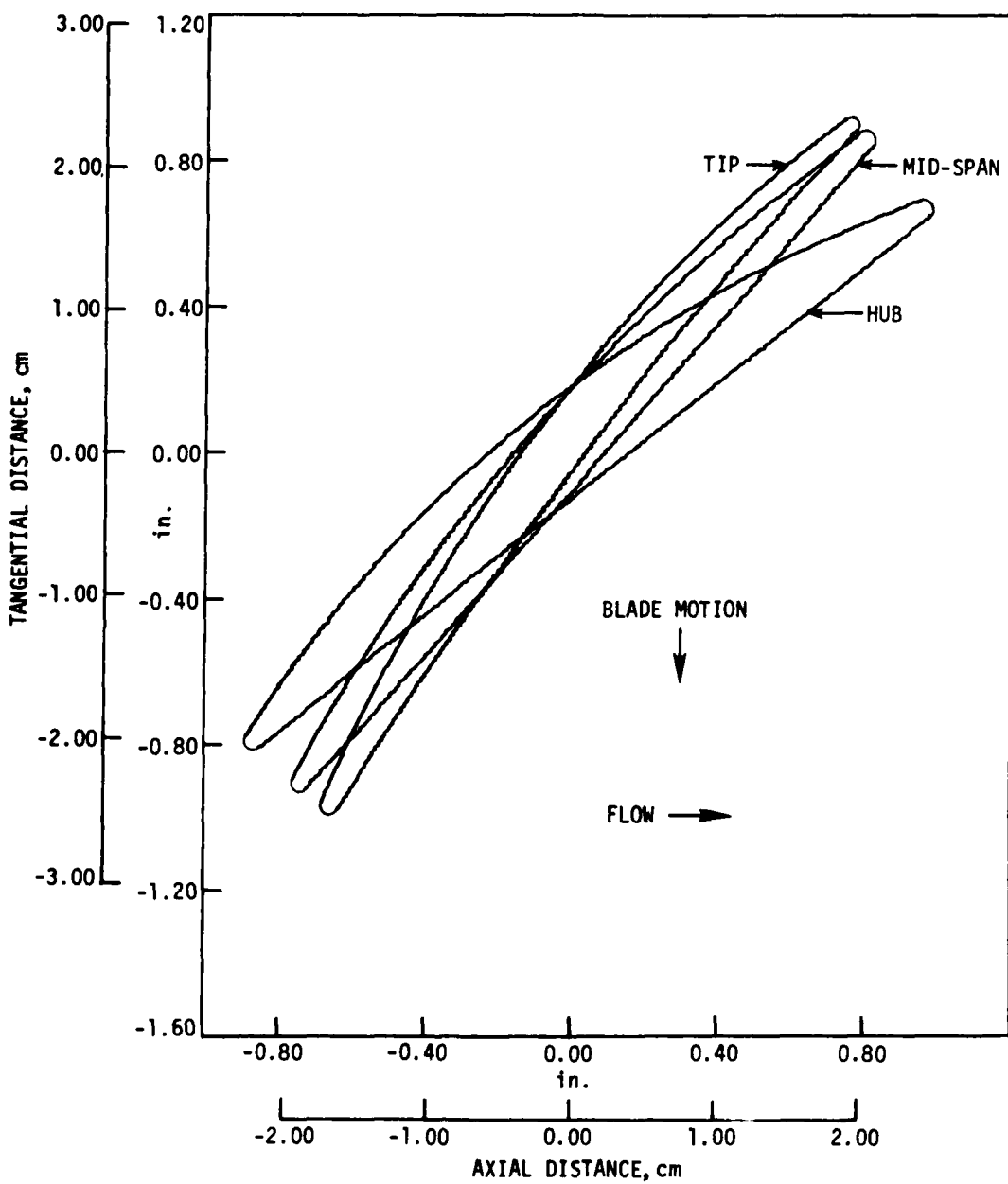


Figure 2.2 Representative rotor blade sections at three spanwise locations.

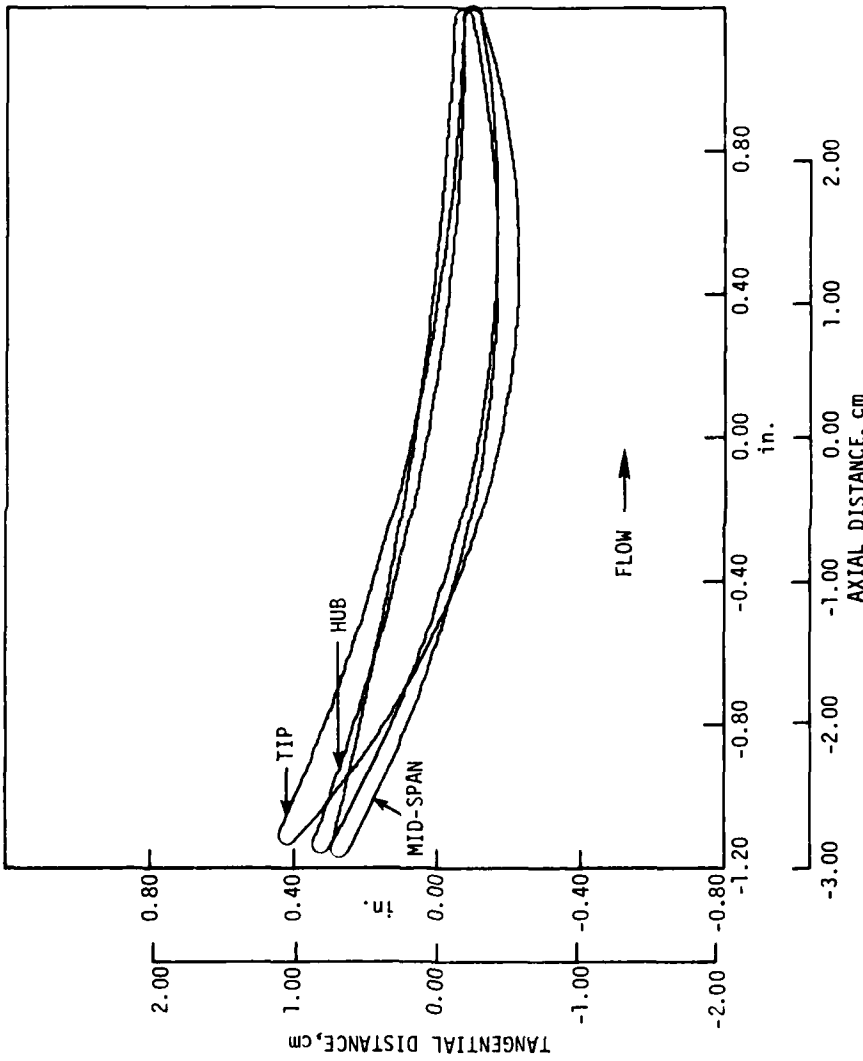


Figure 2.3 Representative stator blade sections at three spanwise locations.

with the codes--with the rotor tip diffusion factor limit specification of 0.4 being the only aerodynamic limit reached during the design process. Circular arc blade-elements were selected as they were considered suitable for the low Mach number service involved. For the baseline configuration, blade chord and leading and trailing edge radii were held constant across the span. The blade maximum thickness to chord ratio was varied linearly from 0.1 at the blade root to 0.06 at the other extremity. In order to maximize the blade chord Reynolds number, the rotor chord length was made as large as possible while still allowing two stages to fit within the predetermined flow path. The selected rotor chord length, 2.39 in (6.07 cm), coupled with a reasonable value of rotor tip solidity (1.0) yielded 21 rotor blades. At design point, the blade chord Reynolds number was on the order of 1.8×10^5 . To achieve a reasonable ratio of number of rotor blades to number of stator blades, the acoustics-related guidelines of Reference [7] were used which set the number of stator blades at 30. A stator chord length equal in value to the rotor chord length resulted in a reasonable stator solidity (1.4 at the tip) and was thus adopted. The aspect ratio of each blade row was 1.0. A radial stacking axis through the center of gravity of each blade element was considered appropriate for the baseline rotor and stator blades. Additional blade parameters and blade fabrication coordinates are given in Appendix B. Annulus-wall blockage factors (see Appendix B) were estimated, keeping in mind that specifying smaller than anticipated blockage is conservative. If blockage is higher than specified, the flow in the mid-span region will be accelerated and loading will be relieved. On the other hand, if

blockage is less than specified, the flow in the mid-span region will tend to be accelerated less and loading will increase. Tabulated velocity diagram output from the NASA aerodynamic design code are provided in Appendix B.

2.1.2. Mechanical Design

Except for the blades, all machining and fabrication of the baseline compressor was performed in the Iowa State University Engineering Research Institute Machine Shop. The geometry of the baseline compressor as well as improvements in the original compressor mechanical design are described in this section.

A meridional-plane view of the redesigned portion of the compressor rig is shown in Figure 2.4. The basic components of the baseline compressor consist of eleven independent rings which facilitate disassembly and reassembly of the compressor flow-path. The five inner rings (MH201 to MH203) which make up the hub flow path are mounted on the original rotor drum and are held in place by friction. Four independent circumferentially and radially interlocking rings (MH101 to MH104) make up the outer casing of the baseline compressor. The two stator blade row supporting rings (MH105) are mounted in circular tracks in the outer casing, formed by rings (MH101 to MH104), to permit independent circumferential positioning of each stator blade row about the compressor axis of rotation. The stator blade rows can, thus, be moved circumferentially during tests by means of a circumferential motion actuator which is mechanically linked to each stator blade row mounting ring (MH105) through slots provided in the outer casing rings. Cylindrical trunnion holes were used in each stator and rotor support ring

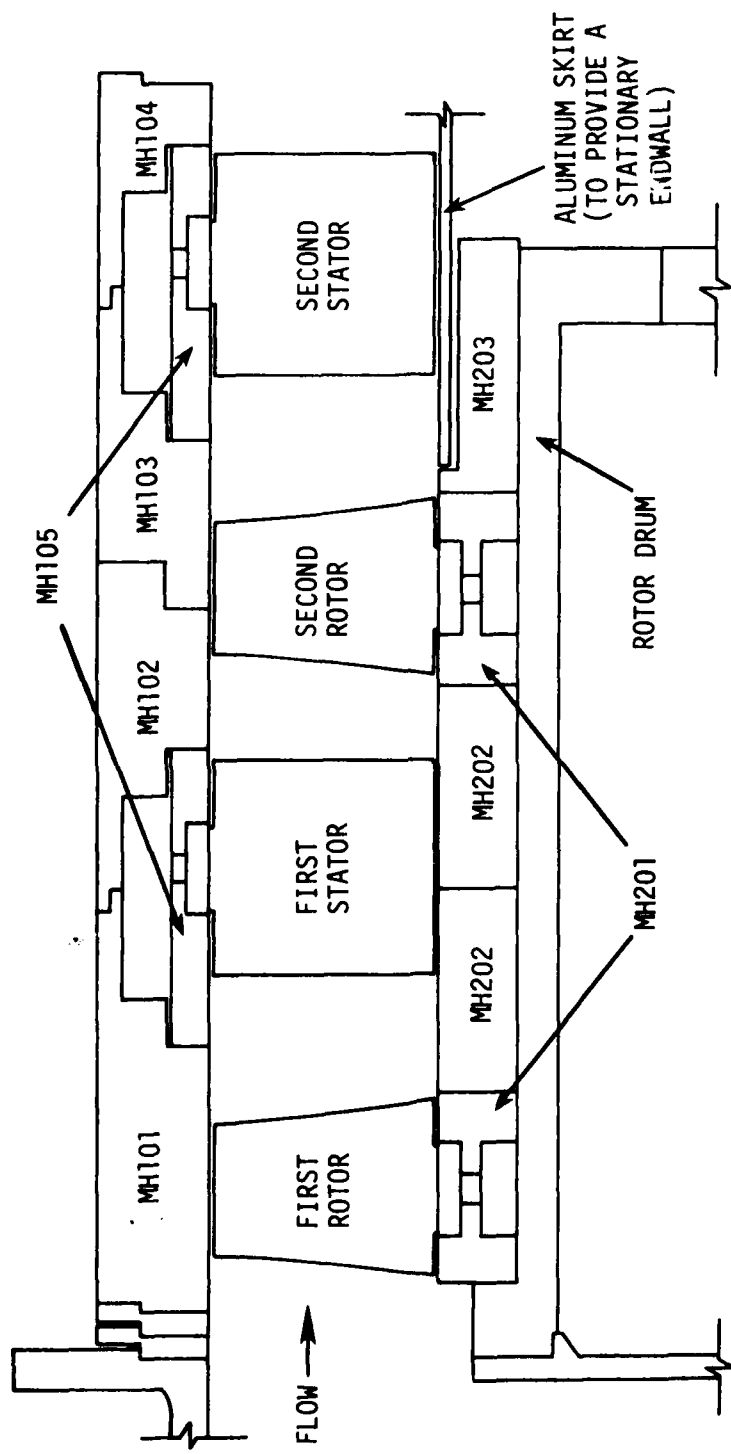


Figure 2.4 Meridional-plane view of redesigned section of baseline compressor with each ring assembly identified.

(MH105, MH201) to facilitate blade attachment and to simplify readjustment of blade setting angles. For the present study, both rotor blade row rings (MH201) were positioned circumferentially during assembly so that the blade stacking axes for each rotor row were in line axially. Since no discernible difference in compressor aerodynamic noise level was noticed for different relative circumferential positions of the stator rows with respect to each other it was decided that, for this study, the stator blade rows would also be aligned so that their stacking axes were in line axially. Probe traversing stations were arranged in line axially and positioned upstream of the first rotor blade row, downstream of the second stator blade row, and between all other blade rows. The axial location of each probe measurement station relative to adjacent blade rows is shown in Figure 2.5. Static pressure-tap holes, spaced 90 degrees apart circumferentially, were also provided at each probe hole axial location.

Several improvements to the original compressor were achieved during the redesign effort and are described herein. Binding and sticking during circumferential rotation of the stator rows was avoided in the baseline compressor with the aid of teflon pads. The teflon pads were placed around the full circumferential extent of both vertical edges of each stator blade row supporting ring (MH105). Ten equally spaced teflon pads were also attached to the outer cylindrical surface of each stator blade row supporting ring. The teflon pads eliminated metal-to-metal contact on all sliding surfaces which resulted in smooth operation of the stator blade row support rings during circumferential positioning. Some of the binding problems

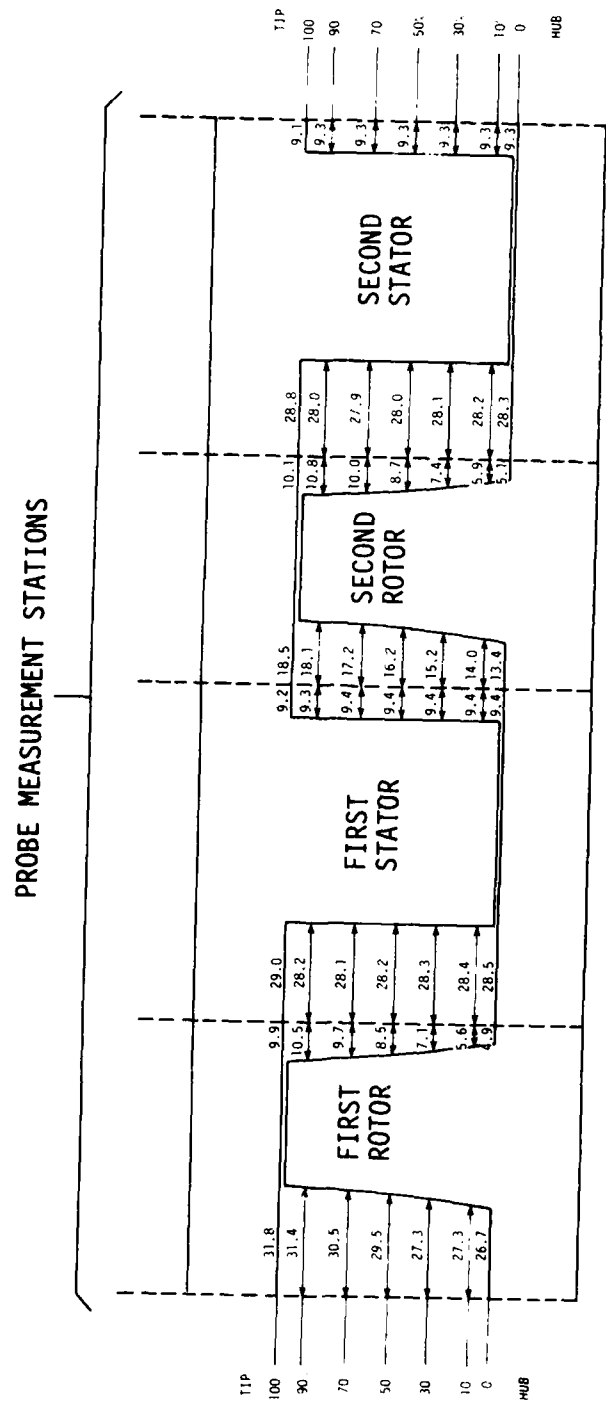


Figure 2.5 Schematic showing axial location of probe measurement stations relative to adjacent blade rows (dimensions in mm).

experienced in an earlier build were attributed to poor radial and circumferential positioning of the outer annulus rings. This problem was eliminated by matching the outer annulus rings so that each ring interlocked both radially and circumferentially with adjacent rings (see Figure 2.6). Reference marks were provided at each coupling point to insure proper circumferential positioning of both stator and rotor blade rows.

Anticipated tests of blade-fillet geometry effects on stator performance required that at least one of the stator blade rows be provided with a stationary flow path at the stator tip. Since the rotor drum surface is the annulus hub, it was necessary to extend an aluminum skirt upstream from the outlet duct hub contour in order to provide a stationary hub surface for the second stage stator. Both the rotor drum and outlet duct hub contour were provided with a circumferential recess to allow for adequate running clearance between the rotor drum and the aluminum skirt, and to insure sufficient continuity of the hub contour. The circumferential recess in the downstream rotor ring (MH203) is shown in Figure 2.4.

The probe access holes were designed to facilitate mounting and dismounting of the probe actuator assembly. A keyway configuration (see Figure 2.7) was chosen since it provided minimal intrusion into the flow path and yet permitted insertion of all anticipated probe configurations.

2.1.3. Blade Fabrication and Installation

Fabrication of the blades for the baseline compressor was performed at Dayton Scale Model Company, Dayton, Ohio. Several materials

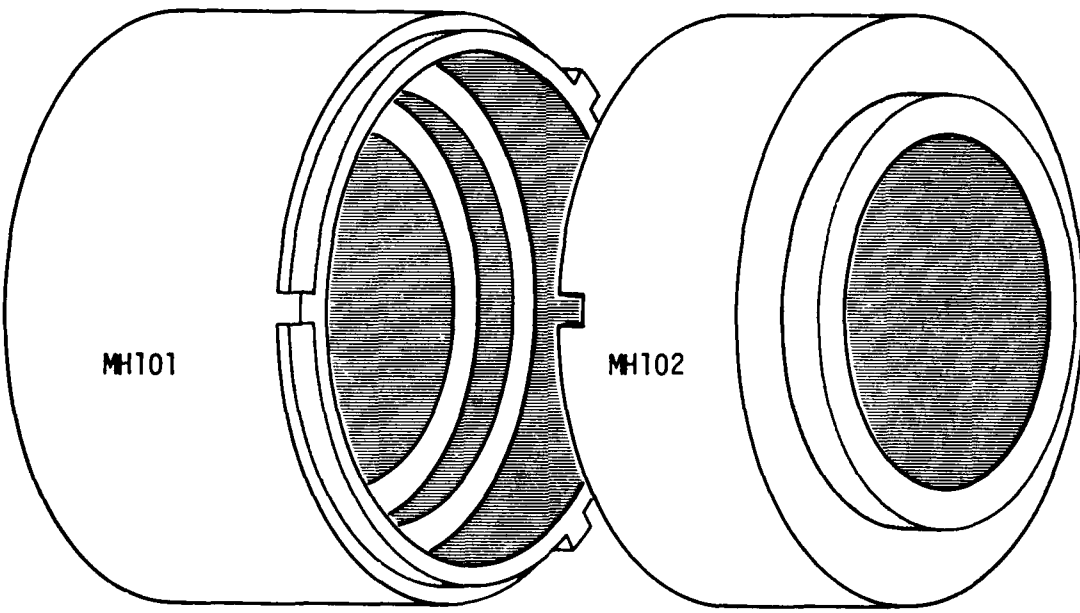
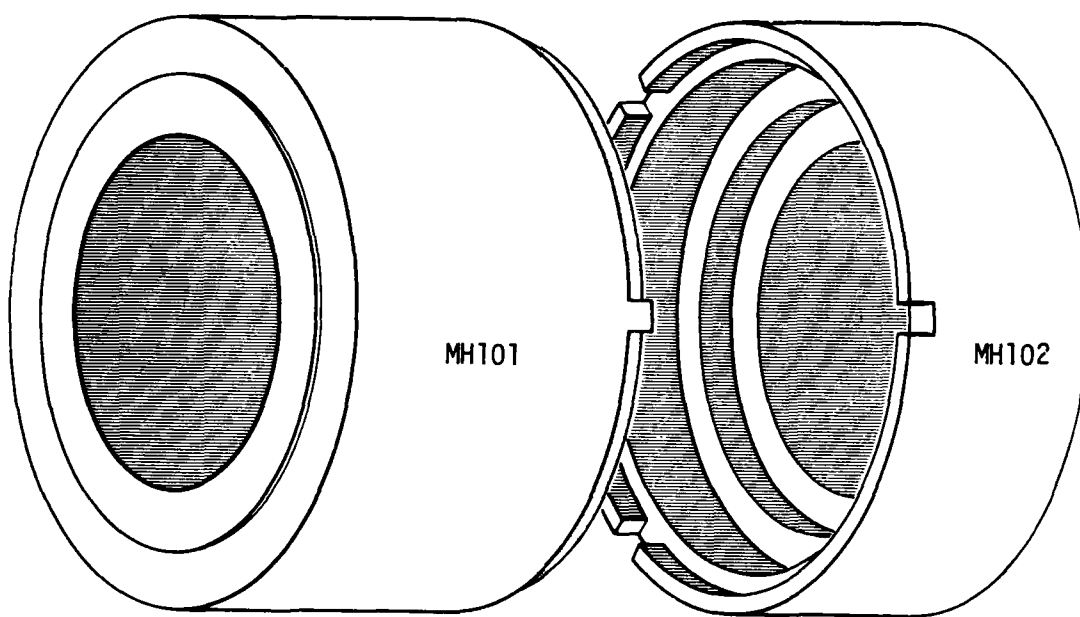


Figure 2.6 Radial and circumferential interlock design of outer ring assembly.

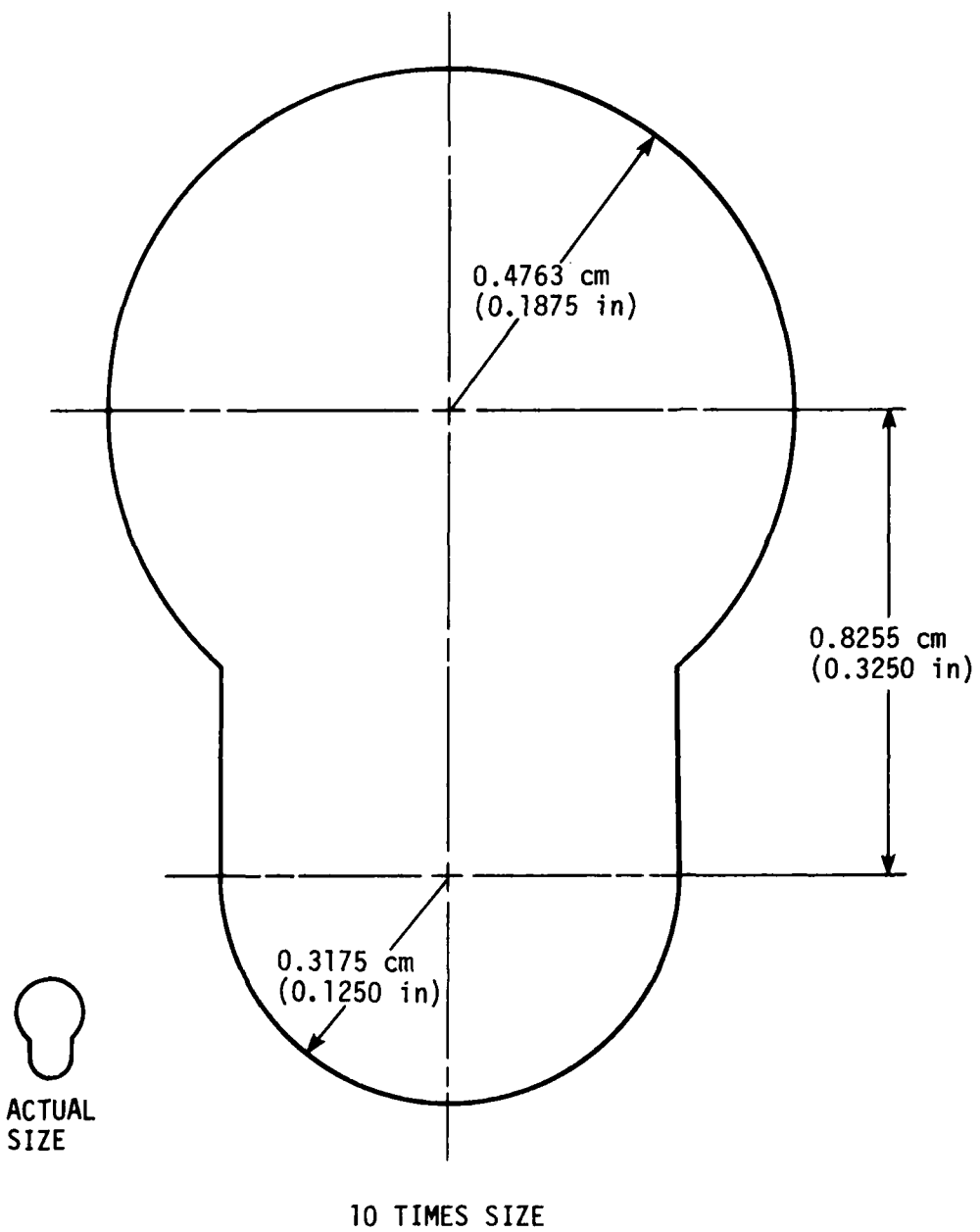


Figure 2.7. Probe access hole configuration.

such as aluminum, plastic, and fiberglass were considered for possible use in the construction of the blades. Molded blades constructed with a fiberglass reinforced epoxy resin material were selected as being most appropriate for this application.

Rotor and stator blade section coordinates at eleven different radii (see Appendix B) were generated from the design code for use in construction of a master rotor blade and master stator blade. These coordinates were also used to produce ten times size drawings of each blade section, on mylar, for use in checking the shape of the master and actual blades. The master blades, constructed of aluminum, were used to manufacture molds for both the rotor and stator blades. The fiberglass reinforced epoxy resin material, in sheet form, was cut to the general shape of the blade and stacked in layers in the mold bottom, sandwiching a spine which protruded from the trunnion base for the blades (see Figure 2.8). Each fiberglass layer was stacked so that the glass fibers of adjacent layers were perpendicular. The mold top was then put in place and the entire mold assembly was placed in a press which slowly applied pressure while also heating the fiberglass to an appropriate temperature to insure complete filling of the mold and bonding of the fiberglass laminates. Upon cooling, each blade was removed from the mold and the leading and trailing edge radii were checked under a microscope and dressed if necessary. Ten times size "eyelash" profiles (see Figure 2.9) of each blade section, corresponding to the blade sections of the mylar drawings, were produced at each step of the manufacturing process. These eyelash drawings of the master blades and a few representative finished blades were compared

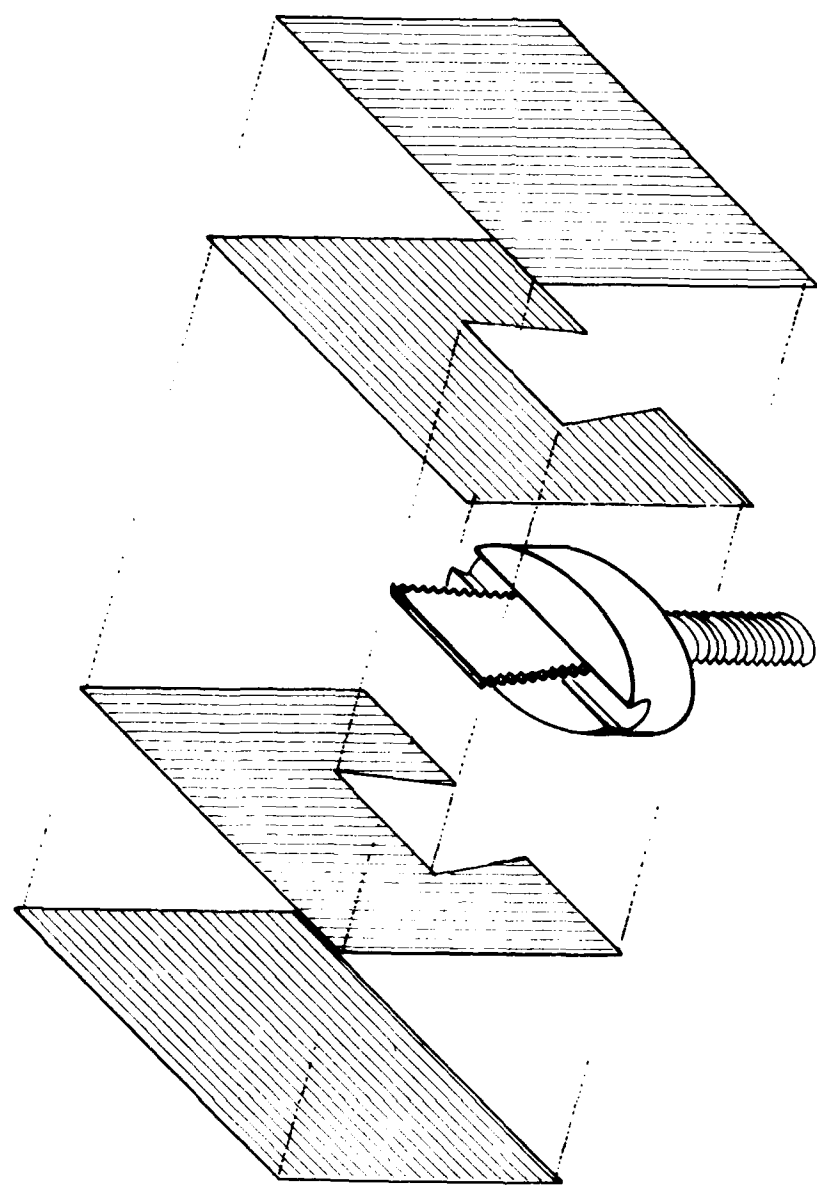


Figure 2.8 Schematic of blade fabrication showing laminates sandwiching trunnion spline.

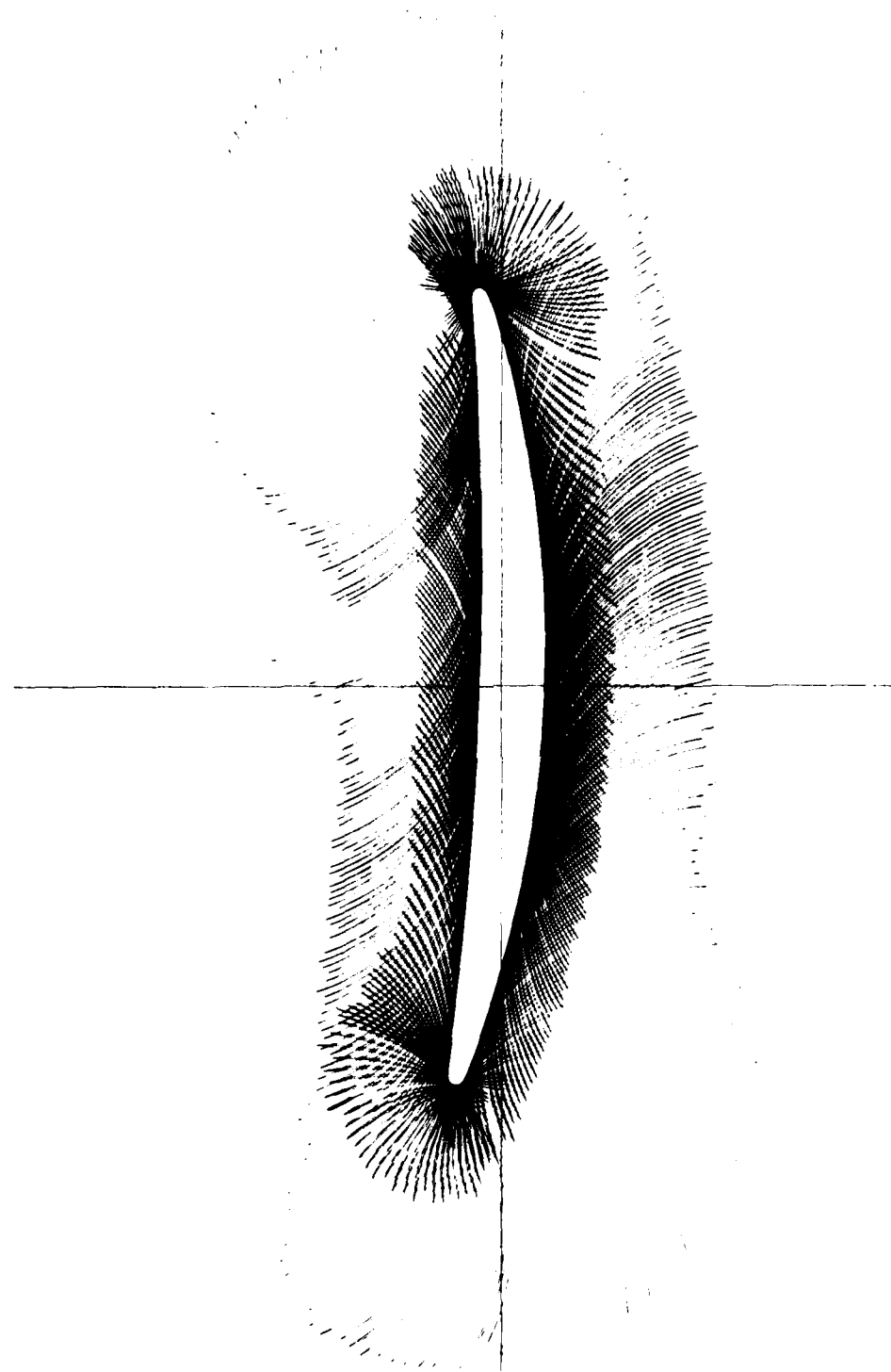


Figure 2.9 Representative eyelash drawing.

to the mylar drawings to insure precision control. The maximum deviation from the mylar drawings was less than 0.005 inches (0.127 mm) along the entire blade surface. The trunnion base for the blades was a machined cylindrical plug with an extended flat spine on one end to which the fiberglass blades could be formed around, and a threaded stud on the other end for attachment to the blade mounting ring (see Figure 2.8). This simple trunnion design allowed for easy adjustment of blade setting angles and facilitated blade attachment to the mounting rings. The length of the trunnion base was made slightly less than the depth of the corresponding holes in the blade mounting rings to prevent any intrusion into the flow. After all stator and rotor blades were attached to their respective blade mounting rings, specially made gauges were used to insure correct adjustment of blade setting angles. The blade setting angles were checked at the blade root and mid-span and found to be within 0.25 degrees of the design setting angles for all blades. The stator blade mounting rings and the rotor drum assembly, with rotor blade mounting rings installed, were placed on a lathe and a high speed grinding tool was used to grind the blade tips to an appropriate radius. The grinding insured that the blades would conform to the curvature of the end-walls with a mean clearance of 0.034 inches (0.864 mm) (1.4% span) for each blade row. Silicon rubber glue was then used to fill in the gap between the rotor root section and rotor hub in order to provide a smooth transition between the blade and the rotor drum surface. A caulking compound, Mortite (Mortell Company, Kankakee, Illinois), was used to seal the gap between the stator blade root and stator blade mounting ring.

No attempt was made to provide a particular fillet radius, however, the fillet was made as small as was practical. The entire rotor drum assembly was dynamically balanced for smooth operation up to 3600 rpm.

2.2. Probe and Stationary Blade Row Actuators

A circumferential motion actuator [4] was used to control circumferential positioning of the stator blade rows during testing. The actuator was connected to each stator blade row mounting ring through an adjustable hand-screw link. Each blade row mounting ring could then be moved independently or simultaneously. The circumferential position of each stator blade row was determined from calibrated scales, marked in degrees, which were attached to the outer casing. The scales were marked such that positive circumferential angles were in the direction of rotor rotation. The zero degree circumferential position was set with the aid of reference scribe marks on the stator blade mounting rings and outer annulus rings such that the probe was positioned circumferentially in the flow midway between two stator stacking axes. The circumferential positions of the actuator were determined by monitoring the voltage from a linear potentiometer. The potentiometer was calibrated to indicate the circumferential position of the actuator through a linear least-squares fit. The circumferential position of each stator blade row was ascertained by recording the circumferential position of the actuator in degrees as determined from the potentiometer voltage and by knowing the circumferential position of each blade row when the circumferential position of the actuator was

at zero. The actuator system could be used to determine the circumferential position of the stator blade rows to within ± 0.05 degrees ($Y/S_S = 0.004$).

A probe actuator (L. C. Smith Company model BBS-3180) was used for probe yaw-angle and immersion positioning. Mechanical digital counters as well as linear potentiometers were used to determine the probe yaw-angle and immersion positions which were calibrated to indicate the extent of their respective motions using a linear least-squares fit. The probe actuator could be used to set the probe yaw-angle and immersion to within ± 0.05 degrees and ± 0.1 mm, respectively. A probe actuator control indicator (L. C. Smith Company model DI-3R) and probe actuator switchbox (L. C. Smith Company model DI-3R-SB4) were used to control the probe actuator.

2.3. Pressure and Temperature Sensing Instrumentation

A scanivalve pressure-port selector actuator system (Scanivalve Company model 48D3-1) including a strain-gauge pressure transducer (Scanivalve Company model PDCR22), a signal conditioner (Endevco model 4470), and an amplified bridge circuit conditioner (Endevco model 4476.2A) were used to obtain all quantitative pressure measurements. A scanivalve actuator control box (Scanivalve Company model CTLR2/S2-S6) was used to control and monitor selection of up to 48 separate pressure ports. Transducer voltage was correlated with pressures from four separate reference columns using a linear least-squares fit. A precision micromanometer (Meriam model 34FB2) was used as a standard for

calibration of all pressure measurements. All pressure probes, static pressure taps, etc., were connected to the pressure-port scanivalve. A cobra probe (United Sensor type CA-120-24-F-18-CD)--capable of measuring flow angle and total pressure--was considered to be most suitable for use in the baseline compressor and was relied on for all slow-response (time-averaged) measurement tests. A Kiel probe (United Sensor type KBC-24-L-22-W) was used as a standard of calibration for all total-pressure measurements. A depth micrometer was used to insure correct radial positioning of the probe in the actuator. The probe yaw-angle was set by placing the probe actuator assembly in a uniform nozzle flow and insuring that the side-port pressures balanced when the actuator yaw-angle counter read zero. Annulus-wall static-pressure taps were provided at all probe axial measurement locations. Static-pressure taps were also located at the inlet and throat of the venturi. Copper-constantan thermocouples were used to measure room air temperature, compressor inlet temperature, and venturi throat temperature. Precision mercury-in-glass thermometers were used to calibrate all thermocouples. A mercury-in-glass barometer (Princo Instruments, Inc. model B-222) was used to measure atmospheric pressure.

2.4. Computer Control System

A desk top computer (Commodore PET model 2001-32) and digital voltmeter (Hewlett Packard model 3455A) were used in conjunction with a multiple channel voltage scanner (Hewlett Packard model 3495A) to provide automatic control of the data acquisition process. A schematic

of the data acquisition system is shown in Figure 2.10. The computer controlled data acquisition system was used to control probe and circumferential motion actuators, to control the scanivalve pressure-port selection actuator, and to allow automatic reading of individual thermocouple voltages and all pressures. The data acquisition system also allowed for on-line calibration of the pressure transducer used for all pressure measurements. A tape cassette and printer were interfaced with the computer to record on tape and paper all pertinent data. The computer was also interfaced with a central disk-storage unit (UNIX) where all pertinent data and computer programs were also stored. Because of limited printing and plotting capabilities of the desk top computer, the Iowa State University Computation Center computing system (National Semiconductor AS6) was utilized for data reduction, tabulation, and plotting.

2.5. Calibration Equipment

An air nozzle, described in detail in Reference [4], provided a uniform nozzle exit velocity suitable for checking probe yaw-angle and total-pressure calibrations. A pressure reference system [8] was used to enable on-line calibration of the scanivalve pressure transducer used for all quantitative pressure measurements. The pressure reference system consisted of four columns of water, balance scales, and glass tubes inserted to an arbitrary depth in each column. The glass tubes were connected with tygon tubing to the scanning valve. The pressures, in volts, from each column were read individually and correlated, using

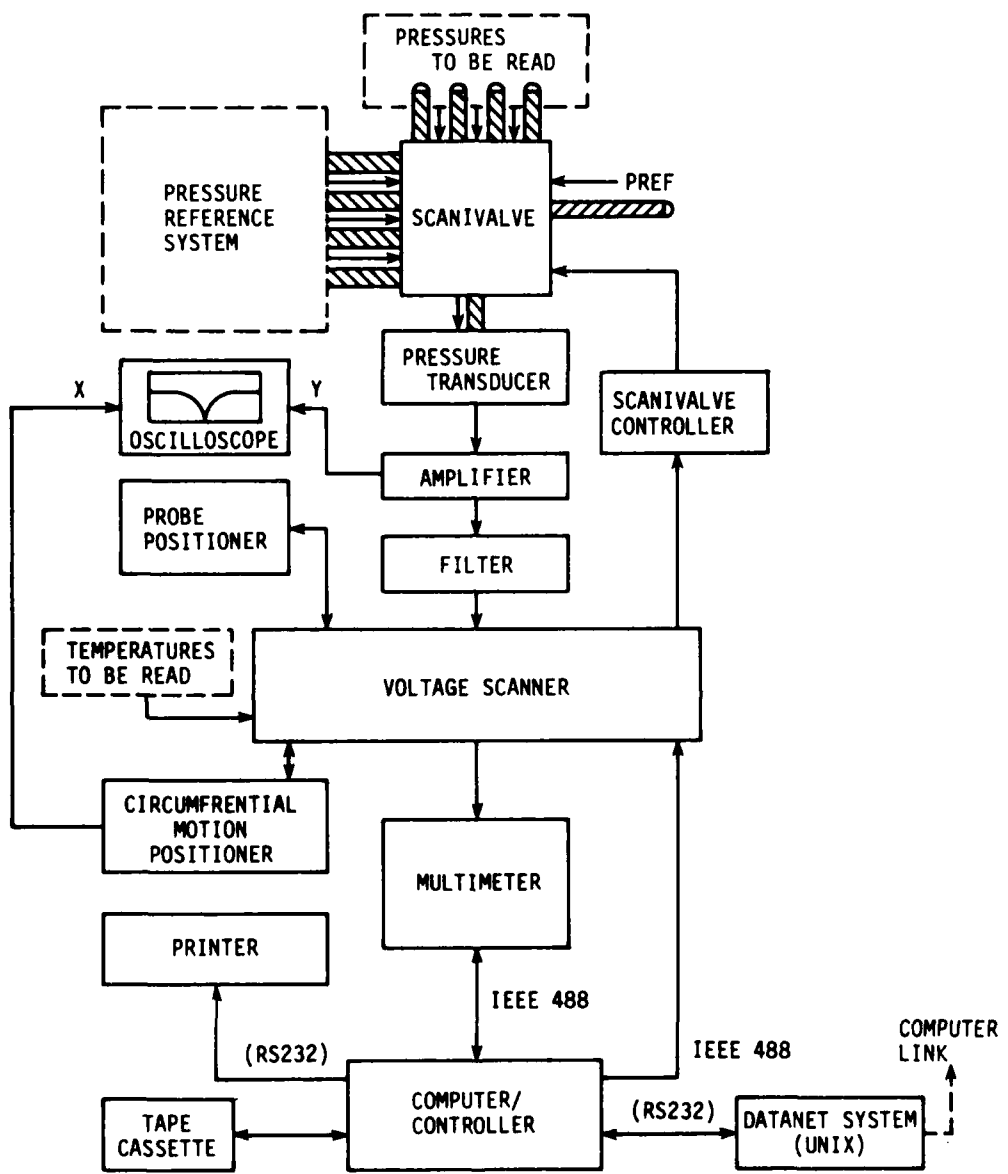


Figure 2.10 Schematic diagram of data acquisition system.

a linear least-squares fit, with the true column pressures. A precision micromanometer was used in conjunction with the balance scales to calibrate, using a linear least-squares fit, the pressure of each column with its corresponding weight. Correlation coefficients of 0.99999 or better could be achieved consistently.

3. EXPERIMENTAL PROCEDURE AND DATA REDUCTION

The objective of the experimental procedure included: 1) generating an accurate overall performance map in order to establish the operating characteristics of the baseline compressor over a large operating range, and 2) obtaining spatially detailed time-averaged measurements of total pressure and flow angle between adjacent blade rows, at one flow rate (design condition), in order to determine pertinent velocity triangle information for comparison with the values associated with the compressor design code.

The time-averaged measurements were obtained at several span locations between blade rows, using appropriate probes, with the compressor operating at the same design point used in the compressor design code; i.e. 2400 rpm, with a flow coefficient of 0.587 as shown in Figure 3.1. The rotor speed was maintained to within ± 1 rpm. The flow coefficient was calculated from equilibrium venturi flow meter data and ambient conditions. Adjustments of the flow to maintain the reference flow coefficient value were made by moving the throttle plate at the exit of the diffuser section. Using this procedure, it was possible to maintain the flow coefficient to within ± 0.0005 of the reference value.

A data acquisition program was written for the PET computer to control the step-by-step procedures of the experimental tests. Data were either entered into the computer by the operator or read by the computer through an interface from the digital voltmeter. The data acquisition program consisted of seven major parts as shown in the

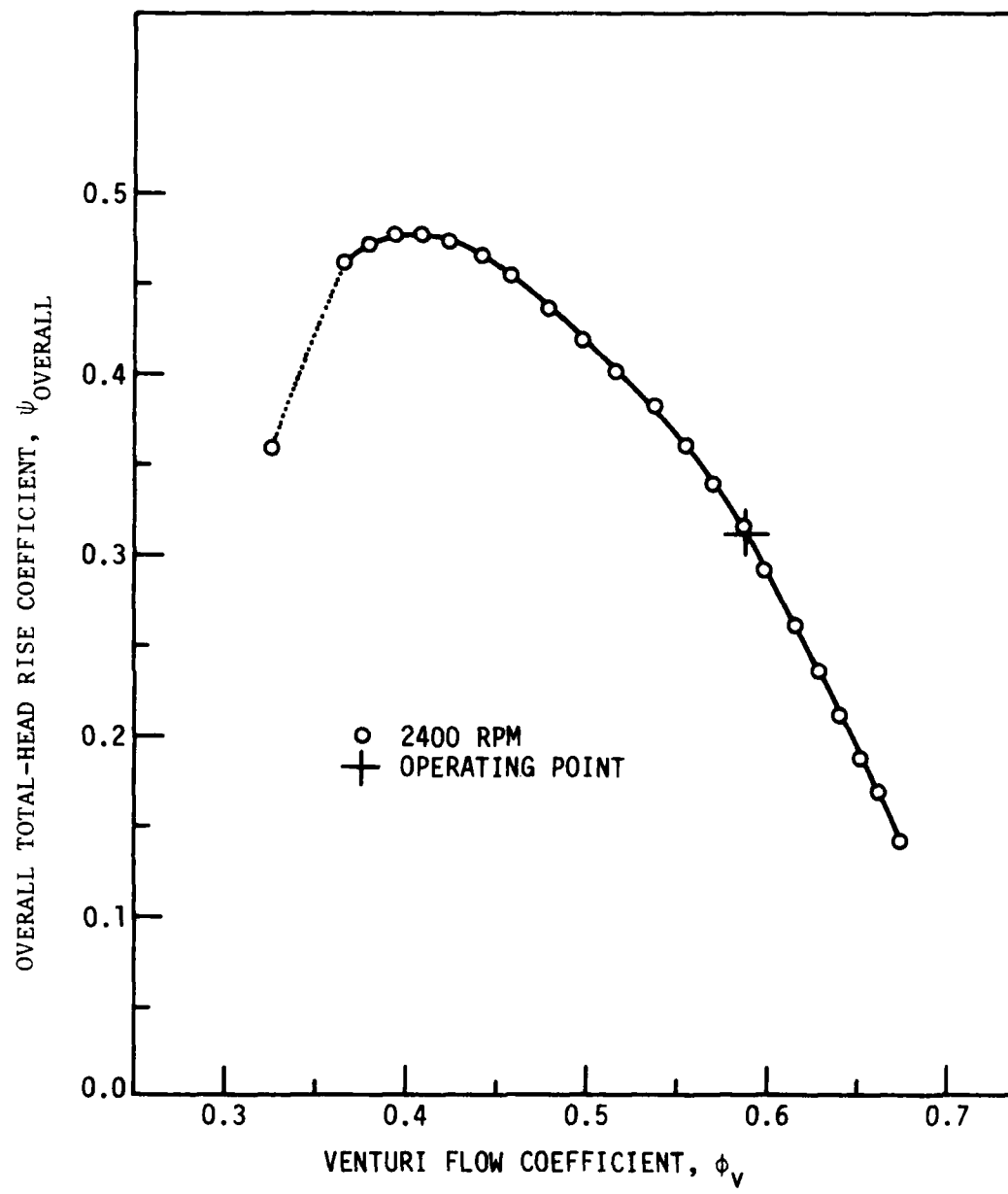


Fig. 3.1 Baseline compressor overall performance curve and operating point.

logic diagram of Figure 3.2. These parts were:

1. Set flow coefficient and measure test conditions.
2. Input probe survey position parameters.
3. Position probe radially and in your plane.
4. Determine circumferential survey parameters with oscilloscope wake trace.
5. Yaw-null cobra probe in free-stream portion of flow.
6. Measure cobra probe pressures and shroud end-wall static pressures.
7. Print out data and store data on magnetic disk.

In addition, data reduction programs were written for the mainframe computer (National Semiconductor AS6) to accept data and preliminary results recorded on disk, and to perform the calculations required to obtain final results. All data and computer programs stored on tape (cassette or reel) are listed in Appendix C.

3.1. Calibration

A micromanometer and a mercury-in-glass thermometer were used respectively as standards for pressure and temperature calibration. Calibrations of all electronic components used in this experimental investigation were performed at the Iowa State University Engineering Research Institute Electronic Shop. Before each test, approximately one hour of running time was allowed for the electronic instrumentation to warm up and for the laboratory and compressor fluid temperatures to reach equilibrium values.

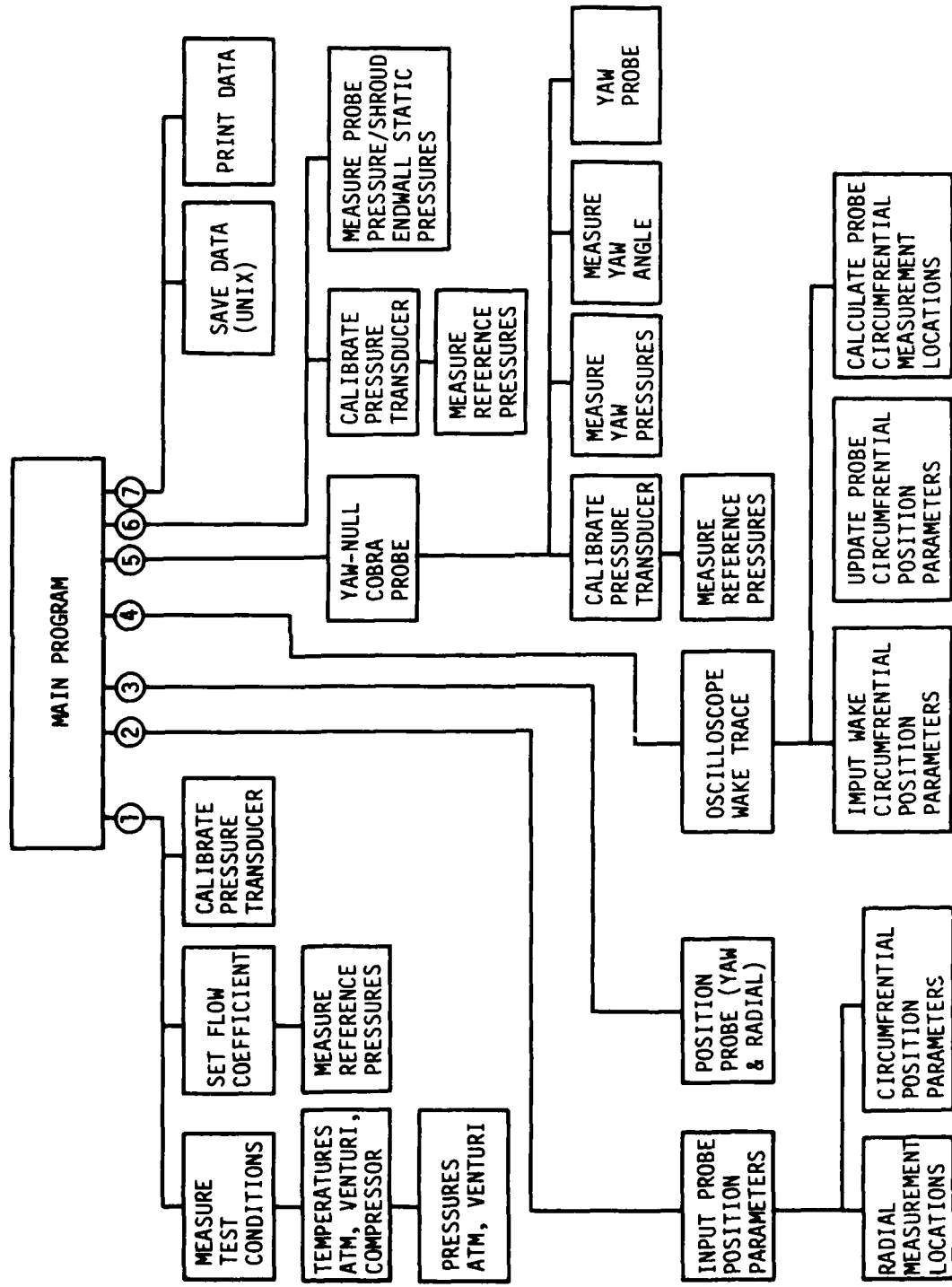


Figure 3.2 Logic diagram of data acquisition system.

All time-averaged measurements of total pressure and flow yaw-angle were obtained using the cobra probe. Extensive total-pressure and yaw-angle measurement calibrations with the cobra probe in a uniform nozzle exit flow have already been documented in Reference [4]. This section will, therefore, deal only with verifying cobra probe measurements in the compressor. Kiel probe data were used to validate the cobra probe measurements. The Kiel probe provides accurate total-pressure information for probe yaw-angles within ± 45.0 degrees of the true flow angle, see Figure 3.3.

3.1.1. Cobra Probe Yaw-Angle Calibration in Free-Stream Portion of Flow

Since total-pressure measurements using the cobra probe are sensitive to flow angle, it is necessary to determine how accurately the probe yaw-angle must be set in order to achieve accurate total-pressure measurements. A comparison of cobra probe and Kiel probe total-pressure measurements from -45.0 degrees to $+45.0$ degrees of probe yaw-angle is shown in Figure 3.3. The test was made behind the first stator, station 3, 50% span, $Y/S_S = 0.0$ (free-stream) operating at the design point flow conditions. The results indicate that the cobra probe will give fairly accurate total-pressure measurements, ± 2.0 Nm/Kg, ($\pm 0.45\%$), if the probe yaw-angle is set within ± 5.0 degrees of the true flow angle.

3.1.2. Cobra Probe Calibration in Wake Portion of Flow

Using the cobra probe to measure total pressures can be very inaccurate if the probe yaw-angle is set too far from the true flow angle (see Figure 3.3). This can be a significant problem in regions of high total-pressure gradients, such as in stator wakes, where the cobra probe cannot be used to accurately determine the true flow angle.

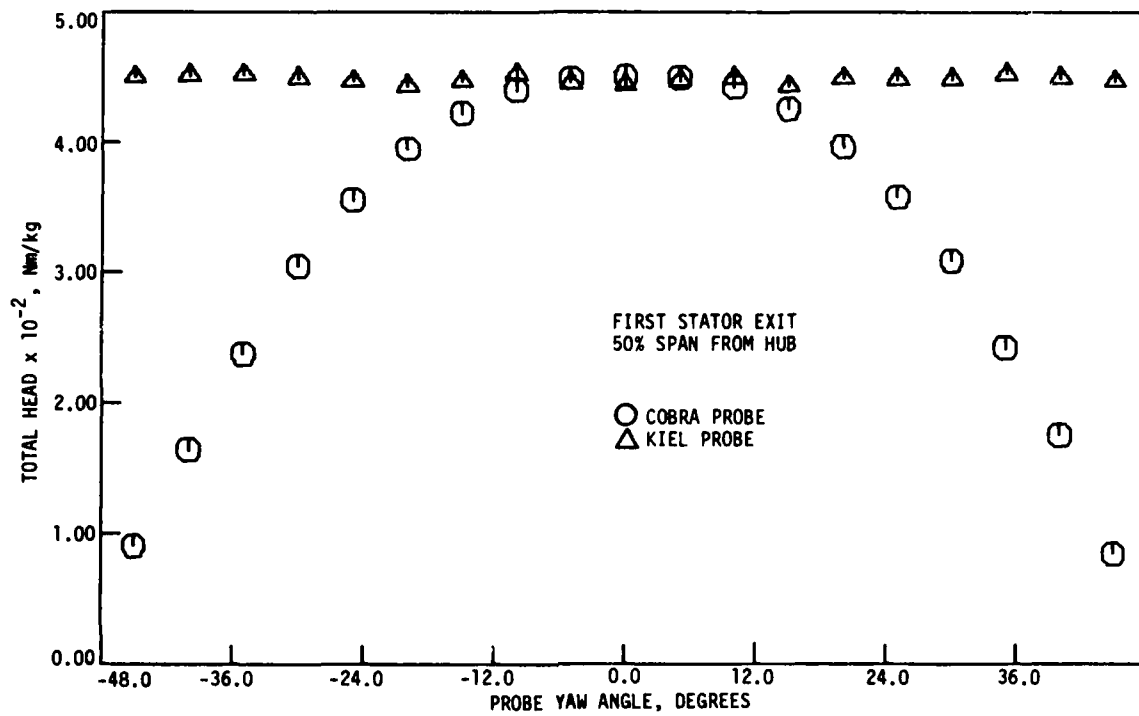


Figure 3.3 Cobra probe yaw-angle total-head calibration curve in free stream portion of flow for flow coefficient = 0.587 at 2400 rpm.

In order to circumvent this problem, the cobra probe yaw-angle in the wake region is set to the integrated-average free-stream flow angle measured by the cobra probe. A comparison of the cobra probe and Kiel probe measurements--with the Kiel probe set at the integrated-average free-stream flow angle--is shown in Figure 3.4. This comparison test was made behind the second stator, station 5, 50% span, operating at the design point flow conditions. The results show very good agreement in the free-stream regions, ± 5.0 Nm/Kg ($\pm 0.6\%$). The wake region data also show good agreement in total-pressure levels, but some slight shifting of the wake position is evident.

3.1.3. Spanwise Calibration of the Cobra Probe

A spanwise comparison of cobra probe and Kiel probe total-head measurements are shown in Figure 3.5 for flows behind the first rotor and first stator. The results show fairly good agreement between the cobra probe and Kiel probe measurements, less than 10.0 Nm/Kg (1.7%) difference, except near the end-walls where the difference was as much as 17 Nm/Kg (4.5%). The larger error near the end-walls was suspected to be due to wall effects. Total-head measurements behind the first rotor were generally better than behind the first stator.

3.1.4. Scanivalve Pressure Transducer Calibration

On line pressure-transducer calibration was accomplished using a pressure reference system consisting of water columns and triple-beam balances. The pressure reference system is described in detail in Reference [8]. The system provides four reference pressures against which the pressure transducer can be calibrated. The pressure transducer is calibrated every time the flow coefficient is to be readjusted

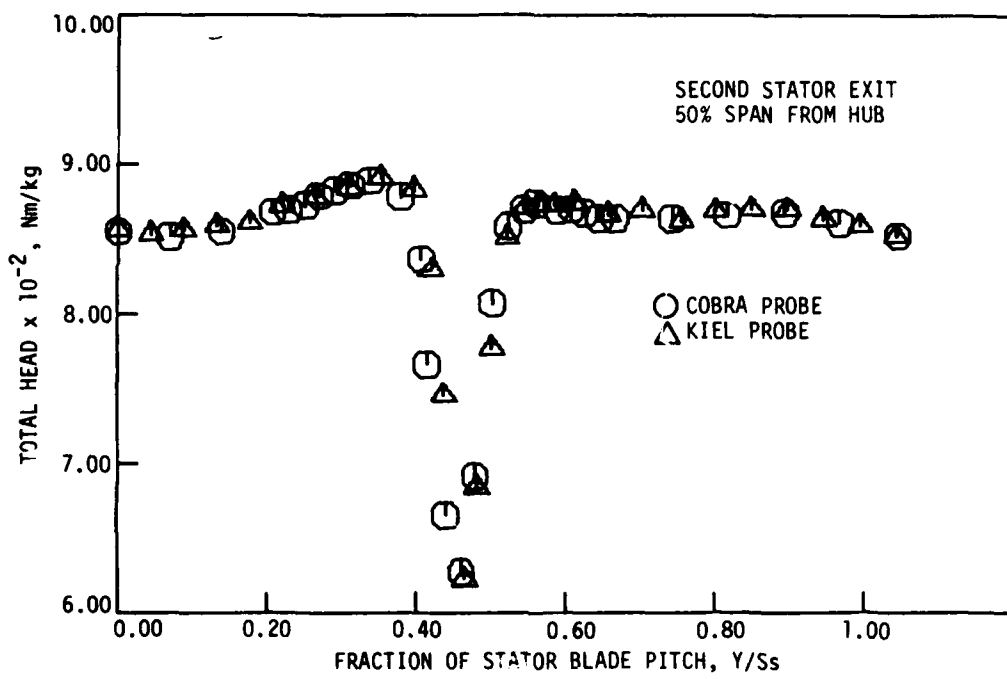


Figure 3.4 Cobra probe total-head calibration curve in wake portion of flow for flow coefficient = 0.587 at 2400 rpm.

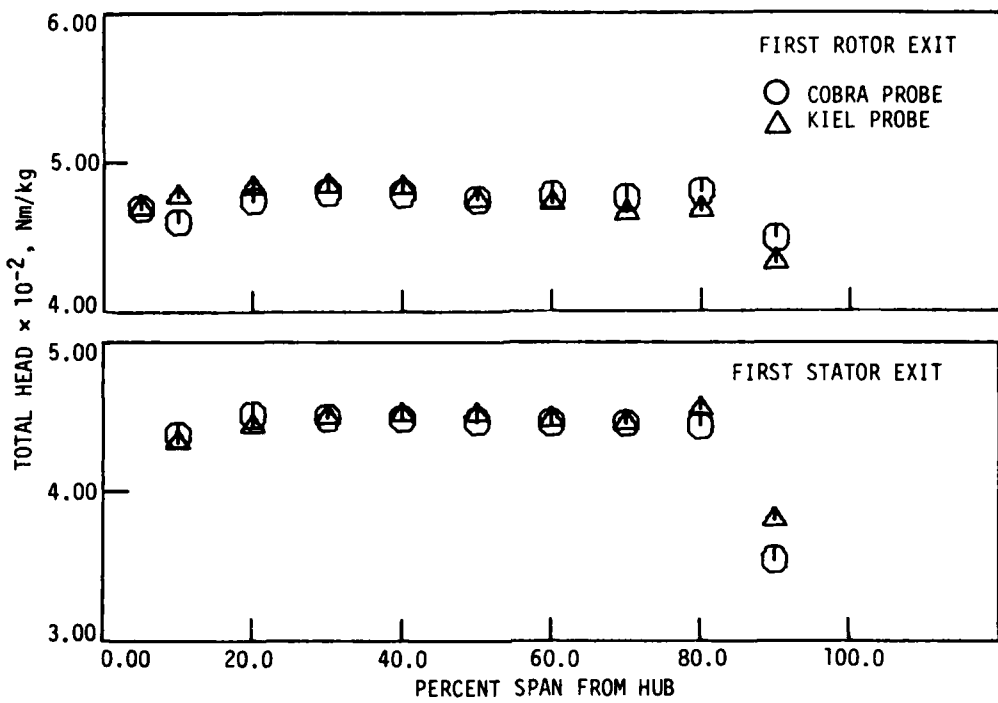


Figure 3.5 Cobra and Kiel probe comparison behind first rotor and first stator for flow coefficient = 0.587 at 2400 rpm ($Y/S_S = 0.0$).

prior to taking any total-pressure measurement. Periodic on-line recalibration of the pressure transducer helps reduce thermal drift and other transient errors inherent in strain-gauge transducers of this type. Tests have shown that the reference pressures can be determined with resolution better than 0.003 inches (0.076 mm) of water. All pressure reference columns are calibrated using the precision micromanometer. Calibration of the pressure reference system is performed once every three months or more often as needed.

An additional water column is used to provide a back pressure to the scanivalve transducer in order to insure that the pressure transducer is always displaced from zero. This eliminates errors from having the transducer pressure fluctuate around zero. On-line calibration of the pressure transducer consists of a linear least-squares correlation of transducer output voltage versus the known reference column pressures. The reference column pressures are determined from linear least-squares correlation equations entered into the computer which have been previously determined from a calibration of column pressure versus column weight. Therefore, it is only necessary to weigh each column prior to testing in order to determine the reference column pressures. During on-line calibration, each column pressure and transducer voltage recorded is referenced to one of the columns, the same column each time. Again, this is done in order to reduce errors due to thermal drift as well as other transient errors between successive readings. In addition, it helps insure that the linear correlation goes through zero, as it should. As mentioned earlier, this procedure consistently provided a linear correlation coefficient

of transducer voltage versus column pressure of 0.99999 or better. The calibration is repeated if this correlation criterion is not met.

3.2. Data Aquisition

The data acquisition procedure consisted of obtaining two types of information: overall performance data, and spatially detailed time-averaged measurements of total pressure and flow angle between adjacent blade rows. The details of obtaining both types of measurements are described below.

3.2.1. Overall Performance Map

The overall performance map parameters are based on compressor drive motor torque meter measurements (to establish the compressor ideal head rise), static-head measurements at the compressor exit (to estimate the actual head rise), and venturi flow rate measurements (to determine the compressor flow coefficient). The above procedure was used to quickly and accurately establish a performance map for the baseline compressor. The method for establishing the compressor exit total head relies on the stator exit swirl being zero and, therefore, the static head at that station being a constant across the span. The venturi-measured flow rate was used to determine the average axial velocity at the compressor exit which, since the swirl is zero, is also the fluid velocity. Using the measured circumferentially-averaged static head and the computed average fluid velocity at the compressor exit, the compressor exit total head was determined. The actual head rise delivered to the working fluid could then be determined by

referencing the compressor exit total head to the total head at the compressor inlet (atmospheric conditions, zero velocity).

The measurements involved in establishing the performance map were obtained as follows. With the compressor operating at 2400 rpm, the diffuser exit throttle plate was adjusted to provide incremental control of the compressor flow rate. At each flow rate, venturi flow meter measurements, torque meter measurements, and compressor exit static-head measurements were recorded along with other pertinent data related to the operating and ambient conditions. The torque meter measurements were obtained with the compressor drive motor floating on air bearings while various weights were added to the torque arm in order to balance the drive motor torque. A calibrated meter employing an incremental load transducer consisting of a solid-state gauge bridge on a cantilevered beam was used to resolve torque arm loads to within ± 0.0125 Kg. The meter was calibrated to read from 0.0 Kg to 1.0 Kg full scale. Meter fluctuations due to motor vibrations and minute torque fluctuations reduced torque measurement accuracy to within ± 0.25 Kg. Static-head measurements at the compressor exit were obtained from four equally spaced (circumferentially) outer annulus-wall static pressure taps. The measurements were made while decreasing the flow rate from maximum flow rate until stall occurred and then repeating the measurements from stall to the maximum flow rate. The stall limit was accurately established by adjusting the flow rate until a slight disturbance at the diffuser exit would instigate a full span stall, which was audibly detectable. Once the stall flow rate was determined, measurements were made just before and after stall.

3.2.2. Time-Averaged Measurements

Time-averaged total pressure and flow angle data variation in the radial, axial, and circumferential directions of the compressor flow field were obtained with the cobra probe set at five passage height locations of 10%, 30%, 50%, 70%, and 90% of span from the hub--ahead of and behind each of the rotating and stationary blade rows--at several circumferential positions over one stator pitch. In addition, outer annulus-wall four-hole-averaged static-pressure measurements were made at each axial measurement location. The steps followed to obtain these data are described below.

Prior to testing, several preliminary setups were accomplished. The cobra probe was mounted in the probe actuator and the probe yaw-angle zero was set by balancing the side-tube pressures with the probe immersed in the calibration nozzle jet. The probe radial positioning was set using a depth micrometer. The probe actuator mechanical counters were set to read zero yaw-angle for compressor axial flow and 5.6 inches (14.22 cm) for contact with the hub surface. Thus, the counters would indicate true probe angular and radial positions. All calibrations were performed through the data acquisition system with the PET computer controlling the calibration procedures. Before each test, the scanivalve pressure reference system columns were refilled with water to predetermined levels and each column was reweighed. The reference column ice bath was checked and reiced if necessary.

The following miscellaneous data were recorded by the computer for each test to insure the attainment of intended measurement conditions.

1. Probe axial measurement station number, (see Figure 2.5)
2. Compressor rpm
3. Static pressure difference across venturi throat, N/m^2
4. Barometer ambient temperature, degrees Kelvin
5. Barometric pressure, N/m^2
6. Temperature at compressor inlet, degrees Kelvin
7. Static pressure at venturi throat, N/m^2
8. Temperature at venturi throat, degrees Kelvin
9. Date
10. Time

The circumferential surveys were made by moving the stators circumferentially past a stationary probe located at one of the probe axial measurement stations at the proper depth of immersion. Figure 3.6 shows, to scale, the axial position and extent of each circumferential measurement window as well as the circumferential survey coordinate direction. A qualitative trace of total pressure versus circumferential position with the probe set at the approximate average flow angle was recorded on an X-Y storage oscilloscope screen from the electrical signals of the strain-gauge pressure transducer and the circumferential motion potentiometer. The trace was used in selecting the spacing of circumferential measurement points and in determining the extent and position of the wake and free-stream regions. For each survey, measurements were made over one stator blade pitch. The circumferential measurement positions in the wake and free-stream regions were determined by the computer, based on the number of free-stream circumferential measurement positions desired and the circumferential measure-

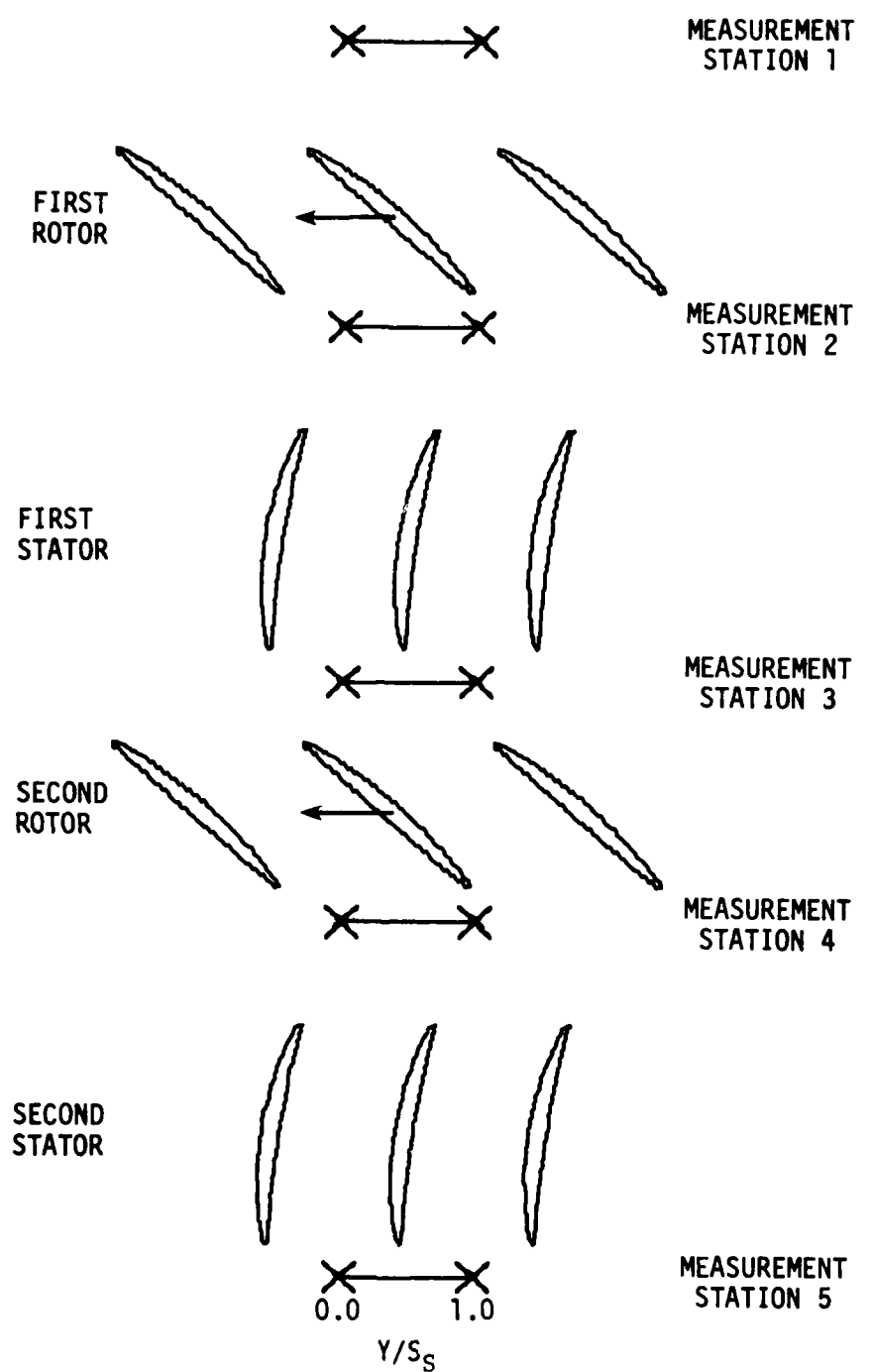


Figure 3.6. Blade cascade showing circumferential measurement window.

ment increment desired in the wake region. Flow angle measurements were made by balancing the cobra probe side-tube pressures through a computer controlled algorithm or by manual over-ride with the aid of a U-tube manometer. Flow angle measurements were made at every flow field measurement point behind a rotor blade row and at free-stream measurement positions only behind stator blade rows. The circumferentially-integrated-average free-stream flow angle was then determined with the computer acquisition program and this flow angle was used when making total-pressure measurements in the corresponding stator wake regions of each circumferential survey. The probe yaw-angle, circumferential position, and total pressure were recorded at each circumferential measurement point. After the last measurement at each circumferential survey was taken, the miscellaneous data, flow-field data, and measured circumferentially-averaged static head were printed out and stored on magnetic disk for reduction at a later time.

3.3. Data Reduction

Preliminary reduction of the time-averaged data was performed during data acquisition and consisted of determining primary flow-field values of total head, static head, and absolute flow angle. These primary values were then read into the data reduction program where other flow-field parameters such as absolute velocity, relative velocity, incidence angle, deviation angle, etc., were calculated along with their circumferentially-averaged values. Finally, overall rotor,

stator, and stage performance parameters such as ideal head-rise (Euler turbine equation based values), actual head-rise, efficiencies, and losses were determined. The flow was assumed incompressible for all calculations as the velocities involved Mach number levels less than 0.2. Integrated values were computed using a spline-fit integration [9]. A complete list of all quantities and equations used in reducing the data is presented in Appendix D.

3.3.1. Flow-Field Parameters

The total head was determined at each flow field measurement point from the cobra probe measured total pressure. Circumferentially-averaged values of total head and absolute flow angle were determined for each radial position at every axial measurement station. All circumferential averages except for flow angle averages behind stator blade rows were determined by integrating over one stator blade pitch. The circumferentially-averaged absolute flow angles behind stator blade rows were obtained by integrating over the free-stream portion only. The static head was assumed to be circumferentially constant, and the radial distribution of static head was determined at each radial position for every axial measurement station by solving the radial equilibrium equation in the following form:

$$\frac{dh}{dr} = \frac{2 \sin^2 \bar{\beta}_y (\bar{H}-\bar{h})}{r}, \text{ (see Reference [4])} \quad 3.1$$

using the Runge-Kutta numerical technique [10]. The circumferential-averaged outer annulus-wall static head was used as an initial value, and the solution was obtained by marching radially toward the hub at

increments of 5% of passage height. The circumferentially-averaged values of total head and absolute flow angle required at each step of the Runge-Kutta solution were obtained by a second-order Lagrange interpolation of their measured radial distributions.

From the radial distributions of total head, absolute flow angle, and static head; the circumferentially-averaged absolute velocity was determined at each radial position for every axial measurement station. With the circumferentially-averaged absolute velocity and the flow angle determined, the following circumferentially-averaged variables were calculated at each radial position for every axial measurement station.

1. Axial velocity, m/s, Eq. 12.16
2. Absolute tangential velocity, m/s, Eq. 12.18
3. Relative tangential velocity, m/s, Eq. 12.20
4. Relative velocity, m/s, Eq. 12.22
5. Relative flow angle, degrees, Eq. 12.24
6. Blade incidence angle, degrees, Eq. 12.25 and Eq. 12.27
7. Blade deviation angle, degrees, Eq. 12.26 and Eq. 12.28
8. Flow coefficient, Eq. 12.29

In addition, for each axial measurement station, an annulus cross-section integrated flow coefficient was calculated for comparison with the flow coefficient determined from venturi flow meter data. In determining the annulus cross-section flow rate and corresponding flow coefficient, the axial velocities at the hub and shroud end-wall surfaces were assumed equal to zero.

3.3.2. Performance Parameters

The actual and ideal (Euler turbine equation based) head-rise coefficients and their ratio (hydraulic efficiency) were determined at each of the five radial positions for both rotor rows, stages, and for the overall compressor. Total-head loss coefficients were also determined for each rotor and stator blade row. In addition, radially mass-averaged values of each of the above quantities were determined for both rotor rows, stages, and for the overall compressor (see Appendix E). The above parameters were calculated from spatially detailed time-averaged measurements and circumferentially-averaged values of the previous section.

Performance map parameters and mechanical efficiency were calculated from motor torque-meter measurements and the overall head-rise across the compressor. The overall head-rise for the performance map was determined from the measured venturi flow rate and the circumferentially-averaged static head at the outer annulus-wall of the last axial measurement station.

4. PRESENTATION AND DISCUSSION OF DATA

The results of the torque meter related performance measurements and the slow-response (time-averaged) data are presented and discussed in this section. Comparisons between these measured results and corresponding calculated values associated with the design code are also presented and discussed. The design code results are tabulated in Appendix B. The experimentally determined data are tabulated in Appendix E. In graphing the results, all data variation curves--except for the performance curves--were drawn with interpolated curves through the actual data points. Smooth curves were drawn through the performance map data using a least-squares fit. All measured data points are graphed with a symbol marking the actual data point. The design code results are represented with continuous curves.

4.1. Error Analysis

Measurement errors associated with the primary measurement quantities and flow-field parameters are presented in Table 4.1. Representative values of each primary measurement quantity and flow-field parameter are presented, along with their estimated uncertainty and percentage of error. The uncertainties of the flow-field parameters were determined using the procedures of Kline and McClintock [11] based on the estimated uncertainties associated with the primary measurement quantities. The estimates of the uncertainties of the primary measurement quantities were based on the repeatability of the measurements and comparisons with the Kiel probe in the case of total pressure

Table 4.1. Uncertainty estimates of measurement parameters.

Flow Parameters	Symbol	Typical Values	Estimated Uncertainty (20-to-1 odds)
<u>Primary measurements</u>			
Temperature	t	299 deg. K	0.25 deg. K (0.08%)
Transducer pressure	P_t	52.0 mm Hg	1.2 mm Hg (2.2%)
Absolute flow angle	B_y	20.0 deg.	1.0 deg. (5.0%)
Barometric pressure	P_{atm}	735 mm Hg	0.03 mm Hg (0.003%)
Torque	T	4.0 Kg	0.03 Kg (0.6%)
<u>Flow field parameters</u>			
Absolute velocity	v	30.0 m/s	0.3 m/s (1.1%)
Axial velocity	v_z	28.0 m/s	0.4 m/s (1.3%)
Absolute tangential velocity	v_y	10.3 m/s	0.5 m/s (4.9%)
Relative flow angle	B'_y	50.0 deg.	0.6 deg. (1.1%)
<u>Performance parameters</u>			
Actual head-rise coefficient	ψ	0.17	0.004 (2.3%)
Ideal head-rise coefficient	ψ_i	0.19	0.02 (8.7%)
Hydraulic efficiency	η	0.88	0.07 (8.0%)
Rotor total-head loss coefficient	w_R	0.05	0.03 (60.0%)
Stator total-head loss coefficient	w_S	0.06	0.02 (33.0%)
Ideal work coefficient	$\psi_{i,pm}$	0.4	0.005 (1.3%)
Mechanical efficiency	η_{me}	0.75	0.01 (1.8%)

measurements. The uncertainty levels given in Table 4.1 are generally consistent with the random scatter observed in the results. It should be noted that the uncertainty levels tend to be higher near the end-walls (see Figure 3.5).

Of the primary measurement quantities, absolute flow angle measurements have the most uncertainty, primarily because of the total-pressure gradients affecting the cobra probe yaw-angle measurements. Behind the stator blade rows, ascertaining the circumferential extent of the free-stream--particularly near the end-walls--was difficult. Comparisons of total-head measurements obtained using a cobra probe and Kiel probe were presented in section 3.1. These comparisons show that even with the uncertainties of determining the absolute flow angle, the cobra probe gives a fairly accurate measure of the total head. Performance parameters based on the Euler turbine equation ideal head-rise, however, are highly dependent on the accuracy of the absolute flow angle measurements (see Table 4.1). It would be reasonable to conclude, therefore, that very little confidence can be afforded the Euler turbine equation based performance parameters. The effect of torque measurement accuracy on the torque based performance parameters is also given in Table 4.1. The torque based efficiencies are more reliable than the Euler turbine equation based efficiencies, but only as an indicator of relative measure. The torque based efficiencies were very repeatable, but were highly dependent on the mechanical characteristics of the compressor and drive motor which affected the absolute measure of the efficiencies. Since the torque meter based efficiencies were affected by bearing friction and other mechanical

losses, they are not reliable as an absolute measure of efficiency. However, with precautions they are a reasonable indicator of relative measure of efficiency.

All time-averaged measurements were obtained with the throttle plate adjusted so that the venturi flow coefficient was within ± 0.0005 of the desired flow coefficient of 0.587. An integrated average flow coefficient based on the spanwise distribution of circumferential-mean axial velocity--as determined from cobra probe measurements--served as a check between venturi based and cobra probe based flow coefficients. Comparisons of the integrated flow coefficients and venturi flow coefficient for each axial measurement station are given in Table 4.2. The integrated flow coefficient was obtained by two different approaches; 1) using the extrapolated circumferential-mean axial velocity at the end-walls, and 2) by considering the circumferential-mean axial velocity to be zero at the end-walls. A spline-fit integration routine [9] was used to perform the integration. Even with only five spanwise measurement locations, the integrated-average flow coefficients--based on zero axial velocity at the end-walls--compared very favorably with the venturi based flow coefficients. The integrated flow coefficients--based on extrapolated circumferential-mean axial velocity at the end-walls--were consistently higher than the venturi based flow coefficients.

Table 4.2. Flow coefficient comparison between venturi and integrated measurement station flow coefficients.

V_z extrapolated to endwall		$V_z = 0.0$ at endwall	
Station	Flow Coefficient Comparison Percent	Station	Flow Coefficient Comparison Percent
1	6.0	1	1.0
2	4.4	2	-0.2
3	2.5	3	-1.9
4	3.4	4	-1.0
5	0.8	5	-2.9

4.2. Overall Performance Map

The results of the torque meter related performance tests are presented in Figure 4.1. Overall compressor head-rise coefficient, work coefficient, and efficiency variations with flow coefficient are plotted. The curves were obtained by recording venturi flow rate, compressor exit (station 5) shroud static pressure, and drive motor torque. The venturi flow rate was used to determine the average axial velocity at the exit of the compressor. Since swirl was virtually non-existent at the compressor exit, the static pressure was presumed constant across the span; thus making it possible to determine representative total pressures and subsequent head-rise coefficient at the compressor exit. The torque meter measurements were used to determine

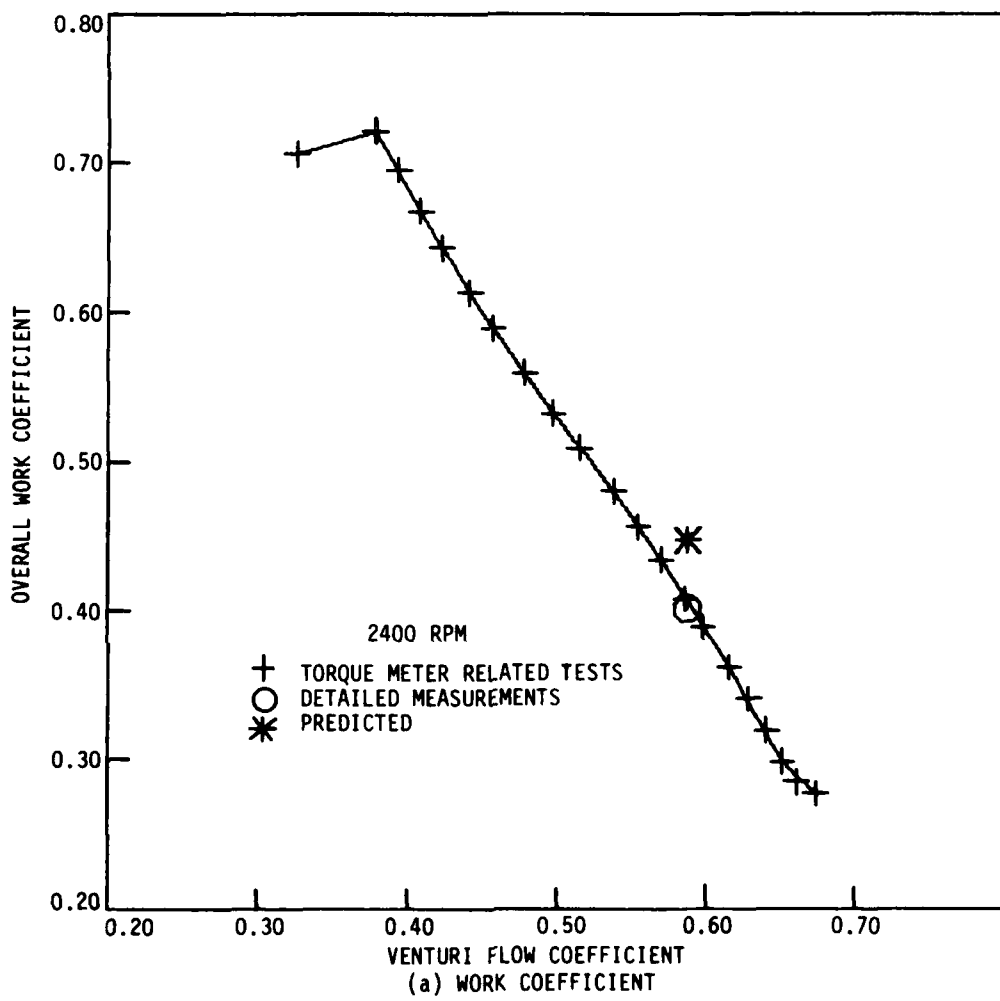


Figure 4.1 Predicted and measured overall performance data.

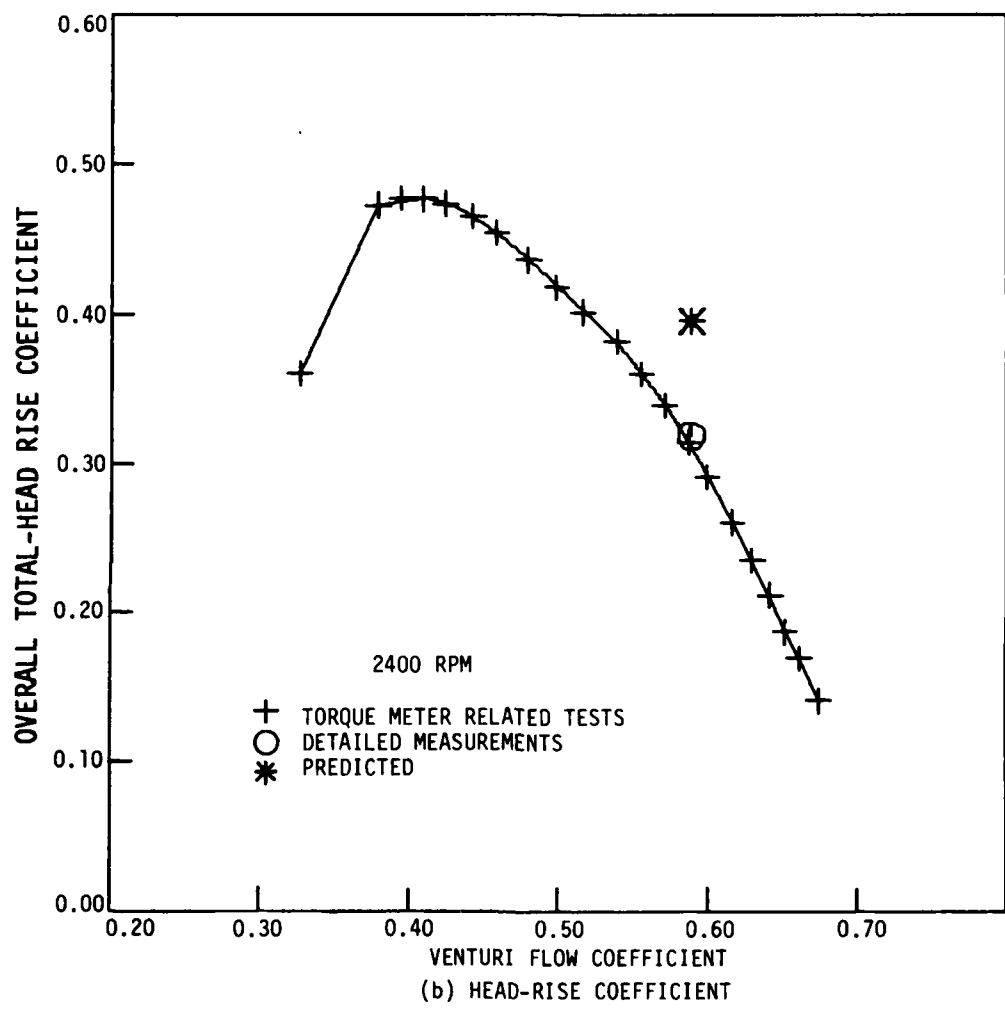


Figure 4.1 continued.

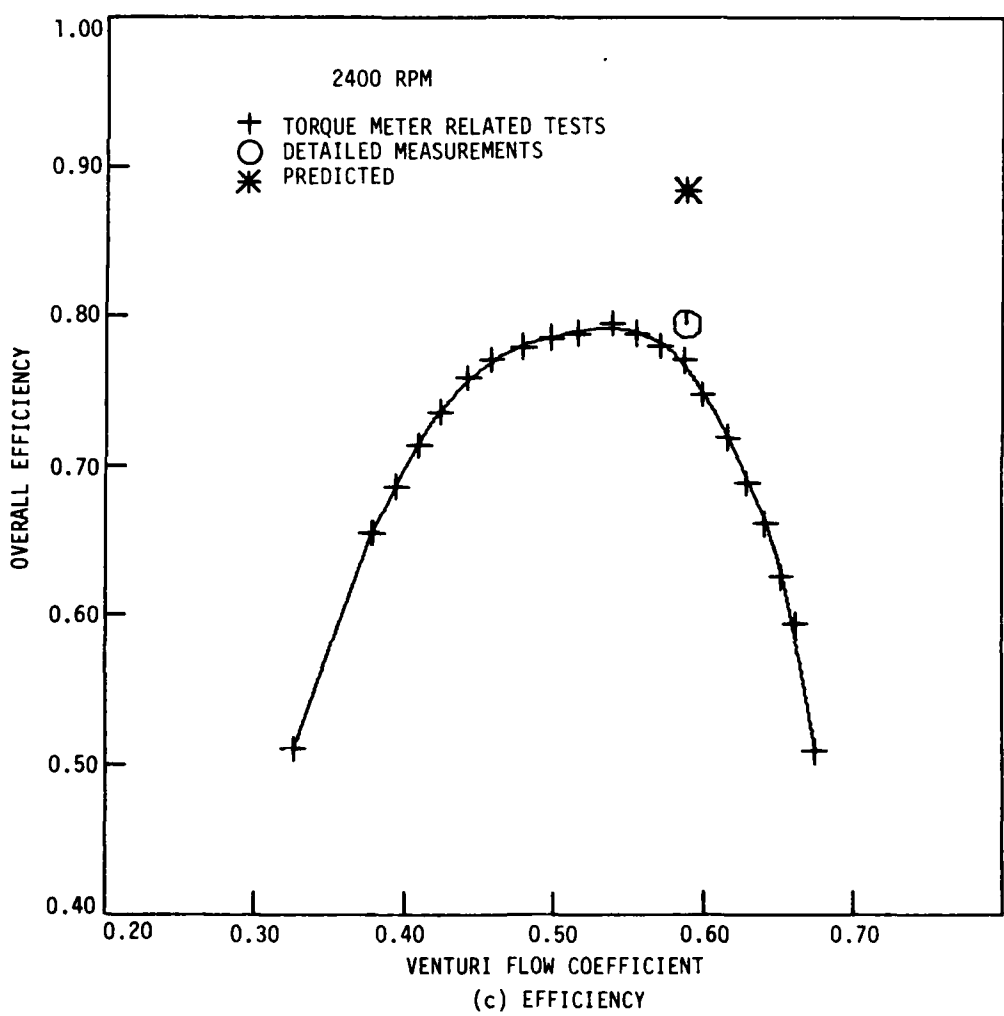


Figure 4.1 concluded.

the work coefficient from Equation 13.50. Also noted in Figure 4.1 are the design point overall head-rise coefficient and hydraulic efficiency as determined from the detailed time-averaged measurements and Euler turbine equation based ideal head-rise, as well as the design point overall hydraulic efficiency and head-rise coefficient predicted from the design code. Both measured efficiencies corresponding to the design point flow coefficient are significantly lower than the predicted efficiency. The reason for this discrepancy will be explored further in a later section (4.4. Comparisons of Circumferential-Mean Data with Design Code Predictions).

As mentioned in the previous section, the Euler turbine equation-based performance parameters are highly dependent on the accuracy of the absolute flow angle measurements and are, therefore, unreliable measures of compressor performance. Although the relative characteristics of the performance curves depicting work coefficient and efficiency variations with flow coefficient proved to very repeatable, the absolute values of each curve were sensitive to the mechanical characteristics of the compressor, such as bearing friction. These mechanical effects appeared as shifts in the absolute magnitudes of the torque measurements which tended to move the level of the work coefficient and efficiency curves, but did not significantly affect the relative aspects of each curve. The head-rise coefficient curve was consistently repeatable and compared favorably with the design point overall head-rise coefficient determined from the detailed time-averaged measurements, thus lending credence to the procedure used in determining the head rise versus flow coefficient performance curve.

Because of the effects of bearing friction on torque measurements, the performance curves could not be used for absolute predictions of the compressor performance. Thus, no means were available for comparing the design program efficiency predictions.

To obtain an accurate performance map which could be used for absolute as well as relative measures of efficiency, the compressor should be run without blading to measure the tare torque; thus obtaining corrections for bearing friction and other mechanical effects. Without regreasing the bearings and with the blades reinstalled, a new performance map could be generated from which the tare torque is subtracted. This procedure was not attempted because of insufficient time.

The curve of compressor efficiency variations with flow coefficient shows an uncharacteristic flat portion where the efficiency is essentially constant over a range of flow coefficient values. The flat portion of the efficiency curve may be due to the fact that blade losses were constant over a range of incidence angles. However, there may also be some over-riding effect that is causing slight improvements in efficiency to be "washed out." For example, Wisler [2] shows a considerable Reynolds number effect on compressor efficiency for a low-speed four-stage axial-flow compressor. Wisler's results show a flattening of the efficiency curves as the Reynolds number is decreased. The Reynolds number range examined by Wisler was 1.0×10^5 to 4.0×10^5 . The Reynolds number for the baseline compressor is about 1.8×10^5 . Further discussion of the constancy of compressor efficiency over a range of flow rates may be found in Reference 12.

4.3. Spatially Detailed Time-Averaged Measurement Results

Detailed time-averaged aerodynamic data were obtained in the baseline compressor at numerous circumferential positions for 10%, 30%, 50%, 70%, and 90% span locations--measured from the hub, ahead of and behind each blade row. The axial measurement locations and circumferential survey windows relative to each blade row are shown in Figure 3.6 for one spanwise location. Figure 3.6 should be referred to when analyzing the figures in this section. All total-head measurements presented in this report are referenced to atmospheric conditions. Graphs of the blade-to-blade distribution of total head for all spanwise locations at each axial measurement station are illustrated. Figure 4.2 is for flows behind the first- and second-stage rotors, and Figure 4.3 is for flows behind the first- and second-stage stators. The data for flow behind the second rotor (Figure 4.2) indicate a peculiar pattern involving two regions of lower total head. This unexpected trend is explained in Reference 12. The detailed time-averaged measurement data were used to obtain circumferential-mean values of total head, flow angle, and absolute velocity. The spanwise distributions of these circumferential-mean quantities are shown in Figure 4.4, for flows behind the first- and second-stage rotors, and in Figure 4.5, for flows behind the first- and second-stage stators. The graphs of the spanwise distributions of circumferential-mean total head and axial velocity behind each blade row (Figure 4.4 and 4.5) show significantly lower total head and axial velocities at the 90% from hub measurement location indicating higher losses near the shroud end-wall there. Evidence

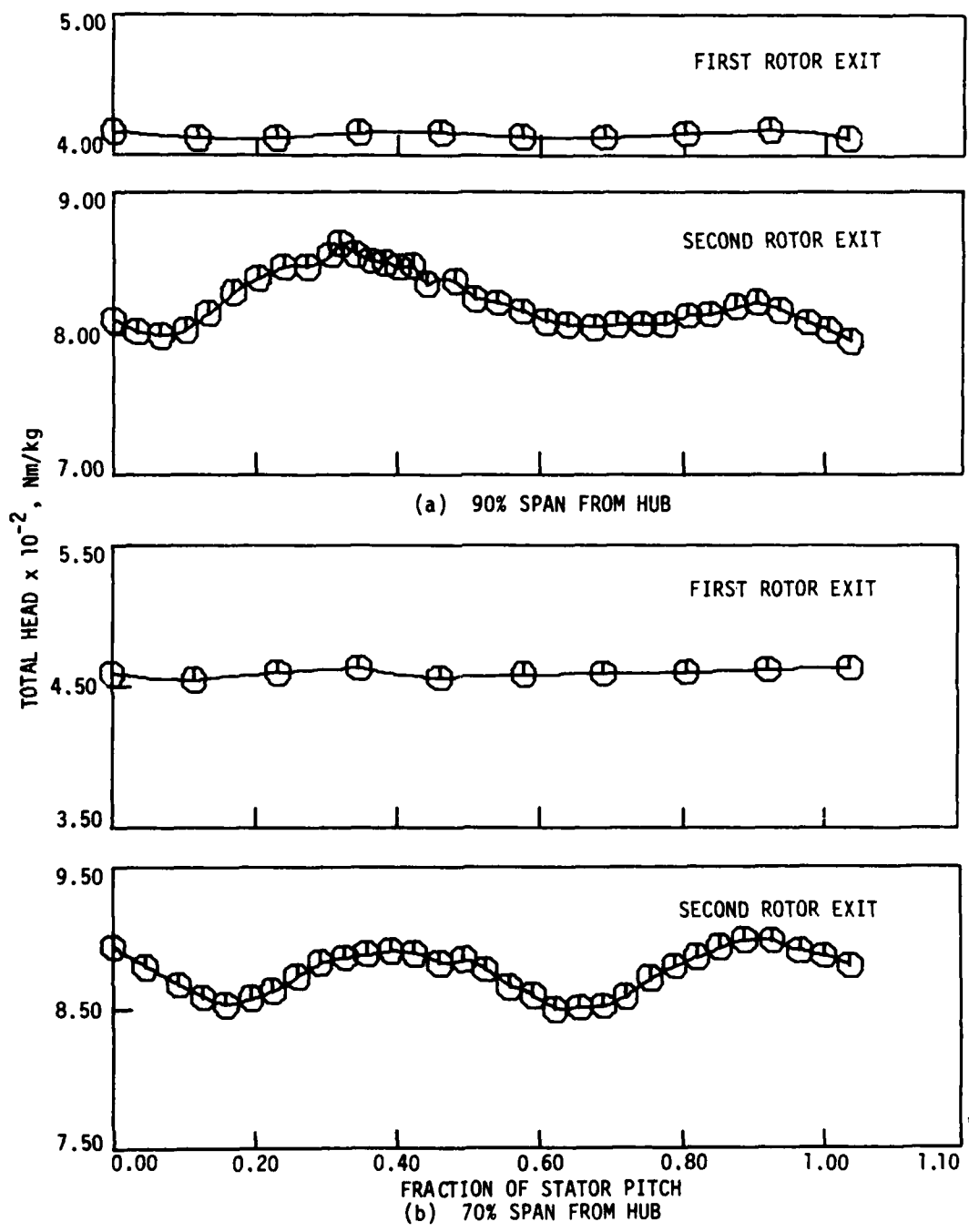


Figure 4.2 Blade-to-blade distribution of time-average total head for flow behind the first and second stage rotors ($\phi = 0.587$ at 2400 rpm).

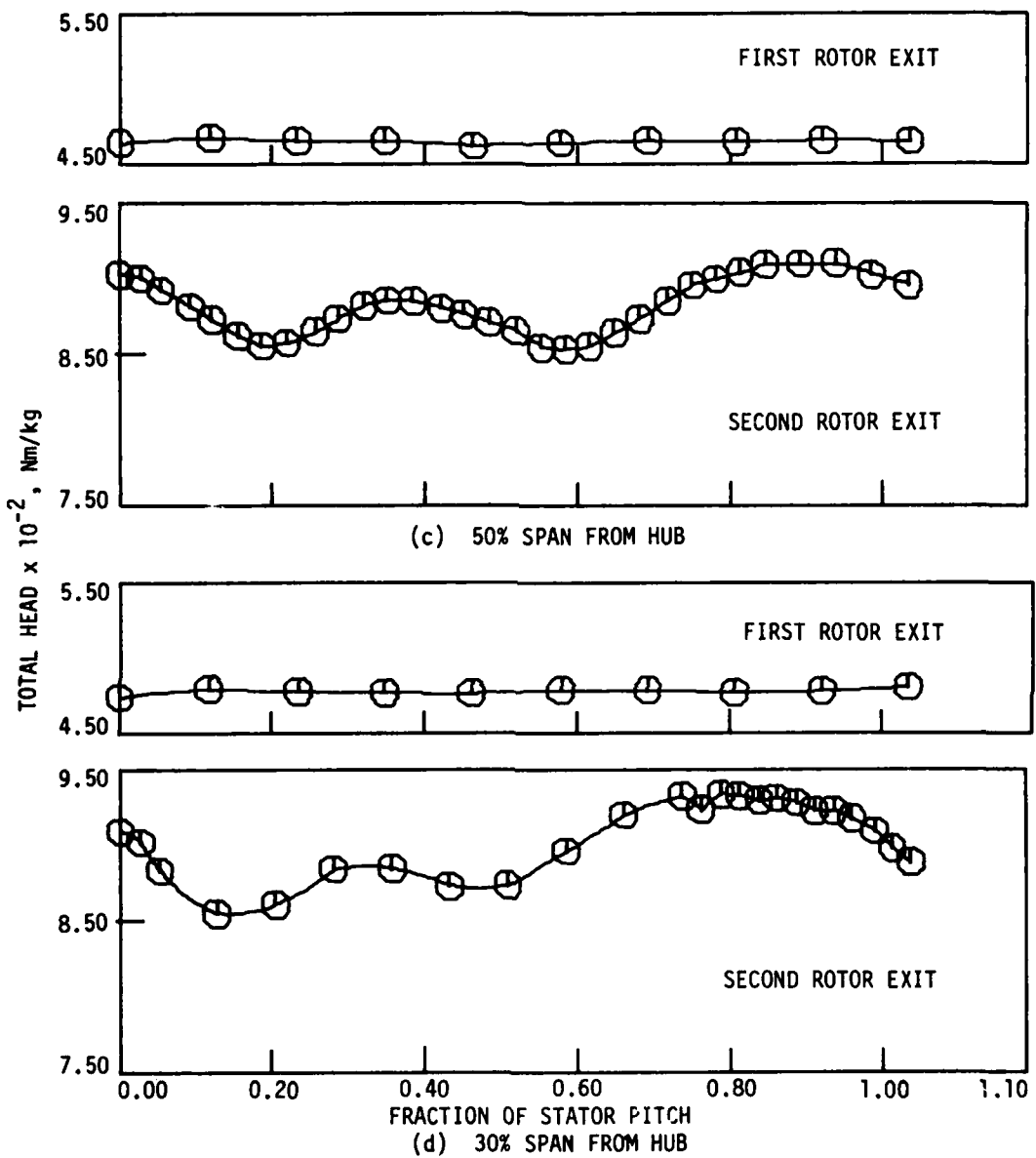


Figure 4.2 continued.

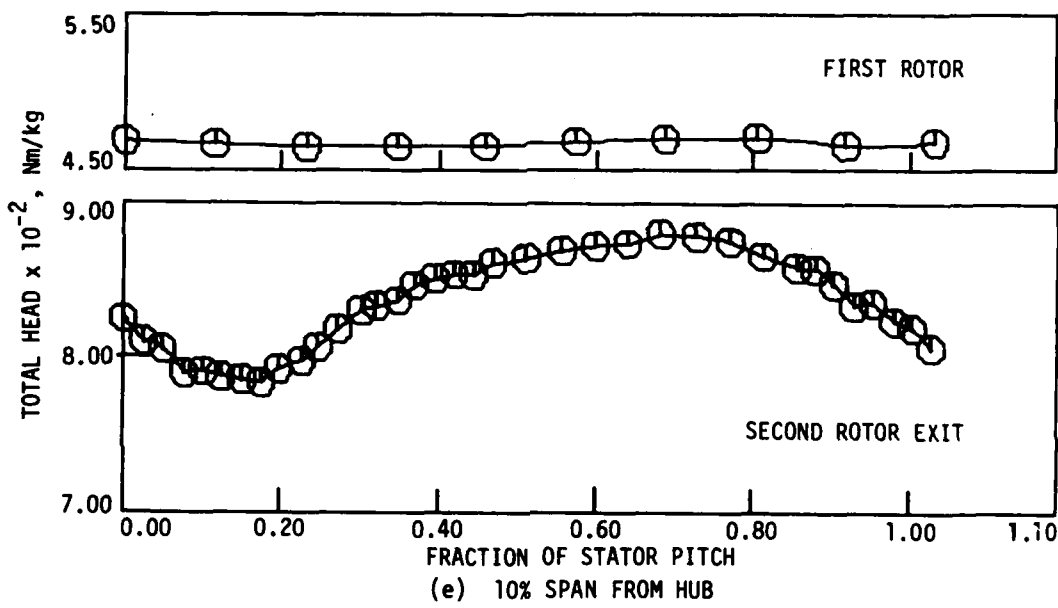


Figure 4.2 concluded.

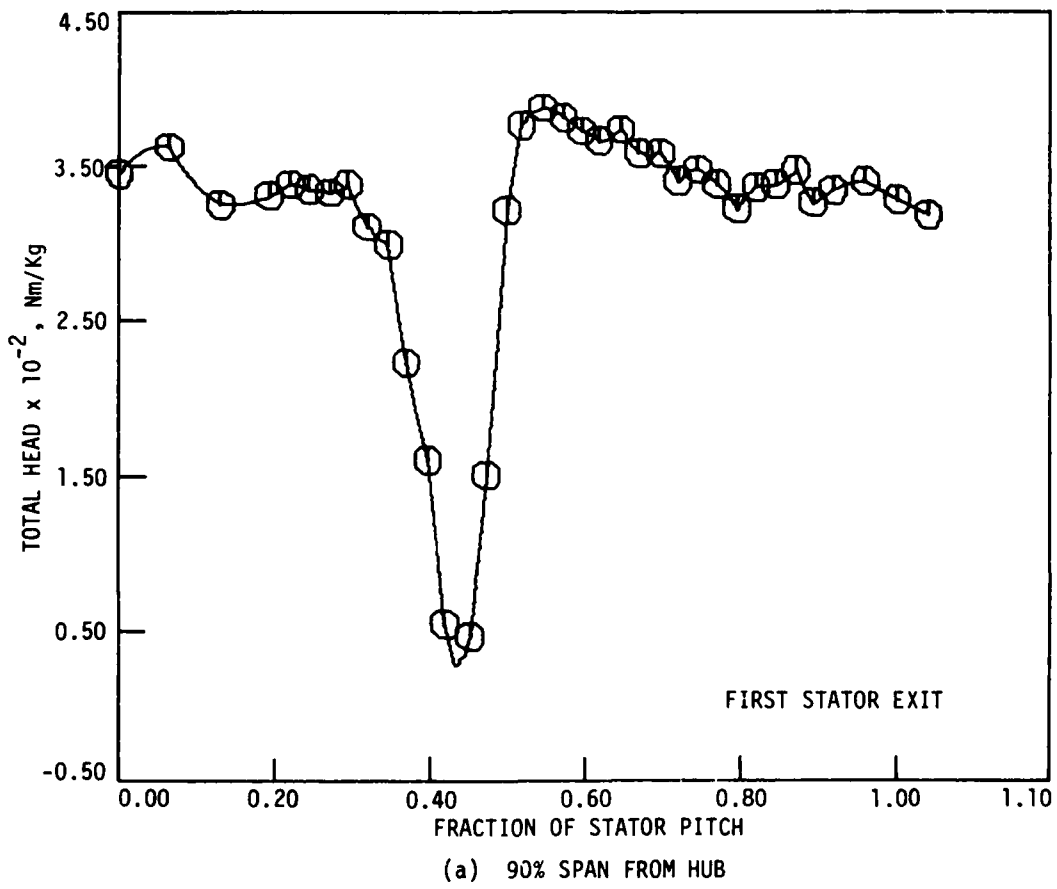


Figure 4.3 Blade-to-blade distribution of time-average total head for flow behind the first and second stage stators ($\phi = 0.587$ at 2400 rpm).

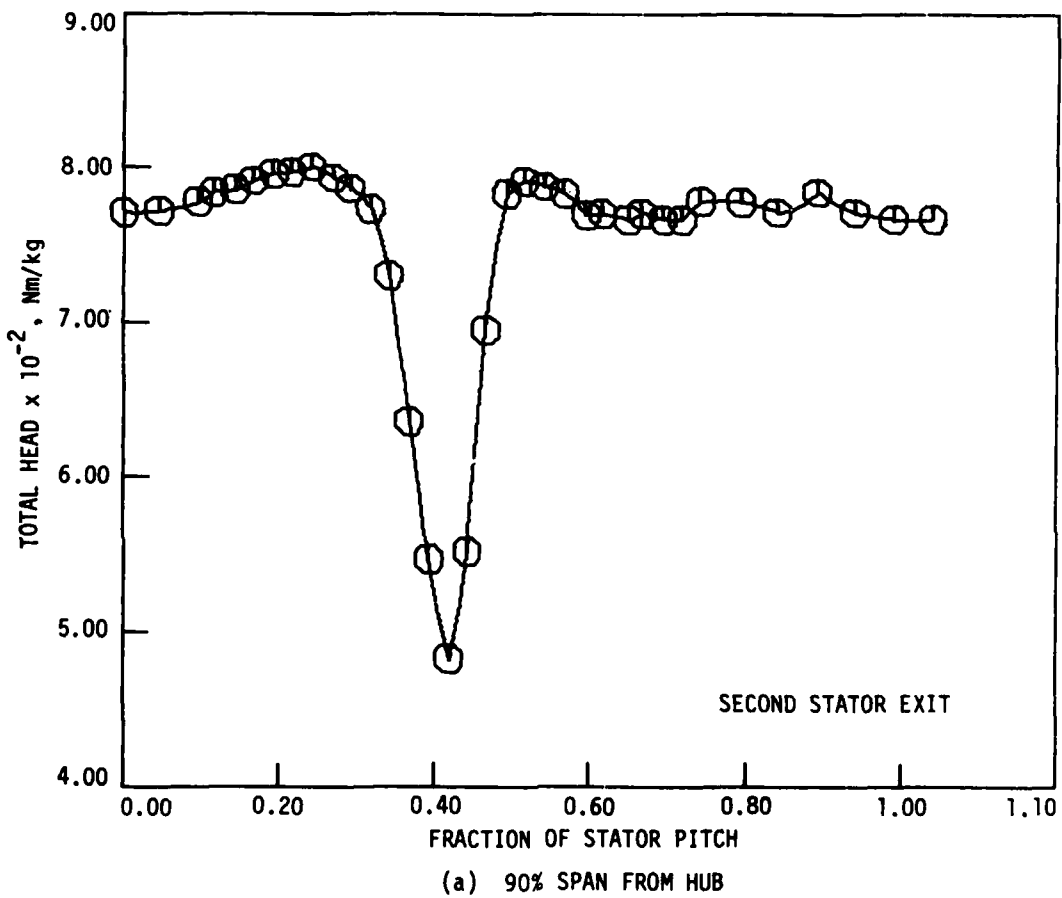


Figure 4.3 continued.

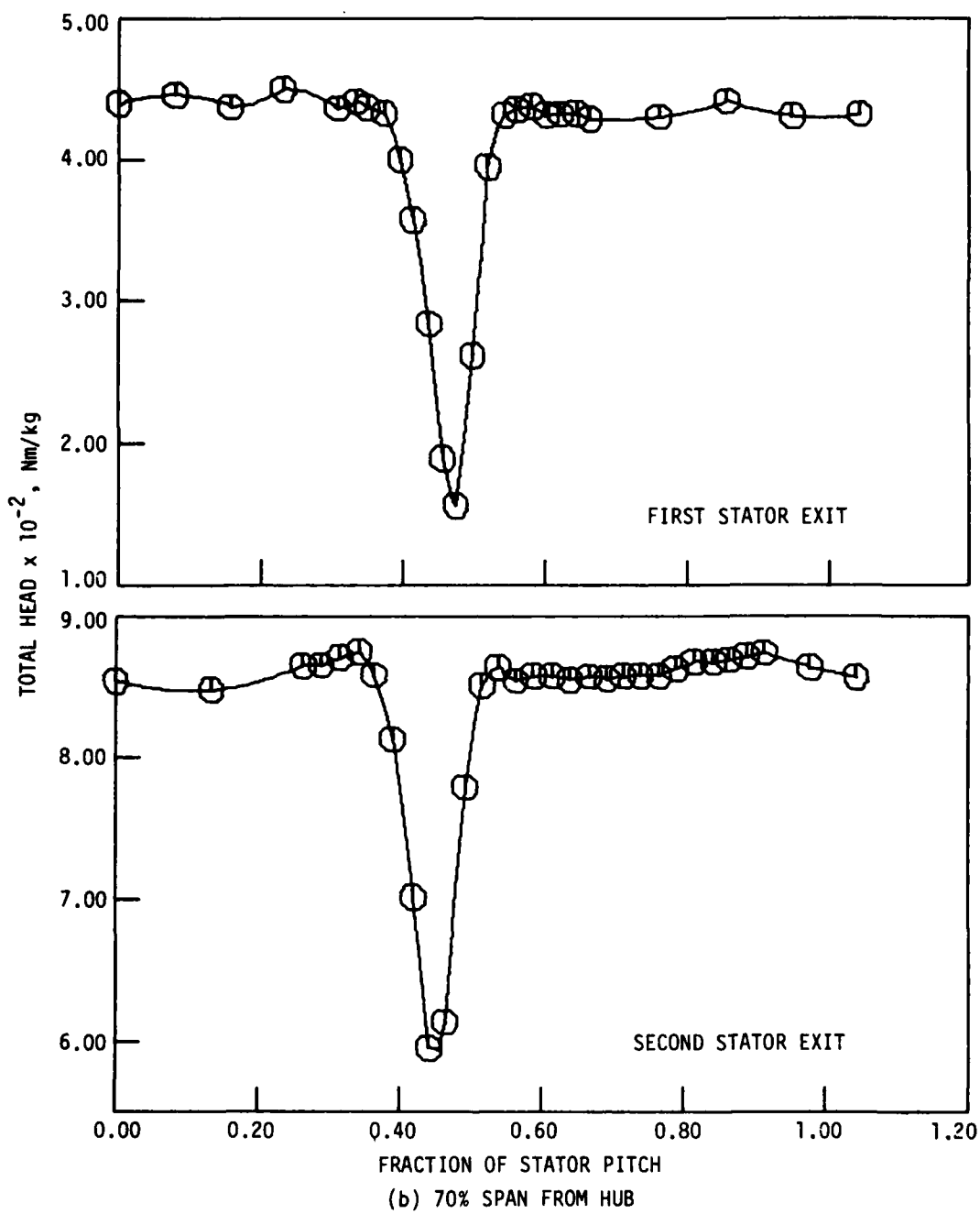


Figure 4.3 continued.

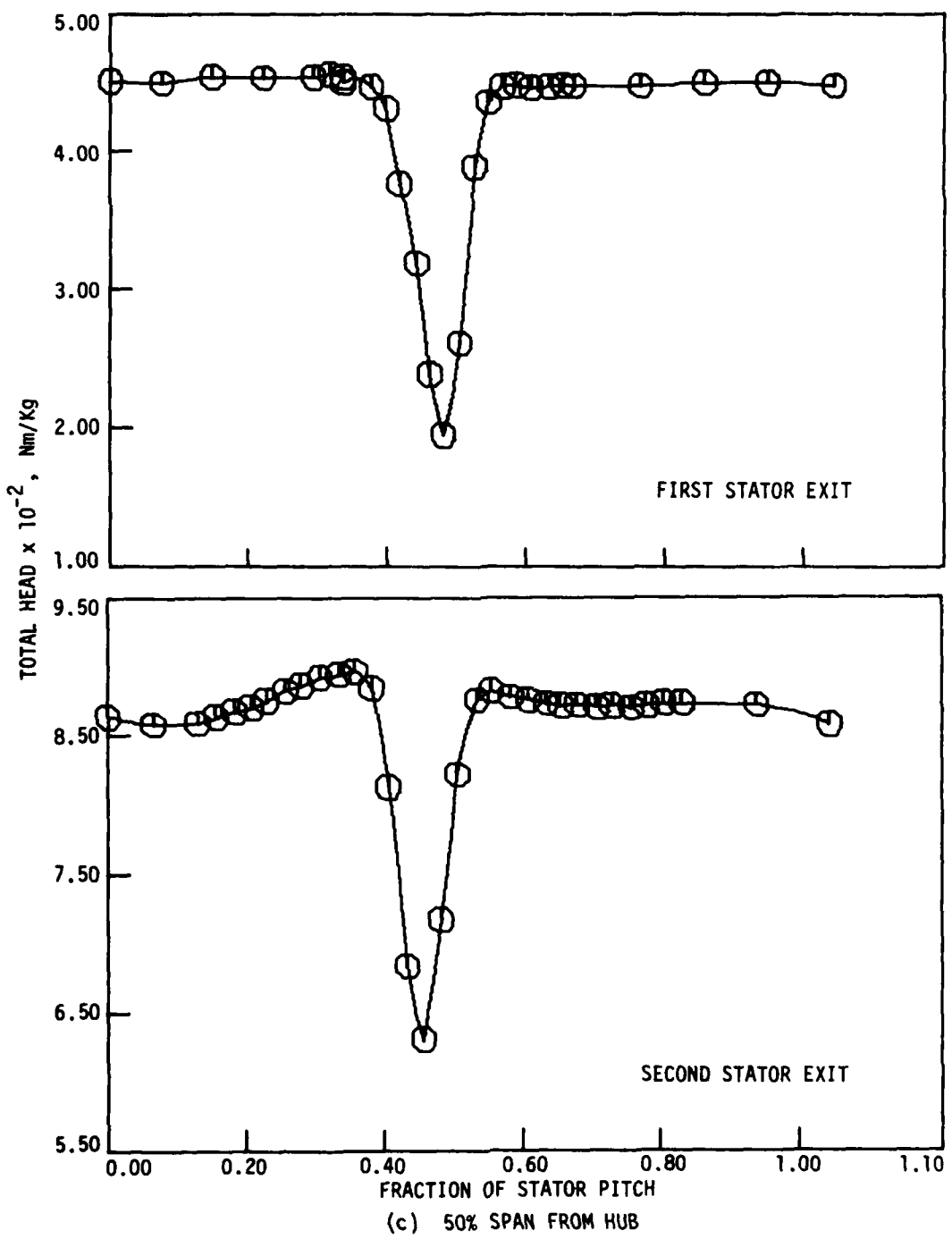


Figure 4.3 continued.

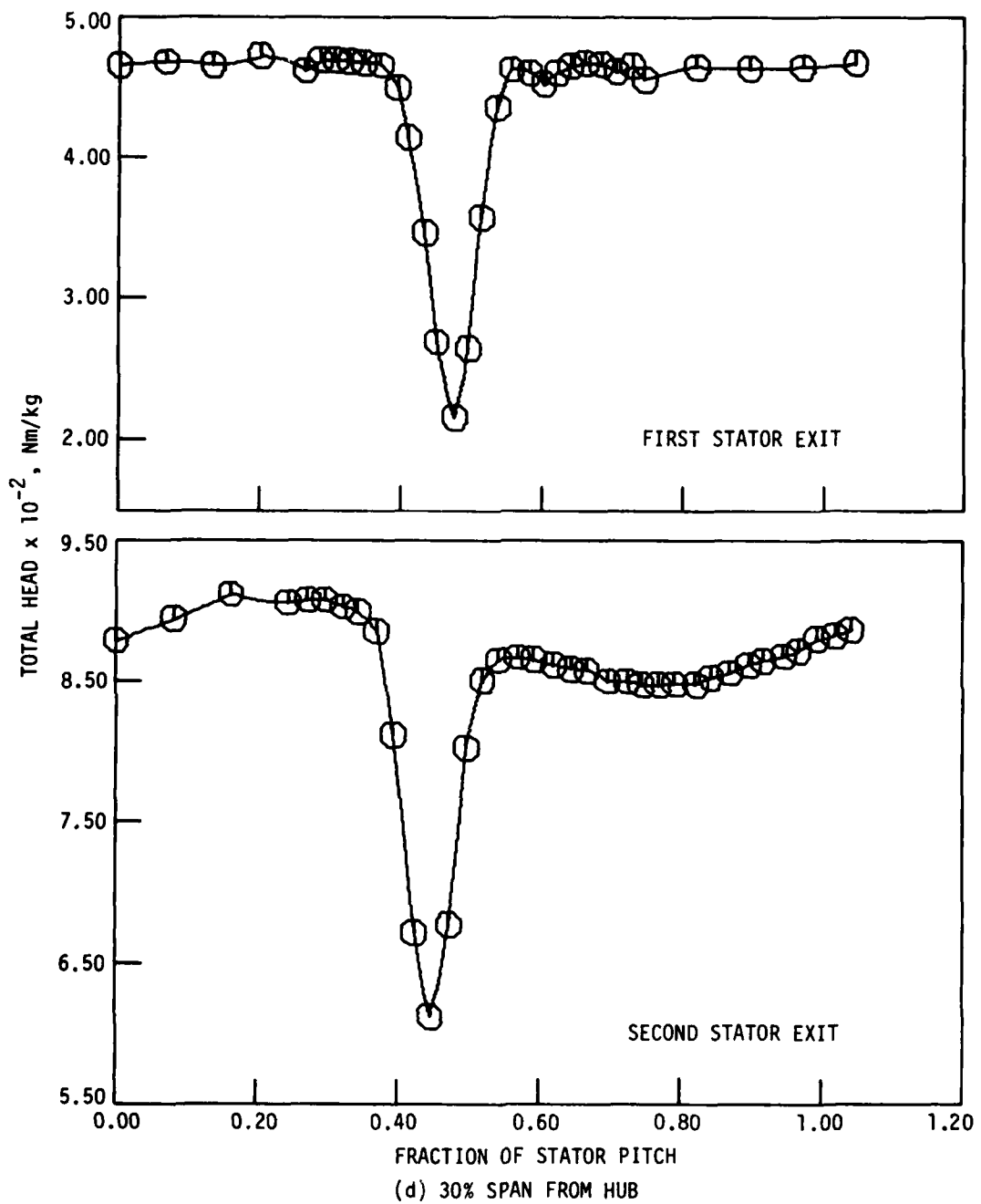


Figure 4.3 continued

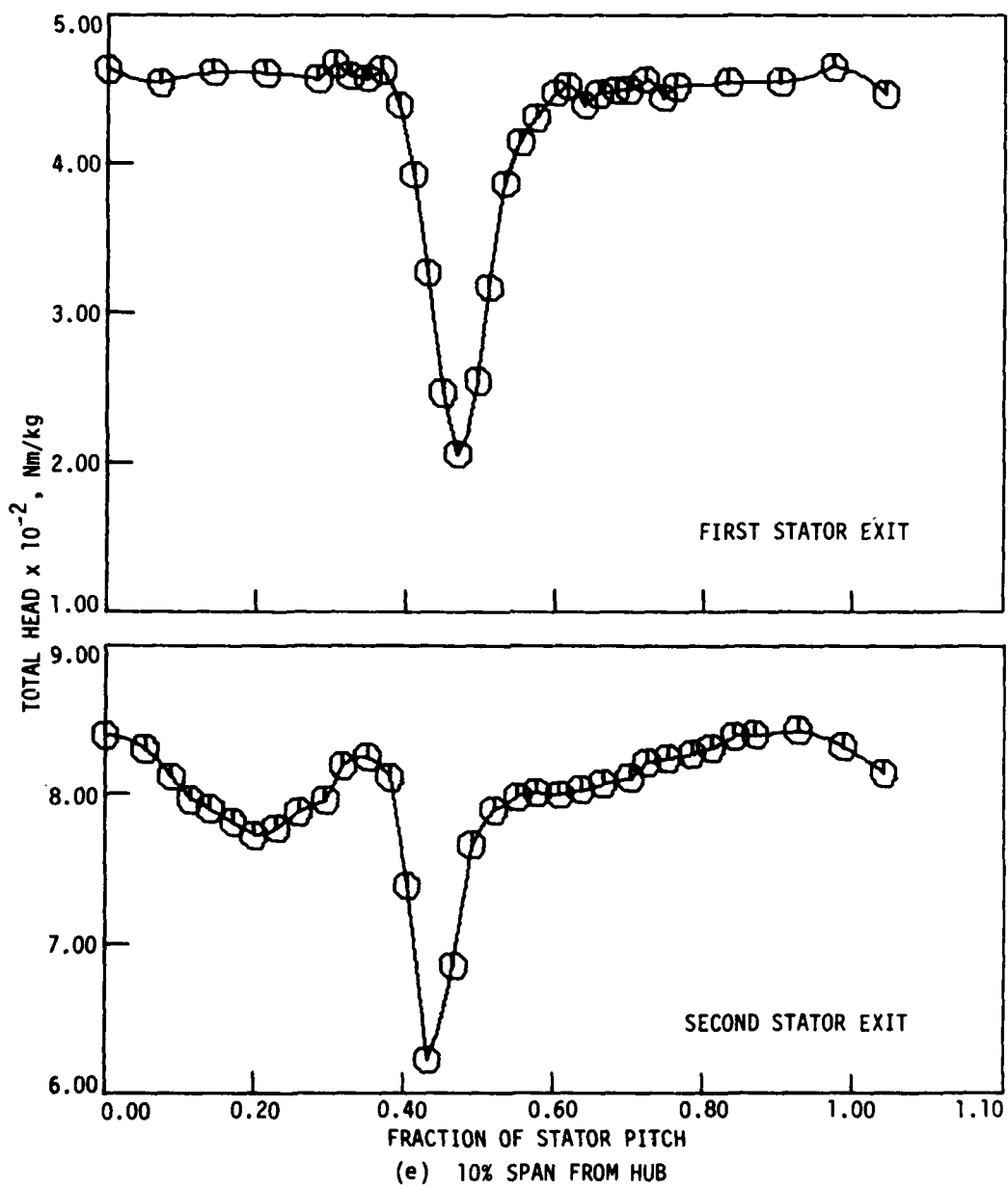


Figure 4.3 concluded.

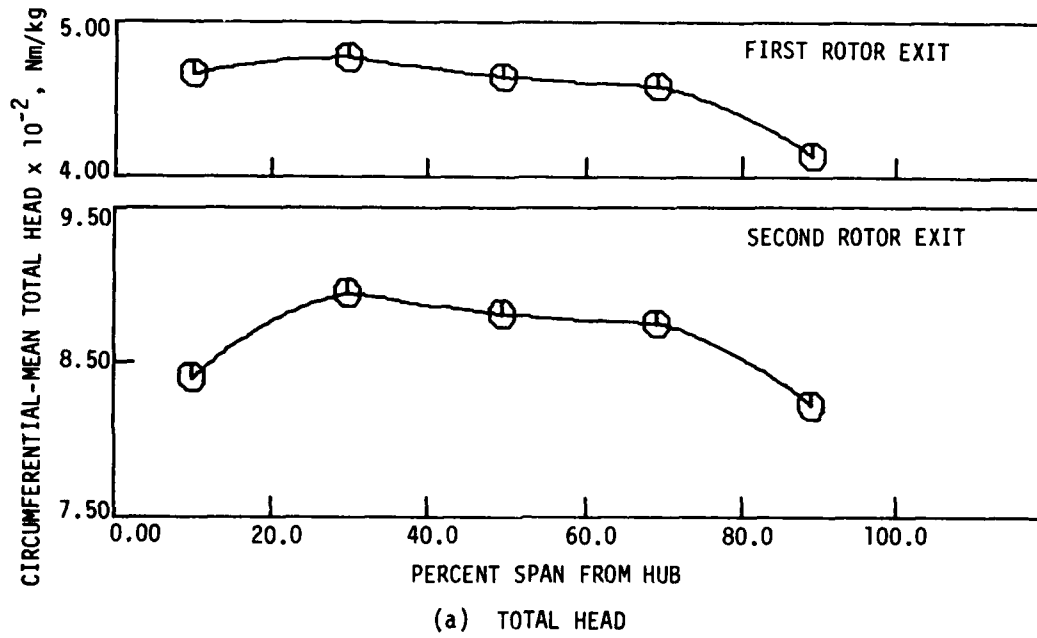


Figure 4.4 Spanwise distribution of circumferential-mean data for flow behind the first and second stage rotors ($\phi = 0.587$ at 2400 rpm).

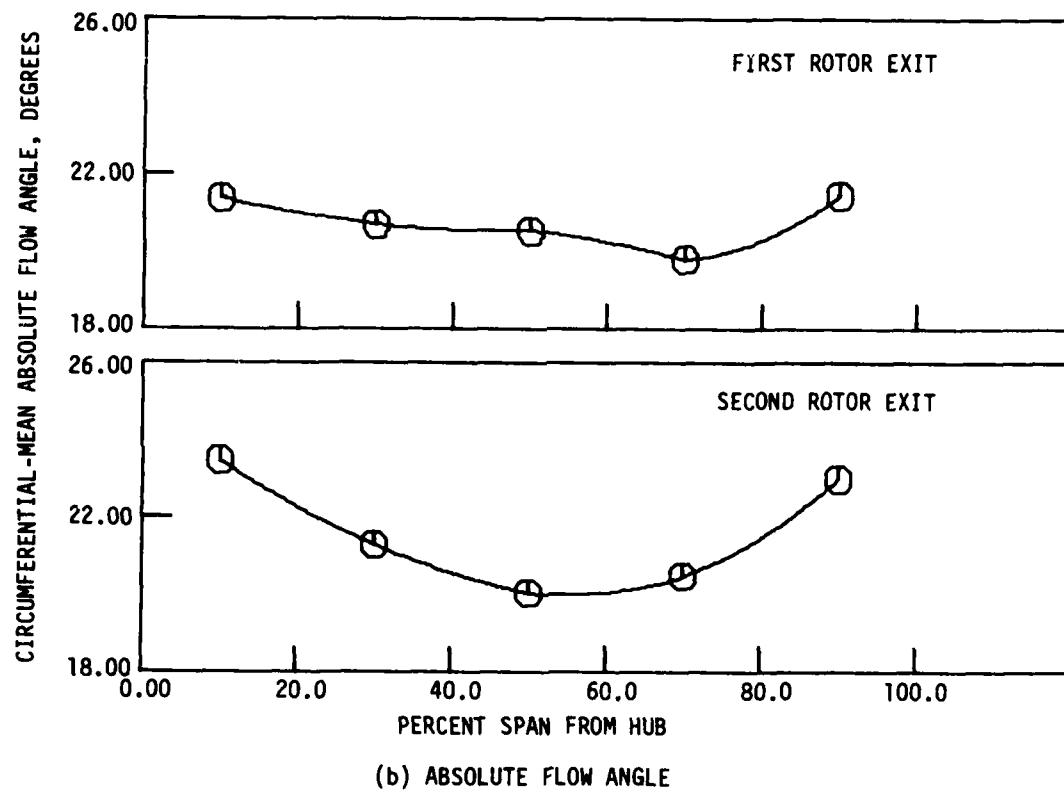


Figure 4.4 continued.

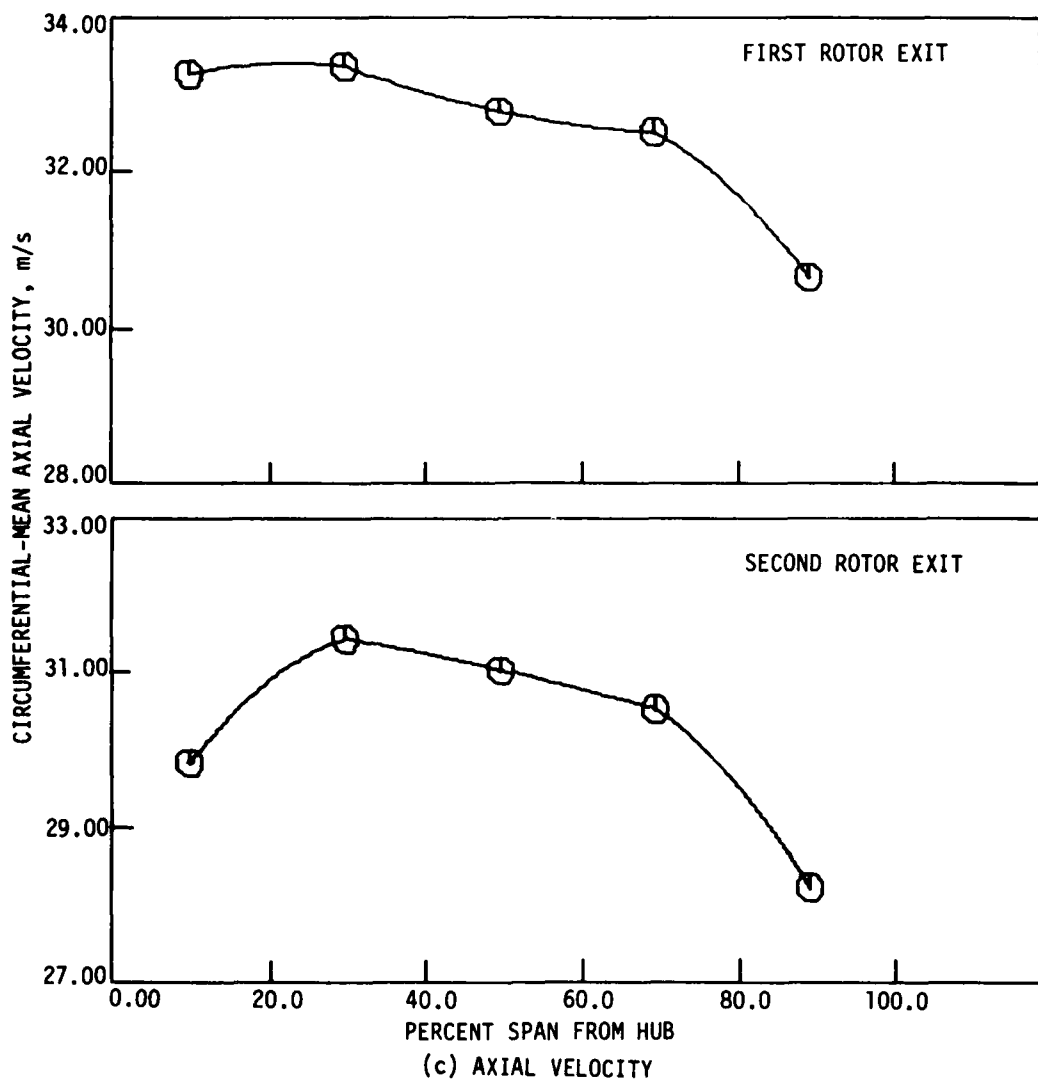


Figure 4.4 concluded.

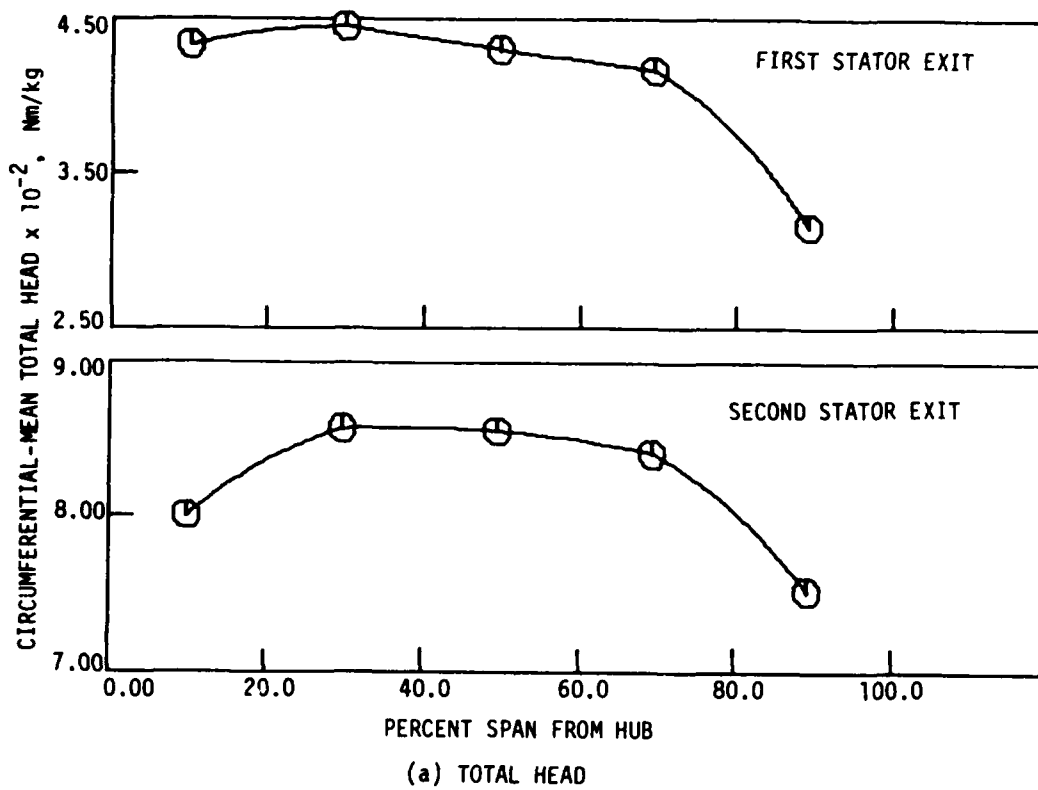


Figure 4.5 Spanwise distribution of circumferential-mean data for flow behind the first and second stage stators ($\phi = 0.587$ at 2400 rpm).

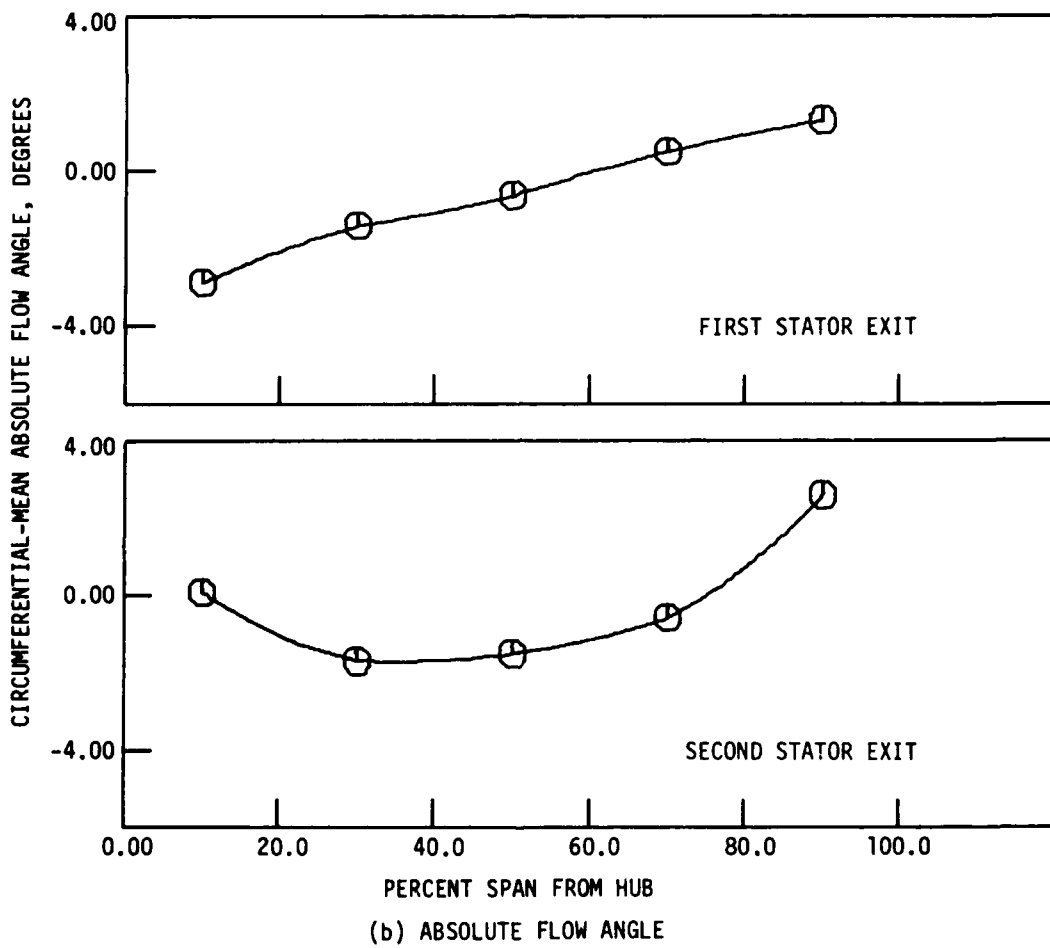


Figure 4.5 continued.

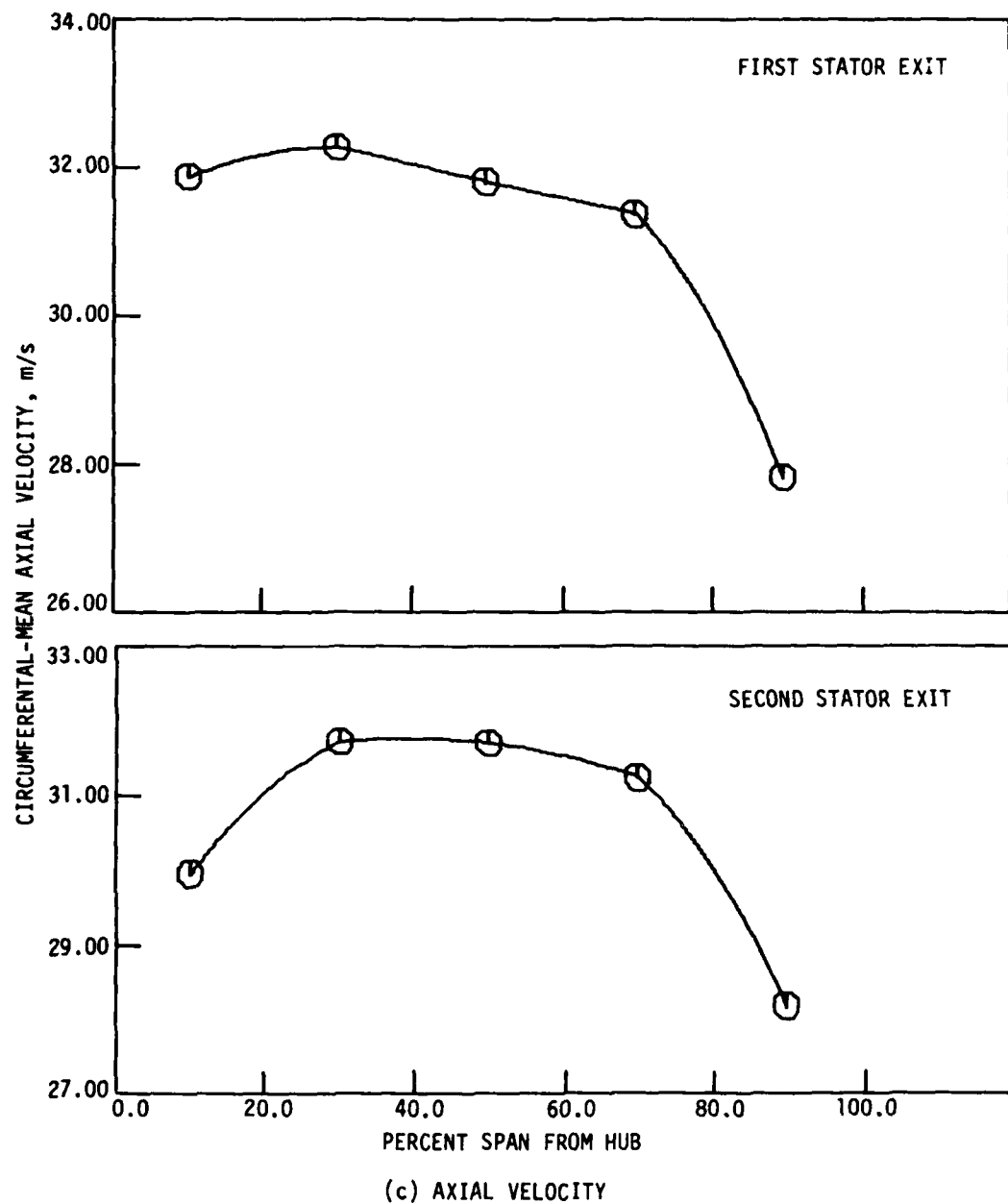


Figure 4.5 concluded.

of hub end-wall effects appears behind the second rotor and stator as seen by the appreciable decrease in total head and axial velocity levels there.

Circumferential-radial plane contour maps of total-head variation at each axial measurement location are presented in Figure 4.6. Figure 4.7 shows the locations of the actual data points used in constructing the contour map for station 3. The single-stator pitch data actually acquired were repeated over two stator blade pitches in order to afford better visualization of the flow pattern. The abscissa and ordinate correspond to fraction of blade pitch, Y/S_S , and percent span location measured from the hub, PHH. The actual data were taken between $Y/S_S = 0.0$ to $Y/S_S = 1.0$. In order to provide a smoother representation of the flow pattern, a data enhancement option provided by the contour plotting program was utilized. The data enhancement option was only employed in the radial direction since there were an adequate number of points available in the circumferential direction. For each contour map, an additional five enhanced data points between each pair of actual data points in the radial direction were requested. For the contour map of station 3, there were five circumferential survey line segments consisting of an equal number of data points--for this case 51--therefore, the total number of enhanced data points was $((5-1)*5*51) = 1020$. The data of station 3 without enhancement are shown in Figure 4.8 for comparison with enhanced data contours of Figure 4.6(b). The contours with enhanced data are a slightly smoother representation of the flow field. Trends, however, are not significantly altered by the enhancement process.

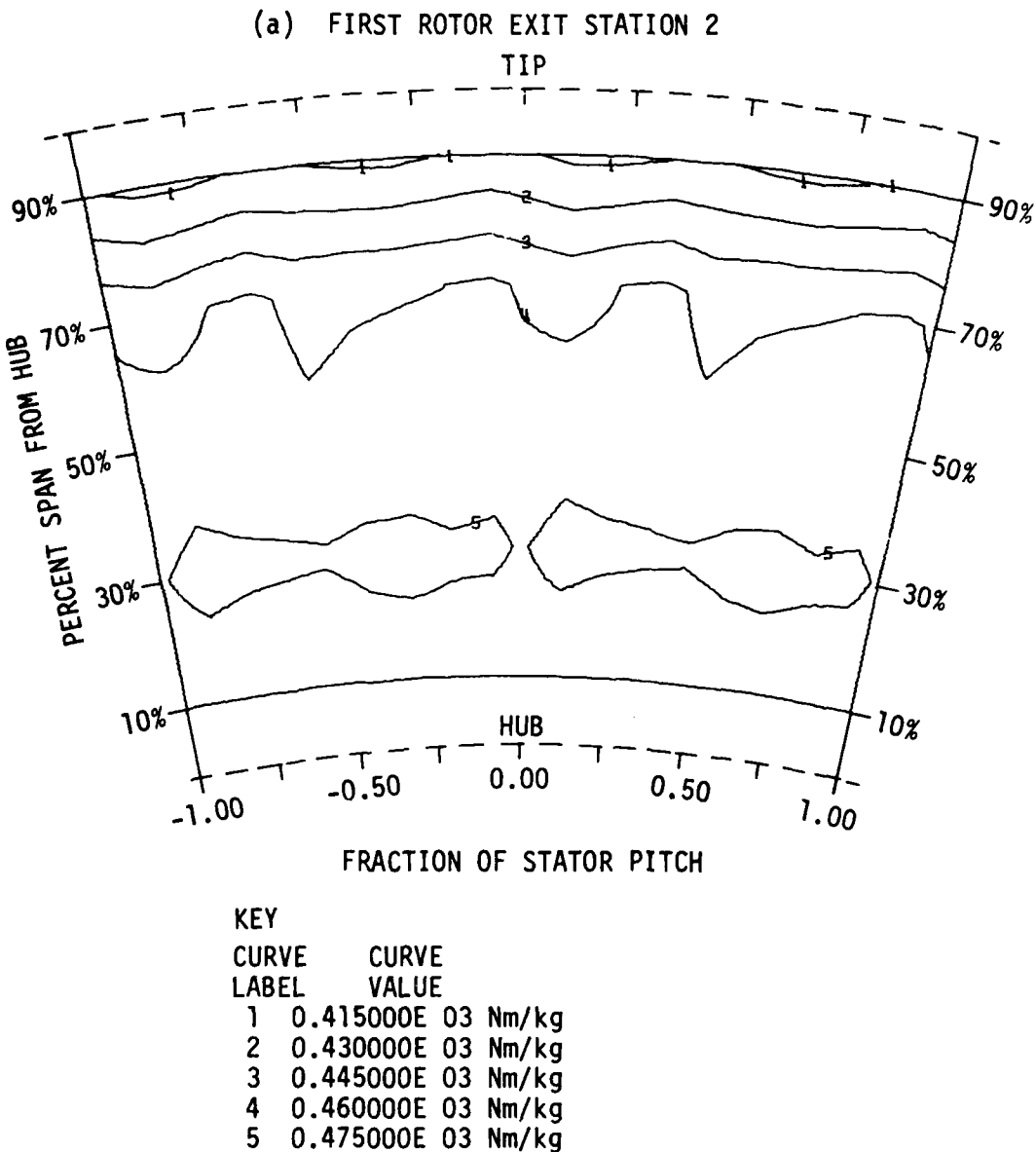
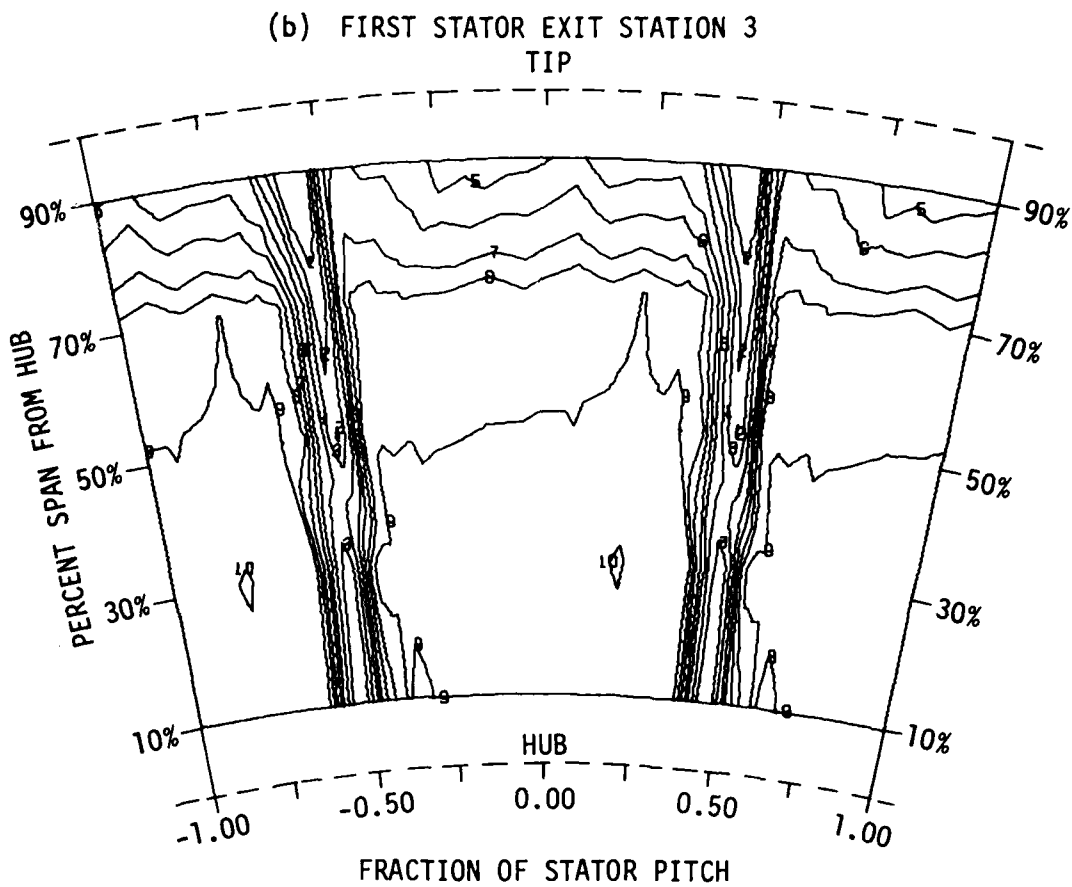
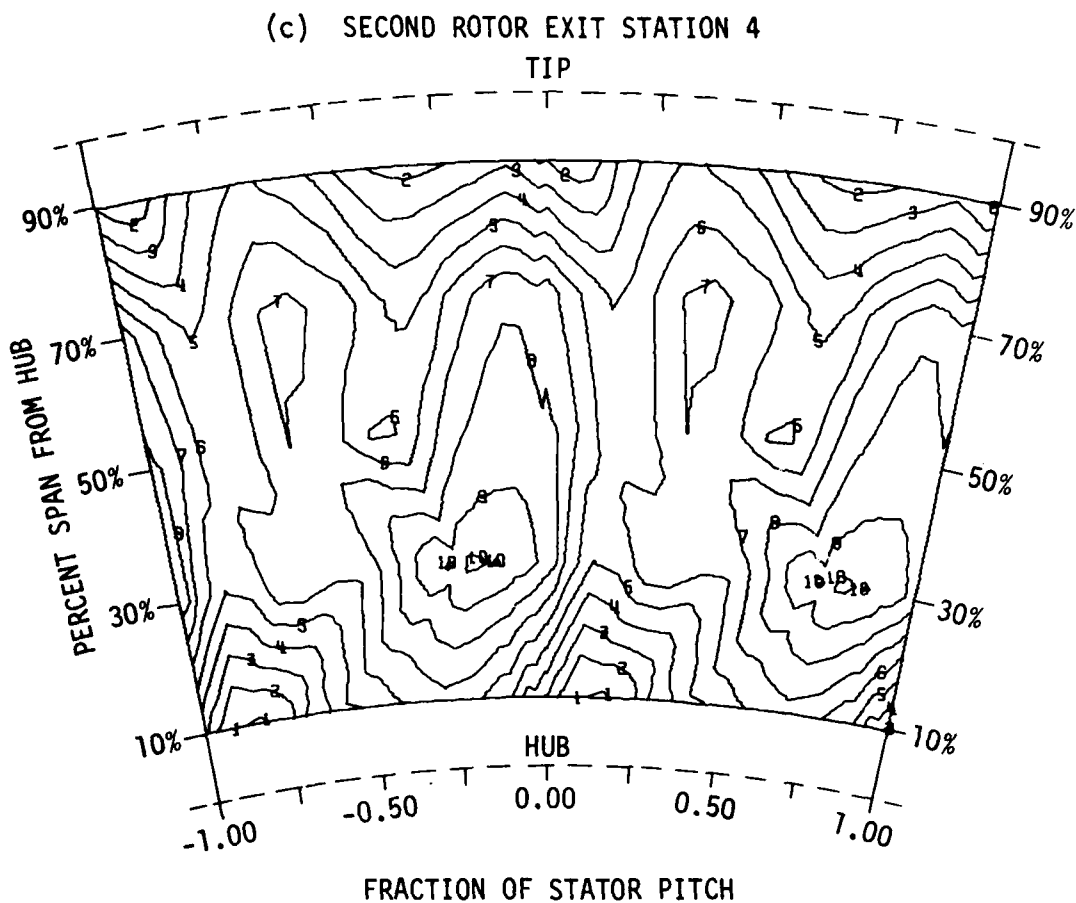


Figure 4.6 Contour map of the distribution of total head behind each blade row ($\phi = 0.587$ at 2400 rpm). Data enhancement employed.



CURVE LABEL	CURVE VALUE
1	0.150000E 03 Nm/kg
2	0.200000E 03 Nm/kg
3	0.250000E 03 Nm/kg
4	0.300000E 03 Nm/kg
5	0.350000E 03 Nm/kg
6	0.380000E 03 Nm/kg
7	0.410000E 03 Nm/kg
8	0.430000E 03 Nm/kg
9	0.450000E 03 Nm/kg
10	0.470000E 03 Nm/kg

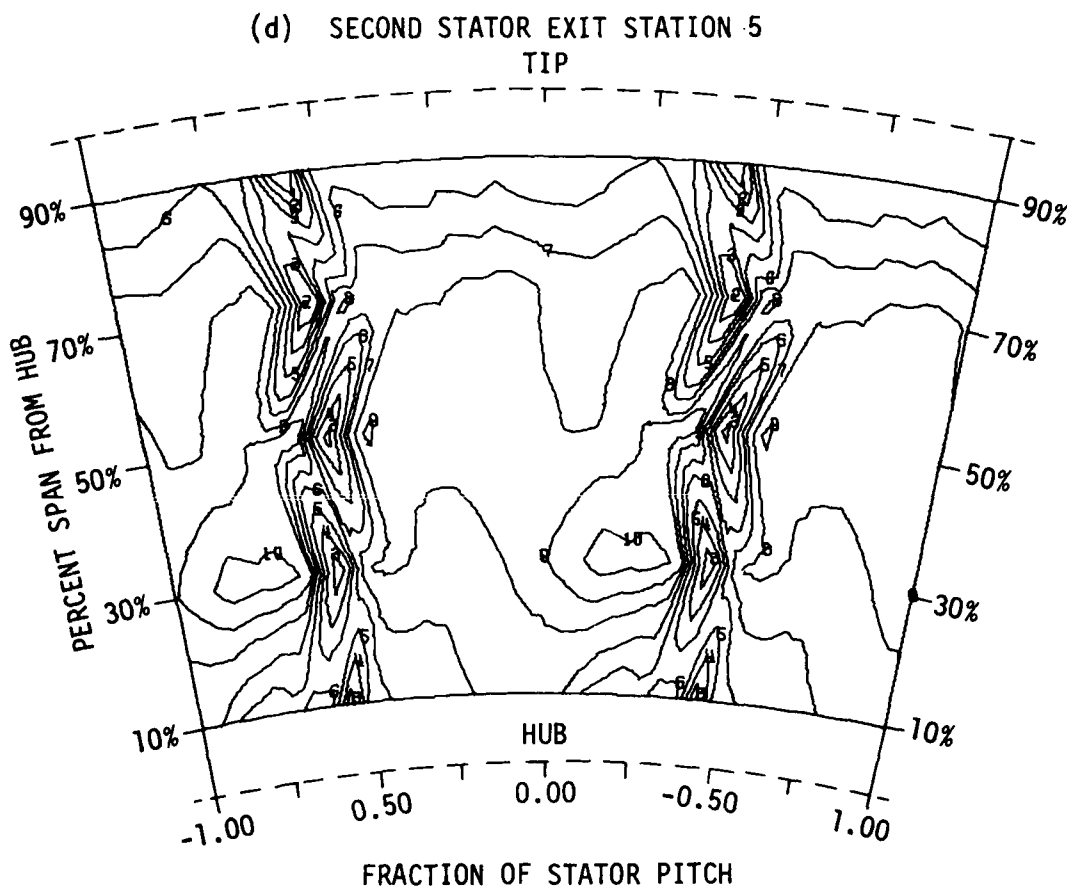
Figure 4.6 continued.



KEY

CURVE LABEL	CURVE VALUE
1	0.790000E 03 Nm/kg
2	0.810000E 03 Nm/kg
3	0.825000E 03 Nm/kg
4	0.840000E 03 Nm/kg
5	0.855000E 03 Nm/kg
6	0.870000E 03 Nm/kg
7	0.885000E 03 Nm/kg
8	0.900000E 03 Nm/kg
9	0.915000E 03 Nm/kg
10	0.930000E 03 Nm/kg

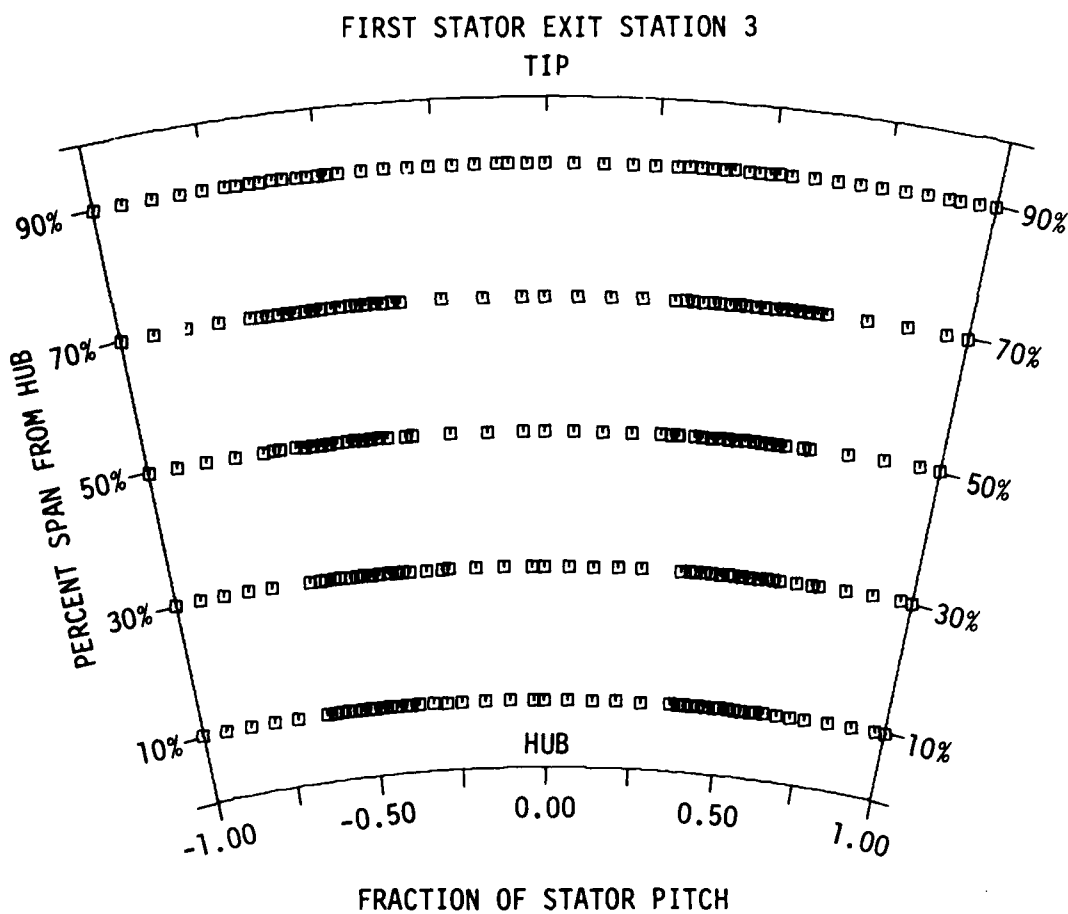
Figure 4.6 continued.



KEY

CURVE LABEL	CURVE VALUE
1	0.550000E 03 Nm/kg
2	0.600000E 03 Nm/kg
3	0.650000E 03 Nm/kg
4	0.700000E 03 Nm/kg
5	0.750000E 03 Nm/kg
6	0.800000E 03 Nm/kg
7	0.830000E 03 Nm/kg
8	0.860000E 03 Nm/kg
9	0.880000E 03 Nm/kg
10	0.900000E 03 Nm/kg

Figure 4.6 concluded.



NOTE: SINGLE PITCH DATA ACTUALLY ACQUIRED REPEATED OVER TWO
STATOR BLADE PITCHES FOR VISUALIZATION ENHANCEMENT

Figure 4.7 Locations of actual data points used in constructing the contour map behind the first stator.

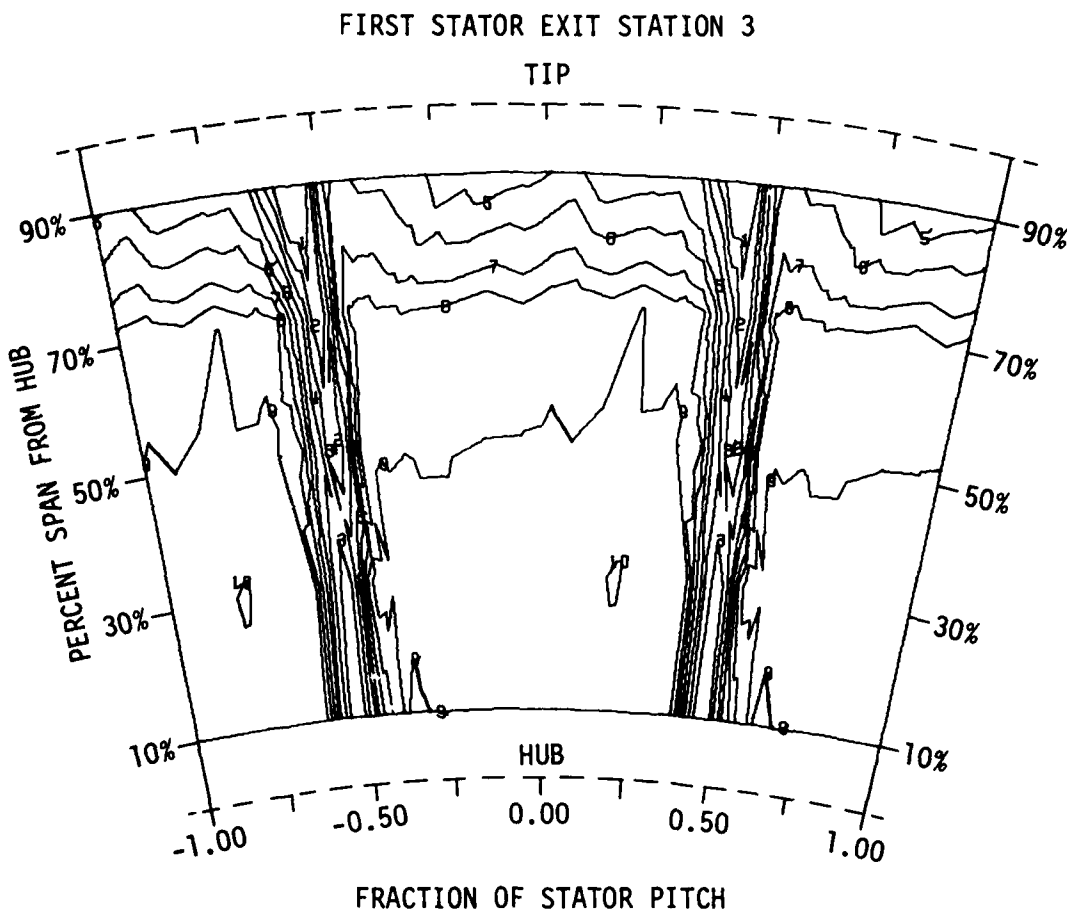


Figure 4.8 Contour map of the distribution of total head behind the first stator ($\phi = 0.587$ at 2400 rpm). No data enhancement.

The contour map of total-head variation behind the first rotor, Figure 4.6(a), indicates a fairly uniform total pressure level distribution with some evidence of an end-wall loss region (lower total head) from about 70% span to the shroud end-wall. The majority of the span from about 10% to 70% span is at about the same total head level, except at about 30% span where there is a core of slightly higher total-head fluid.

The contour map for flow behind the first stator, Figure 4.6(b), shows very well defined stator blade wakes involving steep gradients in total head and the lower total-head values. Again, the shroud end-wall region from about 70% span to the shroud end-wall consists of lower total head fluid associated with end-wall related losses. The highest total head--as for the first rotor exit flow--occurs at about 30% span.

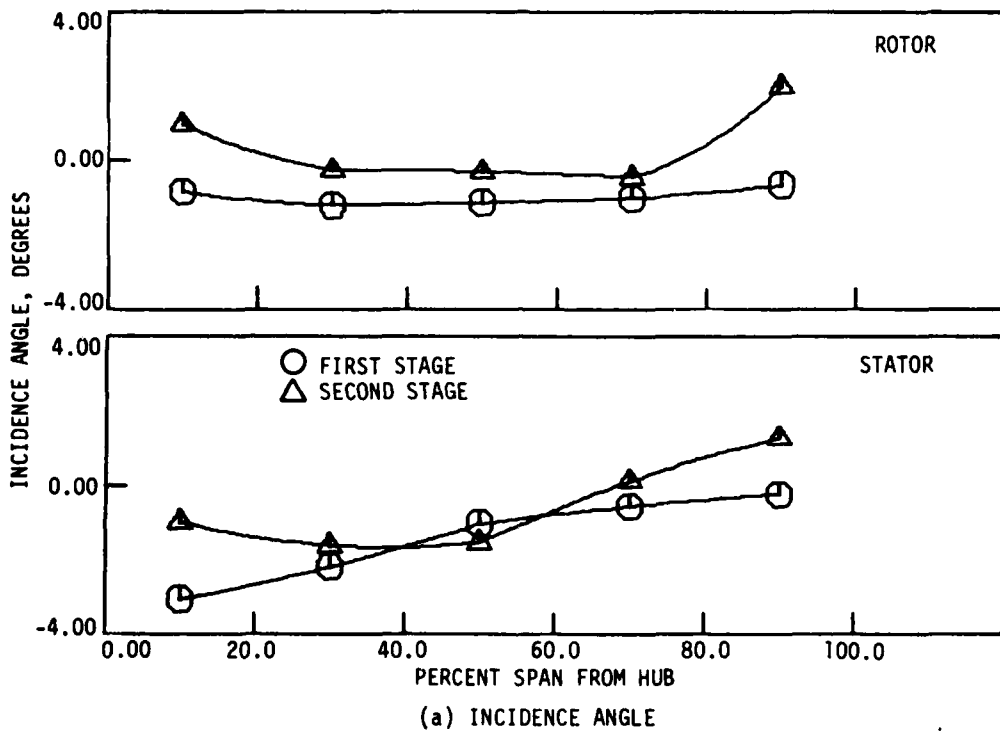
The second rotor exit contour map, Figure 4.6(c), involves a very nonuniform total head variation in contrast to the fairly uniform total head distribution found behind the first rotor. Zierke and Okiishi [13] discussed the large influence of rotor/stator wake interaction on rotor exit total-head distribution when stator wakes are chopped and transported through a downstream rotor blade row. Evident from the contour map of flow behind the second rotor, in Figure 4.6(c), are two regions of lower total-head fluid (as mentioned earlier in discussing Figure 4.2) along the span. Several possible explanations for the occurrence of these two regions of lower total-head fluid were investigated. The wakes of upstream struts used to support the inlet bell housing were eliminated as a possible cause of this trend since they remained stationary relative to the probe during any circumferential

survey and, thus, would not show up as a circumferential variation of total pressure. Only those compressor components which moved relative to the probe were considered further. Potential flow effects upstream from the second stator leading edge were considered next, although they seemed an unlikely cause; no evidence of this kind of effect was observed behind the first rotor. Subsequent tests with the first stage stators held stationary during a circumferential survey demonstrated that as the second stage stators only were traversed circumferentially relative to the probe, the first rotor exit flow total-head remained essentially constant with no evidence of either region of low total-head fluid appearing. Similar tests, with the second stator held stationary while the first stator was circumferentially traversed relative to the probe, resulted in both regions of low total-head fluid appearing. Both regions of low total-head are, thus, quite clearly related to the first stator blade row. This unusual observation has been studied further. Heated first stator wake fluid was tracked through the first rotor row and a logical explanation of the appearance of the two regions of lower total-head fluid behind the first rotor may be found in Reference 12.

The second stator exit contour map, Figure 4.6(a), shows the same end-wall loss region near the shroud end-wall region--from about 70% span to the shroud end-wall--and the same core of high total-head fluid at about 30% span as found in the other contour maps. The unusual wake contours were studied further (Reference 12). Adjustment of the contour plotting procedure resulted in more conventional wake contour lines.

The core of high total-head fluid at about 30% span, apparent at all stations, suggests that there was no significant radial migration of fluid. This is to be partly expected because the hub and shroud end-walls are parallel. Further, the rotor and stator boundary layer flows were probably not substantially separated from the blade surfaces and, thus, as was demonstrated by Dring, Joslyn, and Hardin [14], little radial migration of blade surface flow should have been anticipated. Hub end-wall loss regions could only be detected in the second-stage contour maps. The difference between the extent of hub and shroud loss regions indicates that the shroud losses are higher as discussed further in the next section (4.4. Comparisons of Circumferential-Mean Data with Design Code Predictions).

Comparisons of the spanwise distributions of the measured rotor and stator incidence and deviation angles for both stages are shown in Figure 4.9. Analysis of this figure indicates that the rotor deviation angles are about the same for both stages; whereas, the first rotor is operating with greater negative incidence. The first-stage stator is also operating with slightly more negative incidence and its deviation angles are considerably greater than for the second-stage stator. Although the stator exit circumferential-mean absolute flow angles are difficult to determine accurately, the difference in stator deviation angles are much larger than the estimated uncertainty of the absolute flow angle measurements (see Table 4.1). The negative incidence angles experienced by both stages resulted in the compressor not operating at optimum efficiency--a consequence already seen in the overall performance map results (see Figure 4.1). Table 4.3 shows head-rise coeffi-



(a) INCIDENCE ANGLE

Figure 4.9 Comparisons of measured circumferential-mean incidence and deviation angles for both stages ($\phi = 0.587$ at 2400 rpm).

AD-A141 796

AERODYNAMIC DESIGN AND PERFORMANCE OF A TWO-STAGE
AXIAL-FLOW COMPRESSOR C. (U) IOWA STATE UNIV AMES
ENGINEERING RESEARCH INST M D HATHAWAY ET AL DEC 83

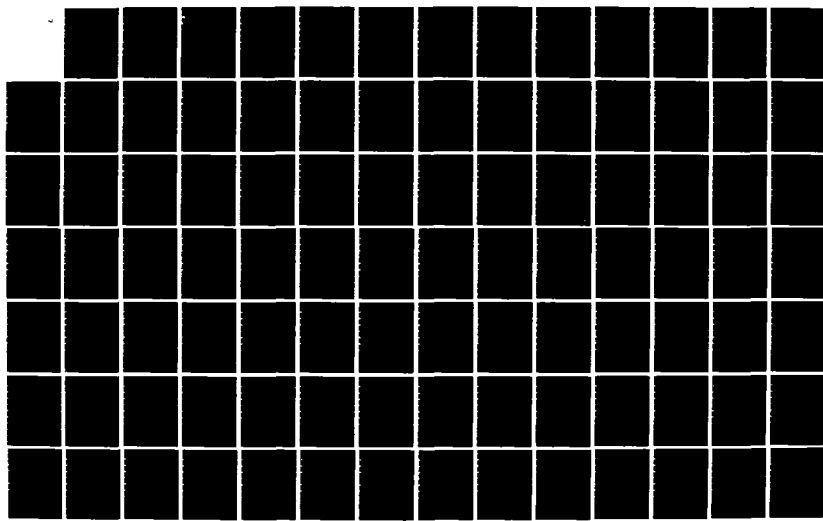
UNCLASSIFIED

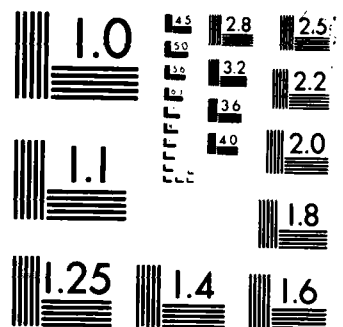
ISU-ERI-AMES-84178 AFOSR-TR-84-8417

F/G 21/5

2/3

NL





MICROCOPY RESOLUTION TEST CHART
NATIONAL BUREAU OF STANDARDS 400-3

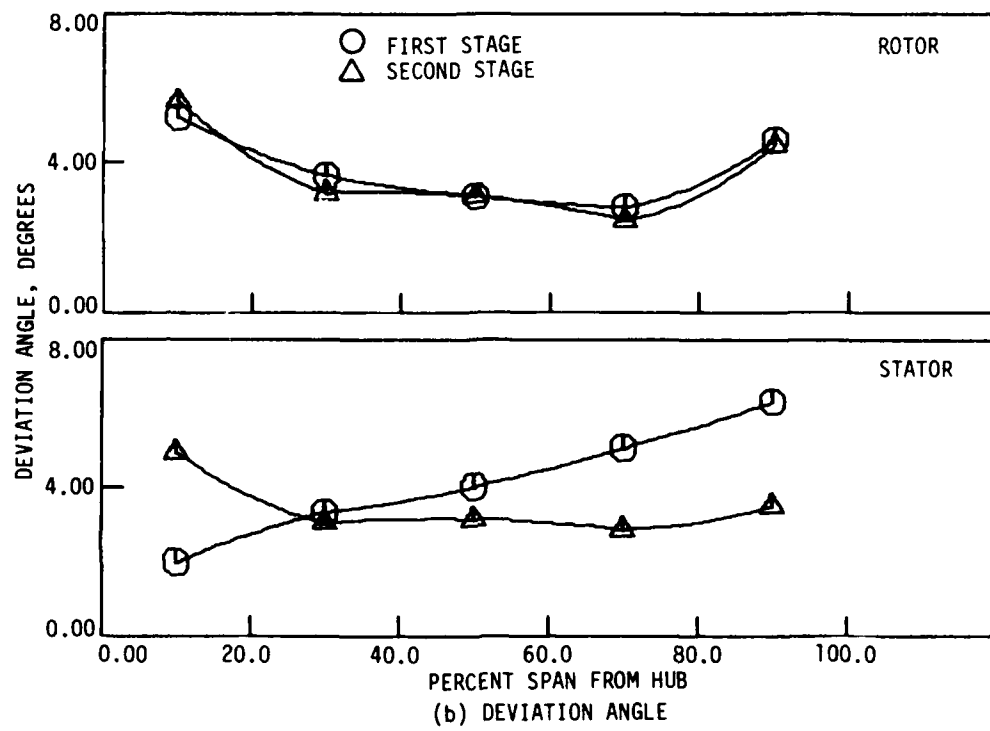


Figure 4.9 concluded.

Table 4.3. Rotor, stator, stage, and overall performance parameters.

<u>First Stage</u>						
PHH	Ψ_R	Ψ_{stage}	w_R	w_S	η_R	η_{stage}
10.0	0.179	0.167	-0.016	0.055	1.042	0.969
30.0	0.183	0.171	-0.014	0.054	1.040	0.971
50.0	0.178	0.165	0.018	0.060	0.949	0.878
70.0	0.176	0.160	0.035	0.075	0.893	0.811
90.0	0.170	0.133	0.078	0.0193	0.769	0.599
Mass Averaged	0.178	0.160	0.025	0.083	0.926	0.833
<u>Second Stage</u>						
PHH	Ψ_R	Ψ_{stage}	w_R	w_S	η_R	η_{stage}
10.0	0.156	0.141	0.120	0.070	0.728	0.658
30.0	0.172	0.158	0.067	0.063	0.830	0.760
50.0	0.173	0.163	0.049	0.044	0.864	0.815
70.0	0.176	0.163	0.049	0.059	0.858	0.796
90.0	0.194	0.168	0.048	0.136	0.870	0.752
Mass Averaged	0.175	0.159	0.063	0.071	0.833	0.760
<u>Overall</u>						
PHH	$\Psi_{overall}$	$\eta_{overall}$				
10.0	0.307	0.796				
30.0	0.329	0.857				
50.0	0.328	0.846				
70.0	0.323	0.803				
90.0	0.300	0.676				
Mass Averaged	0.319	0.795				

cient, blade losses, and hydraulic efficiencies for both stages and for the overall compressor. The performance parameters are based on the Euler turbine equation ideal-head rise and are subject to large errors (see Table 4.1). Even considering these large errors, the first stage is apparently operating more efficiently than the second stage.

4.4. Comparisons of Circumferential-Mean Data with Design Code Predictions

Comparisons of the velocity triangles for the circumferential-mean measurements and the design code calculated results are presented in Figure 4.10 (for flow behind the first rotor), Figure 4.11 (for flow ahead of the second rotor), and Figure 4.12 (flow behind the second rotor). Inspection of these velocity triangles shows very good agreement between the measured and predicted rotor exit relative flow angles, except near the end-walls. This indicates apparent success of the rotor deviation angle prediction option. Also apparent, is the higher axial velocity level of the measured data and the poor agreement between measured and predicted absolute flow angles for almost all cases shown. It is suggested that the differences in measured and predicted absolute flow angles behind the rotors are primarily due to the differences in predicted and measured axial velocity levels. Since the axial velocity levels can be related to the end-wall blockage estimates, this observation indicates that poor blockage estimates were used in the design process. From the calibration tests in section 3.1, the cobra probe was found to be able to accurately measure the total pressure as long as the probe was yawed to within ± 5.0 degrees

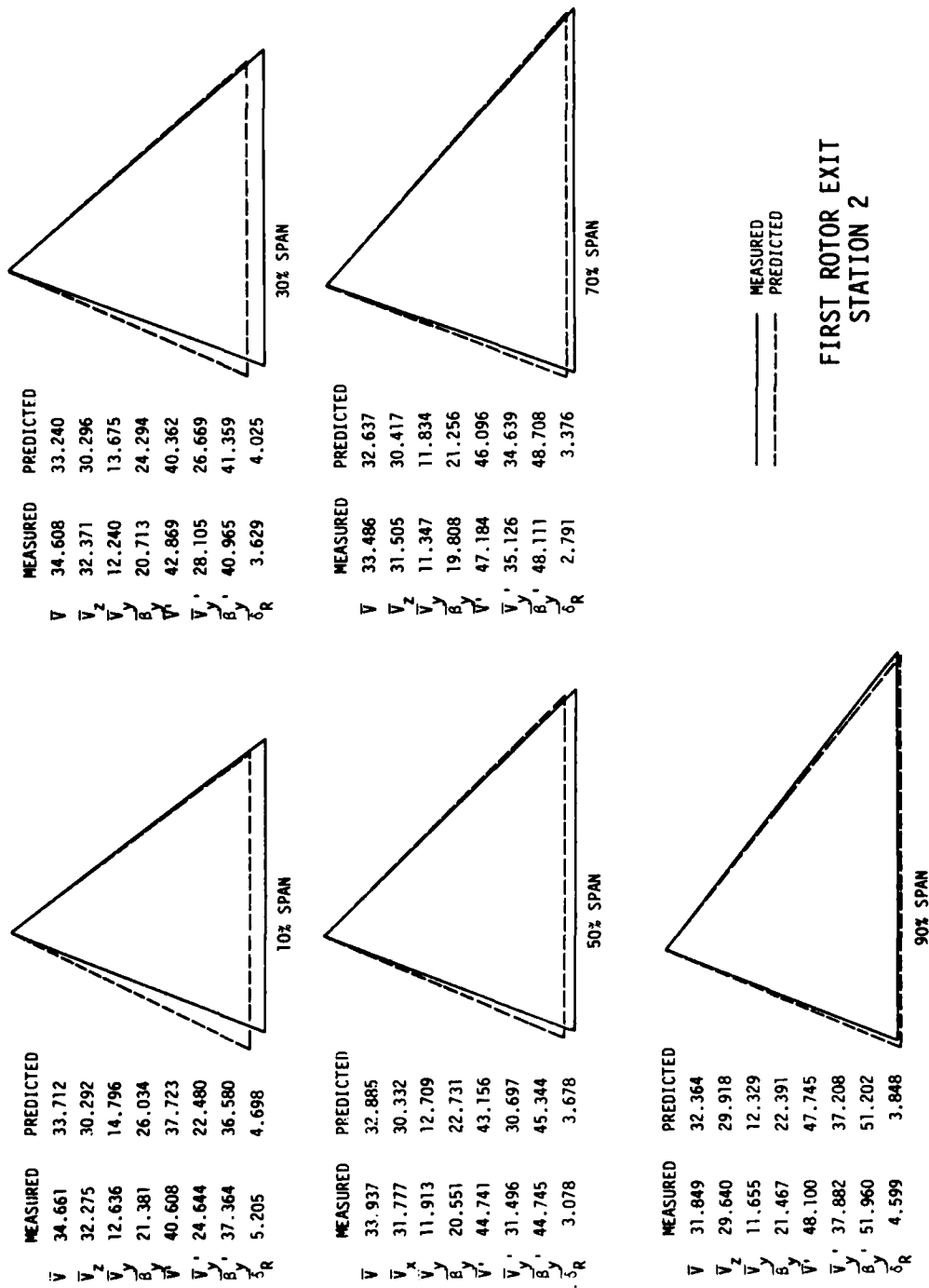


Figure 4.10 Comparisons of measured and predicted velocity triangles behind the first rotor ($\phi = 0.587$ at 2400 rpm).

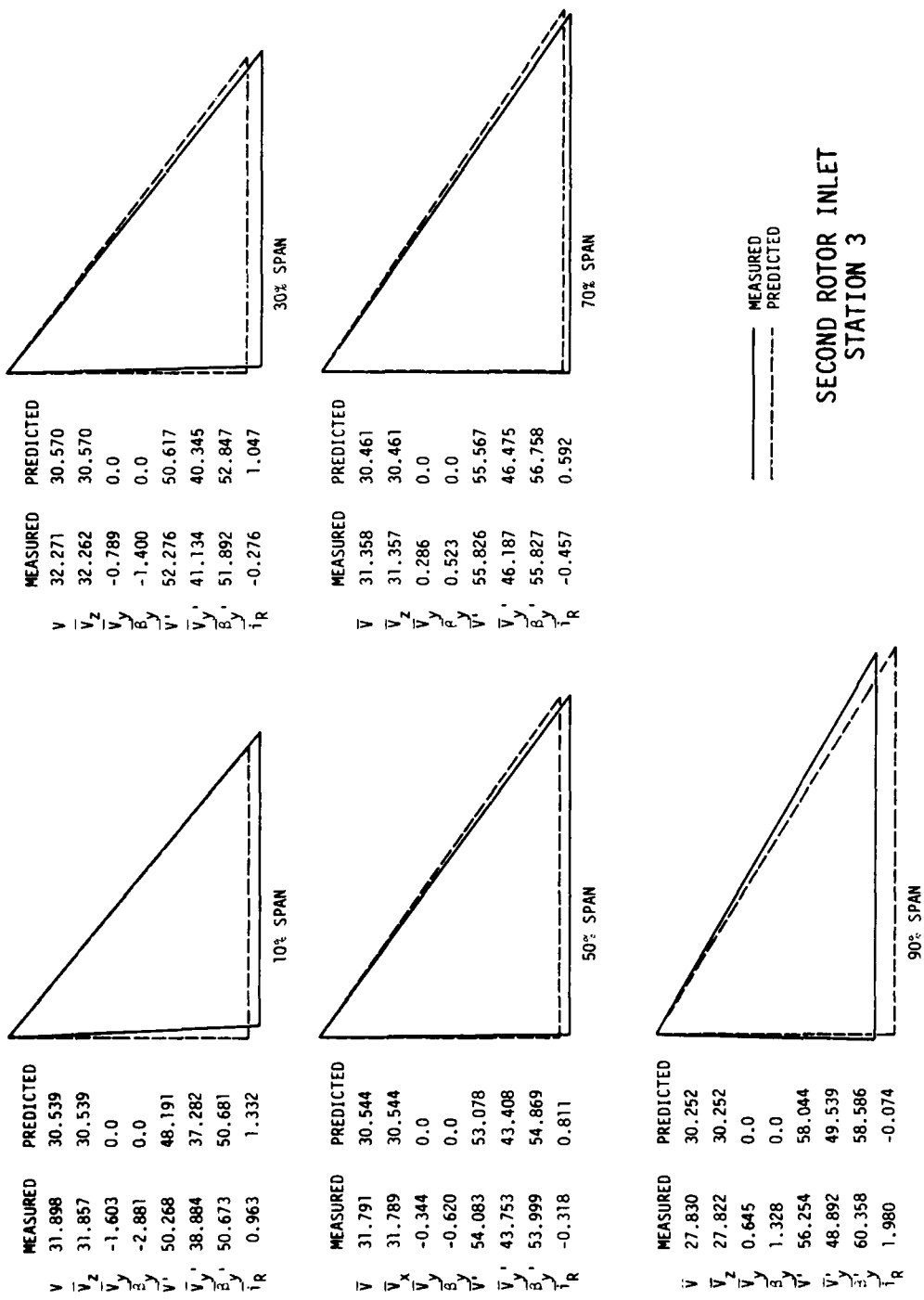


Figure 4.11 Comparisons of measured and predicted velocity triangles ahead of the second rotor ($\phi = 0.587$ at 2400 rpm).

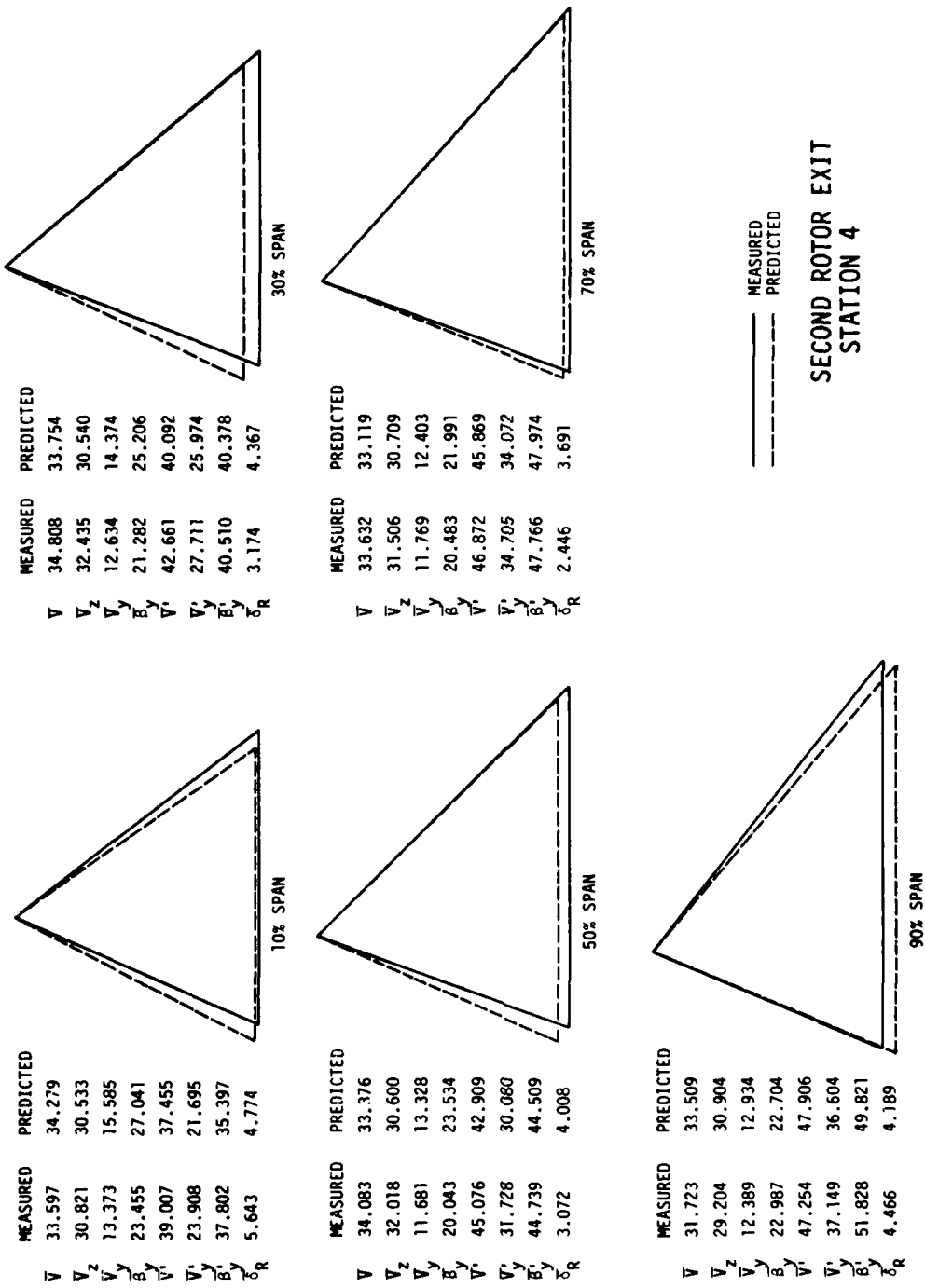


Figure 4.12 Comparisons of measured and predicted velocity triangles behind the second rotor ($\phi = 0.587$ at 2400 rpm).

of the true absolute flow angle. The estimated uncertainty in the absolute flow angle measurement for 20-to-1 odds is ± 1.0 degrees (see Table 4.1). Static head measurements were found to be constant across the span as expected, and were estimated to be accurate to within ± 5.0 Nm/Kg for 20-to-1 odds (see Table 4.1). Since absolute velocity is a function of the difference between the total and static head, it is estimated that the uncertainty in absolute velocity should be no more than ± 0.34 m/s for 20-to-1 odds (see Table 4.1). Given these observations, if the rotor exit absolute flow angle was truly in error by a significant amount, this error should also be evidenced as an error in the rotor exit relative flow angles. Since this is not the case, the large differences in measured and predicted rotor exit absolute flow angles must be predominantly due to the axial velocity discrepancies. Inspection of Figure 4.10--first rotor exit at 90% span--shows good agreement between the measured and predicted axial velocities and, as expected, also shows good agreement between the measured and predicted absolute and relative flow angles. On the other hand, discrepancies between measured and predicted relative flow angles at the inlet of the second rotor were due to errors in measured absolute flow angles as well as differences in axial velocity levels. As mentioned in section 4.1, the difficulty in ascertaining the circumferential extent of the free-stream and wake regions behind the stator blade rows adversely affects the precision of those circumferential-mean absolute flow angles determined from the measured data.

Figure 4.13 shows a comparison between measured and predicted circumferential-mean axial velocities ahead of and behind each blade

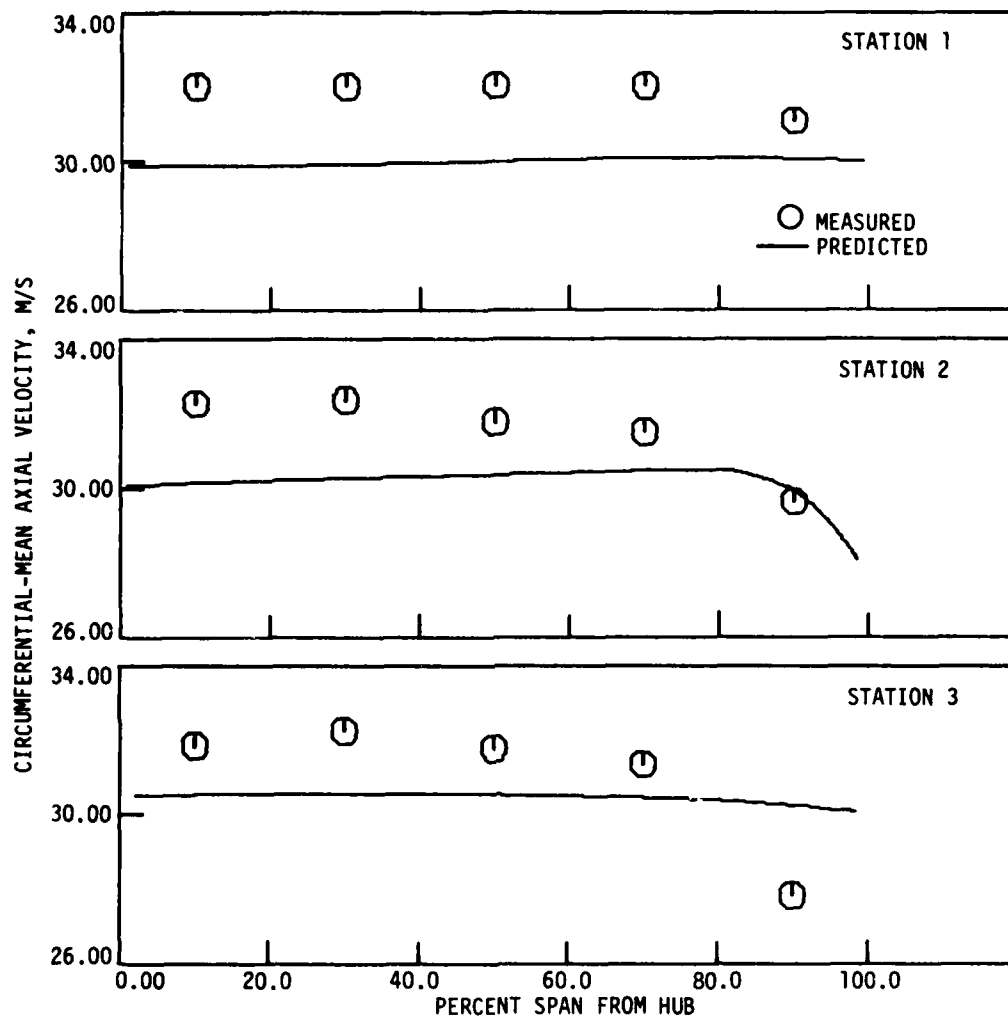


Figure 4.13 Comparisons of the measured and predicted spanwise distributions of circumferential-mean axial velocity ($\phi = 0.587$ at 2400 rpm).

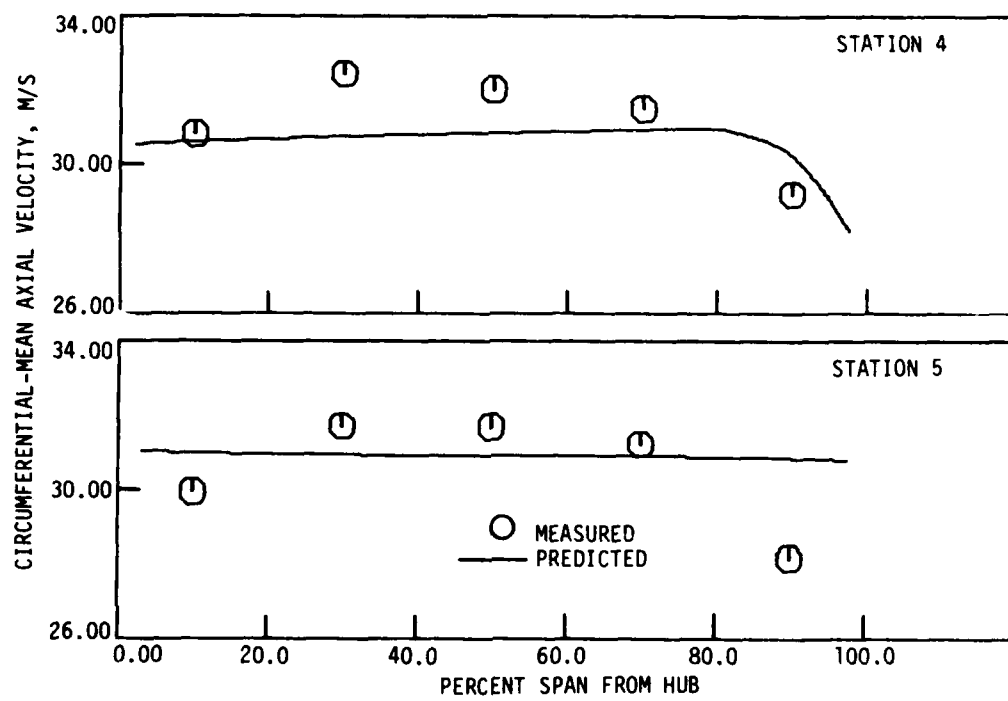
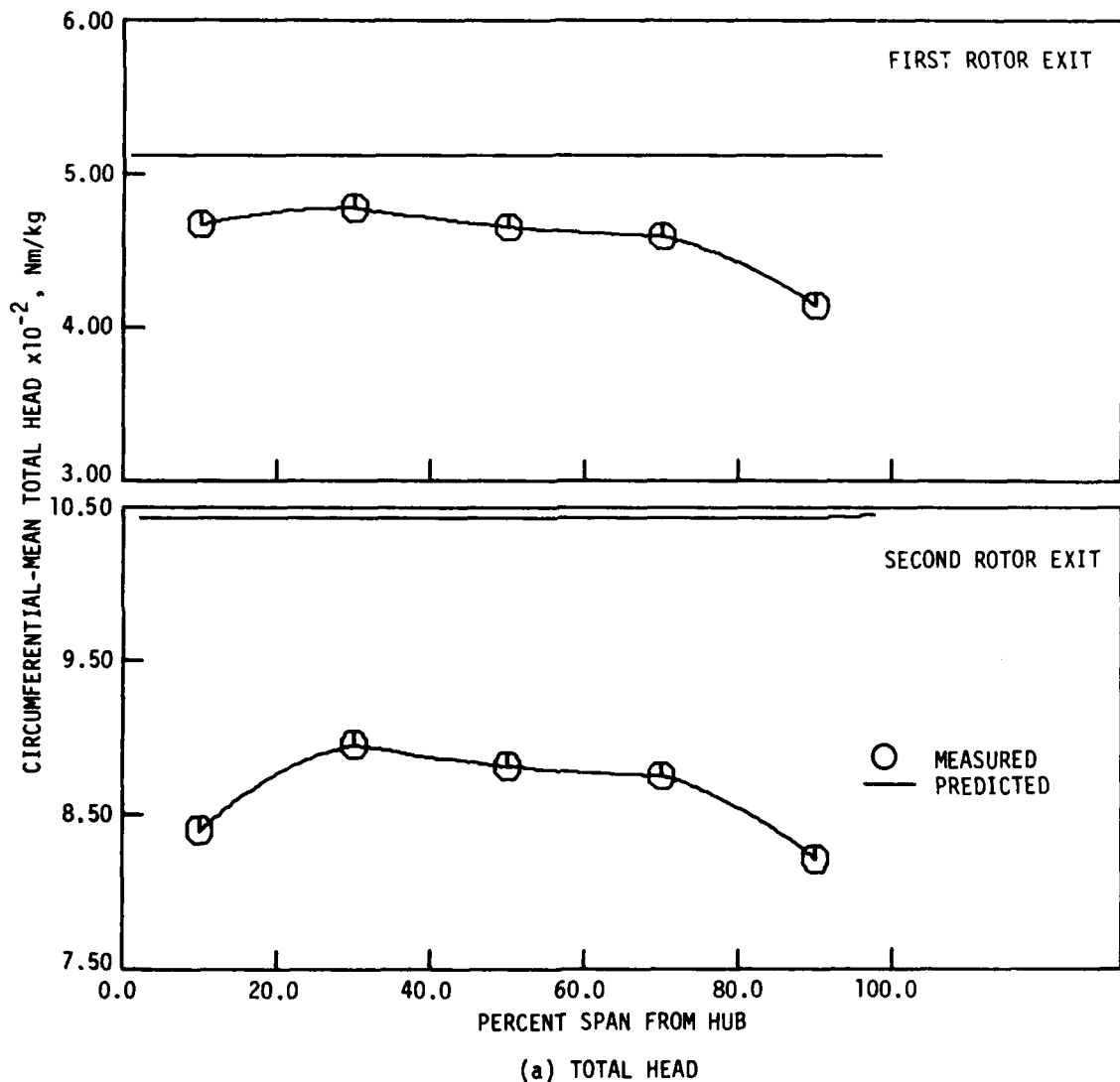


Figure 4.13 concluded.

row. The measured axial velocities are higher than the predicted axial velocities except near the shroud end-wall. As shown in the contour maps of the previous section (see Figure 4.6), there was a loss region (lower total-head fluid) near the shroud end-wall. The lower total-head fluid corresponded to lower axial velocities. In order to achieve the design point flow coefficient, the actual midspan axial velocities would have to be larger to compensate for the lower axial velocities near the shroud end-wall, thus explaining the higher measured midspan axial velocities. Subsequent tests using tuft probes showed that the flow was separating at the shroud lip of the compressor inlet bell housing. This behavior contributed to a larger shroud end-wall boundary layer than might be expected normally. Subsequent tests with a new inlet have all but eliminated flow separation at the inlet of the compressor.

Spanwise distributions of the circumferential-mean values of total head, incidence angles, and deviation angles are shown for the first- and second-stage rotors in Figure 4.14, and for the first- and second-stage stators in Figure 4.15. The comparisons of the measured and predicted spanwise distributions of circumferential-mean total head behind both rotor and stator rows (Figure 4.14 (a) and 4.15 (a)) show significantly lower measured total-head levels than predicted by the design code, and less measured energy addition per stage as well as less overall energy addition than predicted by the design code. As mentioned earlier in connection with the velocity triangle plots (Figures 4.10, 4.11, and 4.12), the measured axial velocities were generally higher than predicted by the design code (also see Figure



(a) TOTAL HEAD

Figure 4.14 Comparisons of the measured and predicted spanwise distributions of circumferential-mean data for the first and second stage rotors ($\phi = 0.587$ at 2400 rpm).

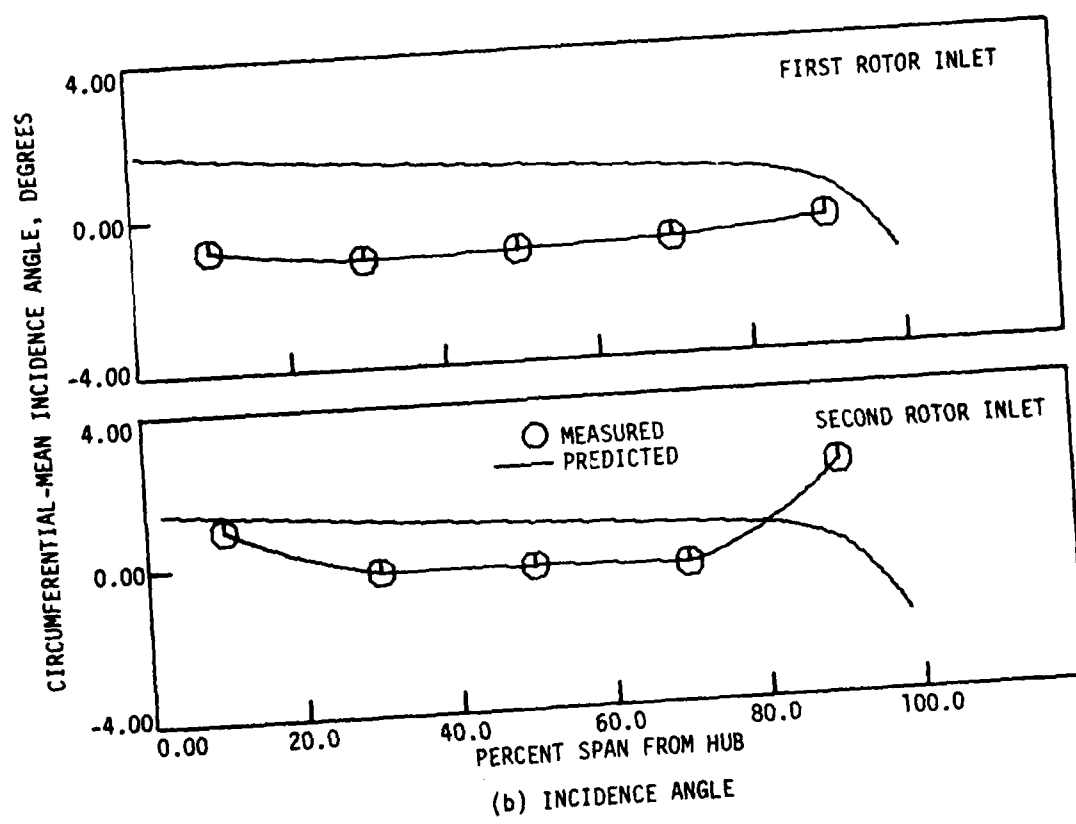


Figure 4.14 continued.

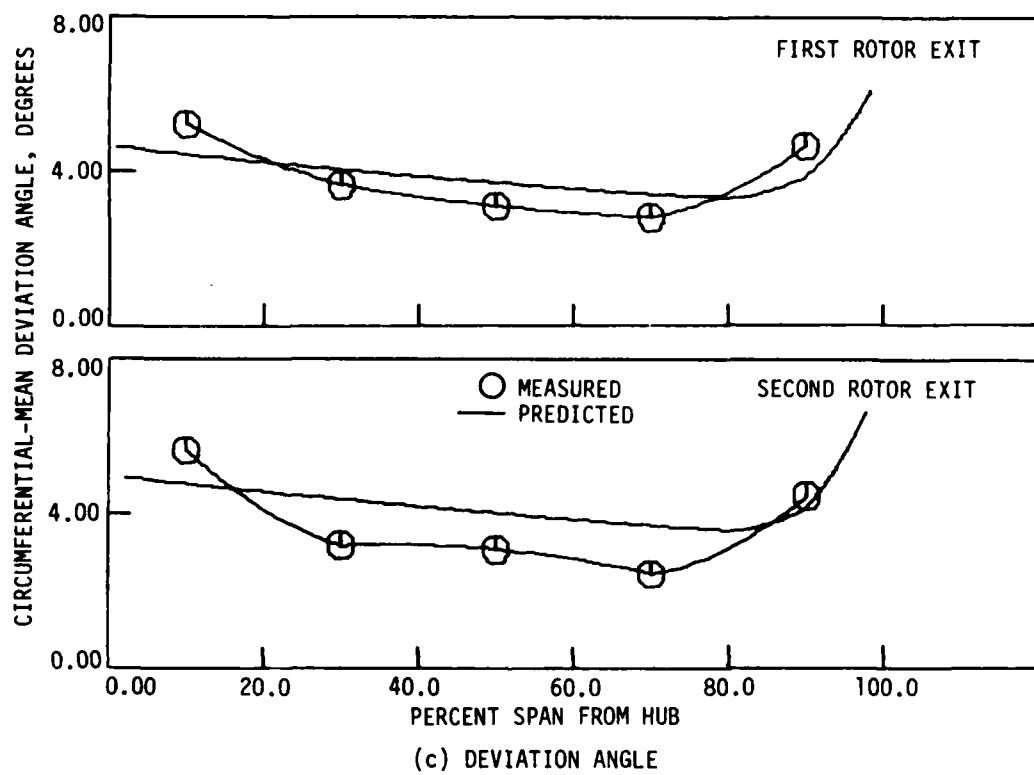


Figure 4.14 concluded.

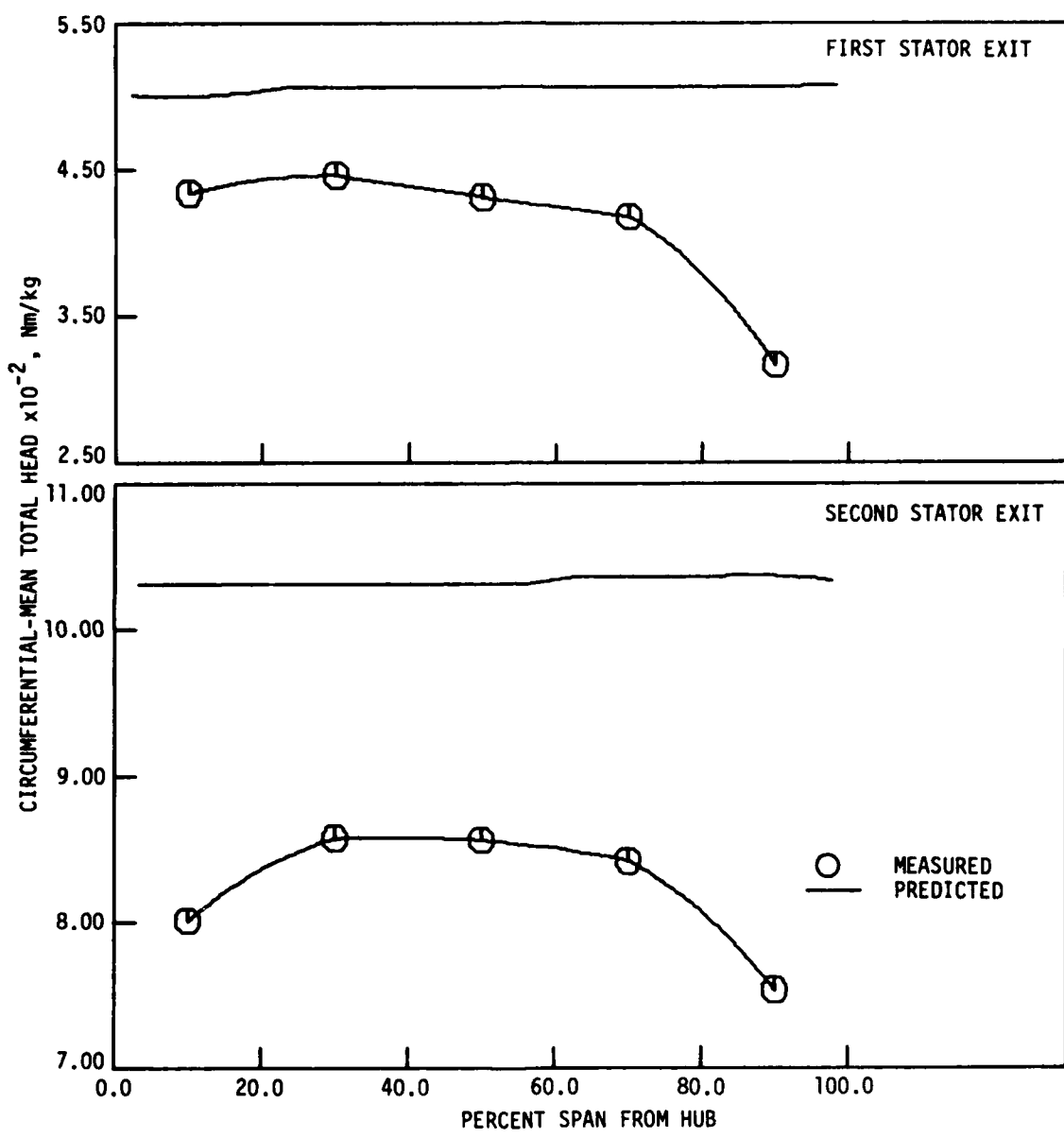


Figure 4.15 Comparisons of the measured and predicted spanwise distributions of circumferential-mean data for the first and second stage stators ($\phi = 0.587$ at 2400 rpm).

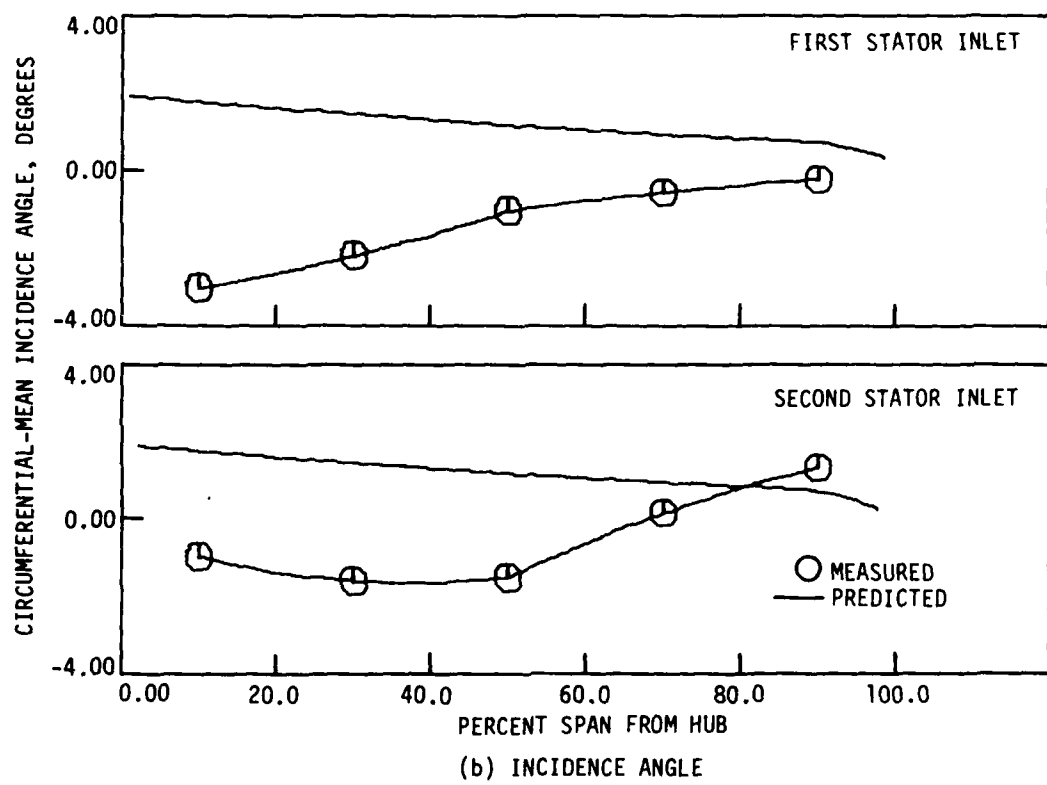


Figure 4.15 continued.

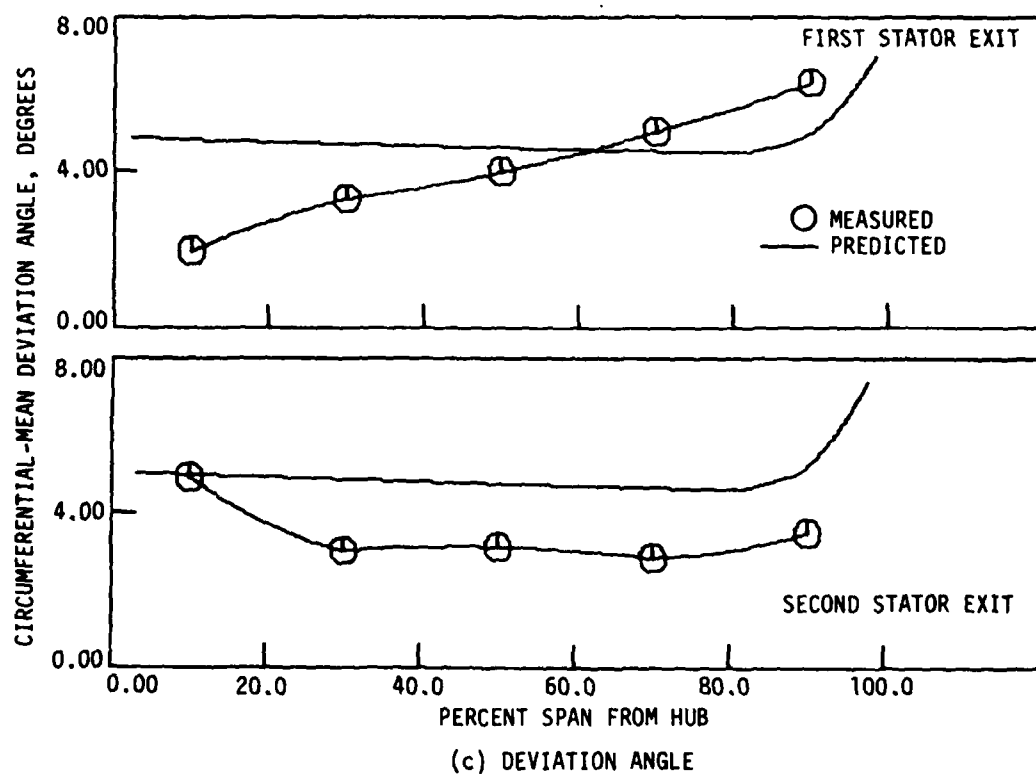


Figure 4.15 concluded.

4.13). The higher measured axial velocities resulted in less measured flow turning than was predicted. With less measured flow, turning the measured energy addition would be less than predicted, as is shown in Figure 4.14 (a) and Figure 4.15 (a). The measured circumferential-mean total head is consistently lowest at the shroud which again shows effects due to the higher shroud end-wall losses as a result of the flow separation at the shroud lip of the inlet bell housing. The measured total head behind the second rotor and stator is also low near the hub which is due to hub end-wall effects beginning to appear there.

As found from inspection of the velocity triangles, the first-stage rotor measured and predicted deviation angles (Figure 4.14 (c)) compared favorably. Flow behind the second rotor exit shows slightly poorer agreement between the measured and predicted deviation angles. The poorer agreement between the measured and predicted deviation angles for the second-stage rotor is due to the fact that the second-stage blade angles for the actual compressor and design code are different (see Figure 4.16). For economic reasons, both stages of the actual compressor were designed based on the first-stage blading of the design code. The actual second-stage rotor exit blade angles are greater than the design code blade angles, and since the measured and predicted relative flow angles were about the same this resulted in smaller deviation angles than predicted by the design code. Figures 4.16 and 4.14 (c) show that the design code blade exit angles for the first rotor are greater than those for the second rotor, and that the design code deviation angles are slightly greater for the second rotor

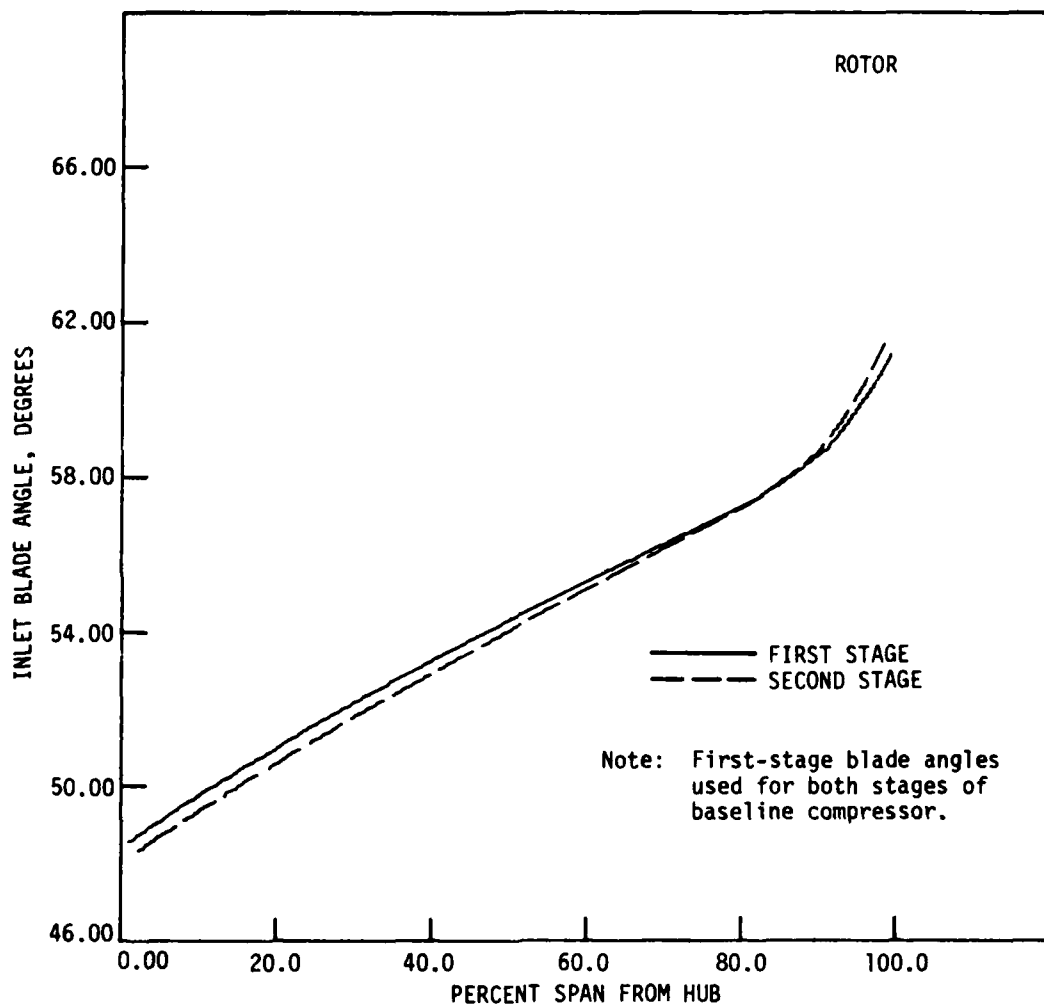


Figure 4.16 Spanwise distributions of design code rotor blade angles.

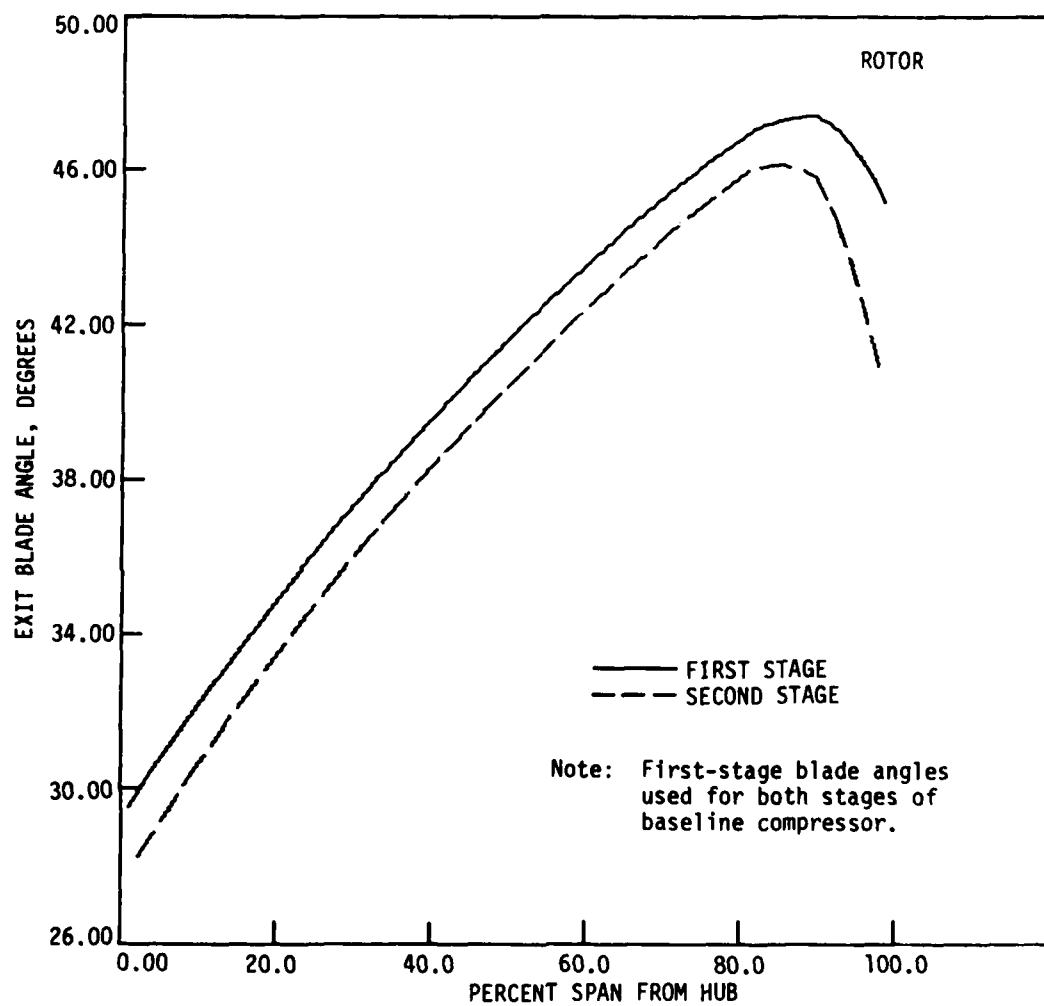


Figure 4.16 concluded

than for the first rotor. The actual blade exit angles for the first and second rotors were the same, and the actual deviation angles for the first and second rotors were about the same. The good agreement between measured and predicted deviation angles indicates that the deviation angle prediction correlation used in the design code (see Appendix A) is quite good. Measured incidence angles (Figure 4.14 (b)) were lower than desired for both rotors. However, these incidence angle differences did not result in appreciable deviation angle differences. Measured stator incidence angles (Figure 4.15 (b)) show poor agreement with predicted stator incidence angles. Comparisons of the measured and predicted stator deviation angles (Figure 4.15 (c)) also show poor agreement. The reason for the poor agreement between measured and predicted stator deviation angles in contrast to the good agreement between measured and predicted rotor deviation angles is partially due to the greater uncertainty in absolute flow angle measurements behind a stator blade row (see Table 4.1). However, not all of the difference between the measured and predicted stator deviation angles can be accounted for by the measurement uncertainty. No satisfactory explanation has been found for the additional differences in measured and predicted stator deviation angles, except to blame the deviation angle prediction method used. A comparison of the stator blade angles for both stages is shown in Figure 4.17.

The spanwise distributions of the measured and predicted blade loss coefficients for each blade row are shown in Figure 4.18. The difficulty in accurately predicting blade losses is evidenced by the large discrepancies between the measured and predicted blade losses.

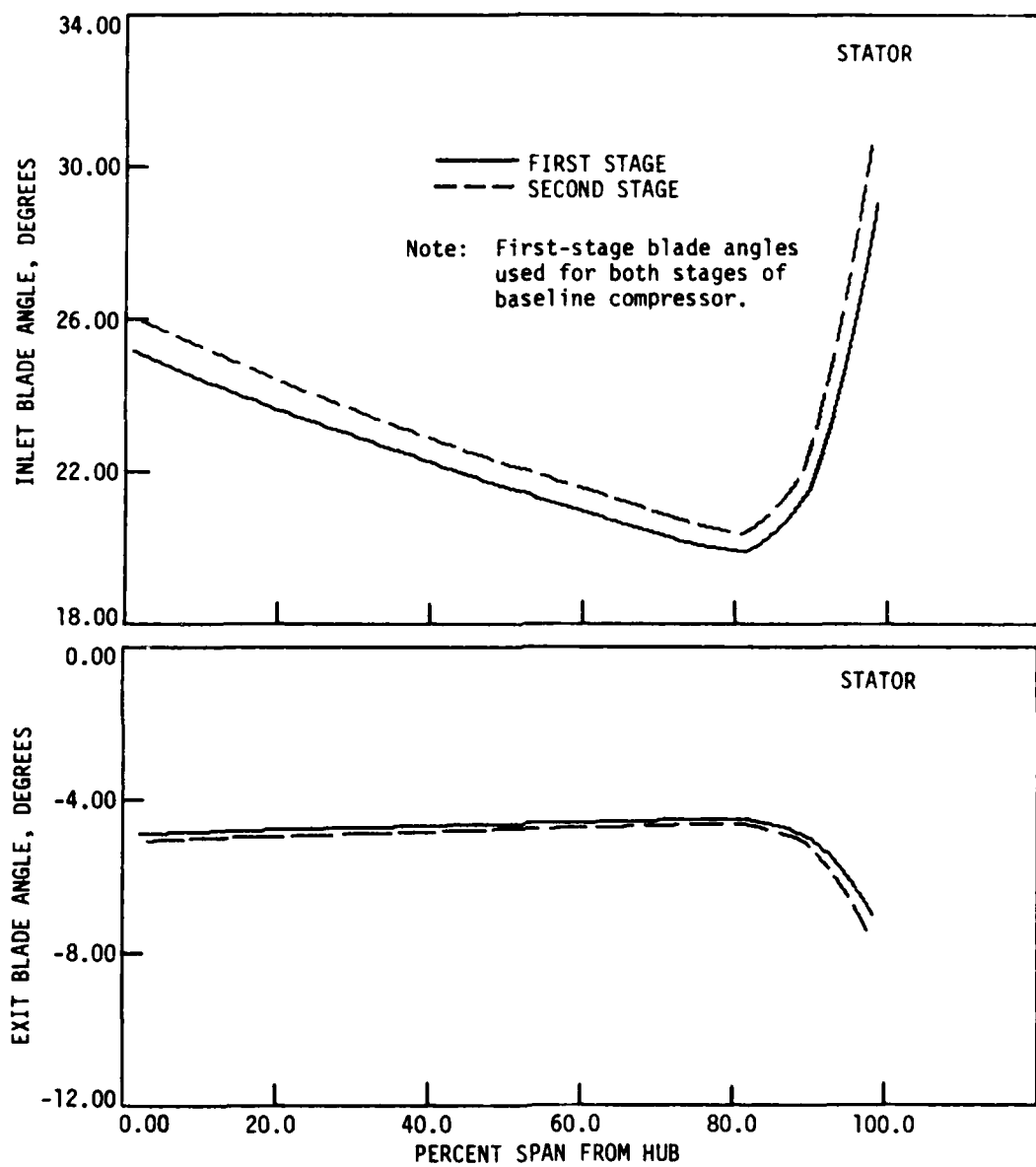


Figure 4.17 Spanwise distributions of design code stator blade angles.

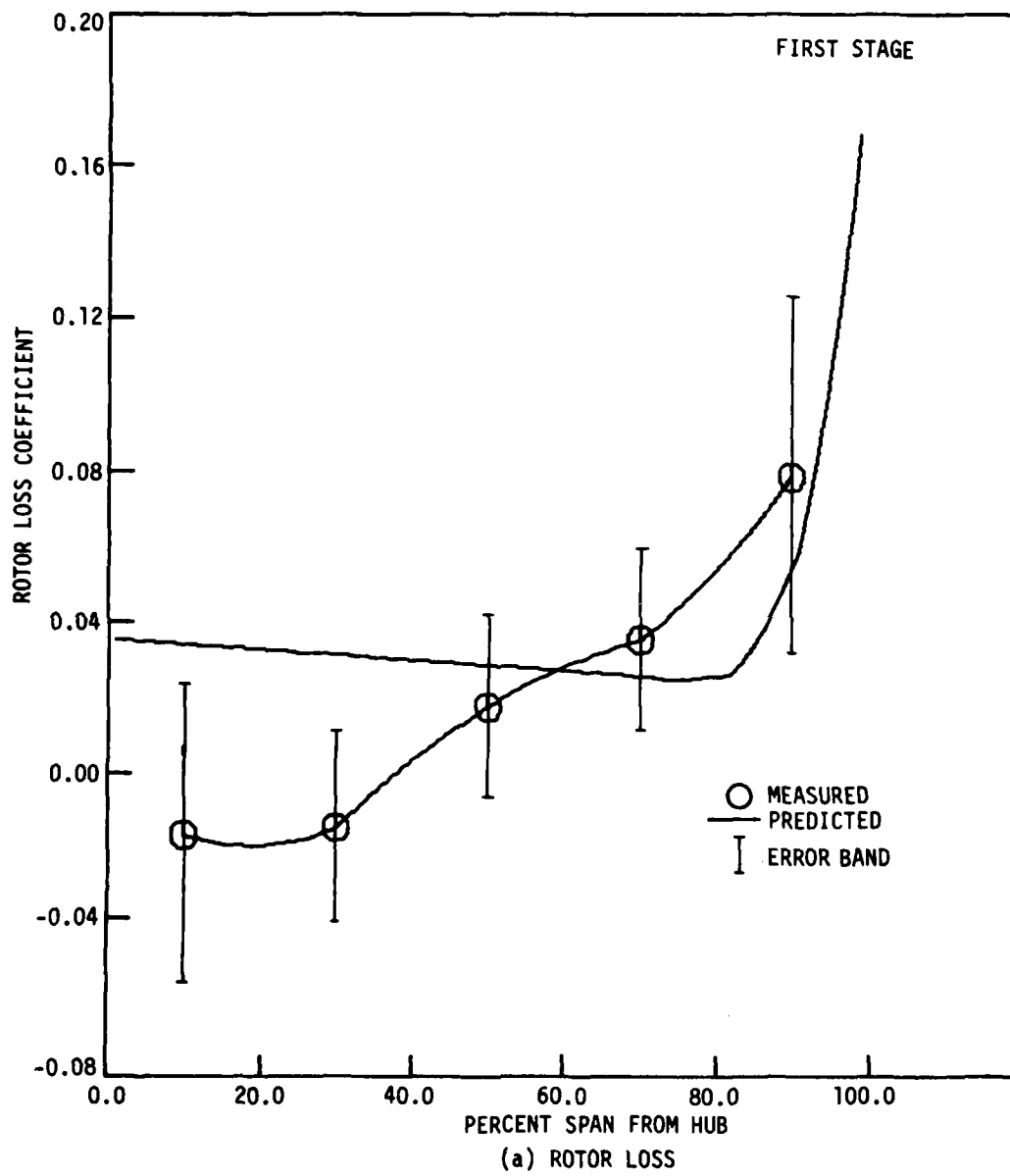


Figure 4.18 Comparisons of measured and predicted spanwise distributions of blade loss for each blade row ($\phi = 0.587$ at 2400 rpm).

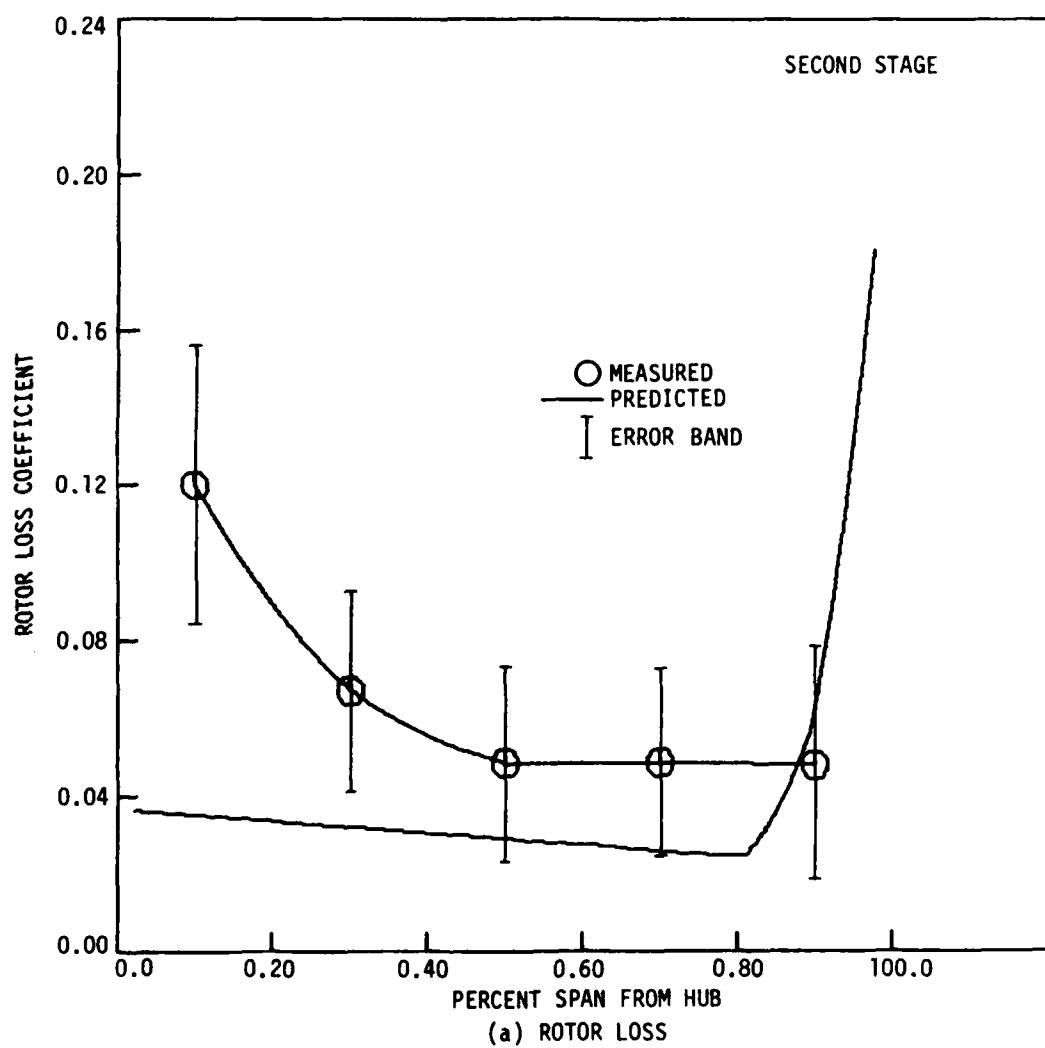
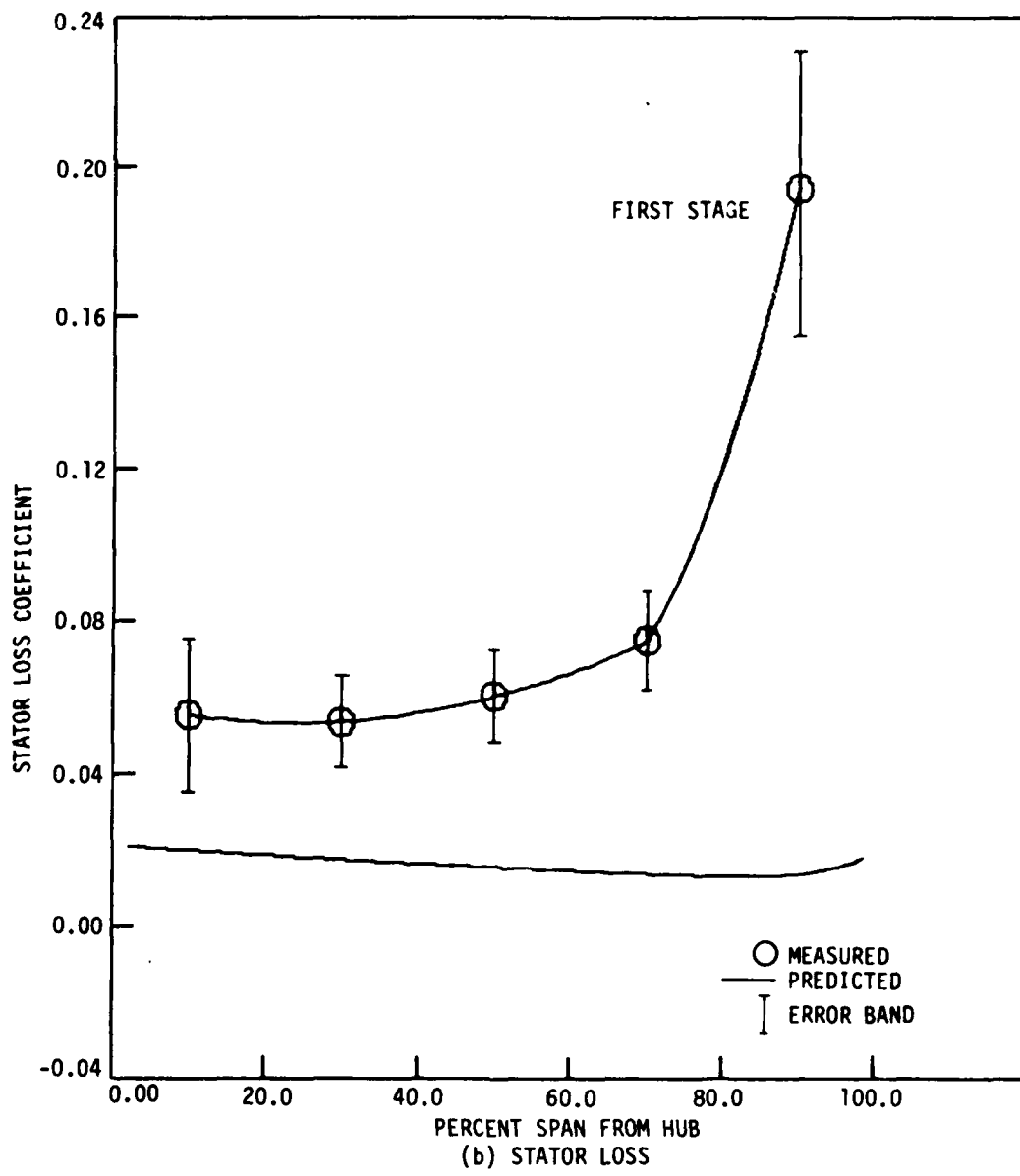


Figure 4.18 Continued.



. Figure 4.18 Continued.

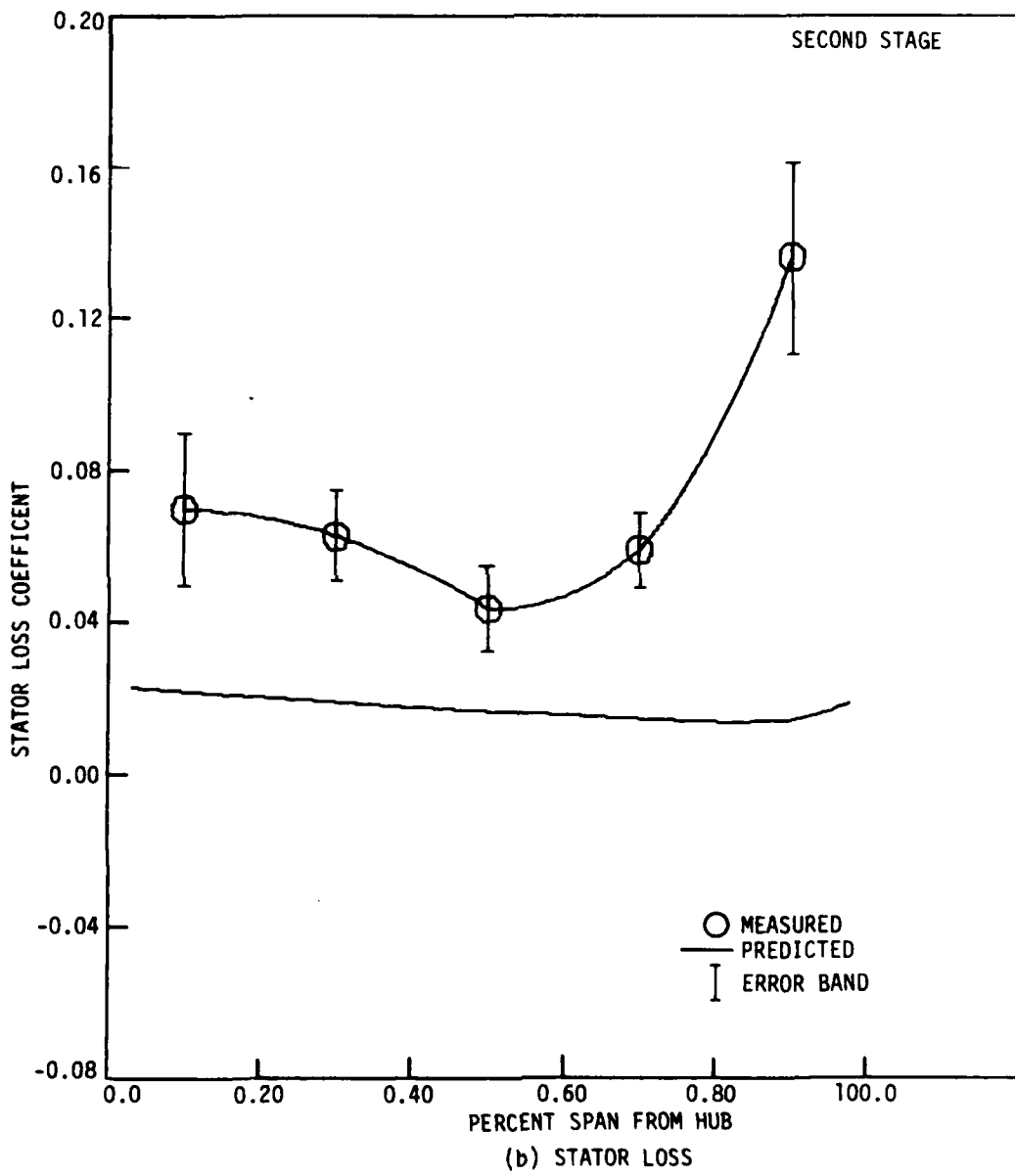


Figure 4.18 Concluded.

Although the uncertainties in the measured loss coefficients are quite large, the design code blade loss predictions are generally lower than the measured losses. Thus, it seems the blade loss correlation used in the design code (see Appendix A) is inadequate. With the lower predicted losses and higher predicted overall energy addition, the predicted overall efficiency would be expected to be much higher than the measured overall efficiency, as is shown in Figure 4.1 (c).

5. SUMMARY AND CONCLUSIONS

A two-stage baseline research compressor has been designed which has resulted in:

1. Higher blade-chord Reynolds numbers than were previously attainable with three-stage compressor blading.
2. A better blade material which would be more durable than that already available.
3. Conventional blade-section shapes.
4. A favorable ratio of number of rotor blades to number of stator blades.
5. Elimination of inlet guide vanes.

This baseline compressor can provide a suitable means for evaluating specific stator blade modifications for possible improved control of end-wall and secondary flows. The data acquisition system and computer programs developed during this research program are expected to aid in the acquisition and reduction of associated time-averaged measurements.

Some limitations of the design code used to design the baseline compressor have been observed. The blade loss prediction correlations (see Appendix A) were shown to be inadequate. The deviation angle correlation (see Appendix A) proved to be quite accurate for predicting rotor but not stator blade deviation angles.

A curious pattern of total head distribution was observed downstream of the second rotor. The relationship between the observed distribution of rotor exit total head and the interaction between

upstream stator wakes and the rotor has been studied further and is discussed in another report (Reference 12).

6. RECOMMENDATIONS FOR FURTHER RESEARCH

The next phase of research included tests of a specific stator blade geometry designed for improved control of end-wall and secondary flows (see Reference 12). A stator blade geometry, designed for improved control of end-wall and secondary flows, was selected and tested in conjunction with the baseline compressor described in this report.

Relative to the compressor design code used to design the baseline compressor, it is clear that improvements in stator blade deviation angle and rotor and stator blade loss prediction correlations are required. These correlation methods were developed in the 1950s from two-dimensional cascade tests of fairly conventional blade sections (i.e., parabolic, circular arc, double circular, etc.). Periodically unsteady effects due to blade wake chopping, transport, and interaction should also be investigated further to help explain the unusual total-head distribution behind the second rotor of the research compressor.

7. REFERENCES

1. Mitchell, W. S., and Soileau, J. F. "Turbine Exit Guide Vane Program." AFAPL-TR-77-75, November 1977.
2. Wisler, D. C. "Core Compressor Exit Stage Study, Volume II-Data and Performance Report for the Baseline Configurations." NACA CR-159498, November 1980.
3. Senoo, Y., Taylor, E. S., Batra, S. K., and Hink, E. "Control of Wall Boundary Layer in an Axial Compressor." Gas Turbine Laboratory Report No. 59, Massachusetts Institute of Technology, June 1960.
4. Schmidt, D. P., and Okiishi, T. H. "Multistage Axial-Flow Turbomachinery Wake Production, Transport, and Interaction." ISU-ERI-Ames-77130, TCRL-7, November 1976.
5. Crouse, J. E., and Gorrell, W. T. "Computer Program for Aerodynamic and Blading Design of Multistage Axial-Flow Compressors." NASA Technical Paper 1946, 1981.
6. Bryans, A. C., and Miller, M. L. "Computer Program for Design of Multistage Axial-Flow Compressors." NASA CR-54530, 1967.
7. Sofrin, T. G. "Aircraft Turbomachinery Noise, Fan Noise." Notes from the Course in the Fluid Dynamics of Turbomachinery, Iowa State University, Ames, Iowa, 1973.
8. Morgan, B. D. "A Water Column Balance Pressure Reference System." Unpublished Report, Department of Mechanical Engineering, Iowa State University, Ames, Iowa 1979.
9. Greville, T. N. E. Theory and Applications of Spline Functions. New York: Academic Press, 1967.

10. Wylie, C. R. Advanced Engineering Mathematics. New York: McGraw-Hill Book Company, Inc., 1975.
11. Kline, S. J., and McClintock, F. A. "Describing Uncertainties in Single Sample Experiments." Mechanical Engineering, 75 (1953), 3-8.
12. Tweedt, D. L., and Okiishi, T. H. "Stator Blade Row Geometry Modification Influence on Two-Stage Axial-Flow Compressor Aerodynamic Performance." ISU-ERI-Ames-84179, TCRL-25, December 1983.
13. Zierke, W. C., and Okiishi, T. H. "Measurement and Analysis of the Periodic Variation of Total Pressure in an Axial-Flow Compressor Stage." ISU-ERI-Ames-81121, TCRL-18, November 1980.
14. Dring, D. P., Joslyn, H. D., and Hardin, L. W. "An Investigation of Axial Compressor Rotor Aerodynamics." Transactions of the ASME, Journal of Engineering for Power 104, No. 1 (January, 1982): 84-96.
15. Johnson, I. A., and Bullock, R. O., eds. "Aerodynamic Design of Axial-Flow Compressors." U.S. NASA SP-36, 1965.

8. ACKNOWLEDGMENTS

We would like to express our appreciation to our colleagues of the Iowa State University Engineering Research Institute/Mechanical Engineering Department Turbomachinery Components Research Laboratory for their assistance and encouragement, in particular, Daniel L. Tweedt for his help in obtaining and reducing data and George K. Serovy for his helpful comments. We are also grateful to Leon Girard and Kurt Ante for their dispatch of related machining, and to the staff of the Iowa State University Engineering Research Institute/Office of Editorial Services/Technical Illustration for their patience and expertise in editing the text and in helping to prepare the many figures and tables in this report. Finally, we acknowledge the support of the Air Force Office of Scientific Research (James D. Wilson - Contract Monitor) throughout.

9. APPENDIX A: USER-DEFINED CORRELATIONS USED IN NASA DESIGN CODE

Advanced compressor design codes frequently require the user to input various empirical correlations of blade profile losses and incidence and deviation angles, and annulus-wall blockage factors. The various user-defined correlations required as input to the NASA design code are presented in this section. The actual tabular input to the design code is given in Appendix B. The variables used in the correlation parameters are defined in the symbols and notation section.

9.1. Blade Loss

The blade loss correlations used are illustrated in Figure 9.1. The loss curves are typical of annular cascade tests of double-circular-arc blades as used in the baseline compressor. The correlating parameters are:

- Loss parameter $\equiv \frac{\bar{w} \cos \beta}{2\sigma} \frac{y_2'}{y_2^2}$ \equiv approximate measure of blade wake momentum thickness to chord ratio.

where $\sigma = c/s$

$$\bullet \text{ D-factor } \equiv 1 - \frac{v_2'}{v_1'} + \frac{(rV_y)_2' - (rV_y)_1'}{\sigma(r_1 + r_2)V_1'}$$

- Percent span from hub

The trends shown are similar to those indicated in Figure 203 of Reference [15].



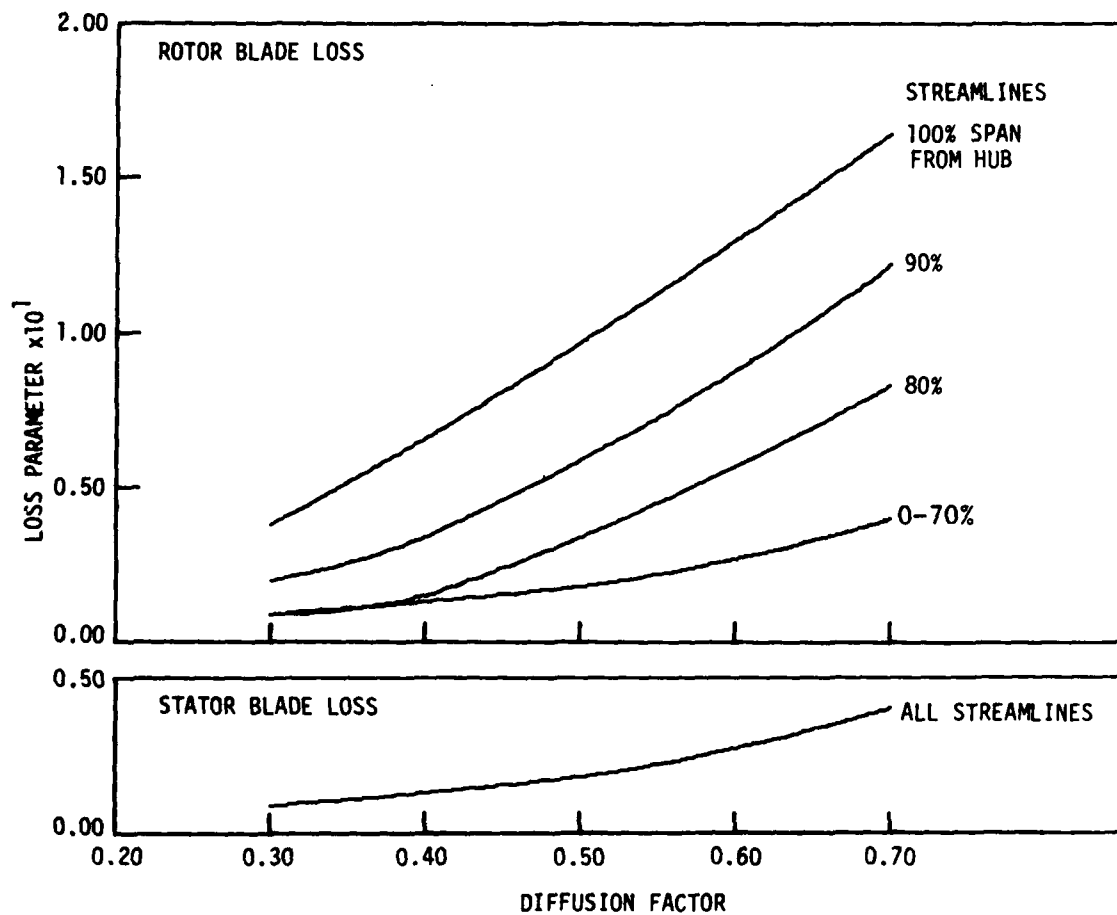


Figure 9.1 Blade loss correlation curves used in NASA design code.

9.2. Incidence and Deviation Angle

The design code provided several options for the incidence and deviation angle correlations. A two-dimensional incidence angle correlation was considered suitable for the baseline compressor design. Carter's rule was selected for the deviation angle correlation. Both correlations are described below.

The incidence angle correlation is described in Chapter VI of Reference 15 in the form of:

$$i = i_0 + n\theta$$

where n is obtained from Figure 138 of Reference 15 as a function of

σ and K_1

θ = blade camber angle

$$i_0 = \frac{(K_i)}{sh} \frac{(K_i)}{t} \frac{(i_0)}{10} = \text{incidence angle for zero camber}$$

where $(i_0)_{10}$ is obtained from Figure 137 of Reference 15

$(K_i)_{sh} = 0.7$ for double circular arc blades

$(K_i)_t$ is obtained from Figure 142 of Reference 15 as a

function of t_{max}/c

The deviation angle correlation (Carter's rule) described in Chapter VII of Reference 15 is

$$\delta = \frac{m_c \theta}{\sqrt{\sigma}}$$

where m_c is obtained from Figure 160 of Reference 15 for circular arc blades.

10. APPENDIX B: NASA DESIGN CODE RESULTS

The output from the NASA design code is presented in the following tables. Table 10.1 lists all input parameters and user-defined correlations, in tabular form, required for the design code analysis. Table 10.2 lists the aerodynamic output (e.g., velocity triangle information, blade element performance, etc.) for 11 streamlines at each axial computation station. The NASA design code gives the streamline radial positions as a percentage of the blade span measured from the shroud end-wall, whereas, the convention used for all data figures in this report is percent span measured from the hub end-wall. Table 10.3 lists the stage and overall mass-averaged aerodynamic performance parameters. Table 10.4 and Table 10.5 list the manufacturing coordinates at 17 spanwise locations for the rotor blade and stator blade, respectively. Only the first stage stator and rotor blade manufacturing coordinates generated from the NASA design code are given as they were used for both stages of the baseline compressor. Figure 10.1 shows representative rotor and stator blade sections and associated manufacturing coordinate nomenclature.

Table 10.1 Design code input parameters.

*** INPUT DATA FOR COMPRESSOR DESIGN PROGRAM ***

AFCOSR/ISU TASK 4 2-STAGE BASE W/SP-36 P-248 LOSS 2400RPM 6SEP79

THE COMPRESSOR ROTATIONAL SPEED IS 2400.0 RPM.
THE DESIRED COMPRESSOR PRESSURE RATIO IS 1.019.
CALCULATIONS WILL BE PERFORMED ON 11 STREAMLINES.

CALCULATIONS WILL BE MADE AT THE BLADE EDGES AND AT 7 ANNULAR STATIONS.

THE INLET FLOW RATE IS 5.250 (LB/SEC).
THE MOLECULAR WEIGHT IS 28.97.
THE COMPRESSOR HAS 4 BLADE ROWS.

STREAMLINE NO.	INLET TOTAL TEMPERATURE (DEG. R.)	INPUT DISTRIBUTIONS BY STREAMLINE OR STREAMTUBE			STREAMTUBE NO.	STREAMTUBE FLOW FRACTION
		INLET TOTAL PRESSURE (PSIA)	INLET MAJIRL VELOCITY (FT/SEC)	*T**4 + 0.0		
1	518.600	14.696	0.0		1	0.1000
2	518.600	14.696	0.0		2	0.2000
3	518.600	14.696	0.0		3	0.3000
4	518.600	14.696	0.0		4	0.4000
5	518.600	14.696	0.0		5	0.5000
6	518.600	14.696	0.0		6	0.6000
7	518.600	14.696	0.0		7	0.7000
8	518.600	14.696	0.0		8	0.8000
9	518.600	14.696	0.0		9	0.9000
10	518.600	14.696	0.0		10	1.0000
11	518.600	14.696	0.0			

Table 10.1 Continued.

INPUT DATA POINTS FOR TIP AND HUB CONTOURS.

TIP AXIAL COORDINATE (INCHES)	TIP RADIUS (INCHES)	HUB AXIAL COORDINATE (INCHES)	HUB RADIUS (INCHES)
-6.000	10.500	-11.530	6.150
-4.100	9.030	-9.100	6.050
-1.750	8.180	-6.100	5.600
0.000	8.000	-5.000	5.400
1.000	8.000	-3.400	5.600
2.500	8.000	0.000	5.600
4.300	8.000	8.000	5.600
7.500	8.000	17.000	5.600
10.500	8.000		
17.000	8.000		

THE INPUT PROFILE LOSS TABLES ~ CMEGA(BAR)*COS(BETA)/(2.0*SIGMA)

** PROFILE LOSS TABLE NO. 1 **									
STREAMLINE	D-FACTOR	LCSS PARAM.	D-FACTOR	LOSS PARAM.	D-FACTOR	LOSS PARAM.	D-FACTOR	LOSS PARAM.	D-FACTOR
1	0.3000	0.0380	0.4000	0.0660	0.5000	0.0970	0.6000	0.1300	0.7000
2	0.3000	0.0380	0.4000	0.0340	0.5000	0.0590	0.6000	0.0880	0.7000
3	0.3000	0.0380	0.4000	0.0150	0.5000	0.0340	0.6000	0.0830	0.7000
4	0.3000	0.0380	0.4000	0.0130	0.5000	0.0180	0.6000	0.0570	0.7000
5	0.3000	0.0380	0.4000	0.0130	0.5000	0.0180	0.6000	0.0270	0.7000
6	0.3000	0.0380	0.4000	0.0130	0.5000	0.0180	0.6000	0.0270	0.7000
7	0.3000	0.0380	0.4000	0.0130	0.5000	0.0180	0.6000	0.0270	0.7000
8	0.3000	0.0380	0.4000	0.0130	0.5000	0.0180	0.6000	0.0270	0.7000
9	0.3000	0.0380	0.4000	0.0130	0.5000	0.0180	0.6000	0.0270	0.7000
10	0.3000	0.0380	0.4000	0.0130	0.5000	0.0180	0.6000	0.0270	0.7000
11	0.3000	0.0380	0.4000	0.0130	0.5000	0.0180	0.6000	0.0270	0.7000
** PROFILE LOSS TABLE NO. 2 **									
STREAMLINE	D-FACTOR	LOSS PARAM.	D-FACTOR	LCSS PARAM.	D-FACTOR	LOSS PARAM.	D-FACTOR	LOSS PARAM.	D-FACTOR
1	0.3000	0.0090	0.4000	0.0130	0.5000	0.0180	0.6000	0.0270	0.7000
2	0.3000	0.0090	0.4000	0.0130	0.5000	0.0180	0.6000	0.0270	0.7000
3	0.3000	0.0090	0.4000	0.0130	0.5000	0.0180	0.6000	0.0270	0.7000
4	0.3000	0.0090	0.4000	0.0130	0.5000	0.0180	0.6000	0.0270	0.7000
5	0.3000	0.0090	0.4000	0.0130	0.5000	0.0180	0.6000	0.0270	0.7000
6	0.3000	0.0090	0.4000	0.0130	0.5000	0.0180	0.6000	0.0270	0.7000
7	0.3000	0.0090	0.4000	0.0130	0.5000	0.0180	0.6000	0.0270	0.7000
8	0.3000	0.0090	0.4000	0.0130	0.5000	0.0180	0.6000	0.0270	0.7000
9	0.3000	0.0090	0.4000	0.0130	0.5000	0.0180	0.6000	0.0270	0.7000
10	0.3000	0.0090	0.4000	0.0130	0.5000	0.0180	0.6000	0.0270	0.7000
11	0.3000	0.0090	0.4000	0.0130	0.5000	0.0180	0.6000	0.0270	0.7000

Table 10.1 Continued.

```

*** PRINTOUT OF INPUT STATION DATA ***

** INPUT SET NO. 1 IS AN ANNULAR STATION **
TIP AXIAL LOCATION      HUB AXIAL LOCATION      TIP BLOCKAGE FACTOR    HUB BLOCKAGE FACTOR    MASS BLEED FRACTION
(INCHES)                  (INCHES)                    (INCHES)                   (INCHES)                   (INCHES)
-5.9500                  -11.4000                     0.0                      0.0                      0.0

** INPUT SET NO. 2 IS AN ANNULAR STATION **
TIP AXIAL LOCATION      HUB AXIAL LOCATION      TIP BLOCKAGE FACTOR    HUB BLOCKAGE FACTOR    MASS BLEED FRACTION
(INCHES)                  (INCHES)                    (INCHES)                   (INCHES)                   (INCHES)
-4.7500                  -8.3500                     0.0030                  0.0030                  0.0

** INPUT SET NO. 3 IS AN ANNULAR STATION **
TIP AXIAL LOCATION      HUB AXIAL LOCATION      TIP BLOCKAGE FACTOR    HUB BLOCKAGE FACTOR    MASS BLEED FRACTION
(INCHES)                  (INCHES)                    (INCHES)                   (INCHES)                   (INCHES)
-3.5800                  -4.9500                     0.0060                  0.0060                  0.0

** INPUT SET NO. 4 IS AN ANNULAR STATION **
TIP AXIAL LOCATION      HUB AXIAL LOCATION      TIP BLOCKAGE FACTOR    HUB BLOCKAGE FACTOR    MASS BLEED FRACTION
(INCHES)                  (INCHES)                    (INCHES)                   (INCHES)                   (INCHES)
-1.4500                  -1.6000                     0.0080                  0.0080                  0.0

```

Table 10.1 Continued.

** INPUT SET NO. 5 IS ROTOR NO. 1 **					
* ALL PROGRAM OPTIONS EXCEPT OFF = DESIGN PUNCH ARE DESIRED FOR THIS BLADE *					
TIP C.G. AXIAL LOCATION (INCHES)	HUB C.G. AXIAL LOCATION (INCHES)	INLET TIP BLOCKAGE	INLET HUB BLOCKAGE	INLET MASS BLEED	
1.03300	1.03300	0.0090	0.0090	0.0	
LOSS SET USED	BLADE TILT ANGLE (DEGREES)	OUTLET TIP BLOCKAGE	OUTLET HUB BLOCKAGE	OUTLET MASS BLEED	
1	0.0	0.0180	0.0090	0.0	
TIP D FACTOR LIMIT	HUB FLOW ANGLE LIMIT (DEGREES)	TIP SOLIDITY	NUMBER OF BLADES	CUM ENERGY ADD FRACT	
0.40000	0.0	1.0027	21	0.5000	
* POLYNOMIAL CONSTANTS FOR THE FOLLOWING *					
TERM	ROTOR OUTLET PRESSURE	L.E. RADIUS/CHORD	T.E. RADIUS/CHORD	MAX. THICKNESS/CHORD	CHORD/TIP CHORD
CONSTANT		0.0100	0.0100	0.0600	0.0
LINEAR	0.0	0.0	0.0	0.0400	0.0
QUADRATIC	0.0	0.0	0.0	0.0	0.0
CUBIC	0.0	0.0	0.0	0.0	0.0
QUARTIC	0.0	0.0	0.0	0.0	0.0
QUINTIC	0.0	0.0	0.0	0.0	0.0
* INPUT BLADE ELEMENT DEFINITION OPTIONS *					
INCIDENCE ANGLE	DEVIATION ANGLE	TURNING RATE RATIO	TRANSITION POINT	MAX. THICKNESS POINT	CHOKE MARGIN
2-D	CARTERS RULE	CIRCULAR ARC	CIRCULAR ARC	TRANS. PT.	NONE
					BLADE MATERIAL DENSITY LB/(IN) ³
					0.10000

Table 10.1 Continued.

*** PRINTOUT OF INPUT STATION DATA ***

** INPUT SET NO. 6 IS A GUIDE VANE OR STATOR **

* ALL PROGRAM OPTIONS EXCEPT OFF - DESIGN PUNCH ARE DESIRED FOR THIS BLADE *

TIP C.G. AXIAL LOCATION (INCHES)	HUB C.G. AXIAL LOCATION (INCHES)	INLET TIP BLOCKAGE	INLET HUB BLOCKAGE	INLET MASS BLEED
5.2600	5.2600	0.0180	0.0090	0.0
LOSS SET USED	BLADE TILT ANGLE (DEGREES)	OUTLET TIP BLOCKAGE	OUTLET HUB BLOCKAGE	OUTLET MASS BLEED
2	0.0	0.0180	0.0180	0.0
HUB D FACTOR LIMIT	INLET HUB MACH LIMIT	TIP SOLIDITY	NUMBER OF BLADES	NTESTK NCVSTK
0.5000	0.5000	1.4324	30	0

* POLYNOMIAL CONSTANTS FOR THE FOLLOWING *

TERM	STATOR OUTLET V(θ)	L.E. RADIUS/CHORD	T.E. RADIUS/CHORD	MAX. THICKNESS/CHORD	CHORD/TIP CHORD
INV.SG.	0.0	0.0100	0.0100	0.1000	0.0
INVERSE	0.0	0.0	0.0	-0.0400	0.0
CONSTANT	0.0	0.0	0.0	0.0	0.0
LINEAR	2.3	0.0	0.0	0.0	0.0
QUADRATIC	3.0	0.0	0.0	0.0	0.0
CUBIC	0.0	0.0	0.0	0.0	0.0

* INPUT BLADE ELEMENT DEFINITION OPTIONS *

INCIDENCE ANGLE	DEVIATION ANGLE	TURNING RATE RATIO	TRANSITION POINT	MAX. THICKNESS POINT	CHOKE MARGIN
2-D	CARTERS RULE	CIRCULAR ARC	CIRCULAR ARC	TRANS. PT.	NONE

Table 10.1 Continued.

** INPUT SET NO. 7 IS ROTOR NO. 2 **

* ALL PROGRAM OPTIONS EXCEPT OFF - DESIGN PUNCH ARE DESIRED FOR THIS BLADE *

TIP C.G. AXIAL LOCATION (INCHES)	HUB C.G. AXIAL LOCATION (INCHES)	INLET TIP BLOCKAGE	INLET HUB BLOCKAGE	INLET MASS BLEED
8.2760	8.2760	0.0180	0.0180	0.0
LOSS SET USED	BLADE TILT ANGLE (DEGREES)	OUTLET TIP BLOCKAGE	OUTLET HUB BLOCKAGE	OUTLET MASS BLEED
1	0.0	0.0270	0.0180	0.0
TIP D FACTOR LIMIT	HUB FLOW ANGLE LIMIT (DEGREES)	TIP SOLIDITY	NUMBER OF BLADES	CUM ENERGY ADD FRAC T
0.4000	0.0	1.0021	21	1.0000

* POLYNOMIAL CONSTANTS FOR THE FOLLOWING *

TERM	ROTOR OUTLET PRESSURE	L.E. RADIUS/CHORD	T.E. RADIUS/CHORD	MAX. THICKNESS/CHORD	CHORD/TIP CHORD
CONSTANT	0.0	0.0100	0.0100	0.0000	0.0
LINEAR	0.0	0.0	0.0	0.0000	0.0
QUADRATIC	0.0	0.0	0.0	0.0000	0.0
CUBIC	0.0	0.0	0.0	0.0000	0.0
QUARTIC	2.0	0.0	0.0	0.0000	0.0
QUINTIC	3.0	0.0	0.0	0.0000	0.0

* INPUT BLADE ELEMENT DEFINITION OPTIONS *

INCIDENCE ANGLE	DEVIATION ANGLE	TURNING RATE RATIO	TRANSITION POINT	MAX. THICKNESS POINT	CHOKE MARGIN	BLADE MATERIAL DENSITY LB/(IN) ³
2-D	CARTERS RULE	CIRCULAR ARC	CIRCULAR ARC	TRANS. PT.	NONE	0.10000

Table 10.1 Continued.

*** PRINTOUT OF INPUT STATION DATA ***

** INPUT SET NO. 9 IS A GUIDE VANE CR STATOR **

* ALL PROGRAM OPTIONS EXCEPT OFF - DESIGN PUNCH ARE DESIRED FOR THIS BLADE *

TIP C.G. AXIAL LOCATION (INCHES)	HUB C.G. AXIAL LOCATION (INCHES)	INLET TIP BLOCKAGE	INLET HUB BLOCKAGE	INLET MASS BLEED
11.7000	11.7000	0.0270	0.0180	0.0
LOSS SET USED	BLADE TILT ANGLE (DEGREES)	OUTLET TIP BLOCKAGE	OUTLET HUB BLOCKAGE	OUTLET MASS BLEED
2	0.0	0.0270	0.0270	0.0
HUB D FACTOR LIMIT	INLET HUB MACH LIMIT	TIP SOLIDITY	NUMBER OF BLADES	NTESTK NCVSTK
0.5000	0.5000	1.4322,	30	0 0

* POLYNOMIAL CONSTANTS FOR THE FOLLOWING *

TERM	STATOR OUTLET V(0)	L-E. RADIUS/CHORD	T-E. RADIUS/CHORD	MAX. THICKNESS/CHORD	CHORD/TIP CHORD
INV SG.	2.0				
INVERSE CONSTANT	0.0	0.0100	0.0100	0.0100	0.0
LINEAR	0.0	0.0	0.0	0.0	0.0
QUADRATIC	0.0	0.0	0.0	0.0	0.0
CUBIC	0.0	0.0	0.0	0.0	0.0

* INPUT BLADE ELEMENT DEFINITION OPTIONS *

INCIDENCE ANGLE	DEVIATION ANGLE	TURNING RATE RATIO	TRANSITION POINT	MAX. THICKNESS POINT	CHOKE MARGIN
2-D	CARTERS RULE	CIRCULAR ARC	CIRCULAR ARC	TRANS. ST.	NONE

*** PRINTOUT OF INPUT STATION DATA ***

** INPUT SET NO. 9 IS AN ANNULAR STATION **		MASS BLEED FRACTION	
TIP AXIAL LOC (INCHES)	FROM HUB AXIAL LOC (INCHES)	TIP BLOCKAGE FACTOR	HUB BLOCKAGE FACTOR
14.5000	14.5000	0.0270	0.0270

Table 10.1 Concluded.

Table 10.2 Design code predictions of aerodynamic parameters.

** VALUES OF PARAMETERS ON STREAMLINES AT STATION. 1. WHICH IS AN ANNULUS **										** VALUES OF PARAMETERS ON STREAMLINES AT STATION. 2. WHICH IS AN ANNULUS **													
STREAMLINE NO.	NO. RADIUS (IN.)	AXIAL COORD. (IN.)	VEL. (FT/SEC)	TANG. VEL. (FT/SEC)	ABS. VEL. (FT/SEC)	ABS. FLOW MACH NO.	ANGLE (DEG)	STREAM SLOPE (1/IN.)	STREAM CURV. (1/IN.)	STREAM PRES. (PSIA)	STATIC TEMP. (DEG.R.)	STREAMLINE NO.	NO. RADIUS (IN.)	AXIAL COORD. (IN.)	VEL. (FT/SEC)	TANG. VEL. (FT/SEC)	ABS. VEL. (FT/SEC)	ABS. FLOW MACH NO.	ANGLE (DEG)	STREAM SLOPE (1/IN.)	STREAM CURV. (1/IN.)	STREAM PRES. (PSIA)	STATIC TEMP. (DEG.R.)
TIP	10.459	-5.950	30.91	42.24	0.0	0.0378	0.0	-4.2-97	0.044	14.696	518.5	TIP	10.459	-5.950	30.91	40.32	0.0361	0.040	14.696	518.6	14.683	518.4	
1	10.459	-5.950	30.91	40.32	0.0	0.0378	0.0	-4.0-97	0.044	14.696	518.5	1	10.459	-5.950	30.91	38.40	0.0344	0.037	14.696	518.6	14.684	518.4	
2	10.459	-5.950	30.91	38.40	0.0	0.0378	0.0	-3.8-98	0.037	14.696	518.5	2	10.459	-5.950	30.91	36.51	0.0327	0.036	14.696	518.6	14.685	518.4	
3	10.459	-5.950	30.91	36.51	0.0	0.0378	0.0	-3.6-97	0.035	14.696	518.5	3	10.459	-5.950	30.91	34.64	0.0310	0.034	14.696	518.6	14.686	518.4	
4	10.459	-5.950	30.91	32.66	0.0	0.0378	0.0	-3.5-97	0.035	14.696	518.5	4	10.459	-5.950	30.91	32.80	0.0294	0.034	14.696	518.6	14.687	518.4	
5	10.459	-5.950	30.91	27.77	0.0	0.0378	0.0	-3.3-98	0.035	14.696	518.5	5	10.459	-5.950	30.91	26.92	0.0279	0.035	14.696	518.6	14.688	518.4	
6	10.459	-5.950	30.91	26.92	0.0	0.0378	0.0	-3.3-98	0.035	14.696	518.5	6	10.459	-5.950	30.91	25.07	0.0265	0.038	14.696	518.6	14.689	518.4	
7	10.459	-5.950	30.91	25.07	0.0	0.0378	0.0	-3.3-98	0.035	14.696	518.5	7	10.459	-5.950	30.91	23.21	0.0265	0.038	14.696	518.6	14.690	518.4	
8	10.459	-5.950	30.91	23.21	0.0	0.0378	0.0	-3.3-98	0.035	14.696	518.5	8	10.459	-5.950	30.91	21.35	0.0265	0.038	14.696	518.6	14.691	518.4	
9	10.459	-5.950	30.91	21.35	0.0	0.0378	0.0	-3.3-98	0.035	14.696	518.5	9	10.459	-5.950	30.91	20.50	0.0254	0.042	14.696	518.6	14.692	518.4	
10	10.459	-5.950	30.91	20.50	0.0	0.0378	0.0	-3.3-98	0.035	14.696	518.5	10	10.459	-5.950	30.91	19.65	0.0247	0.042	14.696	518.6	14.693	518.4	
11	10.459	-5.950	30.91	19.65	0.0	0.0378	0.0	-3.3-98	0.035	14.696	518.5	11	10.459	-5.950	30.91	18.80	0.0247	0.042	14.696	518.6	14.694	518.4	
HUB	8.001	-11.440	19.00	19.00	0.0	0.0378	0.0	-27.0	0.050	14.696	518.5	HUB	8.001	-11.440	19.00	27.20	0.0244	0.050	14.696	518.6	14.695	518.4	

Table 10.2 Continued.

** VALUES OF PARAMETERS ON STREAMLINES AT STATION. 3. WHICH IS AN ANNULUS **									
STREAMLINE NO.	RADIUS (IN.)	AXIAL COORD. (FT/SEC)	MERO. VEL. (FT/SEC)	TANG. VEL. (FT/SEC)	ABS. VEL. (FT/SEC)	ABS. FLOW MACH NO.	STREAM. ANGLE (DEG)	STREAM. CURV. SLOPE (1/IN.)	STATIC PRESS. (PSIA)
1 TIP	6.750	-3.580	70.4	1.4	78.1	0.0700	0.0	0.151	518.0
2	6.520	-3.681	69.1	1.6	75.6	0.0678	-2.5	0.156	518.0
3	6.290	-3.782	73.1	0.0	73.6	0.0656	-2.0	0.121	518.0
4	6.060	-3.883	70.8	0.6	70.8	0.0635	-2.0	0.107	518.0
5	5.830	-4.063	68.6	0.0	68.6	0.0615	-1.8	0.093	518.0
6	5.600	-4.125	66.4	0.0	66.4	0.0595	-1.6	0.079	518.0
7	5.370	-4.177	62.5	0.0	62.5	0.0576	-1.3	0.064	518.0
8	5.140	-4.257	62.3	0.0	62.3	0.0556	-1.0	0.049	518.0
9	4.910	-4.317	62.2	0.8	62.2	0.0536	-0.7	0.034	518.0
10	4.680	-4.359	59.7	79	60.3	0.0516	-0.3	0.020	518.0
11	4.450	-4.390	58.4	0.0	58.4	0.0503	-0.1	0.016	518.0
MUB	5.600	-4.950	56.6	61	56.6	0.0498	0.0	0.012	518.0

** VALUES OF PARAMETERS ON STREAMLINES AT STATION. 4. WHICH IS AN ANNULUS **									
STREAMLINE NO.	RADIUS (IN.)	AXIAL COORD. (FT/SEC)	MERO. VEL. (FT/SEC)	TANG. VEL. (FT/SEC)	ABS. VEL. (FT/SEC)	ABS. FLOW MACH NO.	STREAM. ANGLE (DEG)	STREAM. CURV. SLOPE (1/IN.)	STATIC PRESS. (PSIA)
1 TIP	6.120	-1.450	99.0	0.0	100.0	0.0897	0.0	0.109	518.0
2	6.120	-1.451	98.0	0.6	98.0	0.0872	0.7	0.099	518.0
3	6.120	-1.452	97.0	0.0	96.5	0.0847	0.6	0.097	518.0
4	6.120	-1.453	95.6	0.0	95.6	0.0828	0.6	0.097	518.0
5	6.120	-1.454	93.9	0.6	94.6	0.0803	0.6	0.095	518.0
6	6.120	-1.455	92.3	0.0	92.3	0.0785	0.6	0.093	518.0
7	6.120	-1.456	90.2	0.6	90.2	0.0763	0.5	0.091	518.0
8	6.120	-1.457	89.0	1.1	90.1	0.0743	0.5	0.089	518.0
9	6.120	-1.458	89.7	0.0	89.7	0.0723	0.5	0.088	518.0
10	6.120	-1.459	88.6	0.0	88.6	0.0703	0.5	0.087	518.0
11	6.120	-1.460	87.5	0.0	87.5	0.0683	0.5	0.086	518.0
MUB	5.600	-1.600	87.5	59	87.5	0.0675	0.0	0.016	518.0

Table 10.2 Continue:

** VALUES OF PARAMETERS ON STREAMLINES AT STATION S, WHICH IS THE INLET OF ROTOR NUMBER 1 **											
STREAMLINE NO.	REL. FLOW ANGLE (DEG)	REL. VEL. (FT/SEC.)	VEL. (FT/SEC.)	VEL. (FT/SEC.)	VEL. (FT/SEC.)	VEL. (FT/SEC.)	VEL. (FT/SEC.)	VEL. (FT/SEC.)	VEL. (FT/SEC.)	VEL. (FT/SEC.)	VEL. (FT/SEC.)
Axial coord. (in.)	Axial vel. (ft/sec.)	Merv. vel. (ft/sec.)	Tang. vel. (ft/sec.)	Abs. vel. (ft/sec.)	Abs. mach no.	Abs. flow slope (deg)	Stream curv. (deg)	Total press. (psia)	Total temp. (deg.R.)	Static press. (psia)	Static temp. (deg.R.)
1 1.144	1.143	98.37	98.38	98.38	0.0862	0.0	-0.68	-0.012	14.606	518.60	14.616
2 1.092	1.128	98.59	98.60	98.60	0.0864	0.0	-0.63	-0.008	14.609	518.60	14.616
3 7.779	1.113	98.70	98.71	98.71	0.0865	0.0	-0.68	-0.003	14.603	518.60	14.616
4 7.357	1.097	98.71	98.71	98.71	0.0865	0.0	-0.63	-0.003	14.603	518.60	14.616
5 7.156	1.080	98.64	98.65	98.65	0.0865	0.0	-0.63	-0.004	14.603	518.60	14.616
6 6.908	1.062	98.52	98.53	98.53	0.0864	0.0	-0.63	-0.004	14.603	518.60	14.616
7 6.672	1.042	98.37	98.38	98.38	0.0863	0.0	-0.75	-0.006	14.606	518.60	14.616
8 6.427	1.021	98.22	98.22	98.22	0.0862	0.0	-0.66	-0.005	14.606	518.60	14.616
9 6.172	0.997	98.09	98.09	98.09	0.0860	0.0	-0.57	-0.005	14.606	518.60	14.617
10 5.906	0.971	98.00	98.00	98.00	0.0878	0.0	-0.13	-0.003	14.606	518.60	14.617
11 5.626	0.942	98.01	98.01	98.01	0.0878	0.0	-0.21	-0.005	14.606	518.60	14.617
HUB	5.600	0.940									
STREAMLINE NO. R/TIP	REL. FLOW ANGLE (DEG)	REL. VEL. (FT/SEC.)	REL. VEL. (FT/SEC.)	REL. VEL. (FT/SEC.)	REL. MACH NUMBER	WHEEL SPEED (FT/SEC.)	FLOW COEF.	L/E RAD. /CHORD	MAX. TH. /CHORD	TRANSP. PT./LOC. /CHORD	SEGMENT LAYOUT IN/OUT CONE ANG. TURN RATE (DEG.)
TIP	1.0000	59.52	167.18	193.98	0.1739	167.57	0.5871	0.0100	0.0600	0.5000	1.0000
1 0.9973	56.82	162.93	190.44	0.1707	167.18	0.5883	0.0100	0.0335	0.5000	0.5000	-0.17
2 0.9463	58.10	158.56	186.78	0.1674	162.93	0.5893	0.0100	0.070	0.5000	1.0000	-0.99
3 0.9195	57.35	154.02	182.99	0.1640	158.56	0.5899	0.0100	0.0606	0.5000	1.0000	-0.92
4 0.8919	56.57	149.46	179.08	0.1605	154.08	0.5896	0.0100	0.0744	0.5000	1.0000	-0.81
5 0.8634	55.75	144.69	177.05	0.1569	149.46	0.5879	0.0100	0.0782	0.5000	1.0000	-0.72
6 0.8339	54.86	139.75	170.90	0.1532	139.75	0.5870	0.0100	0.0922	0.5000	1.0000	-0.52
7 0.8033	53.88	134.61	166.64	0.1494	134.61	0.5861	0.0100	0.0964	0.5000	1.0000	-0.41
8 0.7714	52.81	129.27	162.27	0.1454	129.27	0.5853	0.0100	0.0907	0.5000	1.0000	-0.29
9 0.7381	51.61	123.69	157.80	0.1414	123.69	0.5849	0.0100	0.0953	0.5000	1.0000	-0.15
10 0.7032	50.25	117.83	153.26	0.1374	117.83	0.5849	0.0100	0.1000	0.5000	1.0000	-0.00
--- INLET STREAMLINE ---											
STREAMLINE NO.	INC. ANGLE (DEG)	ANGLE (DEG)	ANGLE (DEG)	ANGLE (DEG)	BL. SET (DEG)	BL. ANGLE (DEG)	S. S. C. ANGLE (DEG)	COV. LOC. AS FRACT. LOCATION OF S.S.	MIN. CHK. AREA OF S.S.	MIN. CHK. PT. LOC. IN CIR. CEN. COV. CHAN. R/D# /DR	L.E. EDGE
1	0.77	-1.58	-6.23	61.11	53.17	53.16	12.59	0.2711	0.7927	0.2073	-0.1209
2	1.923	0.52	-4.94	58.70	53.05	53.05	10.71	0.2632	0.7653	0.2338	-0.0661
3	17.91	0.53	-4.84	57.46	52.24	52.24	10.70	0.2453	0.7363	0.2637	-0.0421
4	26.83	0.77	-5.12	56.58	51.44	51.44	11.34	0.2400	0.7049	0.2951	-0.0449
5	36.01	0.87	-5.46	55.71	50.51	50.51	12.02	0.2349	0.6728	0.3272	-0.0481
6	45.50	0.98	-5.79	54.77	49.52	49.52	12.95	0.2293	0.6400	0.3600	-0.0532
7	55.33	1.09	-6.13	53.77	52.76	52.76	13.88	0.2235	0.6063	0.3937	-0.0598
8	65.53	1.21	-6.48	52.67	51.67	51.67	14.91	0.2172	0.5717	0.4283	-0.0663
9	76.16	1.34	-6.84	51.47	51.46	51.46	15.04	0.2105	0.5359	0.4641	-0.0793
10	87.26	1.49	-7.19	50.11	50.12	50.12	15.42	0.2034	0.4988	0.5012	-0.0903
11	98.90	1.67	-7.53	48.57	48.56	48.56	15.87	0.1958	0.4602	0.5398	-0.0982

Table 10.2 Continued.

** VALUES OF PARAMETERS ON STREAMLINES AT STATION. 6. WHICH IS THE OUTLET OF ROTOR NUMBER. 1 **

STREAMLINE NO.	AXIAL COORD. (IN.)	AXIAL VEL. (FT/SEC.)	ZERO VEL. (FT/SEC.)	TANG. VEL. (FT/SEC.)	ABS. VEL. (FT/SEC.)	ABS. FLOW MACH NO.	STREAM SLOPE (DEG)	STREAM CURV. (1./IN.)	TOTAL PRESS. (PSIA)	TOTAL TEMP. (DEG.R.)	STATIC TEMP. (DEG.R.)
TIP	6.000	2.595	92.40	92.40	51.69	105.98	0.0949	29.32	-6.45	0.0118	14.787
1	7.963	2.595	98.26	98.26	40.25	106.19	0.0956	22.27	-6.62	0.0113	14.787
2	7.754	2.595	99.83	99.82	37.72	106.27	0.0956	20.70	-6.70	0.0105	14.787
3	7.547	2.595	99.66	99.66	38.54	107.00	0.0958	21.11	-6.46	0.0098	14.787
4	7.335	2.615	99.62	99.62	39.83	107.32	0.0965	21.78	-6.38	0.0095	14.787
5	7.117	2.637	99.66	99.66	41.14	107.32	0.0965	22.45	-6.31	0.0093	14.787
6	6.891	2.660	99.55	99.55	42.59	108.20	0.0965	23.18	-6.24	0.0093	14.787
7	6.657	2.666	99.47	99.47	44.20	109.00	0.0974	23.97	-6.19	0.0092	14.787
8	6.415	2.713	99.41	99.41	46.00	109.53	0.0981	24.84	-6.14	0.0091	14.787
9	6.163	2.743	99.38	99.38	48.04	110.52	0.0989	25.80	-6.12	0.0091	14.787
10	5.901	2.775	99.38	99.38	50.39	111.44	0.0988	26.88	-6.15	-0.002	14.787
11	5.626	2.810	99.40	99.40							14.787
HUB	5.600	2.814									14.787
<hr/>											
STREAMLINE NO.	REL.FLOW ANGLE (DEG)	REL.TANG. VEL. (FT/SEC.)	REL.MACH NUMBER	WHEEL SPEED (FT/SEC.)	FLOW COEF.	HEAD COEF.	IDEAL HEAD COEF.	ADIA. EFF.	DIFFUSION FACTOR	LOSS COEFF.	SHOCK LOSS COEFF.
TIP	1.0000	51.19	114.98	147.43	0.1320	166.78	0.5514	0.1967	0.3082	0.6381	0.1678
1	0.9954	51.19	120.15	156.77	0.1404	162.40	0.5864	0.1967	0.2330	0.8439	0.068
2	0.9693	51.19	120.34	156.36	0.1400	158.07	0.5958	0.1967	0.2126	0.9250	0.0259
3	0.9434	51.32	152.34	152.34	0.1364	153.63	0.5957	0.1967	0.2111	0.9315	0.045
4	0.9169	49.06	115.09	147.86	0.1324	149.05	0.5941	0.1967	0.2117	0.9292	0.0264
5	0.8896	47.62	109.23	103.18	0.1328	143.38	0.5936	0.1967	0.2117	0.922	0.0277
6	0.8614	46.03	104.23	96.85	0.1284	139.43	0.5933	0.1967	0.2117	0.9291	0.0214
7	0.8322	44.21	90.16	83.90	0.1202	134.36	0.5931	0.1967	0.2116	0.9295	0.005
8	0.8019	42.21	75.54	37.24	0.1160	129.09	0.5930	0.1967	0.2115	0.9298	0.020
9	0.7704	39.90	63.09	37.24	0.1118	123.59	0.5930	0.1967	0.2115	0.9213	0.037
10	0.7376	34.16	67.44	60.076	0.1076	117.83	0.5932	0.1967	0.2114	0.9319	0.0354
11	0.7033										0.020
HUB	0.7000										
<hr/>											
STREAMLINE NO.	PRESS. RATIO [*]	TEMP. RATIO	AERO. CHORD (IN.)	MEAN SPACING (IN.)	LOCAL RADIUS (IN.)	BLADE FORAXIAL TANG. (LBSS/IN.)	OUTLET T.E.RAD. /CHORD (DEG)	STREAMLINE ANGLE (DEG)	CONE ANGLE (DEG)	CUT-BLADE ANGLE (DEG)	LAYOUT CIR. /CHORD (DEG)
1	1.54	1.0062	1.0028	2.3919	2.3854	7.973	0.1643	-0.1957	0.0100	6.02	4.517
2	10.24	1.0062	1.0021	2.3919	2.3238	7.767	0.1807	-0.1512	0.0100	3.80	45.22
3	16.86	1.0062	1.0019	2.3919	2.2616	7.559	0.1794	-0.1394	0.0100	3.29	47.18
4	27.69	1.0062	1.0019	2.3919	2.1979	7.346	0.1732	-0.1385	0.0100	3.35	45.7
5	36.79	1.0062	1.0019	2.3919	2.1322	7.126	0.1663	-0.1387	0.0100	3.48	44.14
6	46.19	1.0062	1.0019	2.3919	2.0644	6.900	0.1592	-0.1386	0.0100	3.62	42.41
7	55.93	1.0062	1.0019	2.3918	1.9941	6.665	0.1517	-0.1384	0.0100	3.77	40.76
8	66.02	1.0062	1.0019	2.3918	6.421	6.421	0.1440	-0.1382	0.0100	3.95	38.76
9	76.51	1.0062	1.0019	2.3918	6.168	6.168	0.1380	-0.1380	0.0100	4.15	35.76
10	87.45	1.0062	1.0019	2.3918	5.903	5.903	0.1272	-0.1379	0.0100	4.37	32.87
11	98.90	1.0062	1.0019	2.3918	5.626	5.626	0.1181	-0.1413	0.0100	4.62	29.95

Table 10.2 Continued:

** VALUES OF PARAMETERS ON STREAMLINES AT STATION. 7. WHICH IS THE INLET OF STATOR NUMBER. 1. OF STAGE NUMBER. 1. *									
STREAMLINE NO.	AXIAL COORD. (IN.)	AXIAL VEL. (FT/SEC.)	TANG. VEL. (FT/SEC.)	ABS. MACH NO. (FT/SEC.)	ABS. FLOW ANGLE (DEG)	STREAM SLOPE (DEG)	STREAM CURV. (1/IN.)	TOTAL PRESS. (PSIA)	STATIC TEMP. (DEG.R.)
1 TIP	4.12	4.117	9.2-18	51.89	10.76	0.052	22.39	0.12	-0.005
2	7.733	4.093	9.8-32	40.51	10.627	0.057	22.29	0.12	0.004
3	7.547	4.089	9.9-97	37.78	10.687	0.057	20.71	0.10	0.006
4	7.335	4.090	10.0-00	38.60	10.719	0.060	21.11	0.09	0.006
5	7.117	4.091	9.9-84	39.88	10.751	0.063	22.45	0.10	0.006
6	6.892	4.093	9.9-70	41.19	10.787	0.066	22.45	0.12	0.006
7	6.652	4.094	9.9-55	42.63	10.829	0.070	23.18	0.14	0.006
8	6.417	4.094	9.9-39	44.23	10.874	0.074	23.99	0.16	0.007
9	6.165	4.095	9.9-21	46.02	10.936	0.079	24.89	0.22	0.008
10	5.902	4.101	9.8-97	48.97	10.985	0.085	25.76	0.27	0.010
11	5.626	4.104	9.8-64	50.39	110.77	0.092	27.06	0.33	0.015
HUB	5.600	4.105						0.015	14.687
STREAMLINE NO. R/TIP	REL. FLOW COEF.	FLOW ANGLE (DEG.)	L-E RAD. /CHORD	MAX. TH. CHORD	MAX. TH. PT./LOC.	TRAN. PT. /CHRD	SEGMENT LOCATION	LAYOUT IN/OUT CONE ANG.	LAYOUT TURN RATE (DEG.)
1 TIP	1.0000	0.5501	51.15	0.100	0.100	0.500	0.500	1.0000	0.01
2	0.9932	0.5868	51.15	0.100	0.064	0.500	0.500	1.0000	0.21
3	0.943	0.5946	50.27	0.000	0.039	0.500	0.500	1.0000	0.44
4	0.949	0.5968	49.00	0.000	0.093	0.500	0.500	1.0000	0.33
5	0.8897	0.5948	48.56	0.000	0.055	0.500	0.500	1.0000	0.23
6	0.8615	0.5949	45.96	0.000	0.081	0.500	0.500	1.0000	0.23
7	0.8221	0.5941	44.21	0.000	0.077	0.500	0.500	1.0000	0.28
8	0.8021	0.5931	42.22	0.000	0.035	0.500	0.500	1.0000	0.33
9	0.7707	0.5920	39.55	0.000	0.092	0.500	0.500	1.0000	0.40
10	0.7358	0.5920	37.36	0.000	0.047	0.500	0.500	1.0000	0.50
11	0.7032	0.5886	34.36	0.000	0.000	0.500	0.500	1.0000	0.64
HUB	0.6999								
--- INLET STREAMLINE --- IN BLADE ANGLE (DEG.)									
INC. S.S. INC. ANGLE (DEG.)									
STREAMLINE NO.	PCT. SPAN	ANGLE (DEG.)	ANGLE (DEG.)	ANGLE (DEG.)	BL. ANGLE (DEG.)	BL. ANGLE (DEG.)	SEG. LOC. (DEG.)	LOC. AT SHOCK (DEG.)	LOC. AT SHOCK (DEG.)
1	0.227	0.33	-8.66	29.11	11.06	11.06	27.04	0.1203	0.2604
2	0.689	0.89	-7.54	21.58	6.17	6.17	22.00	0.1022	0.753
3	2.679	0.89	-7.04	19.91	7.9	7.70	22.55	0.0972	0.753
4	1.162	0.95	-7.04	20.23	7.45	7.66	20.30	0.103	0.843
5	4.6115	1.10	-5.95	20.78	8.17	8.11	20.16	0.1037	0.752
6	5.677	1.23	-5.37	21.34	8.37	8.37	20.04	0.1037	0.752
7	6.594	1.37	-4.37	21.95	8.66	8.66	19.91	0.1096	0.752
8	7.643	1.52	-4.10	22.62	8.93	8.93	19.79	0.1157	0.752
9	8.740	1.70	-3.42	23.36	9.31	9.32	18.60	0.1157	0.752
10	9.811	1.90	-2.66	24.20	9.70	9.71	19.62	0.1157	0.752
11	98.91	1.90	-2.66	25.16	10.15	10.16	19.60	0.1126	0.7803

Table 10.2 Continued.

** VALUES OF PARAMETERS ON STREAMLINES AT STATION, 6, WHICH IS THE OUTLET OF STATOR NUMBER, 1 **											
STREAMLINE NO.	AXIAL COORD. (IN.)	AXIAL VEL. (FT/SEC.)	MERID. VEL. (FT/SEC.)	TANG. VEL. (FT/SEC.)	ABS. VEL. (FT/SEC.)	MACH NO.	ABS. FLOW ANGLE (DEG.)	STREAM SLOPE (1./IN.)	STREAM CURV. (DEG.)	TOTAL PRESS. (PSIA)	STATIC TEMP. (DEG.R.)
TIP	6.000	6.462	99.43	99.43	99.43	0.0890	0.0	0.110	-0.004	14.766	520.04
1	7.963	6.461	99.59	99.59	99.59	0.0892	0.0	0.112	-0.003	14.786	519.69
2	7.762	6.458	99.70	99.70	99.70	0.0893	0.0	0.119	-0.005	14.786	519.59
3	7.556	6.457	99.78	99.78	99.78	0.0893	0.0	0.116	-0.005	14.786	519.59
4	7.345	6.457	99.85	99.85	99.85	0.0894	0.0	0.115	-0.006	14.786	519.59
5	7.127	6.457	99.93	99.93	99.93	0.0895	0.0	0.116	-0.006	14.786	519.59
6	6.902	6.457	100.01	100.01	100.01	0.0896	0.0	0.118	-0.006	14.786	519.59
7	6.671	6.457	100.10	100.10	100.10	0.0896	0.0	0.121	-0.007	14.786	519.59
8	6.431	6.457	100.20	100.20	100.20	0.0897	0.0	0.124	-0.008	14.786	519.59
9	6.182	6.457	100.35	100.35	100.35	0.0899	0.0	0.126	-0.011	14.785	519.59
10	5.923	6.457	100.61	100.61	100.61	0.0901	0.0	0.126	-0.016	14.785	519.59
11	5.652	6.457	100.61	100.61	100.61	0.0901	0.0	0.126	-0.016	14.785	519.59
HUB	5.600	6.457									

STREAMLINE NO. R/R/TIP	FLOW COEF.	HEAD COEF.	IDEAL HEAD COEF.	STATOR PO-RATIO	STAGE PO-RATIO	STAGE AD-EFF.	STAGE FACTOR	DIFFUSION STATOR LOSS COEF.	SHOCK STATOR LOSS COEF.	ELEMENT SOLIDITY	AERO CHORD (IN.)	MEAN SPACING (IN.)
TIP	1.0000	0.5933	0.1931	0.3082	0.9999	1.0061	0.6266	0.2313	0.0179	0.0	1.4324	2.3890
1	0.9954	0.5943	0.1939	0.2330	0.9999	1.0061	0.8322	0.1917	0.0137	0.0	1.4703	2.3890
2	0.9703	0.5943	0.1940	0.2126	0.9999	1.0061	0.9124	0.1840	0.0131	0.0	1.5105	2.3890
3	0.9445	0.5954	0.1940	0.2111	0.9999	1.0061	0.9183	0.1650	0.0136	0.0	1.5540	2.3890
4	0.9181	0.5954	0.1939	0.2111	0.9999	1.0061	0.9153	0.1670	0.0143	0.0	1.6016	2.3890
5	0.8920	0.5959	0.1937	0.2117	0.9999	1.0061	0.9144	0.1890	0.0151	0.0	1.6538	2.3890
6	0.8628	0.5963	0.1936	0.2117	0.9999	1.0061	0.9134	0.1914	0.0160	0.0	1.7114	2.3890
7	0.8338	0.5968	0.1933	0.2117	0.9999	1.0061	0.9124	0.1943	0.0170	0.0	1.7756	2.3890
8	0.8038	0.5972	0.1931	0.2116	0.9999	1.0061	0.9113	0.1973	0.0182	0.0	1.8477	2.3890
9	0.7727	0.5980	0.1928	0.2116	0.9999	1.0061	0.9103	0.2009	0.0195	0.0	1.9293	2.3890
10	0.7403	0.5989	0.1925	0.2115	0.9999	1.0061	0.9086	0.2039	0.0209	0.0	2.0229	2.3891
11	0.7065	0.6004	0.1921	0.2114	0.9999	1.0061	0.9086	0.2039	0.0209	0.0	2.1610	2.3891
HUB	0.7000											

STREAMLINE NO. PCT. SPAN	LOCAL BLADE FORCES (LB/STIN) (LB/STIN)	OUTLET T.E.-RAD. /CHORD	STREAMLINE DEVI. ANGLE (DEG.)	OUT-BLADE ANGLE (DEG.)	MAX. CAMB. (DEG.)	T.E. EDGE CIR. LOC. /CHORD R#D/DR
1	1.53	7.963	0.0344	0.1375	0.0100	6.99
2	9.91	7.758	0.0167	0.1065	0.0100	5.00
3	16.50	7.551	0.0167	0.0983	0.0100	4.52
4	27.31	7.340	0.0169	0.0978	0.0100	4.52
5	36.38	7.122	0.0175	0.0980	0.0100	4.57
6	45.73	6.897	0.0161	0.0980	0.0100	4.61
7	55.39	6.665	0.0188	0.0980	0.0100	4.65
8	65.38	6.424	0.0195	0.0979	0.0100	4.70
9	75.76	6.173	0.0202	0.0979	0.0100	4.75
10	86.56	5.912	0.0211	0.0978	0.0100	4.81
11	97.62	5.639	0.0221	0.0972	0.0100	4.88

Table 10.2 Continued.

** VALUES OF PARAMETERS ON STREAMLINES AT STATION. 9, WHICH IS THE INLET OF ROTOR NUMBER. 2 **

STREAMLINE NO.	RADIUS (IN.)	AXIAL COORD. (IN.)	AXIAL VEL. (FT/SEC.)	TANG. VEL. (FT/SEC.)	ABS. VEL. (FT/SEC.)	MACH NO.	ABS. FLOW ANGLE (DEG)	STREAM SLOPE (DEG)	STREAM CURV. (1./IN.)	TOTAL PRESS. (PSIA)	TOTAL TEMP. (DEG.R.)	STATIC PRESS. (PSIA)	STATIC TEMP. (DEG.R.)
1	7.963	7.579	98.64	98.65	0.0	58.65	0.0883	0.0	-0.41	-0.020	14.766	520.04	14.705
2	7.961	7.552	99.25	99.25	0.0	59.25	0.0889	0.0	-0.54	-0.020	14.766	519.69	14.705
3	7.955	7.536	99.44	99.44	0.0	59.44	0.0892	0.0	-0.47	-0.015	14.766	519.59	14.704
4	7.943	7.520	99.66	99.66	0.0	59.66	0.0894	0.0	-0.38	-0.012	14.786	519.59	14.704
5	7.926	7.512	100.05	100.05	0.0	100.05	0.0896	0.0	-0.31	-0.009	14.786	519.59	14.704
6	6.902	7.444	100.17	100.17	0.0	100.17	0.0897	0.0	-0.23	-0.007	14.786	519.59	14.703
7	6.671	7.424	100.25	100.25	0.0	100.25	0.0898	0.0	-0.17	-0.005	14.786	519.59	14.703
8	6.631	7.429	100.29	100.29	0.0	100.29	0.0898	0.0	-0.12	-0.004	14.786	519.59	14.703
9	6.683	7.429	100.23	100.23	0.0	100.23	0.0898	0.0	-0.07	-0.003	14.786	519.59	14.703
10	5.924	7.424	100.23	100.23	0.0	100.23	0.0898	0.0	-0.04	-0.003	14.785	519.59	14.702
11	5.652	7.376	100.08	100.08	0.0	100.08	0.0896	0.0	-0.05	-0.004	14.785	519.59	14.702
HUB	5.000	7.370											
STREAMLINE NO.	R/TIP	REL FLOW ANGLE (DEG)	REL TANG. VEL. (FT/SEC.)	REL VEL. (FT/SEC.)	REL MACH NUMBER	WHEEL SPEED (FT/SEC.)	FLOW COEF.	L-E-RAD. /CHORD	MAX TH. /CHORD	TRAN-PT. LOCATION /CHORD	SEGMENT LAYOUT IN/OUT CONE ANG. TURN RATE (DEG)		
TIP	1.0000	59.40	166.78	193.77	0.1734	165.75	0.5887	0.100	0.0600	0.5000	1.0000	-0.72	
1	0.9954	59.59	162.55	190.45	0.1705	162.55	0.5923	0.100	0.0635	0.5000	1.0000	-0.51	
2	0.9701	58.59	158.22	186.98	0.1674	158.22	0.5947	0.100	0.0671	0.5000	1.0000	-0.36	
3	0.9443	57.80	153.80	183.38	0.1642	153.80	0.5961	0.100	0.0707	0.5000	1.0000	-0.25	
4	0.9179	57.00	149.54	179.68	0.1609	149.54	0.5975	0.100	0.0745	0.5000	1.0000	-0.17	
5	0.8807	56.16	144.55	175.87	0.1575	144.55	0.5988	0.100	0.0784	0.5000	1.0000	-0.12	
6	0.8427	55.28	139.71	171.96	0.1540	139.71	0.6003	0.100	0.0865	0.5000	1.0000	-0.06	
7	0.8338	53.33	134.70	167.93	0.1504	134.70	0.6018	0.100	0.0908	0.5000	1.0000	-0.04	
8	0.8339	52.24	129.49	163.78	0.1467	129.49	0.6035	0.100	0.0953	0.5000	1.0000	-0.02	
9	0.7729	51.07	124.07	159.49	0.1428	124.07	0.6052	0.100	0.1000	0.5000	1.0000	-0.01	
10	0.7405	49.79	118.38	155.02	0.1388	118.38	0.5992	0.0993	0.1000	0.5000	1.0000	-0.01	
HUB	0.7000												
STREAMLINE NO.	PCT. SPAN	INC. ANGLE (DEG)	INC. ANGLE (DEG)	BLADE ANGLE (DEG)	BLADE ANGLE (DEG)	ANGLE (DEG)	ANGLE (DEG)	ANGLE (DEG)	LAY-OUT CONES NO. OF SCANS DF S.	LAY-OUT CONES NO. OF SCANS DF S.	MIN-CHK. AS FRACT. LOCN.	WIN-CHK. AS FRACT. LOCN.	L-E-EDGE CIR-D/DR COV-CHAN.
1	1.53	-2.00	-6.63	61.40	61.40	51.21	14.82	0.2772	0.7774	0.2226	2.7090	0.0	-0.0758
2	9.96	-0.08	-5.14	58.67	58.67	52.23	11.50	0.2569	0.7602	0.2398	2.6461	0.0	-0.0337
3	16.55	0.44	-5.03	57.36	57.36	51.69	11.77	0.2486	0.7324	0.2676	2.6687	0.0	-0.0374
4	27.37	0.56	-5.34	56.44	56.44	50.56	12.53	0.2470	0.7011	0.2589	2.7189	0.0	-0.036
5	31.42	0.66	-5.67	55.50	55.50	49.50	13.36	0.2476	0.6689	0.3211	2.7726	0.0	-0.021
6	45.75	0.76	-6.01	54.52	54.52	47.93	14.03	0.2476	0.6361	0.3635	2.8289	0.0	-0.053
7	55.38	0.88	-6.35	53.46	53.46	46.51	14.73	0.2476	0.6205	0.3975	2.8885	0.0	-0.097
8	65.36	0.99	-6.70	52.34	52.34	44.73	15.31	0.2476	0.5681	0.4319	2.9522	0.0	-0.054
9	75.71	1.13	-7.06	51.12	51.12	42.84	16.40	0.2476	0.5327	0.4673	3.0208	0.0	-0.023
10	85.51	1.28	-7.41	49.79	49.79	40.71	17.70	0.2476	0.4963	0.5037	3.0955	0.0	-0.006
11	97.81	1.45	-7.74	48.34	48.34	38.29	19.24	0.1990	0.4587	0.5413	3.1776	0.0	-0.092

Table 10.2 Continued.

** VALUES OF PARAMETERS ON STREAMLINES AT STATION. 10. WHICH IS THE OUTLET OF ROTOR NUMBER. 2 **

STREAMLINE NO.	RELATIVE RADIUS (IN.)	Axial coord. (in.)	Axial vel. (ft/sec.)	Mero. vel. (ft/sec.)	Tang. vel. (ft/sec.)	Abs. vel. (ft/sec.)	Abs. mach no.	Abs. flow stream slope (deg)	Stream curv. (1./in.)	Total press. (psia)	Total temp. (deg. r.)	Static press. (psia)	Static temp. (deg. r.)	
1 TIP	8.000	9.086	101.74	101.75	55.08	15.70	0.1034	28.43	-0.49	0.018	14.882	521.57	14.771	
2	7.944	9.076	101.37	101.37	41.92	15.69	0.0981	22.47	-0.62	0.017	14.882	520.82	14.772	
3	7.748	9.040	101.06	101.06	39.37	15.68	0.0970	21.25	-0.54	0.013	14.882	520.63	14.773	
4	7.336	9.064	100.81	100.81	39.37	15.68	0.0970	21.25	-0.54	0.013	14.882	520.62	14.773	
5	7.121	9.086	100.61	100.61	41.69	15.68	0.0972	21.82	-0.33	0.010	14.882	520.62	14.773	
6	6.899	9.109	100.45	100.45	41.69	15.68	0.0974	22.51	-0.33	0.008	14.882	520.62	14.773	
7	6.668	9.135	100.33	100.33	43.08	15.69	0.0978	23.21	-0.26	0.006	14.882	520.62	14.773	
8	6.430	9.162	100.23	100.23	43.62	15.70	0.0978	23.98	-0.20	0.005	14.882	520.63	14.773	
9	6.182	9.192	100.17	100.17	43.84	15.70	0.0982	24.81	-0.15	0.003	14.882	520.63	14.773	
10	5.933	9.224	100.12	100.12	43.84	15.70	0.0985	25.72	-0.11	0.002	14.882	520.63	14.773	
11	5.653	9.259	100.23	100.23	52.40	15.72	0.1003	26.61	-0.09	0.000	14.882	520.63	14.773	
HUB	5.660	9.266			52.66	15.73	0.1014	27.51	-0.08	-0.005	14.882	520.63	14.773	
												14.775	14.775	
STREAMLINE NO. R/R/TIP	REL. FLOW ANGLE (DEG)	REL. TANG. VEL. (FT/SEC.)	REL. VEL. (FT/SEC.)	REL. MACH NUMBER	WHEEL MACH	WHEEL SPEED (FT/SEC.)	FLOW CCOEF.	HEAD CCOEF.	IDEAL HEAD COEF.	ADIAEFF.	DIFFUSION FACTOR	LOSS COEF.	SHOCK LOSS COEF.	ELEMENT SOLIDITY
1 TIP	1.0000	47.57	111.30	150.80	0.1348	166.38	0.6072	0.2066	0.3265	0.3633	0.1805	0.0560	0.0	1.0027
2	0.9930	49.89	120.35	157.35	0.1408	162.27	0.6050	0.2056	0.4240	0.8917	0.2817	0.2666	0.0000	1.0265
3	0.9482	49.59	116.72	155.91	0.1356	158.93	0.6017	0.2055	0.2210	0.9301	0.2210	0.2257	0.0000	1.0563
4	0.9171	48.34	113.29	151.65	0.1357	153.95	0.6017	0.2055	0.2210	0.9319	0.2210	0.2257	0.0000	1.0655
5	0.8901	46.88	107.45	147.20	0.1317	149.07	0.6017	0.2055	0.2210	0.9302	0.2210	0.2257	0.0000	1.1158
6	0.8623	45.27	101.40	142.73	0.1277	144.14	0.5995	0.2060	0.2215	0.9298	0.2218	0.2261	0.0000	1.1558
7	0.8336	43.45	95.04	136.20	0.1237	139.60	0.5989	0.2062	0.2221	0.9295	0.2221	0.2261	0.0000	1.1957
8	0.8037	41.39	86.34	133.60	0.1195	134.66	0.5992	0.2064	0.2224	0.9295	0.2224	0.2261	0.0000	1.2402
9	0.7727	39.04	81.23	128.97	0.1154	129.47	0.5992	0.2067	0.2227	0.9295	0.2227	0.2261	0.0000	1.2920
10	0.7408	36.33	73.65	124.32	0.1112	124.95	0.5992	0.2070	0.2227	0.9295	0.2227	0.2261	0.0000	1.3464
11	0.7056	33.18	65.53	119.75	0.1071	118.39	0.5982	0.2074	0.2229	0.9205	0.2364	0.0364	0.0	1.4109
STREAMLINE NO. PCT. SPAN	PRESS. RATIO	TEMP. RATIO	AERO. CHORD (IN.)	MEAN SPACING (IN.)	RADIUS (IN.)	LOCAL FORCES FOR: AXIAL TANG. (LBS/IN.)	OUTLET BLADE FORCES FOR: AXIAL TANG. (LBS/IN.)	OUTLET T.E.-RAD. /CHORD (DEG)	OUT. BLADE ANGLE (DEG)	OUT. EDGE ANGLE (DEG)	CONC. MAX. CMB. PT. LOC. (DEG)	EDGE CR. GEN. /CHORD	MAX. CMB. PT. LOC. CR. GEN. R#0#DR	
1	2.32	1.0065	1.0023	2.3862	2.3797	7.954	0.1659	-0.2147	0.0100	6.59	40.98	41.02	0.5000	-0.3573
2	16.95	1.0065	1.0022	2.3862	2.3797	7.744	0.1644	-0.1614	0.0100	4.09	45.80	45.93	0.5000	-0.1321
3	2.65	1.0065	1.0020	2.3861	2.3589	7.500	0.1659	-0.1474	0.0100	3.56	46.03	46.03	0.5000	-0.1254
5	36.62	1.0065	1.0020	2.3861	2.3589	7.313	0.1652	-0.1471	0.0100	3.66	44.68	44.68	0.5000	-0.0957
6	45.84	1.0065	1.0020	2.3861	2.3589	7.164	0.1650	-0.1476	0.0100	3.79	43.09	43.10	0.5000	-0.0925
7	55.48	1.0065	1.0020	2.3861	2.3589	6.955	0.1650	-0.1476	0.0100	3.94	41.33	41.34	0.5000	-0.0893
8	65.43	1.0065	1.0020	2.3861	2.3589	6.924	0.1651	-0.1477	0.0100	4.10	39.35	39.36	0.5000	-0.0860
9	75.77	1.0065	1.0020	2.3861	2.3589	6.949	0.1651	-0.1478	0.0100	4.28	37.11	37.12	0.5000	-0.0824
10	86.54	1.0065	1.0020	2.3861	2.3589	7.172	0.1652	-0.1479	0.0100	4.48	34.56	34.57	0.5000	-0.0791
11	97.81	1.0065	1.0020	2.3861	2.3589	7.191	0.1653	-0.1479	0.0100	4.94	28.23	28.24	0.5000	-0.1375

Table 10.2 Continued.

** VALUES OF PARAMETERS ON STREAMLINES AT STATION, 11, WHICH IS THE INLET OF STATOR NUMBER, 1. OF STAGE NUMBER, 2 **

STREAMLINE NO.	AXIAL COORD. (IN.)	RADIAL VEL. (FT/SEC.)	TANG. VEL. (FT/SEC.)	Abs. VEL. (FT/SEC.)	MACH NO. (F/T SEC.)	ABS. FLOW SLOPE (DEG)	STREAM CURV. (1./IN.)	TOTAL PRESS. (PSIA)	STATIC TEMP. (DEG.R.)
TIP	8.000	10.572	92.51	55.09	107.67	0.0962	30.77	0.15	-0.004
1	7.944	10.564	92.51	41.93	101.15	0.0967	22.81	0.25	14.862
2	7.837	10.537	95.69	59.69	100.86	0.0974	21.17	0.23	14.862
3	7.534	10.533	101.51	39.32	100.86	0.0974	21.17	0.004	14.784
4	7.326	10.534	101.51	40.37	109.62	0.0978	21.69	0.020	14.783
5	7.112	10.535	101.38	41.69	109.62	0.0981	22.36	0.19	14.782
6	6.891	10.537	101.26	43.09	110.05	0.0985	23.05	0.19	14.781
7	6.683	10.539	101.13	40.13	110.53	0.0989	23.81	0.20	14.780
8	6.426	10.543	100.97	46.23	111.09	0.0994	24.65	0.22	14.779
9	6.180	10.543	100.77	48.24	111.72	0.1000	25.58	0.07	14.778
10	5.922	10.546	100.51	50.40	112.44	0.1006	26.53	0.027	14.777
11	5.652	10.549	100.15	52.66	113.25	0.1013	27.83	0.015	14.776
HUB	5.600	10.550							519.55
STREAMLINE NO.	R/PTIP	FLOW COEF.	REL.FLOW ANGLE (DEG)	L.E.RAD./CHORD (DEG)	MAX.TH. PT./CHORD	TRAN.PT. /CHORD	SEGMENT LOCN. IN CUT CHORD	LAYOUT TURN RATE (DEG)	SEGMENT LAYOUT IN CUT CONE ANG.
TIP	1.0000	0.5521	50.27	0.0100	0.1000	0.5000	0.5000	1.0000	0.01
1	0.9930	0.5521	50.31	0.0100	0.094	0.5000	0.5000	1.0000	0.25
2	0.9671	0.5559	49.41	0.0100	0.098	0.5000	0.5000	1.0000	0.26
3	0.9417	0.6059	48.04	0.0100	0.082	0.5000	0.5000	1.0000	0.28
4	0.9158	0.6059	46.61	0.0100	0.085	0.5000	0.5000	1.0000	0.29
5	0.8890	0.6051	45.00	0.0100	0.086	0.5000	0.5000	1.0000	0.30
6	0.8614	0.6044	43.19	0.0100	0.076	0.5000	0.5000	1.0000	0.33
7	0.8329	0.6036	42.19	0.0100	0.075	0.5000	0.5000	1.0000	0.37
8	0.8033	0.6026	41.16	0.0100	0.075	0.5000	0.5000	1.0000	0.43
9	0.7724	0.6014	38.86	0.0100	0.0632	0.5000	0.5000	1.0000	0.51
10	0.7403	0.5999	36.23	0.0100	0.0637	0.5000	0.5000	1.0000	0.63
11	0.7065	0.5977	33.19	0.0100	0.0630	0.5000	0.5000	1.0000	
STREAMLINE NO.	FCT. SPAN	INC. S.S. INC. ANGLE (DEG)	IN-BLADE ANGLE (DEG)	BLA.NGLE (DEG)	S.SCAM. ANGLE (DEG)	1ST SEG. AT SHOCK LOCATION	LAYOUT CONE AS FRACT. OF S.S.	SHLOC. AT SHOCK LOCATION	L.E. EDGE COV.CHAN. MARGIN
1	2.32	0.22	-8.74	30.55	11.63	27.97	0.1257	0.2709	0.636
2	10.95	0.70	-8.00	22.11	6.49	22.32	0.0156	0.0594	0.770
3	19.43	0.80	-7.53	20.38	7.87	20.33	0.1011	0.0863	0.686
4	28.08	0.89	-7.03	20.80	8.07	20.64	0.1043	0.0883	0.694
5	36.99	0.99	-6.50	21.37	8.33	20.53	0.0755	0.0888	0.698
6	46.20	1.10	-5.94	21.95	8.60	20.40	0.1104	0.1890	0.698
7	55.71	1.23	-5.36	22.59	8.89	20.28	0.1134	0.1891	0.704
8	65.59	1.36	-4.74	23.29	9.22	20.19	0.1165	0.1891	0.711
9	75.86	1.52	-4.10	24.06	9.58	20.11	0.1197	0.1889	0.720
10	86.58	1.69	-3.41	24.94	9.99	20.07	0.1231	0.1886	0.731
11	97.92	1.88	-2.67	25.97	10.45	20.07	0.1268	0.1882	0.744

Table 10.2 Continued.

** VALUES OF PARAMETERS ON STREAMLINES AT STATION. 12. WHICH IS THE OUTLET OF STATOR NUMBER. 1. OF STAGE NUMBER. 2 **											
STREAMLINE NO.	RADUS (IN.)	AXIAL COORD. (12.901)	TANG. VEL. (FT/SEC.)	MERD. VEL. (FT/SEC.)	ABS. VEL. (FT/SEC.)	ABS. FLOW MACH NO.	ANGLE (DEG.)	STREAM. SLOPE (1./IN.)	STREAM. CURV. (1./IN.)	TOTAL TEMP. (DEG.R.)	STATIC PRESS. (PSIA)
1	1.2	1.7	1.945	1.01	1.01	1.06	0.6	0.093	0.0	-0.02	14.880
2	1.3	1.805	1.01	1.26	1.01	1.26	0.6	0.096	0.0	-0.02	14.881
3	1.4	1.845	1.01	1.36	1.01	1.36	0.6	0.097	0.0	-0.02	14.882
4	1.5	1.894	1.01	1.39	1.01	1.39	0.6	0.097	0.0	-0.02	14.883
5	1.6	1.938	1.01	1.42	1.01	1.42	0.6	0.097	0.0	-0.02	14.884
6	1.7	1.974	1.01	1.44	1.01	1.44	0.6	0.097	0.0	-0.02	14.885
7	1.8	2.007	1.01	1.46	1.01	1.46	0.6	0.098	0.0	-0.02	14.886
8	1.9	2.039	1.01	1.48	1.01	1.48	0.6	0.098	0.0	-0.02	14.887
9	2.0	2.071	1.01	1.50	1.01	1.50	0.6	0.098	0.0	-0.02	14.888
10	2.1	2.103	1.01	1.52	1.01	1.52	0.6	0.098	0.0	-0.02	14.889
11	2.2	2.135	1.01	1.55	1.01	1.55	0.6	0.098	0.0	-0.02	14.890
12	2.3	2.167	1.01	1.58	1.01	1.58	0.6	0.098	0.0	-0.02	14.891
13	2.4	2.200	1.01	1.61	1.01	1.61	0.6	0.098	0.0	-0.02	14.892
14	2.5	2.232	1.01	1.64	1.01	1.64	0.6	0.098	0.0	-0.02	14.893
15	2.6	2.264	1.01	1.67	1.01	1.67	0.6	0.098	0.0	-0.02	14.894
16	2.7	2.296	1.01	1.70	1.01	1.70	0.6	0.098	0.0	-0.02	14.895
17	2.8	2.328	1.01	1.73	1.01	1.73	0.6	0.098	0.0	-0.02	14.896
18	2.9	2.360	1.01	1.76	1.01	1.76	0.6	0.098	0.0	-0.02	14.897
19	3.0	2.392	1.01	1.79	1.01	1.79	0.6	0.098	0.0	-0.02	14.898
20	3.1	2.424	1.01	1.82	1.01	1.82	0.6	0.098	0.0	-0.02	14.899
21	3.2	2.456	1.01	1.85	1.01	1.85	0.6	0.098	0.0	-0.02	14.900
22	3.3	2.488	1.01	1.88	1.01	1.88	0.6	0.098	0.0	-0.02	14.901
23	3.4	2.520	1.01	1.91	1.01	1.91	0.6	0.098	0.0	-0.02	14.902
24	3.5	2.552	1.01	1.94	1.01	1.94	0.6	0.098	0.0	-0.02	14.903
25	3.6	2.584	1.01	1.97	1.01	1.97	0.6	0.098	0.0	-0.02	14.904
26	3.7	2.616	1.01	2.00	1.01	2.00	0.6	0.098	0.0	-0.02	14.905
27	3.8	2.648	1.01	2.03	1.01	2.03	0.6	0.098	0.0	-0.02	14.906
28	3.9	2.680	1.01	2.06	1.01	2.06	0.6	0.098	0.0	-0.02	14.907
29	4.0	2.712	1.01	2.09	1.01	2.09	0.6	0.098	0.0	-0.02	14.908
30	4.1	2.744	1.01	2.12	1.01	2.12	0.6	0.098	0.0	-0.02	14.909
31	4.2	2.776	1.01	2.15	1.01	2.15	0.6	0.098	0.0	-0.02	14.910
32	4.3	2.808	1.01	2.18	1.01	2.18	0.6	0.098	0.0	-0.02	14.911
33	4.4	2.840	1.01	2.21	1.01	2.21	0.6	0.098	0.0	-0.02	14.912
34	4.5	2.872	1.01	2.24	1.01	2.24	0.6	0.098	0.0	-0.02	14.913
35	4.6	2.904	1.01	2.27	1.01	2.27	0.6	0.098	0.0	-0.02	14.914
36	4.7	2.936	1.01	2.30	1.01	2.30	0.6	0.098	0.0	-0.02	14.915
37	4.8	2.968	1.01	2.33	1.01	2.33	0.6	0.098	0.0	-0.02	14.916
38	4.9	3.000	1.01	2.36	1.01	2.36	0.6	0.098	0.0	-0.02	14.917
39	5.0	3.032	1.01	2.39	1.01	2.39	0.6	0.098	0.0	-0.02	14.918
40	5.1	3.064	1.01	2.42	1.01	2.42	0.6	0.098	0.0	-0.02	14.919
41	5.2	3.096	1.01	2.45	1.01	2.45	0.6	0.098	0.0	-0.02	14.920
42	5.3	3.128	1.01	2.48	1.01	2.48	0.6	0.098	0.0	-0.02	14.921
43	5.4	3.160	1.01	2.51	1.01	2.51	0.6	0.098	0.0	-0.02	14.922
44	5.5	3.192	1.01	2.54	1.01	2.54	0.6	0.098	0.0	-0.02	14.923
45	5.6	3.224	1.01	2.57	1.01	2.57	0.6	0.098	0.0	-0.02	14.924
46	5.7	3.256	1.01	2.60	1.01	2.60	0.6	0.098	0.0	-0.02	14.925
47	5.8	3.288	1.01	2.63	1.01	2.63	0.6	0.098	0.0	-0.02	14.926
48	5.9	3.320	1.01	2.66	1.01	2.66	0.6	0.098	0.0	-0.02	14.927
49	6.0	3.352	1.01	2.69	1.01	2.69	0.6	0.098	0.0	-0.02	14.928
50	6.1	3.384	1.01	2.72	1.01	2.72	0.6	0.098	0.0	-0.02	14.929
51	6.2	3.416	1.01	2.75	1.01	2.75	0.6	0.098	0.0	-0.02	14.930
52	6.3	3.448	1.01	2.78	1.01	2.78	0.6	0.098	0.0	-0.02	14.931
53	6.4	3.480	1.01	2.81	1.01	2.81	0.6	0.098	0.0	-0.02	14.932
54	6.5	3.512	1.01	2.84	1.01	2.84	0.6	0.098	0.0	-0.02	14.933
55	6.6	3.544	1.01	2.87	1.01	2.87	0.6	0.098	0.0	-0.02	14.934
56	6.7	3.576	1.01	2.90	1.01	2.90	0.6	0.098	0.0	-0.02	14.935
57	6.8	3.608	1.01	2.93	1.01	2.93	0.6	0.098	0.0	-0.02	14.936
58	6.9	3.640	1.01	2.96	1.01	2.96	0.6	0.098	0.0	-0.02	14.937
59	7.0	3.672	1.01	2.99	1.01	2.99	0.6	0.098	0.0	-0.02	14.938
60	7.1	3.704	1.01	3.02	1.01	3.02	0.6	0.098	0.0	-0.02	14.939
61	7.2	3.736	1.01	3.05	1.01	3.05	0.6	0.098	0.0	-0.02	14.940
62	7.3	3.768	1.01	3.08	1.01	3.08	0.6	0.098	0.0	-0.02	14.941
63	7.4	3.800	1.01	3.11	1.01	3.11	0.6	0.098	0.0	-0.02	14.942
64	7.5	3.832	1.01	3.14	1.01	3.14	0.6	0.098	0.0	-0.02	14.943
65	7.6	3.864	1.01	3.17	1.01	3.17	0.6	0.098	0.0	-0.02	14.944
66	7.7	3.896	1.01	3.20	1.01	3.20	0.6	0.098	0.0	-0.02	14.945
67	7.8	3.928	1.01	3.23	1.01	3.23	0.6	0.098	0.0	-0.02	14.946
68	7.9	3.960	1.01	3.26	1.01	3.26	0.6	0.098	0.0	-0.02	14.947
69	8.0	3.992	1.01	3.29	1.01	3.29	0.6	0.098	0.0	-0.02	14.948
70	8.1	4.024	1.01	3.32	1.01	3.32	0.6	0.098	0.0	-0.02	14.949
71	8.2	4.056	1.01	3.35	1.01	3.35	0.6	0.098	0.0	-0.02	14.950
72	8.3	4.088	1.01	3.38	1.01	3.38	0.6	0.098	0.0	-0.02	14.951
73	8.4	4.120	1.01	3.41	1.01	3.41	0.6	0.098	0.0	-0.02	14.952
74	8.5	4.152	1.01	3.44	1.01	3.44	0.6	0.098	0.0	-0.02	14.953
75	8.6	4.184	1.01	3.47	1.01	3.47	0.6	0.098	0.0	-0.02	14.954
76	8.7	4.216	1.01	3.50	1.01	3.50	0.6	0.098	0.0	-0.02	14.955
77	8.8	4.248	1.01	3.53	1.01	3.53	0.6	0.098	0.0	-0.02	14.956
78	8.9	4.280	1.01	3.56	1.01	3.56	0.6	0.098	0.0	-0.02	14.957
79	9.0	4.312	1.01	3.59	1.01	3.59	0.6	0.098	0.0	-0.02	14.958
80	9.1	4.344	1.01	3.62	1.01	3.62	0.6	0.098	0.0	-0.02	14.959
81	9.2	4.376	1.01	3.65	1.01	3.65	0.6	0.098	0.0	-0.02	14.960
82	9.3	4.408	1.01	3.68	1.01	3.68	0.6	0.098	0.0	-0.02	14.961
83	9.4	4.440	1.01	3.71	1.01	3.71	0.6	0.098	0.0	-0.02	14.962
84	9.5	4.472	1.01	3.74	1.01	3.74	0.6	0.098	0.0	-0.02	14.963
85	9.6	4.504	1.01	3.77	1.01	3.77	0.6	0.098	0.0	-0.02	14.964
86	9.7	4.536	1.01	3.80	1.01	3.80	0.6	0.098	0.0	-0.02	14.965
87	9.8	4.568	1.01	3.83	1.01	3.83	0.6	0.098	0.0	-0.02	14.966
88	9.9	4.600	1.01	3.86	1.01	3.86	0.6	0.098	0.0	-0.02	14.967
89	1.0	4.632	1.01	3.89	1.01	3.89	0.6	0.098	0.0	-0.02	14.968
90	1.1	4.664	1.01	3.92	1.01	3.92	0.6	0.098	0.0	-0.02	14.969
91	1.2	4.696	1.01	3.95	1.01	3.95	0.6	0.098	0.0	-0.02	14.970
92	1.3	4.728	1.01	3.98	1.01	3.98	0.6	0.098	0.0	-0.02	14.971
93	1.4	4.760	1.01	4.01	1.01	4.01	0.6	0.098	0.0	-0.02	14.972
94	1.5	4.792	1.01	4.04	1.01	4.04	0.6	0.098	0.0	-0.02	14.973
95	1.6	4.824	1.01	4.07	1.01	4.07	0.6	0.098	0.0	-0.02	14.974
96	1.7	4.856	1.01	4.10	1.01	4.10	0.6	0.098	0.0	-0.02	14.975
97	1.8	4.888	1.01	4.13	1.01	4.13	0.6	0.098	0.0	-0.02	14.976
98	1.9	4.920	1.01	4.16	1.01	4.16	0.6	0.098	0.0	-0.02	14.977
99	2.0	4.952	1.01	4.19	1.01	4.19	0.6	0.098	0.0	-0.02	14.978
100	2.1	4.984	1.01	4.22	1.01	4.22	0.6	0.098	0.0	-0.02	14.979
101	2.2	5.016	1.01	4.25	1.01	4.25	0.6	0.098	0.0	-0.02	14.980
102	2.3	5.048	1.01	4.28	1.01	4.28	0.6	0.098	0.0	-0.02	14.

Table 10.2 Concluded.

** VALUES OF PARAMETERS ON STREAMLINES AT STATION. 13. WHICH IS AN ANNULUS **

STREAMLINE NO.	RADIUS (IN.)	AXIAL COORD. (IN.)	MERID. VEL. (FT/SEC.)	TANG. VEL. (FT/SEC.)	ABS. VEL. (FT/SEC.)	ABS. FLOW MACH NO.	ANGLE (DEG.)	STREAM SLOPE (1./IN.)	STREAM CURV. (DEG.)	TOTAL PRESS. (PSIA)	TOTAL TEMP. (DEG.R.)
TIP	8.000	14.500	101.45	101.45	0.0	101.45	0.0907	0.0	-0.000	14.880	52.57
1	7.95	14.500	101.45	101.45	0.0	101.45	0.0909	0.0	-0.001	14.881	52.62
2	7.95	14.500	101.45	101.45	0.0	101.45	0.0909	0.0	-0.000	14.881	52.63
3	7.95	14.500	101.45	101.45	0.0	101.45	0.0909	0.0	-0.001	14.881	52.63
4	7.95	14.500	101.45	101.45	0.0	101.45	0.0909	0.0	-0.001	14.881	52.62
5	7.95	14.500	101.45	101.45	0.0	101.45	0.0909	0.0	-0.001	14.881	52.62
6	7.907	14.500	101.45	101.45	0.0	101.45	0.0906	0.0	-0.001	14.881	52.63
7	6.679	14.500	101.45	101.45	0.0	101.45	0.0906	0.0	-0.001	14.880	52.63
8	6.644	14.500	101.45	101.45	0.0	101.45	0.0906	0.0	-0.001	14.880	52.63
9	6.220	14.500	101.45	101.45	0.0	101.45	0.0906	0.0	-0.001	14.880	52.63
10	5.95	14.500	101.45	101.45	0.0	101.45	0.0905	0.0	-0.002	14.880	52.63
11	5.678	14.500	101.45	101.45	0.0	101.45	0.0905	0.0	-0.002	14.880	52.63
HUB	5.000	14.500	100.95	100.95	0.0	100.95	0.0905	0.0	-0.004	14.880	51.978

** VALUES OF PARAMETERS ON STREAMLINES AT STATION. 14. WHICH IS AN ANNULUS **

STREAMLINE NO.	RADIUS (IN.)	AXIAL COORD. (IN.)	MERID. VEL. (FT/SEC.)	TANG. VEL. (FT/SEC.)	ABS. VEL. (FT/SEC.)	ABS. FLOW MACH NO.	ANGLE (DEG.)	STREAM SLOPE (1./IN.)	STREAM CURV. (DEG.)	TOTAL PRESS. (PSIA)	TOTAL TEMP. (DEG.R.)
TIP	8.000	15.500	101.46	101.46	0.0	101.46	0.0907	0.0	-0.000	14.880	52.57
1	7.95	15.500	101.46	101.46	0.0	101.46	0.0907	0.0	-0.000	14.881	52.62
2	7.95	15.500	101.46	101.46	0.0	101.46	0.0907	0.0	-0.000	14.881	52.62
3	7.95	15.500	101.46	101.46	0.0	101.46	0.0907	0.0	-0.000	14.881	52.62
4	7.95	15.500	101.46	101.46	0.0	101.46	0.0907	0.0	-0.000	14.881	52.62
5	7.95	15.500	101.46	101.46	0.0	101.46	0.0907	0.0	-0.000	14.881	52.62
6	6.607	15.500	101.46	101.46	0.0	101.46	0.0907	0.0	-0.000	14.881	52.63
7	6.607	15.500	101.46	101.46	0.0	101.46	0.0907	0.0	-0.000	14.880	52.63
8	6.607	15.500	101.46	101.46	0.0	101.46	0.0907	0.0	-0.000	14.880	52.63
9	6.220	15.500	101.46	101.46	0.0	101.46	0.0907	0.0	-0.000	14.880	52.63
10	5.95	15.500	101.46	101.46	0.0	101.46	0.0907	0.0	-0.000	14.880	52.63
11	5.678	15.500	101.46	101.46	0.0	101.46	0.0907	0.0	-0.000	14.880	52.63
HUB	5.000	15.500	100.95	100.95	0.0	100.95	0.0904	0.0	-0.001	14.880	51.978

** VALUES OF PARAMETERS ON STREAMLINES AT STATION. 15. WHICH IS AN ANNULUS **

STREAMLINE NO.	RADIUS (IN.)	AXIAL COORD. (IN.)	MERID. VEL. (FT/SEC.)	TANG. VEL. (FT/SEC.)	ABS. VEL. (FT/SEC.)	ABS. FLOW MACH NO.	ANGLE (DEG.)	STREAM SLOPE (1./IN.)	STREAM CURV. (DEG.)	TOTAL PRESS. (PSIA)	TOTAL TEMP. (DEG.R.)
TIP	8.000	16.500	101.46	101.46	0.0	101.46	0.0907	0.0	-0.000	14.880	52.57
1	7.95	16.500	101.46	101.46	0.0	101.46	0.0909	0.0	-0.001	14.881	52.62
2	7.95	16.500	101.46	101.46	0.0	101.46	0.0909	0.0	-0.000	14.881	52.62
3	7.95	16.500	101.46	101.46	0.0	101.46	0.0909	0.0	-0.000	14.881	52.62
4	7.95	16.500	101.46	101.46	0.0	101.46	0.0909	0.0	-0.000	14.881	52.62
5	7.95	16.500	101.46	101.46	0.0	101.46	0.0909	0.0	-0.000	14.881	52.62
6	6.607	16.500	101.46	101.46	0.0	101.46	0.0909	0.0	-0.000	14.881	52.63
7	6.607	16.500	101.46	101.46	0.0	101.46	0.0909	0.0	-0.000	14.880	52.63
8	6.607	16.500	101.46	101.46	0.0	101.46	0.0909	0.0	-0.000	14.880	52.63
9	6.220	16.500	101.46	101.46	0.0	101.46	0.0909	0.0	-0.000	14.880	52.63
10	5.95	16.500	101.46	101.46	0.0	101.46	0.0904	0.0	-0.001	14.880	52.63
11	5.678	16.500	101.46	101.46	0.0	101.46	0.0904	0.0	-0.000	14.880	52.63
HUB	5.000	16.500	100.95	100.95	0.0	100.95	0.0904	0.0	-0.002	14.880	51.978

** VALUES OF PARAMETERS ON STREAMLINES AT STATION. 16. WHICH IS AN ANNULUS **

142

Table 10.3 Design code stage and overall performance predictions.

*** COMPUTED COMPRESSOR DESIGN PARAMETERS FOR A ROTATIONAL SPEED OF . 2400.0. RPM ***												
** THE CORRECTED WEIGHTFLOW PER UNIT OF CASING ANNULAR AREA AT THE INLET FACE OF THE FIRST BLADE ROW IS .7.37 LBS/SEC/FT SQ **												
** MASS AVERAGED ROTOR AND STAGE AERODYNAMIC PARAMETERS **												
STAGE NO.	BLADE TYPE	FLOW COEF.	HEAD COEF.	ID. HEAD COEF.	PRESS. TEMP. RATIO	ADIA. POLY. EFF.	ASPECT RATIO	FOR. AX. THRUST (LBS)	GAS BENDING MOMENTS FCR. AX. TANG. (FT-LBS)	TORQUE (FT-LBS)	POWER (HP)	
1	ROTOR	0.5872	0.1697	0.2186	1.0062	1.0020	0.8995	1.00	7.66	0.038	3.99	
1	STATOR	0.5910	0.1733	0.2186	1.0061	1.0020	0.8843	1.00	-13.59	0.022	1.82	
2	ROTOR	0.5965	0.2052	0.2290	1.0065	1.0021	0.9004	1.01	7.58	0.038	4.17	
2	STATOR	0.5999	0.2025	0.2290	1.0064	1.0021	0.8843	1.01	-13.47	0.005	1.91	
** CUMULATIVE SUMS OF MASS AVERAGED ROTOR AND STAGE AERODYNAMIC PARAMETERS **												
STAGE NO.	BLADE TYPE	WEIGHT FLOW (LBS/SEC)	TOTAL PRESS. (PSIA)	TOTAL TEMP. (DEG. R.)	PRESS. RATIO	TEMP. RATIO	HEAD COEF.	IDEAL HEAD COEF.	ADIA. EFF.	POLY. EFF.	FOR. AX. THRUST (LBS)	POWER (HP)
1	INLET	5.25	14.596	518.60	1.0062	1.0020	0.1967	0.2186	0.8995	0.8996	-7.66	3.99
1	ROTOR	5.25	14.587	519.62	1.0061	1.0020	0.1933	0.2186	0.8843	0.8844	-6.93	1.82
2	STATOR	5.25	14.582	520.69	1.0127	1.0040	0.3994	0.4476	0.8924	0.8926	-1.46	0.4005
2	STATOR	5.25	14.580	520.69	1.0125	1.0040	0.3958	0.4476	0.8842	0.8844	-12.01	0.0000

Table 10.4 Rotor blade manufacturing coordinates generated by NASA design code.

Table 10.4 Continued.

Table 10.4 Continued.

BLADE SECTION RAD. NO.	NUMBER OF BLADES = 21.0	AXIAL LOCATION OF STACKING LINE IN COMPRESSOR = 1.030 IN.															
		STACKING POINT COORDINATES			SECTION SETTING ANGLE			BLADE SECTION C.G. COORDINATES			SECTION AREA			MOMENTS OF INERTIA THROUGH C.G.			SECTION STIFFNESS
L (IN.)	H (IN.)	L (IN.)	H (IN.)	L (IN.)	H (DEG.)	L (IN.)	H (IN.)	L (IN.)	H (IN.)	L (IN.)	H (IN.)	L (IN.)	H (IN.)	L (IN.)	H (IN.)	L (IN.)	H (IN.)
9	6.660	1.1934	0.0677	47.355	1.1941	0.0744	0.34764	0.0734	0.00888	0.11829	0.003121	0.043196	0.0003121	0.0003121	0.0003121	0.0003121	
10	6.500	1.1934	0.0716	46.297	1.1941	0.0743	0.35808	0.0733	0.00980	0.12125	0.0012125	0.043366	0.0003426	0.0003426	0.0003426	0.0003426	
11	6.340	1.1937	0.0758	45.184	1.1942	0.0804	0.36855	0.0739	0.01079	0.12424	0.0012424	0.045443	0.0003751	0.0003751	0.0003751	0.0003751	
12	6.180	1.1940	0.0802	44.011	1.1943	0.0839	0.37907	0.0739	0.00186	0.12726	0.00186	0.046310	0.0004097	0.0004097	0.0004097	0.0004097	
SECTION NO.	S COORDINATES	SECTION NO. 10 COORDINATES			SECTION NO. 11 COORDINATES			SECTION NO. 12 COORDINATES			SECTION NO. 13 COORDINATES			SECTION NO. 14 COORDINATES			
L (IN.)	H (IN.)	L (IN.)	H (IN.)	L (IN.)	H (IN.)	L (IN.)	H (IN.)	L (IN.)	H (IN.)	L (IN.)	H (IN.)	L (IN.)	H (IN.)	L (IN.)	H (IN.)	L (IN.)	H (IN.)
0.0	0.0241	0.0241	0.0241	0.0241	0.0241	0.0241	0.0241	0.0241	0.0241	0.0241	0.0241	0.0241	0.0241	0.0241	0.0241	0.0241	0.0241
0.1000	-0.0003	0.0489	0.0673	0.1000	0.0002	0.0684	0.1000	0.0001	0.0001	0.0695	0.1000	0.0001	0.0695	0.1000	0.0001	0.0695	0.1000
0.2000	-0.0008	0.0896	0.1095	0.3000	-0.0007	0.0917	0.2000	-0.0004	0.0004	0.0940	0.3000	-0.0003	0.0940	0.3000	-0.0003	0.0940	0.3000
0.3000	-0.0014	0.1095	0.1261	0.3000	-0.0012	0.1126	0.3000	-0.0008	0.0008	0.1159	0.3000	-0.0007	0.1159	0.3000	-0.0007	0.1159	0.3000
0.4000	-0.0021	0.1271	0.1472	0.4000	-0.0019	0.1311	0.4000	-0.0013	0.0013	0.1353	0.4000	-0.0012	0.1353	0.4000	-0.0012	0.1353	0.4000
0.5000	-0.0028	0.1424	0.1555	0.5000	-0.0025	0.1472	0.5000	-0.0019	0.0019	0.1521	0.5000	-0.0018	0.1521	0.5000	-0.0018	0.1521	0.5000
0.6000	-0.0034	0.1555	0.1665	0.6000	-0.0032	0.1605	0.6000	-0.0025	0.0025	0.1665	0.6000	-0.0024	0.1665	0.6000	-0.0024	0.1665	0.6000
0.7000	-0.0044	0.1752	0.1724	0.7000	-0.0039	0.1724	0.7000	-0.0032	0.0032	0.1785	0.7000	-0.0031	0.1785	0.7000	-0.0031	0.1785	0.7000
0.8000	-0.0051	0.1752	0.1815	0.8000	-0.0047	0.1815	0.8000	-0.0039	0.0039	0.1881	0.8000	-0.0038	0.1881	0.8000	-0.0038	0.1881	0.8000
0.9000	-0.0059	0.1819	0.1885	0.9000	-0.0054	0.1885	0.9000	-0.0046	0.0046	0.1954	0.9000	-0.0045	0.1954	0.9000	-0.0045	0.1954	0.9000
1.0000	-0.0066	0.1864	0.1932	1.0000	-0.0061	0.1932	1.0000	-0.0053	0.0053	0.2004	1.0000	-0.0052	0.2004	1.0000	-0.0052	0.2004	1.0000
1.1000	-0.0072	0.1864	0.1958	1.1000	-0.0067	0.1958	1.1000	-0.0059	0.0059	0.2030	1.1000	-0.0058	0.2030	1.1000	-0.0058	0.2030	1.1000
1.2000	-0.0077	0.1892	0.1962	1.2000	-0.0073	0.1962	1.2000	-0.0065	0.0065	0.2035	1.2000	-0.0064	0.2035	1.2000	-0.0064	0.2035	1.2000
1.3000	-0.0081	0.1875	0.1892	1.3000	-0.0077	0.1944	1.3000	-0.0070	0.0070	0.2017	1.3000	-0.0069	0.2017	1.3000	-0.0069	0.2017	1.3000
1.4000	-0.0084	0.1839	0.1875	1.4000	-0.0080	0.1906	1.4000	-0.0073	0.0073	0.1977	1.4000	-0.0072	0.1977	1.4000	-0.0072	0.1977	1.4000
1.5000	-0.0085	0.1782	0.1847	1.5000	-0.0082	0.1782	1.5000	-0.0075	0.0075	0.1915	1.5000	-0.0074	0.1915	1.5000	-0.0074	0.1915	1.5000
1.6000	-0.0085	0.1706	0.1768	1.6000	-0.0082	0.1768	1.6000	-0.0076	0.0076	0.1832	1.6000	-0.0075	0.1832	1.6000	-0.0075	0.1832	1.6000
1.7000	-0.0083	0.1611	0.1668	1.7000	-0.0080	0.1668	1.7000	-0.0075	0.0075	0.1727	1.7000	-0.0074	0.1727	1.7000	-0.0074	0.1727	1.7000
1.8000	-0.0079	0.1496	0.1547	1.8000	-0.0076	0.1497	1.8000	-0.0071	0.0071	0.1691	1.8000	-0.0070	0.1691	1.8000	-0.0070	0.1691	1.8000
1.9000	-0.0071	0.1361	0.1407	1.9000	-0.0069	0.1407	1.9000	-0.0066	0.0066	0.1454	1.9000	-0.0065	0.1454	1.9000	-0.0065	0.1454	1.9000
2.0000	-0.0061	0.1208	0.1261	2.0000	-0.0060	0.1261	2.0000	-0.0057	0.0057	0.1255	2.0000	-0.0056	0.1255	2.0000	-0.0056	0.1255	2.0000
2.1000	-0.0049	0.1036	0.1146	2.1000	-0.0048	0.1146	2.1000	-0.0046	0.0046	0.1396	2.1000	-0.0045	0.1396	2.1000	-0.0045	0.1396	2.1000
2.2000	-0.0033	0.0800	0.0864	2.2000	-0.0033	0.0864	2.2000	-0.0032	0.0032	0.0895	2.2000	-0.0031	0.0895	2.2000	-0.0031	0.0895	2.2000
2.3000	-0.0014	0.0644	0.0644	2.3000	-0.0014	0.0644	2.3000	-0.0014	0.0014	0.0653	2.3000	-0.0013	0.0653	2.3000	-0.0013	0.0653	2.3000
2.4000	-0.0000	0.0491	0.0491	2.4000	-0.0000	0.0491	2.4000	-0.0000	0.0000	0.0492	2.4000	-0.0000	0.0492	2.4000	-0.0000	0.0492	2.4000
2.5000	0.0242	0.0242	0.0242	2.5000	0.0242	0.0242	2.5000	0.0242	0.0242	0.0242	2.5000	0.0242	0.0242	2.5000	0.0242	0.0242	2.5000

Table 10.4 Continued.

BLADE SECTION NO.	NUMBER OF BLADES = 21.0	AXIAL LOCATION OF STACKING LINE IN COMPRESSOR = 1.830 IN.											
		STACKING POINT COORDINATES (IN.)	SECTION SETTING ANGLE (DEG.)	BLADE SECTION C.G. COORDINATES (IN.)	SECTION AREA (IN.)	MOMENTS OF INERTIA THROUGH C.G. (IN.)**2	MAX. SETTING ANGLE (DEG.)	SECTION CONSTANT STIFFNESS (IN.)**4	SECTION CONSTANT STIFFNESS (IN.)**4	MAX. SETTING ANGLE (DEG.)	SECTION CONSTANT STIFFNESS (IN.)**4	SECTION CONSTANT STIFFNESS (IN.)**4	
13	6.020	1.1943	42.774	(IN.) 1.194	(IN.) 0.0876	(IN.) 0.38964	(IN.) 0.0876	(IN.) 0.001301	(IN.) 0.13030	(DEG.) 42.709	(IN.) 0.04464	(IN.) 0.047327	
14	5.860	1.1945	41.467	(IN.) 1.1946	(IN.) 0.0916	(IN.) 0.40025	(IN.) 0.0916	(IN.) 0.0014261	(IN.) 0.13337	(DEG.) 41.206	(IN.) 0.04853	(IN.) 0.048334	
15	5.700	1.1947	0.0950	(IN.) 1.1947	(IN.) 0.0960	(IN.) 0.41092	(IN.) 0.0960	(IN.) 0.001561	(IN.) 0.13648	(DEG.) 39.908	(IN.) 0.049565	(IN.) 0.049354	
16	5.540	1.1949	0.1010	(IN.) 1.1949	(IN.) 0.1006	(IN.) 0.42166	(IN.) 0.1006	(IN.) 0.001707	(IN.) 0.13964	(DEG.) 38.440	(IN.) 0.050701	(IN.) 0.050393	
SECTION NO. 13 COORDINATES													
L	(IN.)	(IN.)	HS	L	(IN.)	(IN.)	L	(IN.)	(IN.)	HS	L	(IN.)	HS
0.0	0.0241	0.0	0.0241	0.0	0.0241	(IN.) 0.0241	0.0	0.0241	(IN.) 0.0241	0.0	0.0242	(IN.) 0.0242	
0.021	0.0000	0.0	0.0493	0.0	0.0493	(IN.) 0.0493	0.0	0.0000	(IN.) 0.0000	0.0	0.0497	(IN.) 0.0497	
0.100	0.0002	0.0	0.0241	0.0	0.0241	(IN.) 0.0241	0.0	0.0000	(IN.) 0.0000	0.0	0.0242	(IN.) 0.0242	
0.200	0.0004	0.0	0.0718	0.0	0.0718	(IN.) 0.0718	0.0	0.0005	(IN.) 0.0005	0.0	0.097	(IN.) 0.097	
0.300	0.0004	0.0	0.0989	0.0	0.0989	(IN.) 0.0989	0.0	0.0010	(IN.) 0.0010	0.0	0.1000	(IN.) 0.1000	
0.400	0.0004	0.0	0.1230	0.0	0.1230	(IN.) 0.1230	0.0	0.0015	(IN.) 0.0015	0.0	0.1000	(IN.) 0.1000	
0.500	0.0003	0.0	0.1443	0.0	0.1443	(IN.) 0.1443	0.0	0.0013	(IN.) 0.0013	0.0	0.0745	(IN.) 0.0745	
0.600	0.0003	0.0	0.1628	0.0	0.1628	(IN.) 0.1628	0.0	0.0013	(IN.) 0.0013	0.0	0.0016	(IN.) 0.0016	
0.700	0.0004	0.0	0.1786	0.0	0.1786	(IN.) 0.1786	0.0	0.0013	(IN.) 0.0013	0.0	0.0016	(IN.) 0.0016	
0.800	0.0004	0.0	0.1918	0.0	0.1918	(IN.) 0.1918	0.0	0.0013	(IN.) 0.0013	0.0	0.0016	(IN.) 0.0016	
0.900	0.0004	0.0	0.2023	0.0	0.2023	(IN.) 0.2023	0.0	0.0013	(IN.) 0.0013	0.0	0.0016	(IN.) 0.0016	
1.000	0.0004	0.0	0.2103	0.0	0.2103	(IN.) 0.2103	0.0	0.0013	(IN.) 0.0013	0.0	0.0016	(IN.) 0.0016	
1.100	0.0004	0.0	0.2157	0.0	0.2157	(IN.) 0.2157	0.0	0.0013	(IN.) 0.0013	0.0	0.0016	(IN.) 0.0016	
1.200	0.0004	0.0	0.2240	0.0	0.2240	(IN.) 0.2240	0.0	0.0013	(IN.) 0.0013	0.0	0.0016	(IN.) 0.0016	
1.300	0.0004	0.0	0.2271	0.0	0.2271	(IN.) 0.2271	0.0	0.0014	(IN.) 0.0014	0.0	0.0016	(IN.) 0.0016	
1.400	0.0004	0.0	0.2276	0.0	0.2276	(IN.) 0.2276	0.0	0.0014	(IN.) 0.0014	0.0	0.0016	(IN.) 0.0016	
1.500	0.0005	0.0	0.2256	0.0	0.2256	(IN.) 0.2256	0.0	0.0014	(IN.) 0.0014	0.0	0.0016	(IN.) 0.0016	
1.600	0.0005	0.0	0.2231	0.0	0.2231	(IN.) 0.2231	0.0	0.0014	(IN.) 0.0014	0.0	0.0016	(IN.) 0.0016	
1.700	0.0005	0.0	0.2219	0.0	0.2219	(IN.) 0.2219	0.0	0.0014	(IN.) 0.0014	0.0	0.0016	(IN.) 0.0016	
1.800	0.0005	0.0	0.2192	0.0	0.2192	(IN.) 0.2192	0.0	0.0014	(IN.) 0.0014	0.0	0.0016	(IN.) 0.0016	
1.900	0.0005	0.0	0.2172	0.0	0.2172	(IN.) 0.2172	0.0	0.0014	(IN.) 0.0014	0.0	0.0016	(IN.) 0.0016	
2.000	0.0005	0.0	0.2156	0.0	0.2156	(IN.) 0.2156	0.0	0.0014	(IN.) 0.0014	0.0	0.0016	(IN.) 0.0016	
2.100	0.0005	0.0	0.2137	0.0	0.2137	(IN.) 0.2137	0.0	0.0014	(IN.) 0.0014	0.0	0.0016	(IN.) 0.0016	
2.200	0.0005	0.0	0.2113	0.0	0.2113	(IN.) 0.2113	0.0	0.0014	(IN.) 0.0014	0.0	0.0016	(IN.) 0.0016	
2.300	0.0005	0.0	0.2086	0.0	0.2086	(IN.) 0.2086	0.0	0.0014	(IN.) 0.0014	0.0	0.0016	(IN.) 0.0016	
2.3667	0.0005	0.0	0.2064	0.0	0.2064	(IN.) 0.2064	0.0	0.0014	(IN.) 0.0014	0.0	0.0016	(IN.) 0.0016	
2.3890	0.0005	0.0	0.2043	0.0	0.2043	(IN.) 0.2043	0.0	0.0014	(IN.) 0.0014	0.0	0.0016	(IN.) 0.0016	
SECTION NO. 14 COORDINATES													
L	(IN.)	(IN.)	HS	L	(IN.)	(IN.)	L	(IN.)	(IN.)	HS	L	(IN.)	HS
0.0	0.0241	0.0	0.0241	0.0	0.0241	(IN.) 0.0241	0.0	0.0241	(IN.) 0.0241	0.0	0.0242	(IN.) 0.0242	
0.021	0.0000	0.0	0.0493	0.0	0.0493	(IN.) 0.0493	0.0	0.0000	(IN.) 0.0000	0.0	0.0497	(IN.) 0.0497	
0.100	0.0002	0.0	0.0241	0.0	0.0241	(IN.) 0.0241	0.0	0.0000	(IN.) 0.0000	0.0	0.0112	(IN.) 0.0112	
0.200	0.0004	0.0	0.0718	0.0	0.0718	(IN.) 0.0718	0.0	0.0005	(IN.) 0.0005	0.0	0.0759	(IN.) 0.0759	
0.300	0.0004	0.0	0.1230	0.0	0.1230	(IN.) 0.1230	0.0	0.0010	(IN.) 0.0010	0.0	0.1000	(IN.) 0.1000	
0.400	0.0004	0.0	0.1443	0.0	0.1443	(IN.) 0.1443	0.0	0.0013	(IN.) 0.0013	0.0	0.1000	(IN.) 0.1000	
0.500	0.0003	0.0	0.1628	0.0	0.1628	(IN.) 0.1628	0.0	0.0013	(IN.) 0.0013	0.0	0.1000	(IN.) 0.1000	
0.600	0.0004	0.0	0.1786	0.0	0.1786	(IN.) 0.1786	0.0	0.0013	(IN.) 0.0013	0.0	0.1000	(IN.) 0.1000	
0.700	0.0004	0.0	0.1918	0.0	0.1918	(IN.) 0.1918	0.0	0.0013	(IN.) 0.0013	0.0	0.1000	(IN.) 0.1000	
0.800	0.0004	0.0	0.2023	0.0	0.2023	(IN.) 0.2023	0.0	0.0013	(IN.) 0.0013	0.0	0.1000	(IN.) 0.1000	
0.900	0.0004	0.0	0.2103	0.0	0.2103	(IN.) 0.2103	0.0	0.0013	(IN.) 0.0013	0.0	0.1000	(IN.) 0.1000	
1.000	0.0004	0.0	0.2157	0.0	0.2157	(IN.) 0.2157	0.0	0.0013	(IN.) 0.0013	0.0	0.1000	(IN.) 0.1000	
1.100	0.0004	0.0	0.2240	0.0	0.2240	(IN.) 0.2240	0.0	0.0013	(IN.) 0.0013	0.0	0.1000	(IN.) 0.1000	
1.200	0.0004	0.0	0.2271	0.0	0.2271	(IN.) 0.2271	0.0	0.0014	(IN.) 0.0014	0.0	0.1000	(IN.) 0.1000	
1.300	0.0004	0.0	0.2276	0.0	0.2276	(IN.) 0.2276	0.0	0.0014	(IN.) 0.0014	0.0	0.1000	(IN.) 0.1000	
1.400	0.0004	0.0	0.2256	0.0	0.2256	(IN.) 0.2256	0.0	0.0014	(IN.) 0.0014	0.0	0.1000	(IN.) 0.1000	
1.500	0.0005	0.0	0.2231	0.0	0.2231	(IN.) 0.2231	0.0	0.0014	(IN.) 0.0014	0.0	0.1000	(IN.) 0.1000	
1.600	0.0005	0.0	0.2192	0.0	0.2192	(IN.) 0.2192	0.0	0.0014	(IN.) 0.0014	0.0	0.1000	(IN.) 0.1000	
1.700	0.0005	0.0	0.2172	0.0	0.2172	(IN.) 0.2172	0.0	0.0014	(IN.) 0.0014	0.0	0.1000	(IN.) 0.1000	
1.800	0.0005	0.0	0.2156	0.0	0.2156	(IN.) 0.2156	0.0	0.0014	(IN.) 0.0014	0.0	0.1000	(IN.) 0.1000	
1.900	0.0005	0.0	0.2137	0.0	0.2137	(IN.) 0.2137	0.0	0.0014	(IN.) 0.0014	0.0	0.1000	(IN.) 0.1000	
2.000	0.0005	0.0	0.2113	0.0	0.2113	(IN.) 0.2113	0.0	0.0014	(IN.) 0.0014	0.0	0.1000	(IN.) 0.1000	
2.100	0.0005	0.0	0.2086	0.0	0.2086	(IN.) 0.2086	0.0	0.0014	(IN.) 0.0014	0.0	0.1000	(IN.) 0.1000	
2.200	0.0005	0.0	0.2064	0.0	0.2064	(IN.) 0.2064	0.0	0.0014	(IN.) 0.0014	0.0	0.1000	(IN.) 0.1000	
2.300	0.0005	0.0	0.2043	0.0	0.2043	(IN.) 0.2043	0.0	0.0014	(IN.) 0.0014	0.0	0.1000	(IN.) 0.1000	
2.3667	0.0005	0.0	0.2023	0.0	0.2023	(IN.) 0.2023	0.0	0.0014	(IN.) 0.0014	0.0	0.1000	(IN.) 0.1000	
2.3890	0.0005	0.0	0.2043	0.0	0.2043	(IN.) 0.2043	0.0	0.0014	(IN.) 0.0014	0.0	0.1000	(IN.) 0.1000	
SECTION NO. 15 COORDINATES													
L	(IN.)	(IN.)	HS	L	(IN.)	(IN.)	L	(IN.)	(IN.)	HS	L	(IN.)	HS
0.0	0.0241	0.0	0.0241	0.0	0.0241	(IN.) 0.0241	0.0	0.0241	(IN.) 0.0241	0.0	0.0242	(IN.) 0.0242	
0.021	0.0000	0.0	0.0493	0.0	0.0493	(IN.) 0.0493	0.0	0.0000	(IN.) 0.0000	0.0	0.0497	(IN.) 0.0497	
0.100	0.0002	0.0	0.0241	0.0	0.0241	(IN.) 0.0241	0.0	0.0005	(IN.) 0.0005	0.0	0.0112	(IN.) 0.0112	
0.200	0.0004	0.0	0.0718	0.0	0.0718	(IN.) 0.0718	0.0	0.0010	(IN.) 0.0010	0.0	0.0759	(IN.) 0.0759	
0.300	0.0004	0.0	0.1230	0.0	0.1230	(IN.) 0.1230	0.0	0.0015	(IN.) 0.0015	0.0	0.1000	(IN.) 0.1000	
0.400	0.0004	0.0	0.1443	0.0	0.1443	(IN.) 0.1443	0.0	0.0013	(IN.) 0.0013	0.0	0.1000	(IN.) 0.1000	
0.500	0.0003	0.0	0.1628	0.0	0.1628	(IN.) 0.1628	0.0	0.0013	(IN.) 0.0013	0.0	0.1000	(IN.) 0.1000	
0.600	0.0004	0.0	0.1786	0.0	0.1786	(IN.) 0.1786	0.0	0.0013	(IN.) 0.0013	0.0	0.1000	(IN.) 0.1000	
0.700	0.0004	0.0	0.1918	0.0	0.1918	(IN.) 0.1918	0.0	0.0013	(IN.) 0.0013	0.0	0.1000	(IN.) 0.1000	
0.800	0.0004	0.0	0.2023	0.0	0.2023	(IN.)							

Table 10.4 Concluded.

Table 10.5 Stator blade manufacturing coordinates generated by NASA design code.

BLADE SECTION NO.	NUMBER OF BLADES = 30.0	AXIAL LOCATION OF STACKING LINE IN COMPRESSOR = 5.260 IN.									
		STACKING POINT COORDINATES	SECTION ANGLE	BLADE SECTION AREA	MOMENTS OF INERTIA C.G. THROUGH C.G.	SECTION TWIST	MAX. SECTION SETTING ANGLE	CONSTANT STIFFNESS	MAX. SECTION SETTING ANGLE	CONSTANT STIFFNESS	
(IN.)	(IN.)	(IN.)	(IN.)	(IN.)	(IN.)	(IN.)	(DEG.)	(IN.)	(DEG.)	(IN.)	
1	6.020	1.1955	0.1880	12.623	1.195	0.188	0.42756	1.1447	1.2538	0.05732	
2	7.840	1.1933	0.1400	9.134	1.193	0.140	0.40537	0.00898	1.3684	0.049729	
3	7.660	1.1945	0.1215	7.834	1.1945	0.1215	0.39616	0.001595	1.3256	0.048220	
4	7.500	1.1944	0.1187	7.685	1.194	0.1187	0.38548	0.001469	1.2945	0.047187	
SECTION NO.	1	COORDINATES	SECTION NO.	2	COORDINATES	SECTION NO.	3	COORDINATES	SECTION NO.	4	COORDINATES
(IN.)	(IN.)	(IN.)	(IN.)	(IN.)	(IN.)	(IN.)	(IN.)	(IN.)	(IN.)	(IN.)	(IN.)
0.0269	0.0249	0.0249	0.0242	0.0242	0.0242	0.0240	0.0240	0.0240	0.0239	0.0239	0.0239
0.1000	0.1344	0.1456	0.2000	0.0171	0.1213	0.0829	0.0829	0.0829	0.1000	0.1000	0.1000
0.2000	0.3513	0.3888	0.2555	0.2555	0.1553	0.1553	0.1553	0.1553	0.2000	0.2000	0.2000
0.4000	0.6600	0.2664	0.4000	0.3229	0.1851	0.1851	0.1851	0.1851	0.4000	0.4000	0.4000
0.5000	0.7888	0.2587	0.5000	0.3939	0.2111	0.2111	0.2111	0.2111	0.5000	0.5000	0.5000
0.6000	0.8966	0.2862	0.6000	0.4448	0.2333	0.2333	0.2333	0.2333	0.6000	0.6000	0.6000
0.7000	0.986	0.3091	0.7000	0.6494	0.2519	0.2519	0.2519	0.2519	0.7000	0.7000	0.7000
0.8000	0.8000	0.3275	0.8000	0.531	0.2670	0.2670	0.2670	0.2670	0.8000	0.8000	0.8000
0.9000	0.6000	0.3058	0.9000	0.559	0.2765	0.2765	0.2765	0.2765	0.9000	0.9000	0.9000
1.0000	0.4000	0.3416	1.0000	0.578	0.2867	0.2867	0.2867	0.2867	1.0000	1.0000	1.0000
1.1000	0.2000	0.3515	1.1000	0.589	0.2915	0.2915	0.2915	0.2915	1.1000	1.1000	1.1000
1.2000	0.171	0.3575	1.2000	0.591	0.2929	0.2929	0.2929	0.2929	1.2000	1.2000	1.2000
1.3000	0.162	0.3592	1.3000	0.584	0.2909	0.2909	0.2909	0.2909	1.3000	1.3000	1.3000
1.4000	0.134	0.3568	1.4000	0.570	0.2855	0.2855	0.2855	0.2855	1.4000	1.4000	1.4000
1.5000	0.134	0.3502	1.5000	0.547	0.2767	0.2767	0.2767	0.2767	1.5000	1.5000	1.5000
1.6000	0.088	0.3394	1.6000	0.500	0.2645	0.2645	0.2645	0.2645	1.6000	1.6000	1.6000
1.7000	0.027	0.3244	1.7000	0.475	0.2487	0.2487	0.2487	0.2487	1.7000	1.7000	1.7000
1.8000	0.048	0.3050	1.8000	0.427	0.2295	0.2295	0.2295	0.2295	1.8000	1.8000	1.8000
1.9000	0.054	0.2811	1.9000	0.370	0.2066	0.2066	0.2066	0.2066	1.9000	1.9000	1.9000
2.0000	0.064	0.2526	2.0000	0.306	0.1800	0.1800	0.1800	0.1800	2.0000	2.0000	2.0000
2.1000	0.066	0.2192	2.1000	0.232	0.1495	0.1495	0.1495	0.1495	2.1000	2.1000	2.1000
2.2000	0.066	0.1372	2.2000	0.151	0.1053	0.1053	0.1053	0.1053	2.2000	2.2000	2.2000
2.3000	0.026	0.0779	2.3000	0.061	0.0769	0.0769	0.0769	0.0769	2.3000	2.3000	2.3000
2.3674	-0.000	0.0515	2.3645	-0.000	0.0500	0.0500	0.0500	0.0500	2.3650	-0.000	0.0494
2.3913	0.0239	0.0239	2.3884	0.0239	0.0239	0.0239	0.0239	0.0239	2.3891	0.0239	0.0239

Table 10.5 Continued.

BLADE SECTION NO.	NUMBER OF BLADES =		30.0		AXIAL LOCATION OF STACKING LINE IN COMPRESSOR =		5.260 IN.	
	RAD. (IN.)	LOC. (IN.)	STACKING POINT COORDINATES L (IN.)	C.G. COORDINATES H (IN.)	SECTION SETTING ANGLE (DEG.)	BLADE SECTION COORDINATES H (IN.)	SECTION AREA	INERTIA THROUGH C.G.
5	7.340	1.1944	0.1198	7.842	1.194	0.1198	0.001382	(IN.)**4 0.12658
6	7.180	1.1944	0.1214	8.030	1.194	0.1214	0.001304	(IN.)**4 0.12377
7	7.020	1.1944	0.1230	8.220	1.194	0.1230	0.001231	(IN.)**4 0.12095
8	6.860	1.1944	0.1244	8.406	1.194	0.1244	0.001161	(IN.)**4 0.094364
SECTION NO.	S COORDINATES L (IN.)	S COORDINATES H (IN.)	SECTION NO.	6 COORDINATES L (IN.)	6 COORDINATES H (IN.)	SECTION NO.	7 COORDINATES L (IN.)	7 COORDINATES H (IN.)
0	0.0238	0.0238	0	0.0238	0.0238	0	0.0238	0.0238
1	0.0238	0.0238	1	0.0238	0.0238	1	0.0238	0.0238
2	0.0054	0.0492	2	0.0054	0.0492	2	0.0054	0.0492
3	0.0000	0.0761	3	0.0000	0.0761	3	0.0000	0.0757
4	0.2000	0.1083	4	0.2000	0.1083	4	0.2000	0.1078
5	0.3000	0.0181	5	0.3000	0.0181	5	0.3000	0.0174
6	0.4000	0.0235	6	0.4000	0.0235	6	0.4000	0.0167
7	0.5000	0.0282	7	0.5000	0.0282	7	0.5000	0.0162
8	0.6000	0.0323	8	0.6000	0.0323	8	0.6000	0.0159
9	0.7000	0.0359	9	0.7000	0.0359	9	0.7000	0.0155
10	0.8000	0.0387	10	0.8000	0.0387	10	0.8000	0.0152
11	0.9000	0.2340	11	0.9000	0.2340	11	0.9000	0.0149
12	0.9000	0.410	12	0.9000	0.410	12	0.9000	0.0146
13	0.9000	0.442	13	0.9000	0.442	13	0.9000	0.0143
14	1.0000	0.2515	14	1.0000	0.2515	14	1.0000	0.0140
15	1.0000	0.435	15	1.0000	0.435	15	1.0000	0.0137
16	1.0000	0.438	16	1.0000	0.438	16	1.0000	0.0135
17	1.0000	0.435	17	1.0000	0.435	17	1.0000	0.0133
18	1.0000	0.425	18	1.0000	0.425	18	1.0000	0.0131
19	1.0000	0.409	19	1.0000	0.409	19	1.0000	0.0129
20	1.0000	0.409	20	1.0000	0.409	20	1.0000	0.0127
21	1.0000	0.409	21	1.0000	0.409	21	1.0000	0.0125
22	1.0000	0.409	22	1.0000	0.409	22	1.0000	0.0123
23	1.0000	0.409	23	1.0000	0.409	23	1.0000	0.0121
24	1.0000	0.386	24	1.0000	0.386	24	1.0000	0.0119
25	1.0000	0.357	25	1.0000	0.357	25	1.0000	0.0117
26	1.0000	0.322	26	1.0000	0.322	26	1.0000	0.0115
27	1.0000	0.280	27	1.0000	0.280	27	1.0000	0.0113
28	1.0000	0.231	28	1.0000	0.231	28	1.0000	0.0111
29	2.0000	0.176	29	2.0000	0.176	29	2.0000	0.0109
30	2.0000	0.115	30	2.0000	0.115	30	2.0000	0.0107
31	2.0000	0.047	31	2.0000	0.047	31	2.0000	0.0105
32	2.0000	0.000	32	2.0000	0.000	32	2.0000	0.0103
33	2.0000	0.0493	33	2.0000	0.0493	33	2.0000	0.0101
34	2.0000	0.0239	34	2.0000	0.0239	34	2.0000	0.0099
35	2.3869	0.0239	35	2.3869	0.0239	35	2.3869	0.0097

Table 10.5 Continued.

NUMBER OF BLADES = 30.0				AXIAL LOCATION OF STACKING LINE IN COMPRESSOR = 5.260 IN.													
BLADE SECTION RAD. NO.	STACKING POINT COORDINATES (IN.)			BLADE SECTION C.G. COORDINATES (IN.)			SECTION AREA			MOMENTS OF INERTIA THROUGH C.G.			SECTION STIFFNESS				
	L	H	ANGLE	L	H	ANGLE	I _{MIN}	I _{MAX}	I _{MIN}	I _{MAX}	I _{MIN}	I _{MAX}	C.G. (IN.)	ANGLE (DEG.)	CONSTANT STIFFNESS (IN. ³)		
9	6.00	1.1944	0.1259	8.599	1.1944	0.1259	{ 1.1944 } 0.33413	{ 1.1944 } 0.11529	0.001036	0.11247	8.607	0.002114	0.042650	0.002114	0.042650		
10	6.540	1.1943	0.1275	8.800	1.1943	0.1275	{ 1.1943 } 0.3284	{ 1.1943 } 0.10964	0.000939	0.10964	8.805	0.002154	0.041732	0.002154	0.041732		
11	6.380	1.1943	0.1291	9.010	1.1943	0.1291	{ 1.1943 } 0.31355	{ 1.1943 } 0.10681	0.000928	0.10681	9.020	0.002122	0.043019	0.002122	0.043019		
12	6.220	1.1943	0.1307	9.229	1.1943	0.1307	{ 1.1943 } 0.30325	{ 1.1943 } 0.10681	0.000928	0.10681	9.240	0.001985	0.039862	0.001985	0.039862		
SECTION NO.	9	COORDINATES	SECTION NO.	10	COORDINATES	SECTION NO.	11	COORDINATES	SECTION NO.	12	COORDINATES	SECTION NO.	13	COORDINATES	SECTION NO.	14	COORDINATES
L	(IN.)	HP	L	(IN.)	HP	L	(IN.)	HP	L	(IN.)	HP	L	(IN.)	HP	L	(IN.)	HP
0.0	0.238	0.0238	0.0	0.238	0.0238	0.0	0.238	0.0238	0.0	0.238	0.0238	0.0	0.238	0.0238	0.0	0.238	0.0238
0.100	0.090	0.092	0.100	0.089	0.092	0.100	0.089	0.092	0.100	0.089	0.092	0.100	0.089	0.092	0.100	0.089	0.092
0.200	0.0581	0.0575	0.071	0.0689	0.0575	0.071	0.0689	0.0575	0.071	0.0689	0.0575	0.071	0.0689	0.0575	0.071	0.0689	0.0575
0.300	0.0473	0.0454	0.073	0.0500	0.0454	0.073	0.0500	0.0454	0.073	0.0500	0.0454	0.073	0.0500	0.0454	0.073	0.0500	0.0454
0.400	0.0384	0.0354	0.086	0.0400	0.0384	0.086	0.0400	0.0384	0.086	0.0400	0.0384	0.086	0.0400	0.0384	0.086	0.0400	0.0384
0.500	0.0326	0.026	0.096	0.0462	0.0326	0.096	0.0462	0.0326	0.096	0.0462	0.0326	0.096	0.0462	0.0326	0.096	0.0462	0.0326
0.600	0.0288	0.016	0.106	0.0530	0.0288	0.106	0.0530	0.0288	0.106	0.0530	0.0288	0.106	0.0530	0.0288	0.106	0.0530	0.0288
0.700	0.0238	0.0115	0.117	0.0700	0.0238	0.117	0.0700	0.0238	0.117	0.0700	0.0238	0.117	0.0700	0.0238	0.117	0.0700	0.0238
0.800	0.0191	0.0081	0.120	0.0800	0.0191	0.120	0.0800	0.0191	0.120	0.0800	0.0191	0.120	0.0800	0.0191	0.120	0.0800	0.0191
0.900	0.0153	0.0052	0.125	0.0900	0.0153	0.125	0.0900	0.0153	0.125	0.0900	0.0153	0.125	0.0900	0.0153	0.125	0.0900	0.0153
1.000	0.0125	0.0034	0.130	0.1000	0.0125	0.130	0.1000	0.0125	0.130	0.1000	0.0125	0.130	0.1000	0.0125	0.130	0.1000	0.0125
1.100	0.0105	0.0026	0.135	0.1100	0.0105	0.135	0.1100	0.0105	0.135	0.1100	0.0105	0.135	0.1100	0.0105	0.135	0.1100	0.0105
1.200	0.0090	0.0021	0.140	0.1200	0.0090	0.140	0.1200	0.0090	0.140	0.1200	0.0090	0.140	0.1200	0.0090	0.140	0.1200	0.0090
1.300	0.0085	0.0016	0.145	0.1300	0.0085	0.145	0.1300	0.0085	0.145	0.1300	0.0085	0.145	0.1300	0.0085	0.145	0.1300	0.0085
1.400	0.0081	0.0011	0.150	0.1400	0.0081	0.150	0.1400	0.0081	0.150	0.1400	0.0081	0.150	0.1400	0.0081	0.150	0.1400	0.0081
1.500	0.0076	0.0006	0.155	0.1500	0.0076	0.155	0.1500	0.0076	0.155	0.1500	0.0076	0.155	0.1500	0.0076	0.155	0.1500	0.0076
1.600	0.0072	0.0004	0.160	0.1600	0.0072	0.160	0.1600	0.0072	0.160	0.1600	0.0072	0.160	0.1600	0.0072	0.160	0.1600	0.0072
1.700	0.0068	0.0003	0.165	0.1700	0.0068	0.165	0.1700	0.0068	0.165	0.1700	0.0068	0.165	0.1700	0.0068	0.165	0.1700	0.0068
1.800	0.0065	0.0002	0.170	0.1800	0.0065	0.170	0.1800	0.0065	0.170	0.1800	0.0065	0.170	0.1800	0.0065	0.170	0.1800	0.0065
1.900	0.0062	0.0001	0.175	0.1900	0.0062	0.175	0.1900	0.0062	0.175	0.1900	0.0062	0.175	0.1900	0.0062	0.175	0.1900	0.0062
2.000	0.0060	0.0000	0.180	0.2000	0.0060	0.180	0.2000	0.0060	0.180	0.2000	0.0060	0.180	0.2000	0.0060	0.180	0.2000	0.0060
2.100	0.0058	-0.0001	0.185	0.2100	0.0058	0.185	0.2100	0.0058	0.185	0.2100	0.0058	0.185	0.2100	0.0058	0.185	0.2100	0.0058
2.200	0.0056	-0.0002	0.190	0.2200	0.0056	0.190	0.2200	0.0056	0.190	0.2200	0.0056	0.190	0.2200	0.0056	0.190	0.2200	0.0056
2.300	0.0055	-0.0003	0.195	0.2300	0.0055	0.195	0.2300	0.0055	0.195	0.2300	0.0055	0.195	0.2300	0.0055	0.195	0.2300	0.0055
2.365	0.0055	-0.0004	0.200	0.2365	0.0055	0.200	0.2365	0.0055	0.200	0.2365	0.0055	0.200	0.2365	0.0055	0.200	0.2365	0.0055
2.388	0.0055	-0.0005	0.205	0.2388	0.0055	0.205	0.2388	0.0055	0.205	0.2388	0.0055	0.205	0.2388	0.0055	0.205	0.2388	0.0055

Table 10.5 Continued.

Table 10.5 Concluded.

BLADE SECTION RAD. NO.	LOC. (IN.)	NUMBER OF BLADES =	30.0	AXIAL LOCATION OF STACKING LINE IN COMPRESSOR = 5.260 IN.			
				STACKING POINT COORDINATES (IN.)	SECTION SETTING ANGLE (DEG.)	BLADE SECTION C.G. COORDINATES (IN.)	SECTION MOMENTS OF INERTIA AREA
17	8.000			1.1946	0.1609	12.108	$(IN)^{1.02}$
							$(IN)^{1.04}$
							$(IN)^{1.06}$
							$(IN)^{1.08}$
							$(IN)^{1.10}$
							$(IN)^{1.12}$
							$(IN)^{1.14}$
							$(IN)^{1.16}$
							$(IN)^{1.18}$
							$(IN)^{1.20}$
							$(IN)^{1.22}$
							$(IN)^{1.24}$
							$(IN)^{1.26}$
							$(IN)^{1.28}$
							$(IN)^{1.30}$
							$(IN)^{1.32}$
							$(IN)^{1.34}$
							$(IN)^{1.36}$
							$(IN)^{1.38}$
							$(IN)^{1.40}$
							$(IN)^{1.42}$
							$(IN)^{1.44}$
							$(IN)^{1.46}$
							$(IN)^{1.48}$
							$(IN)^{1.50}$
							$(IN)^{1.52}$
							$(IN)^{1.54}$
							$(IN)^{1.56}$
							$(IN)^{1.58}$
							$(IN)^{1.60}$
							$(IN)^{1.62}$
							$(IN)^{1.64}$
							$(IN)^{1.66}$
							$(IN)^{1.68}$
							$(IN)^{1.70}$
							$(IN)^{1.72}$
							$(IN)^{1.74}$
							$(IN)^{1.76}$
							$(IN)^{1.78}$
							$(IN)^{1.80}$
							$(IN)^{1.82}$
							$(IN)^{1.84}$
							$(IN)^{1.86}$
							$(IN)^{1.88}$
							$(IN)^{1.90}$
							$(IN)^{1.92}$
							$(IN)^{1.94}$
							$(IN)^{1.96}$
							$(IN)^{1.98}$
							$(IN)^{2.00}$
							$(IN)^{2.02}$
							$(IN)^{2.04}$
							$(IN)^{2.06}$
							$(IN)^{2.08}$
							$(IN)^{2.10}$
							$(IN)^{2.12}$
							$(IN)^{2.14}$
							$(IN)^{2.16}$
							$(IN)^{2.18}$
							$(IN)^{2.20}$
							$(IN)^{2.22}$
							$(IN)^{2.24}$
							$(IN)^{2.26}$
							$(IN)^{2.28}$
							$(IN)^{2.30}$
							$(IN)^{2.32}$
							$(IN)^{2.34}$
							$(IN)^{2.36}$
							$(IN)^{2.38}$
							$(IN)^{2.40}$
							$(IN)^{2.42}$
							$(IN)^{2.44}$
							$(IN)^{2.46}$
							$(IN)^{2.48}$
							$(IN)^{2.50}$
							$(IN)^{2.52}$
							$(IN)^{2.54}$
							$(IN)^{2.56}$
							$(IN)^{2.58}$
							$(IN)^{2.60}$
							$(IN)^{2.62}$
							$(IN)^{2.64}$
							$(IN)^{2.66}$
							$(IN)^{2.68}$
							$(IN)^{2.70}$
							$(IN)^{2.72}$
							$(IN)^{2.74}$
							$(IN)^{2.76}$
							$(IN)^{2.78}$
							$(IN)^{2.80}$
							$(IN)^{2.82}$
							$(IN)^{2.84}$
							$(IN)^{2.86}$
							$(IN)^{2.88}$
							$(IN)^{2.90}$
							$(IN)^{2.92}$
							$(IN)^{2.94}$
							$(IN)^{2.96}$
							$(IN)^{2.98}$
							$(IN)^{3.00}$
							$(IN)^{3.02}$
							$(IN)^{3.04}$
							$(IN)^{3.06}$
							$(IN)^{3.08}$
							$(IN)^{3.10}$
							$(IN)^{3.12}$
							$(IN)^{3.14}$
							$(IN)^{3.16}$
							$(IN)^{3.18}$
							$(IN)^{3.20}$
							$(IN)^{3.22}$
							$(IN)^{3.24}$
							$(IN)^{3.26}$
							$(IN)^{3.28}$
							$(IN)^{3.30}$
							$(IN)^{3.32}$
							$(IN)^{3.34}$
							$(IN)^{3.36}$
							$(IN)^{3.38}$
							$(IN)^{3.40}$
							$(IN)^{3.42}$
							$(IN)^{3.44}$
							$(IN)^{3.46}$
							$(IN)^{3.48}$
							$(IN)^{3.50}$
							$(IN)^{3.52}$
							$(IN)^{3.54}$
							$(IN)^{3.56}$
							$(IN)^{3.58}$
							$(IN)^{3.60}$
							$(IN)^{3.62}$
							$(IN)^{3.64}$
							$(IN)^{3.66}$
							$(IN)^{3.68}$
							$(IN)^{3.70}$
							$(IN)^{3.72}$
							$(IN)^{3.74}$
							$(IN)^{3.76}$
							$(IN)^{3.78}$
							$(IN)^{3.80}$
							$(IN)^{3.82}$
							$(IN)^{3.84}$
							$(IN)^{3.86}$
							$(IN)^{3.88}$
							$(IN)^{3.90}$
							$(IN)^{3.92}$
							$(IN)^{3.94}$
							$(IN)^{3.96}$
							$(IN)^{3.98}$
							$(IN)^{4.00}$

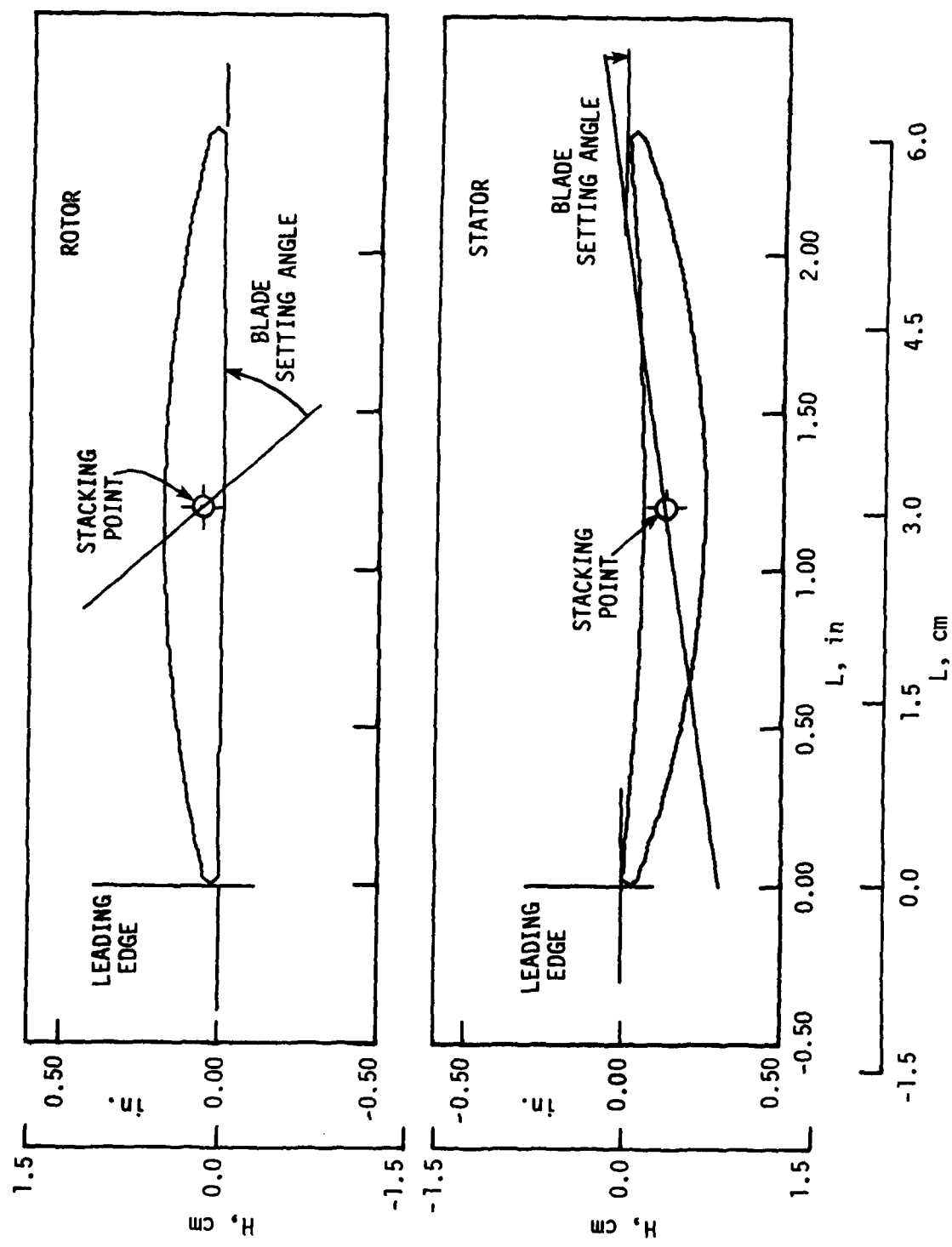


Figure 10.1. Typical rotor and stator blade sections using manufacturing coordinates.

11. APPENDIX C: COMPUTER PROGRAMS AND DATA STORAGE

The computer programs used during this research program are listed in this section. These programs as well as all experimental data and reduced data results are stored on magnetic tapes (cassette or reel) and are indexed according to tape and file numbers as specified below.

Actuator position correlation program: Linear least-squares correlation between actuator potentiometer voltage readout and actuator motion for probe and circumferential positioning actuators; cassette 1, file 1

Slow-response data acquisition program: Acquisition of time-averaged total-head and flow angle survey data; cassette 2, file 1

Compressor overall performance acquisition program: Acquisition of compressor torque meter based performance data; cassette 2, file 2

Time-averaged data reduction program A: Reduction of time-averaged data to obtain point flow-field parameters and circumferentially-averaged flow-field parameters (a plotting option is available); tape DSMDH, file 16

Time-averaged data reduction program B: Reduction of time-averaged data to obtain rotor, stator, stage, and overall performance parameters; cassette 3, file 1

Contour map generation program: Generates contour maps of point flow-field parameters over two stator pitches behind any blade row; tape DSMDH, file 15

Data uncertainty: From estimates of primary measurement uncertainties calculates, using the procedure of Kline and McClintock [11], the uncertainty estimates for all flow-field and performance parameters; cassette 3, file 2

Time-averaged data, station 1: Storage of circumferential survey data at 10%, 30%, 50%, 70%, and 90% span locations including probe data, outer annulus-wall static-head data, and test condition parameters; tape COMP, file 1

Time-averaged data, station 2: Storage of circumferential survey data at 10%, 30%, 50%, 70%, and 90% span locations including probe data, outer annulus-wall static-head data, and test condition parameters; tape COMP, file 2

Time-averaged data, station 3: Storage of circumferential survey data at 10%, 30%, 50%, 70%, and 90% span locations including probe data, outer annulus-wall static-head data, and test condition parameters; tape COMP, file 3

Time-averaged data, station 4: Storage of circumferential survey data at 10%, 30%, 50%, 70%, and 90% span locations including probe data, outer annulus-wall static-head data, and test condition parameters; tape COMP, file 4

Time-averaged data, station 5: Storage of circumferential survey data at 10%, 30%, 50%, 70%, and 90% span locations including probe data, outer annulus-wall static-head data, and test condition parameters; tape COMP, file 5

Reduced time-averaged data, station 1: Storage of results of data reduction program A; tape COMP, file 6

Reduced time-averaged data, station 2: Storage of results of data reduction program A; tape COMP, file 7

Reduced time-averaged data, station 3: Storage of results of data reduction program A; tape COMP, file 8

Reduced time-averaged data, station 4: Storage of results of data reduction program A; tape COMP, file 9

Reduced time-averaged data, station 5: Storage of results of data reduction program A; tape COMP, file 10

12. APPENDIX D: PARAMETER EQUATIONS

The equations used in calculating the time-averaged and performance parameters are presented in this section. The symbols used in the equations are defined in the symbols and notation section and the sign conventions are shown in Figure 12.1. Circumferentially or radially averaged parameters were obtained using a spline-fit integration scheme [9].

12.1. General Parameters12.1.1. Basic Fluid Properties

Barometric pressure, N/m²:

$$P_{atm} = h_{hg@t_{baro}} \cdot (1.0 - 0.00018(t_{baro} - 273.15)) \cdot \gamma_{hg@273^{\circ}K}$$
12.1

Density of air, kg/m³:

$$\rho = \frac{P_{atm}}{R t}$$
12.2

Specific weight of water, N/m³:

$$\gamma_{H_2O} = \frac{g}{g_c} \left(996.86224 + 0.1768124 \left(\frac{9}{5} t - 459.67 \right) - 2.64966 \times 10^{-3} \left(\frac{9}{5} t - 459.67 \right)^2 + 5.00063 \times 10^{-6} \left(\frac{9}{5} t - 459.67 \right)^3 \right)$$
12.3

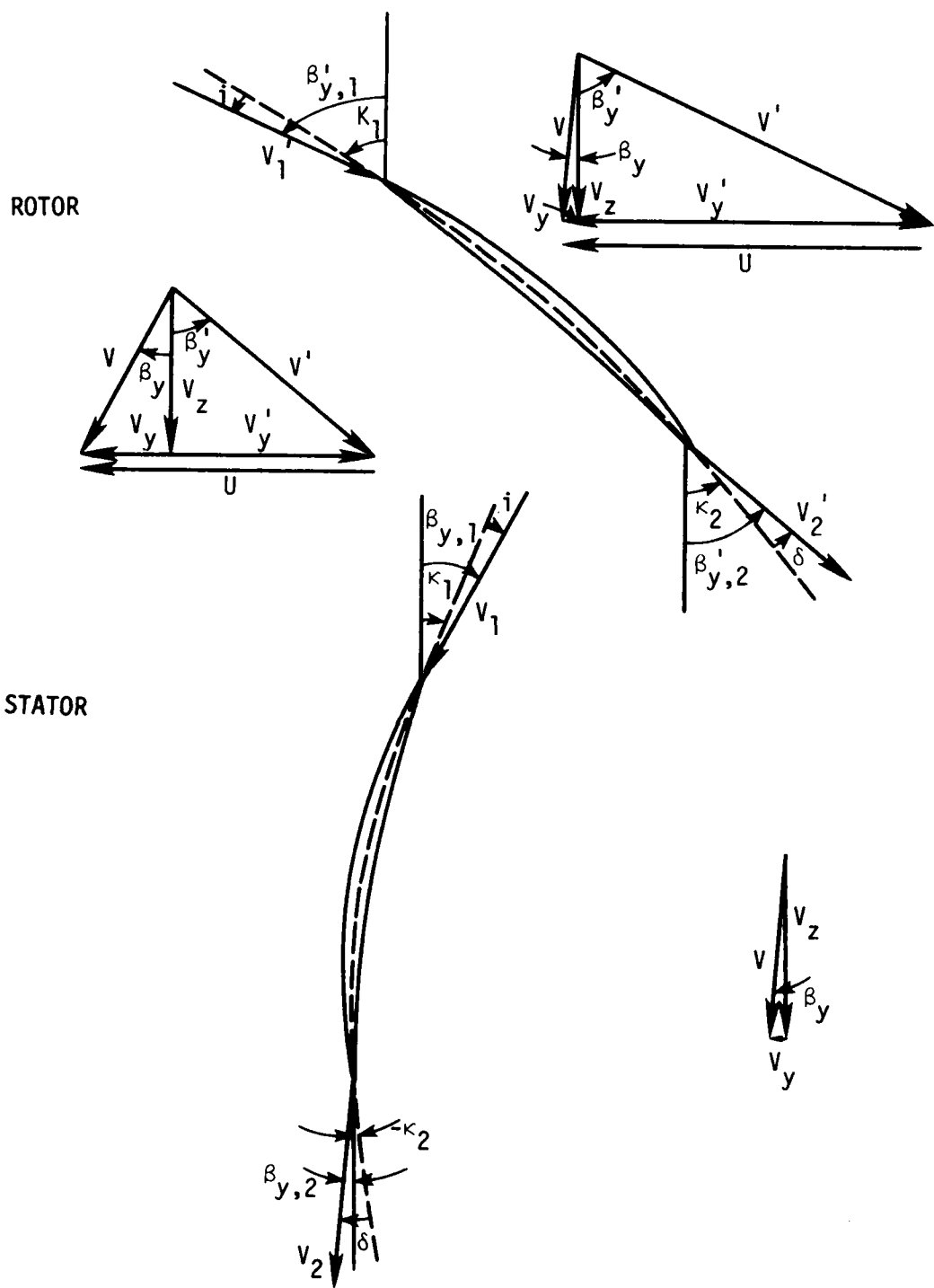


Figure 12.1 Sketch showing nomenclature and sign conventions (all positive except as noted) for slow-response instrument parameters.

12.1.2. Blade-Element location

Percent passage height from hub:

$$PHH = \frac{r-0.14224}{0.06096} \times 100 \quad 12.4$$

12.2. Flow-Field Parameters12.2.1. Point and Circumferential-Average Blade Element Quantities

Total head, Nm/kg:

$$H = \frac{P_t \gamma_{H_2}^0}{\rho} \quad 12.5$$

and

$$\bar{H} = \frac{1}{S_S} \int_0^{S_S} H \, dY \quad 12.6$$

Absolute flow angle behind rotors (see Figure 12.1 for sign convention), degrees:

$$\bar{\beta}_y = \frac{1}{S_S} \int_0^{S_S} \beta_y \, dY \quad 12.7$$

Absolute flow angle behind stators (see Figure 12.1 for sign convention), degrees:

$$\bar{\beta}_y = \frac{1}{Y_{freestream}} \int_{\text{across freestream}} \beta_y \, dY \quad 12.8$$

Annulus outer surface endwall static head, Nm/kg:

$$h_w = \frac{P_w \gamma_{H_2O}}{\rho} \quad 12.9$$

and

$$\bar{h}_w = \frac{1}{S_S} \int_0^{S_S} P_w dY \quad 12.10$$

Static head (radial equilibrium equation), Nm/kg:

$$\frac{dh}{dr} = \frac{2 \sin^2 \beta_y (\bar{H} - h)}{r} \quad 12.11$$

Absolute fluid velocity, m/s:

$$v = \sqrt{2 g_c (H - h)} \quad 12.12$$

and

$$\bar{v} = \frac{1}{S_S} \int_0^{S_S} v dY \quad 12.13$$

Blade velocity, m/s:

$$U = \frac{r\pi RPM}{30.0} \quad 12.14$$

Axial component of absolute fluid velocity, m/s:

$$v_z = v \cos \beta_y \quad 12.15$$

and

$$\bar{v}_z = \bar{v} \cos \bar{\beta}_y \quad 12.16$$

Tangential component of absolute fluid velocity (see Figure 12.1 for sign convention), m/s:

$$v_y = v \sin \beta_y \quad 12.17$$

and

$$\bar{v}_y = \bar{v} \sin \bar{\beta}_y \quad 12.18$$

Tangential component of relative fluid velocity (see Figure 12.1 for sign convention), m/s:

$$v'_y = U - v_y \quad 12.19$$

and

$$\bar{v}'_y = U - \bar{v}_y \quad 12.20$$

Relative fluid velocity, m/s:

$$v' = \sqrt{(v'_y)^2 + (v_z)^2} \quad 12.21$$

and

$$\bar{v}' = \sqrt{(v_y')^2 + (\bar{v}_z)^2} \quad 12.22$$

Relative tangential flow angle (see Figure 12.1 for sign convention), degrees:

$$\beta_y' = \tan^{-1} \left(\frac{v_y'}{\bar{v}_z} \right) \quad 12.23$$

and

$$\bar{\beta}_y = \tan^{-1} \left(\frac{\bar{v}_y}{\bar{v}_z} \right) \quad 12.24$$

Incidence angle for rotors (see Figure 12.1 for sign convention), degrees:

$$\bar{i}_R = \bar{\beta}_{y,1,R} - \kappa_{1,R} \quad 12.25$$

Deviation angle for rotors (see Figure 12.1 for sign convention), degrees:

$$\bar{\delta}_R = \bar{\beta}_{y,2,R} - \kappa_{2,R} \quad 12.26$$

Incidence angle for stators (see Figure 12.1 for sign convention), degrees:

$$\bar{i}_s = \bar{\beta}_{y,1,s} - \kappa_{1,s} \quad 12.27$$

Deviation angle for stators (see Figure 12.1 for sign convention), degrees:

$$\bar{\delta}_s = \bar{\beta}_{y,2,s} - \kappa_{2,s} \quad 12.28$$

Flow coefficient:

$$\bar{\phi} = \frac{\bar{V}_z}{U_t} \quad 12.29$$

12.2.2. Global Parameters

Venturi volume flow rate, m^3/s :

$$Q_v = 0.05229 \sqrt{\frac{2g_c \gamma_{H_2} \Delta P_{vent}}{\rho}} \quad 12.30$$

Venturi flow coefficient:

$$\phi_v = \frac{Q_v}{A U_t} \quad 12.31$$

Integrated volume flow rate at probe axial measurement locations,
 m^3/s :

$$Q_a = 2\pi \int_{r_h}^{r_t} \bar{v}_z r dr \quad 12.32$$

Integrated flow coefficient at probe axial measurement stations:

$$\phi_a = \frac{Q_a}{A U_t} \quad 12.33$$

Integrated and venturi flow-coefficient comparison, percent:

$$FCC = \frac{\phi_a - \phi_v}{\phi_v} \times 100 \quad 12.34$$

General radial mass-average parameter equation (let ξ be any general parameter):

$$\dot{\xi} = \frac{\int_{r_h}^{r_t} \xi \bar{v}_{z,2} r dr}{\int_{r_h}^{r_t} \bar{v}_{z,2} r dr} \quad 12.35$$

12.2.3. Performance Parameters (based on cobra probe measurements)

Actual total-head rise coefficient for rotor:

$$\psi_R = \frac{g_c (\bar{H}_{2,R} - \bar{H}_{1,R})}{U_t^2} \quad 12.36$$

Actual total-head rise coefficient for stage:

$$\psi_{\text{stage}} = \frac{g_c(\bar{H}_{2,S} - \bar{H}_{1,R})}{U_t^2} \quad 12.37$$

Actual total-head rise coefficient for overall compressor:

$$\psi_{\text{overall}} = \frac{g_c(\bar{H}_{2,2S} - \bar{H}_{1,1R})}{U_t^2} \quad 12.38$$

Ideal total-head rise coefficient for rotor:

$$\psi_{i,R} = \frac{U(\bar{V}_{y,2,R} - \bar{V}_{y,1,R})}{U_t^2} \quad 12.39$$

Ideal total-head rise coefficient for stage:

$$\psi_{i,\text{stage}} = \frac{U(\bar{V}_{y,1,S} - \bar{V}_{y,1,R})}{U_t^2} \quad 12.40$$

Ideal total-head rise coefficient for overall compressor:

$$\psi_{i,\text{overall}} = \psi_{1,1R} + \psi_{i,2R} \quad 12.41$$

Hydraulic efficiency for rotor:

$$\eta_R = \frac{\psi_R}{\psi_{i,R}} \quad 12.42$$

Hydraulic efficiency for stage:

$$\eta_{\text{stage}} = \frac{\psi_{\text{stage}}}{\psi_{i,\text{stage}}} \quad 12.43$$

Hydraulic efficiency for overall compressor:

$$\eta_{\text{overall}} = \frac{\psi_{\text{overall}}}{\psi_{i,\text{overall}}} \quad 12.44$$

Total-head loss coefficient for rotor:

$$\omega_R = 2(\psi_{i,R} - \psi_R) \frac{U_t^2}{(V_{1,R})^2} \quad 12.45$$

Total-head loss coefficient for stator:

$$\omega_S = -2g_c \frac{(\bar{H}_{2,S} - \bar{H}_{1,S})}{(\bar{V}_{1,S})^2} \quad 12.46$$

12.2.4. Performance Parameters Used in Generating Performance Map

Cross-section average absolute velocity at the exit of the second stator assuming zero swirl, m/s:

$$\bar{\bar{v}}_{z,2,2S,pm} = \frac{Q_v}{A} \quad 12.47$$

Cross-section average total-head at the exit of the second stator assuming constant circumferentially average static-head, Nm/kg:

$$\bar{\bar{H}}_{2,2S,pm} = \bar{h}_{w,2,2S,pm} + \bar{\bar{v}}_{2,2S,pm}^2 \quad 12.48$$

Actual head-rise coefficient for overall compressor:

$$\psi_{\text{overall,pm}} = \frac{\bar{H}_{2,2S,pm}}{U_t^2} \quad 12.49$$

Ideal work coefficient:

$$\psi_{i,pm} = \frac{T\pi RPM}{30\rho Q_v U_t^2} \quad 12.50$$

Mechanical efficiency:

$$\eta_{me} = \frac{\psi_{\text{overall,pm}}}{\psi_{i,pm}} \quad 12.51$$

13. APPENDIX E: TABULATION OF EXPERIMENTALLY DETERMINED DATA

The time-averaged data obtained ahead of and behind each blade row are tabulated in this section. All data were obtained at the design point flow condition predicted by the design code (i.e., 2400 rpm at a flow coefficient of 0.587). The measured point-by-point distributions of various flow-field parameters are listed in Table 13.1. The corresponding circumferentially-averaged flow-field parameters are listed in Table 13.2. The axial locations of the measurement locations with respect to the blade rows are depicted in Figure 2.5, for a radial (spanwise) view, and Figure 3.6, for the circumferential survey window. Total head and static head were measured with respect to atmospheric pressure. The sign conventions for flow angles, incidence angles, and deviation angles are shown in Figure 12.1. A complete listing of mathematical symbols is given in the SYMBOLS AND NOTATION section. The definitions of the Fortran variables used in the computer output listings of Tables 13.1 and 13.2 are:

- o BETA R = Relative flow angle, β_y .
- o BETA Y = Absolute flow angle, β'_y .
- o FC = Flow coefficient, $\bar{\phi}$.
- o HS = Static head with respect to atmospheric pressure, h,
Nm/kg.
- o HT = Total head with respect to atmospheric pressure, H,
Nm/kg.
- o PHH = Percent passage height from hub, PHH.
- o V = Absolute velocity, V, m/s.

- o VR = Relative velocity, V' , m/s.
- o VY = Tangential component of absolute fluid velocity, V_y , m/s.
- o VZ = Axial component of fluid velocity, V_z , m/s.
- o VYR = Tangential component of relative fluid velocity, V'_y , m/s.
- o Y/SS = Circumferential spacing, Y/S_S .

Table 13.1 Point-by point distributions of circumferential survey data.

STATION 1 / PHH= 10.00									
Y/SS	BETA Y DEG.	HT N#M/KG	V M/S	VZ M/S	VY M/S	BETA R DEG.	VR M/S	VYR M/S	
0.0	0.483	0.301	32.062	32.060	0.270	49.099	48.966	37.010	
0.118	0.652	0.575	32.070	32.068	0.365	49.020	48.899	36.916	
0.234	0.946	0.493	32.068	32.063	0.529	48.897	48.772	36.751	
0.350	0.968	-0.479	32.037	32.033	0.541	48.916	48.743	36.740	
0.467	1.106	-1.355	32.010	32.004	0.618	48.882	48.667	36.563	
0.584	1.097	-0.575	32.034	32.028	0.613	48.864	48.686	36.668	
0.700	1.100	-0.545	32.004	31.998	0.615	48.889	48.665	36.448	
0.814	1.493	-2.079	31.987	31.976	0.833	48.739	48.486	36.291	
0.928	1.769	0.191	32.058	32.043	0.990	48.557	48.413	36.869	
1.042	0.738	-1.805	31.996	31.993	0.412	49.050	48.815		
STATION 1 / PHH= 30.00									
Y/SS	BETA Y DEG.	HT N#M/KG	V M/S	VZ M/S	VY M/S	BETA R DEG.	VR M/S	VYR M/S	
0.0	1.661	-0.637	32.025	32.012	0.929	50.919	50.778	39.417	
0.117	1.661	1.470	32.061	32.047	0.930	50.887	50.800	39.416	
0.233	0.549	0.549	32.068	32.058	0.822	50.954	50.889	39.523	
0.350	1.624	-1.071	32.016	32.005	0.907	50.940	50.790	39.438	
0.467	1.495	-1.907	31.992	31.981	0.834	51.013	50.832	39.511	
0.583	1.493	-0.741	32.028	32.017	0.835	50.981	50.855	39.511	
0.700	1.493	-0.137	32.047	32.036	0.835	50.964	50.866	39.510	
0.814	1.323	-0.467	32.037	32.028	0.739	51.038	50.935	39.606	
0.929	1.746	0.494	32.067	32.052	0.977	50.849	50.766	39.368	
1.042	1.072	-0.838	32.025	32.019	0.599	51.145	51.039	39.746	
STATION 1 / PHH= 50.00									
Y/SS	BETA Y DEG.	HT N#M/KG	V M/S	VZ M/S	VY M/S	BETA R DEG.	VR M/S	VYR M/S	
0.0	1.113	0.275	32.058	32.052	0.623	53.162	53.461	42.787	
0.117	1.113	0.646	32.070	32.064	0.623	53.152	53.468	42.786	
0.233	1.113	0.028	32.074	32.068	0.623	53.149	53.470	42.834	
0.350	1.028	-0.165	32.065	32.040	0.575	53.204	53.491	42.834	
0.467	1.107	0.357	32.061	32.055	0.620	53.162	53.465	42.790	
0.584	1.106	0.316	32.060	32.054	0.619	53.164	53.465	42.791	
0.700	1.102	-1.085	32.016	32.010	0.616	53.203	53.441	42.794	
0.814	1.156	-0.652	32.023	32.017	0.646	53.178	53.421	42.763	
0.928	1.154	-0.687	32.028	32.022	0.645	53.174	53.425	42.764	
1.042	1.197	0.261	32.058	32.051	0.670	53.133	53.422	42.740	

Table 13.1 Continued.

STATION 1 / PHH = 70.00							STATION 1 / PHH = 90.00													
V/SS	BETA V DEG.	HT NM/KG	V M/S	VZ M/S	VY M/S	BETA R DEG.	VR M/S	VYR M/S	V/SS	BETA V DEG.	HT NM/KG	V M/S	VZ M/S	VY M/S	BETA R DEG.	VR M/S	VYR M/S			
0.0	-0.028	0.344	32.060	32.021	-0.015	55.409	56.472	46.489	0.0	-0.117	0.523	32.024	32.064	0.458	55.167	56.061	46.016			
0.234	0.819	-0.798	32.024	32.021	0.458	55.322	55.210	56.197	0.233	-0.101	0.248	32.014	32.014	0.230	56.305	56.244	46.152			
0.351	0.412	-1.101	32.066	32.015	0.230	55.277	55.243	56.228	0.467	0.496	0.248	32.057	32.056	0.277	56.223	56.196	46.243			
0.584	0.487	-0.427	32.036	32.036	0.272	55.263	56.221	46.201	0.584	0.487	0.757	32.026	32.024	0.280	55.267	56.221	46.201			
0.701	0.501	-0.751	32.019	32.019	0.317	55.252	56.174	46.156	0.814	0.568	-0.963	32.018	32.018	0.183	55.335	56.281	46.290			
0.928	0.327	-1.197	32.012	32.011	0.183	55.383	56.401	46.417	1.042	0.101	-0.275	32.041	32.041	0.057	55.383	56.401	46.417			
0.0	-0.230	-30.140	31.095	31.094	-0.125	57.949	58.594	49.663	0.117	-0.150	-31.064	31.065	-0.081	57.950	58.541	49.619				
0.233	-0.442	-29.964	31.064	31.099	-0.240	58.004	58.694	49.777	0.350	0.483	-31.032	31.066	0.262	57.771	58.250	49.275				
0.467	0.146	-29.286	31.066	31.065	0.262	57.719	57.819	49.458	0.583	0.146	-30.521	31.122	0.079	57.852	58.435	49.458				
0.700	0.148	-29.147	31.082	31.127	0.080	58.437	58.615	49.457	0.814	0.006	-35.255	30.930	0.03	58.019	58.398	49.534				
0.928	-0.254	-27.588	31.177	31.176	-0.138	57.988	58.648	49.676	1.042	-0.232	-30.191	31.093	-0.126	57.951	58.594	49.664				

Table 13.1 Continued.

STATION 2 / PHH= 10.00									
Y/SS	BETA Y DEG.	HT N:M/KG	V M/S	VZ M/S	VY M/S	BETA R DEG.	VR M/S	VYR M/S	
0.0	21.210	468.700	34.711	32.360	12.558	37.379	40.723	24.723	
0.116	21.210	456.600	34.651	32.304	12.536	37.452	40.692	24.745	
0.233	21.220	464.700	34.596	32.250	12.522	37.514	40.658	24.759	
0.350	21.340	465.000	34.605	32.232	12.593	37.450	40.601	24.688	
0.464	21.470	465.600	34.688	32.203	12.666	37.393	40.534	24.584	
0.581	21.470	467.900	34.740	32.281	12.696	37.292	40.577	24.571	
0.696	21.460	469.700	34.763	32.332	12.710	37.234	40.609	24.563	
0.815	21.460	470.500	34.816	32.353	12.718	37.206	40.621	24.539	
0.929	21.470	465.400	34.683	32.278	12.689	37.379	40.539	24.592	
1.044	21.460	467.700	34.683	32.278	12.689	37.303	40.579		
STATION 2 / PHH= 30.00									
Y/SS	BETA Y DEG.	HT N:M/KG	V M/S	VZ M/S	VY M/S	BETA R DEG.	VR M/S	VYR M/S	
0.0	20.670	474.000	34.505	32.263	12.180	41.103	42.843	28.165	
0.118	20.670	479.300	34.658	32.427	12.234	40.923	42.914	28.111	
0.235	20.670	477.700	34.612	32.384	12.217	40.977	42.894	28.128	
0.349	20.670	476.800	34.586	32.359	12.208	41.007	42.881	28.137	
0.463	20.740	476.500	34.568	32.328	12.242	41.001	42.836	28.103	
0.581	20.740	478.200	34.626	32.382	12.262	40.933	42.863	28.083	
0.696	20.740	478.300	34.629	32.385	12.263	40.930	42.865	28.082	
0.811	20.740	476.600	34.580	32.339	12.246	40.987	42.841	28.099	
0.927	20.740	477.700	34.612	32.369	12.257	40.950	42.856	28.086	
1.041	20.740	480.000	34.678	32.431	12.280	40.872	42.888		
STATION 2 / PHH= 50.00									
Y/SS	BETA Y DEG.	HT N:M/KG	V M/S	VZ M/S	VY M/S	BETA R DEG.	VR M/S	VYR M/S	
0.0	20.530	464.200	33.913	31.759	11.893	44.780	44.742	31.516	
0.119	20.530	467.400	34.007	31.847	11.926	44.671	44.782	31.483	
0.233	20.780	465.500	33.951	31.742	12.045	44.656	44.624	31.364	
0.349	20.530	465.300	33.945	31.789	11.904	44.743	44.756	31.505	
0.465	20.530	462.100	33.851	31.701	11.871	44.852	44.717	31.538	
0.580	20.530	464.000	33.907	31.753	11.891	44.787	44.740	31.518	
0.696	20.530	465.600	33.954	31.797	11.908	44.732	44.760	31.502	
0.812	20.530	464.700	33.927	31.773	11.898	44.763	44.749	31.511	
0.927	20.490	465.600	33.954	31.806	11.886	44.745	44.781	31.524	
1.042	20.530	465.100	33.939	31.784	11.902	44.749	44.754	31.507	

Table 13.1 Continued.

STATION 2 / PHH= 70.00									
Y/SS	BETA Y DEG.	HT N#M/KG	V M/S	VZ M/S	YY M/S	BETA R DEG.	VR M/S	VYR M/S	
0.0	19.700	458.700	33.473	31.514	11.284	48.154	47.238	35.190	
0.116	19.780	454.300	33.342	31.374	11.283	48.281	47.146	35.190	
0.235	19.780	459.800	33.506	31.529	11.339	48.096	47.207	35.135	
0.349	19.790	462.900	33.599	31.614	11.376	47.989	47.237	35.098	
0.464	19.910	456.000	33.393	31.397	11.372	48.169	47.094	35.102	
0.582	19.990	458.200	33.458	31.443	11.438	48.093	47.076	35.035	
0.695	19.990	458.900	33.479	31.462	11.445	48.070	47.083	35.028	
0.812	19.780	459.900	33.509	31.532	11.340	48.092	47.208	35.134	
0.926	19.600	462.100	33.575	31.629	11.263	48.067	47.331	35.211	
1.043	19.600	462.900	33.599	31.652	11.271	48.040	47.340	35.203	
STATION 2 / PHH= 90.00									
Y/SS	BETA Y DEG.	HT N#M/KG	V M/S	VZ M/S	YY M/S	BETA R DEG.	VR M/S	VYR M/S	
0.0	20.820	416.300	31.922	29.838	11.346	52.001	48.465	38.191	
0.119	20.910	411.700	31.778	29.685	11.341	52.147	48.375	38.196	
0.231	21.670	411.700	31.778	29.532	11.734	52.003	47.971	37.803	
0.348	21.670	415.400	31.804	29.640	11.777	51.870	48.004	37.760	
0.464	21.670	415.600	31.900	29.646	11.779	51.863	48.006	37.758	
0.579	21.630	412.500	31.803	29.563	11.723	51.982	47.999	37.815	
0.696	21.630	411.900	31.784	29.546	11.716	52.003	47.994	37.822	
0.811	21.340	415.000	31.881	29.636	11.752	51.892	48.022	37.786	
0.930	21.340	417.800	31.959	29.777	11.634	51.847	48.202	37.904	
1.041	21.340	411.200	31.762	29.584	11.558	52.083	48.142	37.979	

Table 13.1 Continued.

STATION 3 / PHH= 10.00									
V/SS	BETA Y DEG.	HT NM/KG	V M/S	VZ M/S	VY M/S	VR M/S	BETA R DEG.	VR M/S	VYR M/S
0.0	-3.545	463.600	32.837	32.774	-2.030	50.182	51.181	39.311	
0.070	-4.095	454.800	32.568	32.485	-2.326	50.642	51.224	39.607	
0.141	-3.500	462.100	32.791	32.730	-2.002	50.199	51.131	39.283	
0.211	-3.205	461.500	32.773	32.722	-1.832	50.085	50.995	39.113	
0.281	-2.819	457.400	32.647	32.608	-1.606	50.019	50.749	38.886	
0.304	-2.505	459.600	32.958	32.927	-1.440	49.624	50.828	38.721	
0.323	-2.489	459.100	32.715	32.684	-1.421	49.818	50.656	38.702	
0.346	-2.489	458.500	32.669	32.638	-1.419	49.857	50.625	38.700	
0.367	-2.489	463.000	32.834	32.803	-1.426	49.720	50.737	38.707	
0.390	-2.489	460.500	32.110	32.080	-1.396	50.325	50.248	38.675	
0.409	-2.489	393.100	30.615	30.586	-1.330	51.615	49.257	38.610	
0.428	-2.487	326.900	28.370	28.343	-1.231	53.648	47.817	38.512	
0.449	-2.487	246.700	25.386	25.362	-1.102	56.544	46.005	38.382	
0.469	-2.487	206.000	23.729	23.706	-1.030	58.251	45.052	38.311	
0.496	-2.486	254.500	25.692	25.667	-1.146	56.237	46.165	38.395	
0.510	-2.487	317.000	28.019	27.992	-1.216	53.978	47.598	38.497	
0.533	-2.487	386.900	30.411	30.383	-1.320	51.793	49.123	38.600	
0.553	-2.486	415.000	31.322	31.292	-1.359	50.997	49.721	38.639	
0.574	-2.487	431.700	31.851	31.821	-1.382	50.545	50.074	38.663	
0.600	-2.487	448.100	32.361	32.331	-1.404	50.113	50.416	38.685	
0.615	-2.486	453.000	32.512	32.482	-1.410	49.986	50.518	38.691	
0.638	-2.486	439.900	32.107	32.077	-1.393	50.327	50.245	38.674	
0.657	-2.486	447.800	32.352	32.322	-1.403	50.120	50.410	38.684	
0.680	-2.487	450.000	32.420	32.389	-1.407	50.064	50.456	38.688	
0.698	-2.487	450.600	32.439	32.408	-1.408	50.048	50.469	38.688	
0.720	-2.487	457.100	32.638	32.608	-1.416	49.881	50.604	38.697	
0.744	-2.486	445.000	32.265	32.235	-1.400	50.193	50.351	38.680	
0.761	-2.486	452.800	32.506	32.492	-1.479	49.661	50.194	38.259	
0.831	-2.609	455.200	32.580	32.546	-1.483	49.983	50.615	38.764	
0.901	-3.115	455.500	32.589	32.541	-1.771	50.196	50.833	39.052	
0.972	-3.472	465.800	32.904	32.843	-1.993	50.095	51.197	39.274	
1.042	-3.580	447.600	32.346	32.283	-2.020	50.599	50.860	39.301	

Table 13.1 Continued.

STATION 3 / PHH= 30.00					
V/SS	BETA Y DEG.	H/T NM/KG	V Y M/S	VZ M/S	VY M/S
0.0	-1.177	465.600	32.894	32.887	-0.676
0.066	-1.599	468.000	32.954	-0.925	51.280
0.132	-1.786	465.700	32.897	-1.025	51.389
0.199	-2.203	472.200	33.094	-1.272	51.523
0.262	-2.780	462.100	32.749	-1.590	51.529
0.284	-1.516	469.200	33.003	-0.874	52.013
0.304	-1.518	469.300	33.006	-0.874	51.327
0.325	-1.520	468.300	32.994	-0.874	52.796
0.345	-1.520	467.500	32.951	-0.874	52.780
0.368	-1.518	466.100	32.909	-0.872	52.764
0.393	-1.520	449.400	32.398	-0.859	52.736
0.408	-1.518	414.300	31.295	-0.829	52.733
0.433	-1.497	346.400	29.045	-0.759	52.712
0.450	-1.493	268.900	26.241	-0.684	51.324
0.475	-1.493	215.700	24.129	-0.629	51.350
0.495	-1.493	264.700	26.061	-0.679	51.370
0.512	-1.493	357.400	29.421	-0.767	51.405
0.534	-1.493	435.400	31.962	-0.853	51.409
0.554	-1.493	463.000	32.815	-0.855	51.420
0.580	-1.493	460.800	32.747	-0.847	51.420
0.600	-1.493	452.500	32.493	-0.853	51.420
0.619	-1.493	460.800	32.747	-0.857	51.420
0.637	-1.493	465.200	32.882	-0.857	51.417
0.658	-1.491	467.200	32.942	-0.857	51.366
0.682	-1.491	466.500	32.921	-0.857	51.366
0.702	-1.493	461.500	32.769	-0.854	51.511
0.725	-1.493	465.200	32.882	-0.857	51.417
0.743	-0.241	455.600	32.736	-0.870	51.137
0.817	-0.532	464.800	32.588	-0.868	51.043
0.892	-0.833	463.500	32.869	-0.826	51.043
0.968	-1.253	464.700	32.859	-0.719	51.334
1.042	-1.252	467.200	32.942	-0.720	51.270

Table 13.1 Continued.

STATION 3 / PHH = 50.00									
Y/SS	BETA Y DEG.	HT N & N/KG	V M/S	VZ M/S	VY M/S	BETA R DEG.	VR M/S	VYR M/S	VYR M/S
0-0	-0.625	451.200	32.452	32.450	-0.354	53.443	54.482	43.763	43.763
0-0.74	-0.920	450.000	32.415	32.411	-0.521	53.581	54.592	43.930	43.930
0-1.46	-1.299	454.200	32.544	32.536	-0.738	53.610	54.841	44.147	44.147
0-2.20	-1.687	454.100	32.541	32.524	-1.072	53.626	55.103	44.481	44.481
0-2.92	-2.355	454.700	32.560	32.532	-1.338	53.982	55.323	44.747	44.747
0-3.17	-0.727	456.700	32.621	32.619	-0.414	53.339	54.630	43.823	43.823
0-3.35	-0.726	454.300	32.548	32.545	-0.412	53.400	54.585	43.821	43.821
0-3.56	-0.726	450.600	32.434	32.431	-0.411	53.495	54.516	43.820	43.820
0-3.76	-0.751	447.200	32.329	32.326	-0.424	53.592	54.464	43.833	43.833
0-3.97	-0.731	431.600	31.842	31.840	-0.406	53.995	54.162	43.815	43.815
0-4.18	-0.729	376.300	30.056	30.053	-0.383	55.539	53.112	43.792	43.792
0-4.40	-0.729	319.000	28.085	28.082	-0.357	57.314	52.001	43.767	43.767
0-4.61	-0.731	238.400	25.051	25.049	-0.320	60.195	50.395	43.729	43.729
0-4.80	-0.729	194.800	23.245	23.243	-0.296	61.995	49.501	43.705	43.705
0-5.04	-0.729	260.900	25.933	25.931	-0.330	59.338	50.848	43.739	43.739
0-5.25	-0.729	368.700	30.465	30.463	-0.388	55.179	53.349	43.797	43.797
0-5.44	-0.729	435.900	31.977	31.975	-0.407	53.880	54.242	43.816	43.816
0-5.65	-0.729	447.600	32.341	32.338	-0.412	53.574	54.461	43.821	43.821
0-5.85	-0.729	446.400	32.366	32.363	-0.412	53.553	54.476	43.821	43.821
0-6.06	-0.731	446.400	32.304	32.301	-0.412	53.606	54.440	43.821	43.821
0-6.32	-0.729	447.700	32.349	32.342	-0.412	53.571	54.463	43.821	43.821
0-6.52	-0.731	448.700	32.375	32.372	-0.413	53.546	54.483	43.822	43.822
0-6.68	-0.729	448.000	32.353	32.352	-0.340	53.068	53.866	43.069	43.069
0-7.64	-0.322	448.100	32.357	32.356	-0.182	53.185	53.995	43.227	43.227
0-8.56	-0.029	450.200	32.421	32.421	-0.017	53.255	54.194	43.426	43.426
0-9.48	-0.197	450.700	32.437	32.437	-0.111	53.302	54.279	43.521	43.521
1.044	-0.616	447.900	32.360	32.348	-0.348	53.525	54.416	43.757	43.757

Table 13.1 Continued.

STATION 3 / PHH= 70.00						
V/SS	BETA Y DEG.	HT NM/KG	V M/S	VZ M/S	VY M/S	BETA R DEG.
0.0	0.664	440.500	32.121	32.119	0.372	55.135
0.079	0.363	446.600	32.310	32.309	0.205	55.073
0.157	-0.244	438.100	32.046	32.046	-0.137	55.491
0.232	-0.666	450.700	32.437	32.434	-0.377	55.305
0.308	-1.763	437.000	32.012	32.012	-0.985	56.012
0.384	0.349	442.100	32.170	32.170	0.157	55.212
0.374	0.302	437.600	32.030	32.030	0.168	55.328
0.396	0.413	433.300	31.896	31.895	0.168	55.441
0.436	0.301	400.500	30.850	30.850	0.163	56.330
0.456	0.302	357.700	29.430	29.430	0.154	57.569
0.474	0.301	284.100	26.813	26.813	0.142	59.942
0.498	0.302	189.300	23.007	23.007	0.121	63.602
0.519	0.302	156.700	21.544	21.544	0.113	65.076
0.542	0.301	261.600	25.960	25.960	0.137	60.740
0.559	0.301	395.700	30.694	30.694	0.162	56.465
0.581	0.301	432.600	31.874	31.873	0.167	55.460
0.601	0.301	436.600	32.005	32.005	0.168	55.349
0.620	0.301	438.200	32.049	32.049	0.168	55.312
0.643	0.301	432.500	31.871	31.870	0.167	55.462
0.662	1.787	429.500	31.902	31.902	0.167	55.449
0.759	1.554	431.100	31.776	31.776	0.091	55.073
0.855	1.452	442.000	32.167	32.157	0.815	54.843
0.947	1.031	431.300	31.833	31.828	0.573	55.262
1.042	0.715	433.000	31.886	31.884	0.398	55.317

Table 13.1 Continued.

STATION 3 / PHH = 90.00									
Y/SS	BETA Y DEG.	H/H/KC	Y M/S	Y2 M/S	YY M/S	YY M/S	DETA R DEG.	VR M/S	VYR M/S
0.0	2.082	345.800	29.023	29.004	1.054	59.111	56.496	48.483	48.703
0.064	1.616	362.900	29.606	29.594	0.835	58.715	56.989	49.061	49.061
0.131	1.005	325.800	28.325	28.321	0.497	59.994	56.631	49.416	49.416
0.194	0.244	331.500	28.526	28.526	0.122	50.004	57.058	48.803	48.803
0.221	1.131	339.100	28.791	28.785	0.568	59.552	56.738	48.972	48.972
0.244	1.131	335.300	28.659	28.653	0.566	59.668	56.739	48.973	48.973
0.271	1.131	333.000	28.578	28.573	0.564	59.576	56.789	48.970	48.970
0.294	1.131	338.300	28.763	28.758	0.568	59.576	56.789	48.970	48.970
0.319	1.131	310.900	27.794	27.789	0.549	60.436	56.322	48.989	48.989
0.347	1.131	299.500	27.381	27.376	0.540	60.807	56.126	48.997	48.997
0.370	1.131	222.900	24.424	24.419	0.482	63.537	54.797	49.056	49.056
0.398	1.133	160.600	21.724	21.719	0.430	66.141	53.697	49.108	49.108
0.419	1.131	54.470	16.114	16.111	0.318	71.875	51.789	49.220	49.220
0.452	1.133	46.510	15.612	15.609	0.309	72.408	51.644	49.229	49.229
0.474	1.131	150.400	21.249	21.245	0.419	66.610	53.516	49.118	49.118
0.499	1.133	321.400	28.169	28.164	0.557	60.101	56.501	48.943	48.943
0.518	1.133	376.600	30.065	30.059	0.594	58.443	57.437	48.943	48.943
0.545	1.133	388.100	30.445	30.439	0.602	58.117	57.630	48.936	48.936
0.572	1.131	381.600	30.231	30.225	0.597	58.301	57.522	48.941	48.941
0.595	1.131	372.900	29.942	29.936	0.591	58.550	57.375	48.947	48.947
0.618	1.133	366.500	29.727	29.722	0.588	58.734	57.267	48.950	48.950
0.646	1.133	374.000	29.979	29.973	0.593	58.518	57.393	48.945	48.945
0.669	1.131	358.800	29.467	29.462	0.582	58.961	57.133	48.956	48.956
0.696	1.133	358.600	29.460	29.455	0.583	58.966	56.821	48.968	48.968
0.719	1.133	340.200	28.829	28.823	0.570	59.518	56.953	48.962	48.962
0.745	1.133	348.000	29.098	29.093	0.575	59.282	56.789	48.969	48.969
0.769	1.133	338.300	28.763	28.758	0.569	59.576	56.519	48.980	48.980
0.796	1.133	322.500	28.208	28.203	0.558	60.066	56.719	48.970	48.970
0.820	1.133	336.800	28.711	28.705	0.568	59.622	56.763	48.970	48.970
0.845	1.131	338.200	28.760	28.754	0.568	59.579	56.788	48.970	48.970
0.871	1.131	347.200	29.071	29.065	0.574	59.306	56.941	48.964	48.964
0.893	1.131	326.500	28.350	28.344	0.560	59.941	56.588	48.978	48.978
0.920	2.630	334.800	28.641	28.606	1.414	59.271	55.984	48.124	48.124
0.961	2.830	340.300	28.833	28.797	1.424	59.098	56.074	48.114	48.114
1.002	2.429	328.200	28.410	28.384	1.204	59.576	56.052	48.334	48.334
1.042	1.777	318.800	28.077	28.064	0.871	60.030	56.179	48.667	48.667

Table 13.1 Continued.

		STATION 4 / PHH = 10.00					
VSS	BETA Y DEG.	HT NM/KG	V M/S	VZ M/S	VY M/S	BETA R DEG.	VR M/S
0.0	23.447	824.988	33.148	30.411	13.014	38.386	24.091
0.026	23.447	810.439	32.707	30.006	12.953	38.591	24.067
0.050	23.447	805.480	32.555	29.867	12.953	38.521	24.327
0.078	23.447	789.719	32.067	29.419	12.759	39.812	24.522
0.103	23.447	790.924	32.104	29.453	12.774	39.762	24.507
0.125	23.449	787.553	31.999	29.357	12.733	39.902	24.548
0.153	23.447	785.329	31.930	29.293	12.705	39.996	24.576
0.178	23.447	783.684	31.878	29.246	12.684	40.065	24.597
0.200	23.447	792.828	32.164	29.508	12.798	39.683	24.483
0.230	23.447	797.817	32.318	29.650	12.859	39.477	24.421
0.250	23.447	806.705	32.592	29.901	12.968	38.413	24.313
0.276	23.447	818.214	32.943	30.223	13.108	38.653	24.173
0.307	23.447	830.723	33.321	30.570	13.258	38.161	24.023
0.326	23.447	833.200	33.395	30.638	13.288	38.914	23.993
0.354	23.447	837.021	33.509	30.743	13.333	37.918	23.969
0.375	23.449	846.993	33.606	31.014	13.452	37.536	23.829
0.401	23.449	851.450	33.937	31.135	13.505	37.368	23.776
0.426	23.449	853.853	34.006	31.200	13.533	37.277	23.749
0.451	23.449	853.755	34.005	31.197	13.532	37.281	23.749
0.476	24.453	861.394	34.229	31.159	14.169	36.566	23.112
0.519	24.240	864.415	34.317	31.292	14.069	36.544	23.949
0.565	24.051	869.365	34.461	31.469	14.045	36.441	23.192
0.608	23.990	872.521	34.553	31.568	14.048	36.351	23.079
0.650	23.734	874.057	34.597	31.671	13.925	36.407	23.356
0.693	23.441	880.269	34.776	31.906	13.834	36.511	23.447
0.739	22.971	878.589	34.728	31.974	13.553	36.579	23.728
0.782	22.661	875.485	34.638	31.964	13.345	36.827	23.933
0.825	22.590	866.098	34.366	31.729	13.202	37.195	23.832
0.869	22.589	858.369	34.141	31.521	13.114	39.719	24.079
0.893	22.3449	857.657	34.120	31.302	13.577	39.135	23.704
0.917	22.3447	847.788	33.829	31.036	13.461	37.507	23.820
0.943	22.3447	833.828	33.414	30.655	13.295	38.041	23.986
0.968	22.3447	835.205	33.455	30.693	13.312	37.988	23.969
0.996	22.3449	823.735	33.111	30.376	13.176	38.434	24.105
1.018	22.3447	819.234	32.974	30.252	13.120	38.613	24.160
1.042	23.447	806.290	32.579	29.889	12.963	39.131	24.318

Table 13.1 Continued.

Y/SS	BETA Y DEG.	HT NSH/KG	STATION 4 / PHH= 30.00			BETA R DEG.	YR M/S
			Y M/S	YZ M/S	YY M/S		
0.0	21.281	909.1*	35.212	32.811	12.780	40.034	42.853
0.026	21.283	901.6/c	35.005	32.618	12.706	40.276	42.753
0.052	20.825	883.031	34.463	32.211	12.252	41.093	42.741
0.127	21.354	854.542	33.626	31.317	12.246	41.901	42.076
0.205	22.154	860.518	33.803	31.308	12.747	41.396	41.735
0.282	21.675	883.939	34.489	32.051	12.738	42.301	27.607
0.359	21.022	884.463	34.504	32.208	12.378	40.969	27.968
0.435	20.728	872.561	34.158	31.947	12.089	42.656	42.649
0.512	20.977	873.376	34.182	31.916	12.237	41.370	28.256
0.589	21.276	896.138	34.841	32.466	12.642	40.473	42.529
0.666	21.402	919.865	35.516	32.067	12.960	39.631	42.679
0.763	21.315	932.395	35.967	33.413	13.037	43.153	27.705
0.768	21.283	923.245	35.611	33.182	12.926	39.258	27.308
0.794	21.283	933.693	35.903	33.454	13.032	43.045	27.419
0.818	21.283	932.698	35.875	33.428	13.022	39.230	43.188
0.844	21.283	929.480	35.785	33.345	12.989	39.262	43.174
0.867	21.281	930.854	35.824	33.381	13.002	39.365	43.130
0.893	21.283	927.948	35.742	33.305	12.973	39.322	27.363
0.917	21.281	922.679	35.595	33.167	12.920	43.109	27.372
0.943	21.281	922.703	35.595	33.168	12.919	39.587	43.037
0.967	21.281	917.151	35.439	33.023	12.862	39.769	27.425
0.998	21.281	908.987	35.208	32.807	12.778	40.039	42.963
1.020	21.281	897.845	34.890	32.511	12.663	40.413	42.851
1.044	21.281	888.448	34.620	32.259	12.565	42.700	27.567

Table 13.1 Continued.

STATION 4 / PHH = 50.00						
Y/SS	BETA Y DEG.	HT N#H/KG	V M/S	VZ M/S	YY M/S	VYR M/S
0.0	19.987	902.528	34.704	32.614	11.862	44.047
0.027	19.819	899.881	34.628	32.577	11.741	44.190
0.054	19.820	892.045	34.401	32.363	11.664	44.447
0.093	20.030	881.072	34.081	32.019	11.673	44.746
0.121	20.030	872.222	33.820	31.774	11.584	45.082
0.156	20.030	861.294	33.495	31.469	11.473	45.422
0.187	20.030	854.927	33.305	31.290	11.407	45.644
0.220	20.028	857.121	33.370	31.352	11.429	45.568
0.257	20.030	864.281	33.584	31.553	11.503	45.319
0.287	20.028	872.888	33.840	31.793	11.590	45.024
0.322	20.028	881.506	34.093	32.031	11.676	44.732
0.353	20.028	885.049	34.197	32.129	11.712	44.612
0.387	20.028	884.480	34.180	32.113	11.706	44.632
0.424	20.028	879.800	34.043	31.984	11.659	44.789
0.454	20.030	875.685	33.922	31.970	11.619	45.067
0.487	20.030	870.274	33.762	31.720	11.614	44.928
0.523	20.030	864.311	33.565	31.553	11.503	45.113
0.557	20.032	853.816	33.271	31.258	11.397	45.318
0.588	20.030	852.501	33.232	31.222	11.382	45.729
0.620	20.030	854.511	33.292	31.278	11.403	45.659
0.653	20.030	863.247	33.553	31.524	11.495	45.355
0.687	20.030	872.691	33.834	31.787	11.589	45.030
0.724	20.030	884.637	34.185	32.117	11.709	44.626
0.757	20.030	894.483	34.483	32.397	11.811	44.285
0.788	20.030	899.144	34.607	32.513	11.853	44.144
0.820	20.028	903.151	34.722	32.622	11.892	44.013
0.854	20.028	908.594	34.879	32.725	12.066	43.765
0.900	20.028	909.058	34.892	32.738	12.070	43.749
0.947	20.027	909.359	34.901	32.746	12.072	43.740
0.995	20.028	901.750	34.682	32.585	11.878	44.059
1.044	20.021	894.692	34.478	32.394	11.804	44.294

Table 13.1 Continued.

STATION 4 / PHH = 70.00						
V/S	BETA Y DEG.	HT NM/KG	V M/S	VZ M/S	VY M/S	VR M/S
						BETA R DEG.
0.0	20.030	893.910	34.189	32.121	11.710	47.263
0.045	19.932	879.718	33.771	31.748	11.512	47.225
0.092	19.928	866.940	33.390	31.391	11.381	34.961
0.126	20.610	858.008	32.922	31.002	11.659	35.093
0.158	20.610	852.729	32.962	30.852	11.603	48.187
0.194	20.610	857.158	33.096	30.976	11.650	48.499
0.224	20.610	862.313	33.252	31.123	11.705	48.345
0.260	20.610	872.514	33.557	31.409	11.812	48.167
0.292	20.610	882.379	33.850	31.683	11.915	47.816
0.326	20.612	886.144	33.961	31.787	11.955	47.884
0.357	20.612	888.336	34.025	31.847	11.978	46.924
0.392	20.612	890.676	34.094	31.911	12.002	47.286
0.425	20.612	888.786	34.038	31.859	11.983	47.208
0.461	20.612	881.537	33.825	31.660	11.907	47.271
0.495	20.612	884.417	33.910	31.739	11.937	47.513
0.526	20.612	877.094	33.693	31.536	11.861	47.662
0.559	20.610	864.580	33.320	31.187	11.729	48.089
0.593	20.610	856.330	33.132	31.011	11.663	48.304
0.624	20.612	848.594	32.836	30.734	11.559	48.643
0.659	20.612	849.917	32.877	30.772	11.574	48.590
0.693	20.612	851.120	32.913	30.806	11.586	48.554
0.724	20.612	857.462	33.106	30.987	11.654	48.333
0.759	20.610	870.489	33.496	31.353	11.791	47.887
0.794	20.610	879.053	33.751	31.591	11.880	47.597
0.825	20.610	865.297	33.936	31.764	11.945	47.388
0.857	20.610	892.279	34.141	31.956	12.018	47.156
0.893	20.520	897.433	34.291	32.116	12.020	47.011
0.932	20.180	896.941	34.277	32.173	11.825	47.122
0.972	20.306	889.605	34.062	31.946	11.821	47.328
1.006	20.104	885.875	33.953	31.884	11.670	47.200
1.043	20.102	879.057	33.751	31.695	11.600	47.125

Table 13.1 Continued.

STATION 4 / PHH= 90.00									
V/SS	BETA Y DEG.	HT NM/KG	V M/S	VZ M/S	VY M/S	VY M/S	BETA R DEG.	VR M/S	VR M/S
0.033	22.964	809.741	31.346	28.862	12.230	52.274	47.169	37.308	
0.067	22.987	801.446	31.080	28.612	12.138	52.582	47.089	37.400	
0.102	22.987	798.766	30.994	28.533	12.104	52.684	47.068	37.433	
0.133	22.987	802.569	31.117	28.646	12.152	52.540	47.098	37.386	
0.168	22.987	814.427	31.495	28.994	12.500	52.095	47.194	37.238	
0.203	22.989	829.165	31.960	29.422	12.481	51.551	47.316	37.056	
0.240	22.984	839.738	32.289	29.725	12.611	51.167	47.404	36.927	
0.273	22.955	847.661	32.533	29.951	12.703	50.885	47.474	36.834	
0.306	23.682	856.111	32.792	30.031	12.688	50.890	47.490	36.849	
0.321	23.069	864.516	32.047	30.341	13.171	50.451	47.163	36.366	
0.341	23.069	856.738	32.811	30.188	12.856	50.218	47.417	36.439	
0.362	23.111	851.951	32.665	30.043	12.822	50.708	47.506	36.681	
0.383	22.855	850.746	32.628	30.067	12.633	50.800	47.441	36.716	
0.401	22.770	847.460	32.627	29.992	12.589	50.933	47.571	36.865	
0.422	22.643	848.297	32.553	30.044	12.532	50.927	47.589	36.848	
0.442	22.645	835.188	32.148	29.670	12.377	51.395	47.666	37.005	
0.462	22.980	837.445	32.218	29.661	12.578	51.252	47.552	36.959	
0.510	22.984	824.614	31.817	29.291	12.424	51.718	47.280	37.144	
0.542	22.987	821.869	31.731	29.211	12.392	51.819	47.256	37.146	
0.577	22.959	815.986	31.545	29.046	12.305	52.042	47.223	37.133	
0.611	22.989	808.706	31.313	28.826	12.230	52.308	47.147	37.308	
0.642	22.984	806.386	31.239	28.759	12.198	52.396	47.131	37.340	
0.679	22.960	804.556	31.180	28.710	12.163	52.469	47.129	37.374	
0.711	22.989	806.554	31.244	28.763	12.203	52.389	47.130	37.335	
0.748	22.987	806.919	31.256	28.774	12.207	52.375	47.133	37.330	
0.779	22.987	806.619	31.246	28.765	12.203	52.387	47.131	37.335	
0.813	22.989	812.977	31.449	28.952	12.283	52.148	47.182	37.255	
0.843	22.989	813.966	31.481	28.980	12.295	52.112	47.190	37.243	
0.880	22.986	819.230	31.647	29.135	12.358	51.917	47.235	37.179	
0.910	22.986	822.210	31.742	29.221	12.395	51.807	47.259	37.143	
0.943	22.987	816.750	31.569	29.062	12.329	52.008	47.214	37.209	
0.983	22.989	808.132	31.295	28.809	12.222	52.330	47.142	37.315	
1.013	22.986	802.292	31.108	28.638	12.148	52.551	47.097	37.390	
1.043	22.986	794.791	30.866	28.415	12.053	52.836	47.037	37.485	

RD-A141 796

AERODYNAMIC DESIGN AND PERFORMANCE OF A TWO-STAGE
AXIAL-FLOW COMPRESSOR (U) IOWA STATE UNIV AMES
ENGINEERING RESEARCH INST M D HATHAWAY ET AL. DEC 83
ISU-ERI-AMES-84178 AFOSR-TR-84-0417

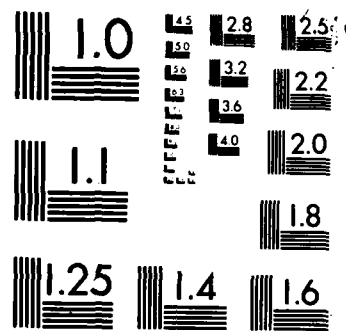
3/3

UNCLASSIFIED

F/G 21/5

NL





MICROCOPY RESOLUTION TEST CHART
NATIONAL BUREAU OF STANDARDS-1963-A

Table 13.1 Continued.

STATION 5 / PHM= 10.00					
V/SS	BETA Y DEG.	HT NKG	V M/S	VZ M/S	YY M/S
0.0	-0.263	839.574	31.246	31.246	0.143
0.053	-0.455	830.206	30.945	30.944	48.639
0.089	0.050	812.021	30.351	30.351	48.053
0.114	0.048	796.722	29.843	29.843	47.735
0.140	0.049	790.410	29.631	29.631	47.602
0.172	0.048	781.186	29.318	29.318	47.409
0.199	0.048	772.833	29.032	29.032	47.232
0.229	0.048	777.658	29.197	29.197	47.334
0.260	0.048	788.737	29.574	29.574	47.568
0.295	0.048	796.385	29.832	29.832	47.728
0.318	0.048	819.845	30.608	30.608	48.216
0.352	0.048	825.212	30.783	30.783	48.327
0.381	0.049	811.794	30.344	30.344	48.049
0.404	0.049	738.910	27.839	27.839	46.509
0.432	0.048	622.984	23.305	23.305	43.949
0.467	0.048	686.000	25.868	25.868	45.359
0.492	0.048	766.389	28.609	28.609	47.096
0.522	0.048	789.629	29.908	29.908	47.588
0.552	0.048	798.652	29.908	29.908	47.775
0.579	0.046	801.748	30.011	30.011	47.841
0.609	0.048	800.108	29.956	29.956	47.806
0.637	0.048	803.286	30.062	30.062	47.872
0.667	0.046	807.786	30.212	30.212	47.967
0.703	0.048	811.155	30.323	30.323	48.036
0.725	0.046	821.533	30.663	30.663	48.252
0.754	0.048	824.742	30.768	30.768	48.316
0.786	0.046	827.781	30.866	30.866	48.381
0.811	0.048	831.776	30.995	30.995	48.463
0.842	0.048	839.606	31.247	31.247	48.624
0.870	1.011	840.426	31.273	31.268	48.236
0.927	0.693	843.298	31.363	31.363	48.429
0.988	0.085	832.221	31.010	31.010	48.456
1.042	-1.289	814.687	30.439	30.439	48.657

Table 13.1 Continued.

STATION 5 / PHH = 30.00											
V/SS	BETA Y DEG.	N/M/KG	HT	V M/S	VZ M/S	VY M/S	VY M/S	VR M/S	VR M/S	BETA R DEG.	VYR M/S
0.0	-0.941	878.933	32.481	32.477	-0.533	51.534	52.209	40.879	40.879	52.627	41.036
0.081	-1.202	894.460	32.955	32.948	-0.691	51.239	52.320	41.276	41.276	51.239	41.036
0.162	-1.593	905.903	33.483	33.470	-0.931	51.962	53.320	41.663	41.663	51.962	41.036
0.243	-2.269	908.016	33.364	33.351	-1.318	51.387	53.140	41.374	41.374	51.387	41.036
0.271	-1.766	908.992	33.364	33.351	-1.028	51.130	53.140	41.028	41.028	51.130	41.036
0.295	-1.766	902.860	33.209	33.194	-1.028	51.131	53.039	41.024	41.024	51.131	41.036
0.322	-1.766	899.458	33.107	33.091	-1.019	51.257	53.039	41.365	41.365	51.257	41.036
0.343	-1.765	899.366	32.663	32.651	-1.019	51.341	52.972	41.365	41.365	51.341	41.036
0.370	-1.765	811.593	30.370	30.322	-1.006	52.695	52.695	41.351	41.351	52.695	41.036
0.393	-1.766	811.593	30.370	30.322	-0.935	53.701	51.220	41.280	41.280	53.701	41.036
0.424	-1.766	671.640	22.507	22.529	-0.780	58.406	48.281	41.125	41.125	58.406	41.036
0.446	-1.765	612.652	22.507	22.526	-0.704	60.901	48.978	41.049	41.049	60.901	41.036
0.472	-1.766	677.228	25.526	25.514	-0.787	58.188	48.403	41.132	41.132	58.188	41.036
0.497	-1.765	802.516	30.036	30.022	-0.925	53.966	51.035	41.270	41.270	53.966	41.036
0.521	-1.765	850.213	31.584	31.569	-0.973	52.618	51.998	41.318	41.318	52.618	41.036
0.543	-1.765	865.065	32.051	32.036	-0.987	52.221	52.221	41.322	41.322	52.221	41.036
0.570	-1.765	866.995	32.011	32.006	-0.989	52.171	52.332	41.324	41.324	52.171	41.036
0.593	-1.765	865.432	32.063	32.047	-0.983	52.216	52.216	41.326	41.326	52.216	41.036
0.621	-1.765	861.452	31.929	31.914	-0.983	52.325	52.325	41.328	41.328	52.325	41.036
0.645	-1.765	858.569	31.848	31.833	-0.981	52.393	52.393	41.330	41.330	52.393	41.036
0.668	-1.765	857.519	31.815	31.800	-0.980	52.421	52.421	41.332	41.332	52.421	41.036
0.698	-1.765	849.935	31.574	31.560	-0.972	52.625	51.992	41.334	41.334	52.625	41.036
0.725	-1.765	849.899	31.574	31.559	-0.972	52.626	51.992	41.336	41.336	52.626	41.036
0.745	-1.766	847.439	31.496	31.481	-0.971	52.694	51.943	41.337	41.337	52.694	41.036
0.770	-1.765	847.298	31.492	31.477	-0.970	52.697	51.943	41.338	41.338	52.697	41.036
0.793	-1.765	848.135	31.518	31.504	-0.971	52.674	51.950	41.339	41.339	52.674	41.036
0.822	-1.766	847.761	31.507	31.492	-0.971	52.685	51.950	41.340	41.340	52.685	41.036
0.844	-1.766	852.718	31.664	31.648	-0.976	52.651	52.651	41.342	41.342	52.651	41.036
0.871	-1.766	856.119	31.771	31.756	-0.979	52.460	52.460	41.344	41.344	52.460	41.036
0.893	-1.766	861.503	31.940	31.925	-0.985	52.316	52.316	41.346	41.346	52.316	41.036
0.918	-1.766	864.562	32.035	32.020	-0.986	52.235	52.235	41.348	41.348	52.235	41.036
0.947	-1.766	868.058	32.144	32.129	-0.991	52.143	52.143	41.350	41.350	52.143	41.036
0.968	-1.765	871.504	32.251	32.236	-0.993	52.052	52.052	41.352	41.352	52.052	41.036
1.019	-1.002	882.668	32.520	32.505	-1.001	51.827	51.827	40.915	40.915	51.827	40.915
1.042	-1.084	886.560	32.715	32.591	-0.570	51.461	52.309	40.964	40.964	51.461	40.964
					-0.619	51.392					

Table 13.1 Continued.

STATION 5 / PHH = 50.00						
V/SS	BETA Y DEG.	WT NIN/KG	V M/S	VZ M/S	VY M/S	VR M/S
0.0	-1.847	863.063	32.005	31.988	-1.031	54.254
0.066	-2.122	856.063	31.929	31.806	-1.179	54.497
0.129	-2.220	859.063	31.861	31.837	-1.234	54.102
0.156	-1.404	863.062	32.122	32.112	-0.777	54.506
0.163	-1.386	867.387	32.214	32.205	-0.779	54.555
0.207	-1.386	870.358	32.214	32.205	-0.783	54.622
0.229	-1.386	875.371	32.369	32.360	-0.788	54.679
0.257	-1.386	882.610	32.592	32.583	-0.791	53.773
0.279	-1.386	886.210	32.702	32.702	-0.795	53.511
0.306	-1.386	892.468	32.887	32.878	-0.797	53.360
0.333	-1.386	894.468	32.954	32.944	-0.798	53.305
0.356	-1.386	896.374	33.022	33.013	-0.798	53.249
0.381	-1.386	898.751	33.045	33.036	-0.798	53.558
0.405	-1.386	901.275	33.073	33.064	-0.798	53.477
0.432	-1.386	903.913	33.095	33.085	-0.798	53.022
0.456	-1.386	905.403	33.123	33.112	-0.798	51.935
0.481	-1.386	907.586	33.154	33.143	-0.798	51.938
0.504	-1.386	921.673	33.173	33.161	-0.798	51.938
0.534	-1.386	932.031	33.205	33.193	-0.798	51.938
0.554	-1.386	935.751	33.235	33.223	-0.798	51.938
0.582	-1.386	939.922	33.265	33.255	-0.798	51.938
0.609	-1.386	942.786	33.282	33.273	-0.798	51.938
0.634	-1.386	945.145	33.300	33.291	-0.798	51.938
0.655	-1.386	948.404	33.320	33.298	-0.798	51.938
0.679	-1.386	952.677	33.344	33.298	-0.798	51.938
0.707	-1.386	957.161	33.325	33.214	-0.798	51.938
0.729	-1.386	961.535	33.244	33.214	-0.798	51.938
0.757	-1.386	969.935	33.201	33.191	-0.798	51.938
0.779	-1.386	971.804	33.259	33.249	-0.798	51.938
0.804	-1.386	973.371	33.307	33.298	-0.798	51.938
0.830	-0.815	973.196	33.320	33.299	-0.798	51.938
0.938	-1.624	971.935	33.263	33.250	-0.798	51.938
1.043	-2.172	957.685	31.818	31.795	-1.206	54.615

Table 13.1 Continued.

STATION 5 / PHH= 70.00									
V/SS	BETA Y DEG.	HT NM/KG	V N/S	VZ H/S	VY H/S	VR H/S	BETA R DEG.	VY H/S	VY N/S
0.0	0.274	854.738	31.724	-0.151	55.768	56.396	46.625		
0.0	0.696	848.277	31.518	56.073	56.470	46.856			
0.0	1.415	865.736	32.059	-0.383	56.073	56.470			
0.0	2.63	866.059	32.079	-0.792	55.851	57.112	47.265		
0.0	2.88	871.304	32.242	-0.276	55.851	56.696	46.769		
0.0	3.15	875.332	32.367	-0.277	55.408	56.790	46.751		
0.0	3.42	875.492	32.366	-0.278	55.305	56.862	46.752		
0.0	3.63	858.916	31.855	-0.274	55.729	56.569	46.767		
0.0	3.89	812.892	30.376	-0.261	56.978	55.739	46.734		
0.0	4.18	701.192	26.444	-0.227	60.479	53.666	46.701		
0.0	4.40	595.587	22.094	-0.190	64.664	51.629	46.663		
0.0	4.63	614.094	22.916	-0.197	63.849	51.993	46.670		
0.0	4.91	779.037	29.241	-0.251	57.962	55.120	46.720		
0.0	5.14	851.376	31.618	-0.273	55.927	56.434	46.746		
0.0	5.37	864.492	32.034	-0.275	55.580	56.671	46.747		
0.0	5.62	700.494	31.726	-0.274	55.835	56.497	46.747		
0.0	5.87	704.492	31.841	-0.274	55.741	56.560	46.747		
0.0	6.14	858.461	31.840	-0.284	56.746	56.569	46.757		
0.0	6.38	855.631	31.753	-0.277	55.817	56.513	46.750		
0.0	6.65	858.145	31.931	-0.278	55.752	56.558	46.751		
0.0	6.90	856.500	31.771	-0.278	55.801	56.524	46.750		
0.0	7.14	700.500	31.833	-0.278	55.769	56.560	46.751		
0.0	7.38	700.500	31.841	-0.278	55.736	56.569	46.751		
0.0	7.64	10.501	31.847	-0.279	55.739	56.568	46.752		
0.0	7.87	10.500	32.004	-0.279	55.608	56.656	46.752		
0.0	8.13	10.501	32.166	-0.281	55.474	56.750	46.755		
0.0	8.41	10.500	32.152	-0.280	55.465	56.741	46.754		
0.0	8.65	10.500	32.198	-0.281	55.447	56.768	46.754		
0.0	8.87	10.501	31.850	-0.278	55.384	56.813	46.756		
0.0	9.12	10.236	875.064	32.274	55.074	56.520	46.360		
0.0	9.77	10.227	864.500	32.359	55.127	55.498	46.600		
1.042	0.433	857.686	32.031	32.030	55.241	56.520	46.714		
			31.817	31.816	55.742				

Table 13.1 Concluded.

STATION 5 / PHH = 90.00						
V/SS	BETA Y DEG.	HT NAN/XC	V H/S	VZ H/S	YY M/S	BETA R DEG.
0.0	2.0208	770.615	28.951	28.930	1.115	59.144
0.045	2.169	770.585	28.964	29.175	1.097	59.124
0.095	1.659	777.481	29.016	29.369	1.085	59.071
0.143	2.069	783.741	29.401	29.419	1.372	58.413
0.166	2.069	785.198	29.453	29.611	1.361	58.413
0.192	2.069	790.813	29.600	29.777	1.368	58.148
0.216	2.069	796.727	29.642	29.807	1.390	58.148
0.242	2.069	800.040	29.714	29.842	1.395	58.148
0.269	2.069	800.028	29.746	29.874	1.395	58.148
0.317	2.069	802.940	29.750	29.874	1.395	58.148
0.341	2.069	805.758	29.745	29.874	1.395	58.148
0.368	2.069	806.490	29.746	29.874	1.395	58.148
0.419	2.069	819.142	19.160	19.175	1.028	63.811
0.466	2.069	841.442	19.160	19.196	1.028	63.811
0.503	2.069	841.442	19.160	19.196	1.028	63.811
0.541	2.069	841.442	19.160	19.196	1.028	63.811
0.585	2.069	841.442	19.160	19.196	1.028	63.811
0.616	2.069	841.442	19.160	19.196	1.028	63.811
0.649	2.069	841.442	19.160	19.196	1.028	63.811
0.677	2.069	841.442	19.160	19.196	1.028	63.811
0.718	2.069	841.442	19.160	19.196	1.028	63.811
0.745	2.069	841.442	19.160	19.196	1.028	63.811
0.795	2.069	841.442	19.160	19.196	1.028	63.811
0.841	2.069	841.442	19.160	19.196	1.028	63.811
0.894	2.069	841.442	19.160	19.196	1.028	63.811
0.942	2.069	841.442	19.160	19.196	1.028	63.811
1.042	2.020	841.442	19.160	19.196	1.028	63.811

Table 13.2 Circumferentially-averaged flow-field parameters.

STATION 1		PHM	HT N _{EM} /KG	HS N _{EM} /KG	BETA Y DEG.	V M/S	VZ M/S	VY M/S	BETA R DEG.	VR M/S	VYR M/S	FC
10.00	-0.576	-513.672	1.093	32.034	32.028	0.611	0.865	48.685	36.670	39.490	0.627	
30.00	-0.395	-513.639	1.530	32.039	32.027	0.855	0.957	50.845	39.490	42.766	0.627	
50.00	-0.681	-513.597	1.114	32.048	32.042	0.623	1.171	53.454	56.221	46.204	0.627	
70.00	-0.521	-513.590	0.482	32.032	0.269	0.269	0.269	55.268	56.490	49.545	0.609	
90.00	-30.398	-513.578	-0.014	31.086	-0.007	0.007	0.007	57.894	58.490	49.545	0.609	
STATION 2		PHM	HT N _{EM} /KG	HS N _{EM} /KG	BETA Y DEG.	V M/S	VZ M/S	VY M/S	BETA R DEG.	VR M/S	VYR M/S	FC
10.00	466.945	-133.744	21.381	34.661	32.275	12.636	37.364	40.608	24.644	28.105	0.632	
30.00	477.577	-121.283	20.713	34.608	32.371	12.240	40.965	42.869	31.496	35.126	0.624	
50.00	465.037	-110.834	20.551	33.937	31.777	11.913	44.745	44.741	47.184	35.126	0.617	
70.00	459.121	-101.534	19.808	33.486	31.505	11.347	48.111	48.100	37.882	0.582		
90.00	413.978	-93.210	21.467	31.849	29.640	11.655	51.960					
STATION 3		PHM	HT N _{EM} /KG	HS N _{EM} /KG	BETA Y DEG.	V M/S	VZ M/S	VY M/S	BETA R DEG.	VR M/S	VYR M/S	FC
10.00	433.708	-75.529	-2.881	31.848	31.007	-1.601	50.715	50.234	38.892	41.132	0.623	
30.00	445.518	-75.400	-1.400	32.222	32.012	-0.787	51.934	52.245	54.026	53.750	0.631	
50.00	430.839	-75.372	-0.615	31.757	31.556	-0.361	51.934	52.245	54.026	53.750	0.621	
70.00	417.081	-75.369	0.523	31.307	31.306	0.286	55.871	55.798	46.188	46.188	0.613	
90.00	315.919	-75.360	1.328	27.771	27.764	0.644	60.411	56.226	48.894		0.544	
STATION 4		PHM	HT N _{EM} /KG	HS N _{EM} /KG	BETA Y DEG.	V M/S	VZ M/S	VY M/S	BETA R DEG.	VR M/S	VYR M/S	FC
10.00	840.398	275.580	23.455	33.597	30.021	13.373	37.802	39.007	23.908	27.711	0.606	
30.00	895.271	261.186	21.282	34.808	32.355	12.634	42.661	45.076	31.728	34.705	0.635	
50.00	881.291	300.329	20.043	34.083	32.018	11.681	46.739	46.872	34.705	37.149	0.627	
70.00	875.145	300.461	20.483	33.632	31.506	11.769	47.766	47.254				
90.00	821.798	318.448	22.987	31.723	29.204	12.389	51.828					
STATION 5		PHM	HT N _{EM} /KG	HS N _{EM} /KG	BETA Y DEG.	V M/S	VZ M/S	VY M/S	BETA R DEG.	VR M/S	VYR M/S	FC
10.00	801.050	351.415	0.081	29.944	29.944	0.042	51.197	47.784	37.239	41.279	0.586	
30.00	857.284	351.426	-1.666	31.733	31.710	-0.034	52.461	52.458	44.433	44.433	0.621	
50.00	855.956	351.486	-1.497	31.711	31.700	-0.828	54.375	56.266	46.778	46.778	0.612	
70.00	841.706	351.519	-0.559	31.238	31.237	-0.305	56.228	55.870	48.248	48.248	0.552	
90.00	753.235	351.528	2.621	28.200	28.170	1.290	59.721					

END

FILMED

34

ADHIC